Universidade do Minho
Escola de Engenharia

Tírcia Susete Xavier Carlos dos Santos

In vivo assessment of the host reactions to natural origin biomaterials aimed to be used as wound dressers and as bone tissue engineering scaffolds

Novembro de 2009

In vivo assessment of the host reactions to natural origin biomaterials aimed to be used as wound dressers and as bone tissue engineering scaffolds
Tírcia Susete Xavier Carlos dos Santos
UMinho | 2009

Universidade do Minho
Escola de Engenharia

Tírcia Susete Xavier Carlos dos Santos

In vivo assessment of the host reactions to natural origin biomaterials aimed to be used as wound dressers and as bone tissue engineering scaffolds

Tese de Doutoramento
Ramo de Ciência e Tecnologia de Materiais
Área de Engenharia de Tecidos - Materiais Híbridos

Trabalho efectuado sob a orientação do
Professor Doutor Rui Luís Gonçalves dos Reis
e do
Professor Doutor António Gil Castro

Novembro de 2009

To my parents

Acknowledgments

When I made the decision to suspend my staff position as a Pathology Technician in my hometown Hospital and choose to dedicate most of my life to research, I thought: “maybe this is not a very wise decision and it will not be an easy task”! But I could survive and here I’m after these 5 years, with a finished PhD. Obviously, this important achievement in my life would not be possible without the involvement of many people to whom I would like to recognize my gratitude.

First of all, to Prof. Rui Reis, who incited me to make that difficult decision by showing me what the research world is. He opened the research door and encouraged me to follow my ambitions. Even when FCT seemed not to trust in my competence and in my effort to accomplish a research work, he was always supporting me, giving me the right opportunities and confidence to go forward. Particularly when he convinced me that the collaboration with the LBI (Vienna, Austria) would be the better option to complete this work, gaining further knowledge and experience in animal experimentation. For all that and for supervising my work, THANK YOU!

To Prof. Gil Castro, I have to show my appreciation for his wise advises and for accompanying me all these years of my short scientific career, from the trainee in Applied Biology to this important step of accomplish a PhD. Also for all the talks we had, not as much as I would like, but always very fruitful.

I would like to express my gratitude to Prof. Martijn van Griensven for all the time and effort he did dedicate to my work. I have to be grateful for our work meetings when you always came up with a solution to any problem, mainly when things seemed to be wrong and worst every day.

I would like to acknowledge the European Network of Excellence EXPERTISSUES (NMP3-CT-2004-5000283) for partially support the work developed in this thesis. To the Marie Curie European program for providing me a short-term scholarship in the Alea Jacta EST project (MEST-CT-2004-008104), allowing the performance of some experiments at the LBI (Vienna, Austria). Finally to the Portuguese Foundation for Science and Technology (FCT), for funding my PhD grant (SFRH/ BD/ 40861/ 2007).

To Xana, which have been more than a “mother”, a “sister”, a scientific and a personal adviser. She opened the window of cell culture and taught me everything I’m able to do in the CCL lab. Thank you for your support, confidence, and determination. I also have to thank you for all your patience, in particular during the writing of this thesis and for teach me how to write science. When everything seemed to be lost, you were always there, trying to “annoying” me when my great pessimism put everything down. Actually, I do not really find the right words to express all the gratitude and appreciation I feel for you. THANK YOU for all our discussions!

I would like to thank to Ana Frias for her friendship and confidence outside the lab. In the lab, finally I have someone to discuss with, and to “lend a hand” on go forward with the “civic” work. Thanks for show up in the 3B’s and for being the “engineer” I can always count on to the rational

thinking. To Mariana, my “little” desk neighbour, thank you for your friendship, good mood and understanding. I also need to express my appreciation to Manela for all her opinions, help and recognition during my stay at the 3B’s.

To Belinha and Helena, whose advices and presence have been important for me, to grow up as a scientist and as a person.

There are many people from the 3B’s to whom I should address my gratitude, but I must confess that this is a very difficult task for me. To Rogério and Tommaso, thank you for all the fun and hard work. I also like to thank Ana Regina, for her help and comprehension, in particular in this final stage of my PhD.

At the LBI ... thank to all the people I had to work with, but specially:
To Kathi and Naime ... hey caramelas ... THANK YOU for make me feel at home in Vienna. You were my real colleagues and friends in a foreign country with very strange language! Thanks for the “survival kit” in a very depressing time and for the time we had.
Bernhard, who taught me everything I know on surgical procedures in animals. Thank you for your patience when I insisted in picking the scissors and forceps in the wrong position! You made our long days in that OP room much more agreeable. Thanks for being also my friend.
Tatjana, Sabine and Martina, the “mice team”! Thank you girls, for all the time we spent in and out of the LBI, and for everything I could learn you. You made my stay in Vienna even better. Thank you for your support and friendship. Also to Asmita and Daniela, the “cells team”, I do appreciate your advises on cell culture and also your friendship as office neighbours.

To my husband, Fizé, I have to address all my recognition for his support. I must thank his comprehension and patience, particularly during the time I was in Vienna. It was not easy for both! THANK YOU for being always there.

My final words are going to my parents to whom I dedicate this thesis. They were always supporting me and encouraging me to pursue my ambitions. At all difficult times they were there for me to get up and to show me that “life goes on”.

SHORT *CURRICULUM VITAE*

Tírcia Santos was born in 1977 in Chaves, Portugal. Since February 2004, she has been a researcher at the 3B's Research Group - Biomaterials, Biodegradables and Biomimetics.

Her background includes the Baccalaureate in Pathology in 1998, from the Superior School of Health Technology, Porto, and the BSc in Applied Biology in 2003 from the University of Minho, Braga. From July 1998 to January 2004 developed her Pathology Technician activity at the Curry Cabral Hospital (Lisbon) and at the Hospital of the District of Chaves, where she was responsible for the re-opening of the Pathology laboratory in 2000. From February 2004 she integrated the 3B's Research Group where she has been involved in a line of research related with the understanding of the inflammatory/immune reactions to biomaterials. The research work was developed in collaboration with the Ludwig Boltzmann Institute, Vienna, Austria, under the supervision of Prof. Martijn van Griensven. A total of one year was spent in this institution, which is one of the partners of the European Tissue Engineering Network EXPERTISSUES.

At the 3B's Research Group she is one of the responsible for the training of new researchers on the cell culture and histology laboratories. At the moment she is also responsible for the setting up of the animal facilities.

Furthermore, during her PhD activities, she integrated interdisciplinary teams involved in writing proposals for the 7th Framework Programme.

In 2005 attended the Course on Laboratory Animal Science, which provided her with the C level of graduation from The Federation of Laboratory Animal Science Associations (FELASA).

As a result of her research work, Tírcia Santos has attended relevant conferences in her research field. Presently, she is author of 11 papers in international refereed journals (7 submitted, 1 *in press* and 3 published), 2 book chapters and 3 chapters in national and international conference proceedings.

LIST OF PUBLICATIONS

This thesis is based on the following publications:

PAPERS IN INTERNATIONAL REFEREED JOURNALS

1. **T.C. Santos**, A.P. Marques, S.S. Silva, J.M. Oliveira, J.F. Mano, A.G. Castro and R.L. Reis, 2007, *In vitro* evaluation of the behaviour of human polymorphonuclear neutrophils in direct contact with chitosan-based membranes, *Journal of Biotechnology*, **132 (2)** : 218-226.

2. **T.C. Santos**, A.P. Marques and R.L. Reis, 2009, Animal models for host reactions and skin and bone tissue engineering approaches, *Submitted*.

3. **T.C. Santos**, A.P. Marques, S.S. Silva, J.M. Oliveira, J.F. Mano, A.G. Castro, M. van Griensven and R.L. Reis, 2007, Chitosan improves the biological performance of soy-based biomaterials, *Submitted*.

4. **T.C. Santos**, B. Hoering, K. Reise, A.P. Marques, S.S. Silva, J.M. Oliveira, J.F. Mano, A.G. Castro, R.L. Reis and M. van Griensven, 2009, *In vivo* performance of chitosan/soy-based membranes as wound dressing devices for acute skin wounds, *Submitted*.

5. **T.C. Santos**, A.P. Marques, B. Hoering, A.R. Martins, K. Tuzlakoglu, A.G. Castro, M. van Griensven and R.L. Reis, 2009, *In vivo* short and long term reaction to starch-based scaffolds, *Submitted*.

6. **T.C. Santos**, T. Morton, M. Moritz, S. Pfeiffer, K. Reise, A.P. Marques, A.G. Castro, R.L. Reis and M. van Griensven, 2009, *In vivo* evaluation of the suitability of starch-based constructs for tissue engineering applications, *Submitted*.

BOOK CHAPTERS

1. **T.C. Santos**, A.P. Marques and R.L. Reis, 2008, In vivo tissue responses to natural-origin biomaterials, In Natural-based polymers for biomedical applications, eds. R.L. Reis, N.M. Neves, J.F. Mano, M.E. Gomes, A.P. Marques, H.S. Azevedo, Woodhead Publishing in Materials, Cambridge, 683-698.

2. H.S. Azevedo, **T.C. Santos** and R.L. Reis, 2008, Controlling the Degradation of Natural Polymers for Biomedical Applications, In Natural-based Polymers for Biomedical Applications,

eds. R.L. Reis, N.M. Neves, J.F. Mano, M.E. Gomes, A.P. Marques, H.S. Azevedo, Woodhead Publishing Limited, Cambridge, 106-128.

CONFERENCE PROCEEDINGS

1. **T.C. Santos**, A.P. Marques, A.G. Castro, M. van Griensven, H .Redl and R.L. Reis, 2008, Long term in vivo performance of starch-based scaffolds, Tissue Engineering Part A, **14 (5)** : 752-753.

2. **T.C. Santos**, A.P. Marques, S.S. Silva, J.M. Oliveira, J.F. Mano, A.G. Castro, M. van Griensven, H. Redl and R.L. Reis, 2008, Chitosan/soy-based membranes enhance wound reepithelialization in partial thickness skin wounds, Tissue Engineering Part A, **14 (5)** : 711-711.

COMMUNICATIONS IN INTERNATIONAL CONFERENCES

1. **T.C. Santos**, A.P. Marques, S.S. Silva, J.M. Oliveira, J.F. Mano, A.G. Castro and R.L. Reis, *In vitro* evaluation of the behaviour of polymorphonuclear neutrophils in direct contact with chitosan-based membranes, 6th European Symposium on Biochemical Engineering Science, Austria, 2006.

2. **T.C. Santos**, B. Hoering, A.P. Marques, A.G. Castro, H. Redl, M .van Griensven and R.L. Reis, *In Vivo* Performance of Starch-based Scaffolds: Assessment of the Inflammatory Response, TERMIS NA 2007, Canada, 2007.

3. **T.C. Santos**, B. Hoering, A.P. Marques, A.G. Castro, H. Redl, M. van Griensven and R.L. Reis, *In Vivo* Assessment of the Inflammatory Response of Starch-based Scaffolds, 4th Marie Curie Cutting Edge Conference Biocompatibility evaluation and biological behaviour of polymeric biomaterials, Portugal, 2007.

4. **T.C. Santos**, T. Morton, K. Reise, A.P. Marques, A.G. Castro, H. Redl, M. van Griensven and R.L. Reis, 2008, Adipose stem cells and starch-based constructs performance on VEGFR2-LUC transgenic mice, SPCE-TC08, Portugal, 2008.

5. **T.C. Santos**, B. Hoering, A.P. Marques, A.G. Castro, H. Redl, M. van Griensven and R.L. Reis, Different implantation models for biomaterials host response evaluation, 1st SPCAL Meeting, Portugal, 2009.

Abstract

The development, in recent years, of novel biomaterials for tissue engineering (TE) and regenerative medicine, is an attempt to give an answer to the rising needs of the new tissue replacement/regeneration strategies. However, the increasing complexity of TE devices, comprising cells and/or bioactive agents within 3D scaffolding structures, implies additional concerns regarding adverse host reactions to the implantable constructs. Despite all the investment in the research on stem cells technology, as well as in the identification of key mediators in inflammation/immune reaction and differentiation pathways, the role of support biomaterials in the host reaction has been somewhat neglected.

Natural-origin biomaterials have been considered for many years as a way to improve, in comparison to synthetic polymers, *in vivo* biofunctionality and to modulate/avoid a harmful host response due to its similarities with biological molecules. This PhD work attempted to gather deeper knowledge on the host reactions elicited by natural-origin biomaterials processed under different conditions and aimed at skin wound dressing and bone TE applications.

In a first approach, chitosan/soy membranes were tested for their *in vitro* ability to activate human polymorphonuclear neutrophils (PMNs), assessed by the quantification of lysozyme activity and reactive oxygen species (ROS) production. Chitosan/soy membranes were not able to activate PMNs *in vitro* thus the analysis of the *in vivo* performance of those materials was pursued. The influence of chitosan and soy on the elicited inflammation was quantified after intraperitoneal implantation in rats. Soy isolate protein induced the recruitment of higher numbers of leukocytes and elicited a considerable reaction from the host in comparison to chitosan. Additionally, the chitosan/soy-membranes induced of a normal host response after subcutaneous implantation in rats while soybean membranes elicited a severe tissue reaction. In conclusion, an improved host response, considering inflammatory cells' recruitment and overall inflammatory reaction, was observed when chitosan was combined with soybean. Considering a potential application of these chitosan/soy membranes as wound dressers, a rat partial-thickness skin wound model was used to assess the suitability of the membranes in promoting wound healing. A rapid but, most importantly, functional regeneration was achieved in the chitosan/soy membranes dressed wounds. The re-epithelisation, observed only one week after wounding, was followed by the cornification of the outermost epidermal layer indicating a functional recovery of the excised tissue. These new chitosan/soy membranes showed to possess the desired features in terms of healing stimulation, ease of handling and final aesthetic appearance to be considered useful as wound dressers.

Starch-based biomaterials have been extensively studied *in vitro* aiming at different TE applications. Previous *in vitro* studies with starch and polycaprolacatone (SPCL) scaffolds have proved the great potential of these structures. Thus, an *in vivo* systematic study was carried out using two different rat implantation models, subcutaneous (SC) and intramuscular (IM), and aiming at primarily understand the tissue reaction to two SPCL-based scaffolds produced by different methodologies, wet spinning (SPCL-WS) and fibre-bonding (SPCL-FB), both at short and long term implantation periods. SPCL-WS scaffolds seemed to induce a lower inflammatory/immune reaction in both types of implantation models even if when comparing the two models, the IM implantation resulted in a higher inflammatory response than the SC implantation, with early activation of the lymph nodes for both scaffolds. The overall data suggested a good integration of the polymeric structures in the host, independently of the implantation site, with a normal progression of the inflammatory reaction for all the conditions.

Different biomaterials, cells, growth factors and stimulation conditions, as well as numerous combinations among them, have been widely proposed as potential routes to achieve the perfect bone TE construct. Despite this, in bone TE, vascularisation remains a rather big concern, not yet perfectly addressed. A valuable alternative to tackle the vascularisation of bone TE constructs relies on the incorporation in the construct of important mediators, such as vascular endothelial growth factor (VEGF) and fibroblast growth factor (FGF), which can be released in a controlled manner from the scaffolding material. To pursue this, SPCL-WS and SPCL-FB scaffolds were seeded with transfected human Adipose-derived Stem Cells (hASCs) and their movement was followed after implantation of the constructs into *nude* mice. Additionally, bone TE constructs were assembled using the SPCL scaffolds, fibrin sealant (Baxter®), hASCs, and growth factors (VEGF or FGF-2), and implanted in vascular endothelial growth factor receptor-2 (*VEGFR2)-luc* transgenic mice. The behaviour of transfected hASCs after transplantation was similar for both the SPCL-WS and the SPCL-FB scaffolds. Furthermore a mild inflammatory reaction was observed after transplantation of the assembled constructs and, as expected, the release of VEGF and FGF-2 from the constructs enhanced the expression of VEGFR-2 as well as specific molecular markers of neovascularisation.

The overall data confirmed that the developed chitosan/soy membranes represent a valuable alternative for wound dressing applications and that starch-based constructs are promising approaches for bone TE applications.

Resumo

O desenvolvimento de novos biomateriais para Engenharia de Tecidos (ET) e medicina regenerativa representa uma tentativa de responder à necessidade de novas estratégias para a regeneração e substituição de tecidos. No entanto, a crescente complexidade dos dispositivos de ET, que compreendem células e/ou agentes bioactivos no interior de estruturas de suporte tridimensionais, implica novas preocupações relativamente a reacções adversas desencadeadas pelo hopedeiro a esses mesmos dispositivos. Apesar de todo o investimento na investigação relacionada quer com as células estaminais, quer com a identificação de mediadores chave na reacção inflamatória e vias de diferenciação, o papel dos materiais de suporte na reacção imune do hospedeiro tem sido algo negligenciada.

Os biomateriais de origem natural têm sido considerados, desde há alguns anos, como uma forma de melhorar, comparativamente aos polímeros sintéticos, aspectos da biofuncionalidade *in vivo* e de modular/evitar uma recção adversa do hospedeiro, devido às suas semelhanças com moléculas biológicas. Este trabalho de doutoramento foi desenvolvido de forma a adquirir um conhecimento mais profundo das reacções do hospedeiro, desencadeadas por biomateriais de origem natural, processados em diferentes condições, e produzidos para utilização em revestimento/protecção de lesões de pele, bem como em aplicações de ET ósseos.

Numa primeira fase, foi testada a capacidade de membranas de quitosano/soja activarem neutrófilos (PMNs) humanos em cultura, através da quantificação da actividade da lisozima e da produção de espécies reactivas de oxigénio (ROS). As referidas membranas não foram capazes de activar os PMNs em cultura, procedendo-se, de seguida, à análise da performance daqueles materiais após implantação. A influência do quitosano e da soja na inflamação provocada foi quantificada após implantação intraperitoneal em ratos. O isolado de proteína de soja induziu o recrutamento de um número mais alto de leucócitos e provocou uma reacção considerável do hospedeiro, em comparação com o quiotosano. Adicionalmente, as membranas de quitosano/soja induziram uma resposta normal do hospedeiro após implantação subcutânea em ratos, enquanto que as membranas de soja provocaram uma reacção tecidular severa. Em conclusão, foi observada uma melhoria na reacção do hospedeiro, do ponto de vista do recrutamento de células inflamatórias e reacção inflamatória geral, quando o quitosano foi combinado com a soja. Considerando uma potencial aplicação destas membranas de quitosano/soja como revestimento e protecção de lesões, foi utilizado um modelo de lesão de espessura parcial de pele em rato, para determinar a capacidade das membranas de auxiliarem

a regeneração das lesões. Uma regeneração mais rápida e, ainda mais relevante, funcional foi conseguida nas lesões revestidas com as membranas de quitosano/soja. A re-epitelização, observada apenas uma semana após a lesão, foi seguida pela cornificação da camada exterior da epiderme, indicando uma recuperação funcional do tecido excisado. Estas novas membranas de quitosano/soja mostraram possuir características adequadas em termos de estimulação da regeneração, facilidade de manipulação e aparência estética final, de forma a serem consideradas como boas opções para o revestimente e protecção de lesões cutâneas.

Os biomateriais à base de amido têm sido extensivamente estudados *in vitro* tendo em vista diferentes aplicações de ET. Estudos *in vitro* anteriores utilizando suportes de amido e policaprolactona (SPCL) provaram já o grande potencial destas estruturas. Assim, foi elaborado um estudo *in vivo* sistemático, utilizando dois modelos de implantação em ratos, subcutâneo (SC) e intramuscular (IM), com o objectivo de compreender a reacção tecidular a dois suportes tridimensionais de SPCL, produzidos de duas formas distintas, *wet spinning* (SPCL-WS) e *fibre bonding* (SPCL-FB) em ambos períodos de implantação, curto e longo. Os suportes de SPCL-WS induziram uma reacção inflamatória/imune menor nos dois tipos de modelo de implantação, mesmo tendo em conta que, comparando os dois modelos, o modelo IM revelou uma resposta inflamatória mais intensa do que o modelo SC, com uma activação inicial dos nódulos linfáticos para ambos os suportes. A totalidade dos dados sugeriu uma boa integração das estruturas poliméricas nos tecidos do hospedeiro, independentemente do local de implantação, com uma progressão normal da reacção inflamatória para todas as condições.

Diferentes biomateriais, células, factores de crescimento e condições de estimulação, bem como várias combinações entre estes factores, têm sido largamente propostos como potenciais formas de atingir o dispositivo de ET ósseos perfeito. No entanto, a vascularização permanece como uma grande preocupação na ET de osso e ainda não correctamente estudada. Uma possível alternativa para ultrapassar o problema da vascularização de dispositivos para ET ósseos consiste na incorporação no próprio dispositivo, de importantes mediadores, como o factor de crescimento endotelial vascular (VEGF) e o factor de cresciemento fibroblástico (FGF). Estes factores podem ser libertados de uma forma controlada do material que compõe os dispositivos. Para avaliar, na prática, esta tecnologia, suportes de SPCL-WS e SPCL-FB foram semeados com células estaminais humanas do tecido adiposo (hASCs) transfectadas e o seu movimento foi seguido após implantação em ratinhos immunossuprimidos (*nude*). Além disso, os dispositivos para ET de osso foram produzidos utilizando suportes de SPCL, selante de fibrina (Baxter®), hASCs e factores de crescimento (VEGF ou FGF-2) e implantados em ratinhos

transgénicos *VEGFR2-luc*. O comportamento das hASCs transfectadas foi similar para ambos os tipos de suportes, SPCL-WS e SPCL-FB. Mais ainda, foi observada uma ligeira reacção inflamatória após a transplantação dos suportes e, tal como o esperado, a libertação de VEGF e FGF-2 dos suportes induziu o aumento da expressão de VEGFR-2, bem como de marcadores moleculares específicos de neo-vascularização.

No seu conjunto, estes resultados confirmaram que as membranas de quitosano/soja desenvolvidas representam uma valiosa alternativa para aplicação em revestimento e protecção de lesões cutâneas, e que a utilização de suportes baseados em amido é uma estratégia promissora para aplicações em ET ósseos.

Table of Contents

List of Figures

Chapter 2

Chapter 3

Chapter 4

Chapter 5

Chapter 6

Chapter 7

List of Tables

List of Abbreviations

A

Adipose Tissue-Derived Stem Cells – ASCs

Antigen-Presenting Cells – APCs

Arg-Gly-Asp Peptide Sequence – RGD

B

Basic Fibroblast Growth Factor – bFGF

Body Weight – BW

Bone Morphogenetic Proteins – BMPs

C

Calcium – Ca^{2+}

Calcium Chloride – $CaCl_2$

Carbon Dioxide – CO_2

Chitosan – Cht

Chitosan Powder – Cht-P

Chitosan/Soy – Cht/Soy

Chitosan/Soy 75/25% – CS75

Chitosan/Soy Membrane – Cht/Soy-M

Chitosan/Soy Protein Hybrid – Cht/Soy-TEOS

Chloridric Acid – HCl

Cluster of Differentiation -3, -18 – CD3, CD18

Complement Component 3b – C3b

Complimentary Deoxyribonucleic Acid – cDNA

D

Denaturated Soybean Protein Isolate – dSI

Denaturated Soybean Protein Isolate Membrane – dSI-M

Deoxyribonucleic Acid – DNA

E

Extracellular Matrix – ECM

F

Fibre Bonding – FB

Fibrin Sealant – FS

Fibroblast Growth Factor – FGF

Fibroblast Growth Factor-2 – FGF-2

Foetal Calf Serum – FCS

Foreign Body Reaction – FBR

Foreign-Body Giant Cells – FBGCs

Formyl-methionyl-leucyl-phenylalanine – fMLP

G

Gamma-Aminobutyric Acid – GABA

Glycosaminoglycans – GAGs

H

Haematoxylin and Eosin – HE

Horseradish Peroxidase – HRP

Human Adipose Tissue-Derived Stem Cells – hASCs

Human Recombinant Osteogenic Protein-1 – rhOP-1

Human Umbilical Cord Endothelial Cells – HUVEC

Hydrogen Peroxide – H_2O_2

Hydroxyl Anion – HO^-

I

Immunoglobulin G – IgG

Insulin Growth Factor -1 and -2 – IGF-I and IGF-II

Interferon Gamma – IFN-γ

Interleukin -1α, -4, -6. -8, -10, -12, -13, -18 – IL-1α, I-4, IL-6, I-8, IL-10, IL-12, IL-13, IL-18

Intramuscular – IM

Intraperitoneal – IP

L

Lymph Nodes – LN

M

Macrophages – MO

Magnesium – Mg^{2+}

Major Histocompatibility Complex Class II – MHC class II

Masson Goldner Trichrome – MGT

Mesenchymal Stem Cells – MSCs

Messenger Ribonucleic Acid – mRNA

N

Nicotinamide Adenine Dinucleotide Phosphate – NADPH

O

Operation Day – OpD

Optical Density – OD

Osteogenic Protein-1 – OP-1

Oxygen – O_2

P

Phorbol 12-Myristate 13-Acetate – PMA

Phosphate Buffer Saline – PBS

Phosphoinositide 3-Kinase – Pi3K

Plasma Fibronectin – p(FN)

Platelet Derived Growth Factor – PDGF

Poly(L-lactide) Acid – PLLA

Polymorphonuclear Neutrophils – PMNs

Pro-His-Ser-Arg-Asn Peptide Sequence – PHSRN

R

Reactive Oxygen Species – ROS

Reverse Transcriptase Polymerase Chain Reaction – RT-PCR

Ribonucleic Acid – RNA

S

Singlet Oxygen – $^1O_2$

Soybean Protein Isolate – SI

Soybean Protein Isolate Membrane – SI-M

Soybean Protein Isolate Powder – SI-P

Starch /Poly-ε-Caprolactone – fibre bonding – SPCL-FB

Starch /Poly-ε-Caprolactone – SPCL

Starch /Poly-ε-Caprolactone - wet spinning – SPCL-WS

Subcutaneous – CS

Superoxide Anion – O_2^-

T

Tetraethyl Orthosilicate – TEOS

T_H2 subset – T_H2

Tissue Culture Polystyrene – TCPS

Tissue Engineering – TE

Transforming Growth Factor Beta – TGF-β

Transgenic FVB/N-Tg(VEGF-r2-luc)Xen mice – VEGFR2-LUC

Tumour Necrosis Factor Alpha – TNF-α

V

Vascular Endothelial Growth Factor – VEGF

Vascular Endothelial Growth Factor Receptor 1 – VEGF-R1

Vascular Endothelial Growth Factor Receptor 2 – VEGF-R2

W

Wet Spinning – WS

Chapter I

Animal models for host reactions and skin and bone tissue engineering approaches

1.1 Abstract

The study of host reactions in the field of implantable materials is a key issue. The type of material, its shape and final application, are important features to consider when choosing an appropriate animal model. Every day new biomaterials, as well as their based constructs for tissue engineering (TE) applications, are being developed and presented to the scientific community. Their properties are very wide including, among others, mechanical and physicochemical properties, surface chemistries and degradability. Eventually all of them will influence the host reaction and performance of the implant and reliable animal models have to be used in order to closely evaluate those properties. Due to the specific anatomical and physiological features of each tissue, significant information can be extrapolated to humans and to a particular clinical situation. Although in most cases there is no question on the reliability of the results obtained from animal experimentation, there are increasing discussions regarding the limitation of the number of animals used in research that might limit the achievement of some scientific developments. The rational of this review exercise is to highlight key issues in animal experimentation used to test implantable materials. An overview of the elicited host reactions after implantation of biomaterials is made. Special attention is given to the state of the art in animal models available for skin and bone tissue engineering. The most widely used animal models are discussed in order to gain further insight on the advantages and disadvantages in extrapolating the obtained results to human health care procedures.

***This chapter is based on the following publication:**

T. C. Santos, A. P. Marques, R. L. Reis, Animal models for host reactions and skin and bone tissue engineering approaches, **2009. *Submitted***.

1.2 Host Reactions to Biomaterials Implantation

The induced host tissue trauma and the inflammatory process resulting from the implantation of a medical device [1-4] are of outmost importance for its successful clinical application. To the host response towards the implant are usually attributed features of a chronic inflammation, while an early acute inflammatory response is mainly endorsed by the implantation procedure. Nevertheless, no matter what, the final purposes of inflammation are to destroy (or control) the invading agent, to initiate the repair process, and to re-establish tissue function as a continuous event [3, 5].

As a wound is created, coagulation takes place in the context of acute inflammation. Simultaneously, the complement system, which has the capability to distinguish "self" from "non-self" [6, 7] is activated [3, 8, 9]. The interaction of plasma proteins such as immunoglobulins and fibrin [3, 4, 8, 9] with the surface of the material, or through an inadequate down-regulation of convertase, which enables Complement component 3b (C3b) binding to plasma proteins, such as albumin, immunoglobulin G (IgG) and fibrinogen [9] is the main responsible for this activation. In addition to that, the adsorbed proteins onto the surface of the implanted materials act as strong chemoatractants to polymorphonuclear neutrophils (PMNs) at a first stage and blood monocytes within 24 hours. Macrophages derived from blood monocytes continue the phagocytic work initiated by neutrophils [3, 10], although they might also act as antigen-presenting cells (APCs) after processing the material [4], instigating specific immunological responses in which also participate lymphocytes [3]. In general, the formation of foreign-body giant cells (FBGCs) indicates the transition to a chronic inflammatory process [2, 11]. However, the same features may co-exist, attesting the simultaneous development of the acute and chronic inflammation [12]. As the FBGCs persist, unable to resolve the inflammation, cytokines and chemokines are released, inducing delayed-type hypersensitivity and forming a granuloma at the injury/implant site [13-15]. Granuloma formation is often a reason for implant rejection [16-20], or additionally induces latent auto-immune diseases [21]. Some authors defend [16, 22-24] that at the implant site, the foreign body induces chronic stress bringing forward the formation of granulomas. However, that is not always true and implants can be well tolerated and integrated in the host tissue without eliciting a persistent acute inflammation [25]. Conversely, when collagen synthesis is likely to surpass its degradation [26], excessive fibrotic tissue surrounds the implant impeding the interaction of the host with the implanted material [15, 26-28]. This diminished interaction may protect the host from eventual material debris, but more importantly, will not allow the integration of the implant into the host tissue. Therefore, thick fibrotic capsule formation is considered to be a

detrimental consequence of biomaterial implantation and a negative feature needed to be overcome in order to improve host reaction and eventually avoid rejection of the implant.

Ideally, an implanted biomaterial would interact with and integrate the host tissue [29, 30], allowing the functional re-establishment and a complete recovery of the injured tissue. The resolution of inflammation with concomitant integration of the implant in the host tissue precedes the healing process. In a tissue engineered construct where the scaffolding material works as a temporary structure, the constant mutation of the implanted material will influence the reaction from the host. Additionally, the release of the degradation products should not adversely interact with the host and should be physiologically discarded. Moreover, the presence of cells and bioactive agents influencing the properties of the biomaterial further hurdles the ideal scenario and raises further concerns still to be overcome.

1.3 Skin Healing

Skin is the largest and the heaviest organ of the body, constituting the main physical barrier to invading pathogens and foreign bodies [31]. For this reason rapid reconstitution of wounded skin is typically required. As a wound is created a complex set of systems interact in order to establish skin physical integrity, homeostasis and functionality [32, 33]. The reepithelialisation process begins few days after skin injury. It happens concomitantly to blood coagulation, inflammation, repair and new tissue formation [34, 35], as it is the precursor of tissue repair. As tissue is remodelling, blood supply becomes essential to feed newly formed tissue. It was shown that blood flow after skin excision is significantly high at the reepithelialisation stage and decreases, as the tissue remodels, to similar values observed in non-injured skin [36]. Thus, these intrinsically connected processes are fundamental for the enhancement of healing and functional tissue formation. Nonetheless, this cascade of events inevitably leads to scar formation in skin wounds. The type of the fibrous tissue in the scar, as well as the degree of scarring is dependent on the deposition of collagen and can be controlled, at some extent, by dressings that enhance healing by promoting the reepithelialisation and vascularisation of the wounded skin [37, 38].

The lack of fibrin and platelet degranulation, the reduced inflammatory reaction and the raised levels of skin morphogenesis and growth molecules [39-42] observed in the embryos scar-free healing, may be the key for improving adult wound healing. Many useful models [43-49] have allowed the numerous studies on the features, players and mechanisms of wounding, inflammation and progression to wound healing and tissue regeneration. Epidermal growth factor receptor [47] was proved to be a key molecule in wound healing. Being able to regulate inflammation, wound contraction, cell migration and proliferation, and angiogenesis [47] might be

used as a promoter of skin regeneration. Other molecules present at the inflammatory milieu, such as reactive oxygen species, although directly delaying skin wound repair, are inherent detoxifying agents of the wounded area [46, 49]. The pro-healing effect of the non-protein amino acid gamma-aminobutyric acid (GABA) was also demonstrated by suppressed inflammation and stimulated reepithelialisation in excisional wounds in rats [48]. Hence, very different types of molecules involved in a variety of mechanisms and processes may be useful tools to provide a better understanding on the wound healing mechanisms. Additionally, those molecules represent promising tools to assist skin regeneration [37, 47, 50, 51] in the different strategies that have been proposed either for acute or chronic, as well as deep and superficial wounds healing.

1.4 Bone Healing

Bone tissue is a quite hard tissue with very particular mechanical properties. It is highly vascularised, with several anastomoses between inner medullary and outer periosteal vessels [52, 53], and mineralized [54, 55].

The cellular component of bone, constituted by osteocytes, osteoblasts and osteoclasts, is responsible for specific functions, such as filling up the bone matrix, synthesise the organic components of the matrix, and resorption and remodelling, respectively [53, 54]. The balance existing between osteoblasts and osteoclasts is the main responsible for the stability of bones [53, 56]. Hence, to reconstruct bone healing process after fractures or implantation procedures represents a challenge, not only because remodelling mechanisms in either situations are different [57], but also because new bone deposition in bone tissue defects showed to be different in different species [57, 58].

Contrarily to highly vascularised tissues, such as muscle, bone is able to heal and remodel without scarring [59]. It heals by different mechanisms with the same functional end. Endochondral bone repair occurs when bone is subjected to some mobility and also is the mechanism that allows bone growth. It is the only mechanism where a preliminary cartilage phase (callus formation), synthesised by the inner periosteal layer and marrow tissue, followed by woven and then lamellar bone formation. Primary and direct bone repair do not comprehend a cartilage phase and require a rigid stability of the gaps between edges, as in the case of fractures or osteotomies. The first is mediated by the intraosseous Haversian system osteoblasts and osteoclasts occurring in a non intrafragmentary space, and the direct bone repair has the participation of marrow derived vessels and mesenchymal cells [56]. By its turns, in distraction osteogenesis, woven and then lamellar bone is synthesised as the gap slowly expands, also without primary cartilage formation, as in bone elongation clinical situations [60].

Independently of the repair mechanisms, cells from the inner osteogenic layer of the periosteum [59], circulating osteoprogenitor cells [61], endosteum cells [59], and undifferentiated mesenchymal cells from either the bone marrow [62] or from soft tissues are key players in bone repair [54, 55, 59, 61-63].

Within the repairing niche, each intervenient cell type produce growth factors and proteins that determine the progression of bone healing. Bone morphogenic proteins (BMPs), such as BMP-2 [58, 64], BMP-3 [65], BMP-7 [66] and BMP-13 [67] have been show to induce osteogenic differentiation [68]. With the similar objective of bone regeneration, transforming growth factor beta (TGF-β1) [69, 70], insulin growth factors 1 and 2 (IGF-I and IGF-II) [71], basic fibroblast growth factor (bFGF) [72, 73] and platelet derived growth factor (PDGF) [74, 75] have been used with very rewarding results. Additionally, platelet-rich plasma demonstrated to be an excellent autologous source of a cocktail of key growth factors to induce bone regeneration [76, 77].

The relevance of some of those growth factors over bone regeneration has been highlighted in different bone tissue engineering (TE) approaches [71, 73, 74]. However, issues such as the need of very high concentration and difficulties in their controlled release from incorporating TE constructs are still to be addressed.

1.5 Animal models for Biomaterials Evaluation

Animal models have been extensively developed in the last few decades in the biomedical field. Despite major advances regarding *in vitro* models aiming to mimic the complexity and the cellular interaction existing within tissues, *in vivo* testing is essential to safely conclude about the biological performance of newly developed devices when implanted in a living system. A better characterization of such response, at the cellular and molecular level, is demanded and is being extensively investigated in the last decades [14, 78-80]. However, the complexity of the *in vivo* responses to implanted biomaterials renders this assessment as a challenging issue to be addressed. For this reason the establishment and the choice of a specific animal model must not only consistently answer to the posed hypothesis but also to mimic, as much as possible, the clinical situation that permits a correct extrapolation to humans.

1.5.1 - Host reaction models

Subcutaneous [81, 82], intraperitoneal [81, 83] and intramuscular [84, 85] mice [86, 87] and rat [81, 85] models are the most commonly used animal models to assess, at an early stage, the *in vivo* performance of newly developed biomaterials. Despite the well known influence of the

processing methodologies over materials surface properties and degradation behaviour, usually these implantation models do not deal with the final shape of the device. Nevertheless valuable considerations can be obtained with these models regarding acute [30, 81, 88, 89] or chronic inflammation [30, 81, 89, 90], as well as long term reactions with fully integration of the implant into the host tissue [29, 30]. Additionally, comparative works using different models allow for the local [30, 81, 91], or systemic [81, 91, 92] analysis of the implant effect over the host. While the subcutaneous and the intramuscular models are mainly related to the direct effect of the device over the implantation site, the intraperitoneal models have been useful in evaluating the reaction of abdominal organs, such as spleen [81, 91, 92], liver [81, 91], kidney [81], mesenteric lymph nodes [92] as well as the adjacent adipose tissue [92]. Moreover, the antigenic potential of a material and consequent acquired immunity by the host has also been studied after repeated implantations either in subcutaneous [93] and intraperitoneal [94] rat models.

Classically, researchers in the biomedical field tend to consider the implant/host interface as a key issue in evaluating tissue reactions to implants. In fact, great efforts have been made to develop materials whose surfaces are less immunogenic [94-98]. The reduced number and the lack of validation of *in vitro* models to assess the immunogenic potential of newly developed materials still renders *in vivo* tests as more reliable for testing the success of those imunomodulatory approaches. The effect of key molecules such as dexamethasone [99], nitric oxide [100], tumour necrosis factor alpha (TNF-α) and interferon gamma (IFN-γ) [101], vascular endothelial growth factor (VEGF) and fibroblast growth factor-beta (FGF-β) [102] has been tested in both subcutaneous rat [99, 100] and mouse [101] models, as well as in the intramuscular rat model [102]. Parameters such as inflammatory tissue reaction, foreign body reaction (FBR), phagocytic potential of macrophages and giant cells formation, fibrotic capsule thickness and vascularisation were targeted. However, due to given differences on the test model and consequent reaction mechanisms [101, 102], or on the carrier materials, and thus the surface properties [99-102], few remarks regarding the potential of the tested molecules in modulating host response can be extracted. Given the interest to avoid immunessupression, it is imperative to proceed with this line of research, which envisages materials that elicit moderate host response or controlled inflammatory/immune reactions. Moreover, comparative studies of specific biomolecule/carrier systems in different animal models are demanded for concluding about the potential of those strategies.

Macrophages, always a major player in the host reaction, recognize and react with the proteins adsorbed to the materials surface [103]. Although some lights have been thrown regarding this interaction [80, 104-106], the mechanisms by which macrophages adhere and react to the

different surfaces are still far from being revealed. However, some indications on the mechanisms of monocyte recruitment and sub-population differentiation in response to biomaterials implantations have been achieved [107]. A subcutaneous cage implant rat model [80] allowed to show that specific fibronectin peptide sequences such as Pro-His-Ser-Arg-Asn (PHSRN) and Arg-Gly-Asp (RGD) elicited an early stage FBGC reaction. These domains were identified as being important factors mediating macrophage adhesion to biomaterials surfaces in the FBGC formation [80]. This assumptions were further explored in a transgenic mice model where plasma fibronectin [p(FN)] was depleted [105]. Besides being an important regulator of FBGC reaction, Keselowsky and co-workers [105] demonstrated that p(FN) plays a role in the fibrotic capsule formation [105]. Additionally, two other transgenic mice models, where either fibrinogen or plasminogen was depleted, were used to evaluate the role of these proteins in the recruitment and adhesion of leukocytes to the intraperitoneal implanted biomaterials [108]. This work proved that leukocyte recruitment to the intraperitoneal environment is plasminogen-dependent, while leukocyte adhesion is fibrinogen-dependent [108].

Ultimately the specific cellular response to the materials surface determines the deposition of collagen by the tissue repairing cells and consequently the nature and the extent of the fibrotic capsule around the implant [105, 109-111] . Due to the muscle high degree of vascularisation that assist complement and clot systems' activation, intramuscular models can be considered more reliable for providing information on the fibrotic capsule formation and development throughout the implantation [84, 85].

The postulation that the implant/host interface is considered of major importance must not diminish the importance of cell recruitment mechanisms and its relevance in the onset of inflammation, tissue regeneration and implant integration. Intraperitoneal models are the most suitable to evaluate cell recruitment and activation status [92], at short [92, 98, 108, 112] and long time periods [92, 94] of reaction. Besides injection of particles suspensions [91, 92], those models also permit materials implantation [94, 98, 108, 112], allowing to establish a parallel between the implant/host interface analysis and the surrounding cellular milieu. The cytokine profile resulting from the materials implantation is an example of an extremely powerful measure of this crosstalk. In fact, the cytokines in the exudate samples are released by recruited cells that received the information from mediators, by its turn, secreted by surface adherent cells [112-115]. Additionally, direct cell response to the implant surface may elicit the release of several reactive species which induce either cell death or concomitant secretion of mediators, such as new reactive species [112]. Variations of the classical subcutaneous implantations, such as subcutaneous air pouches [82, 116, 117], dorsal skin fold chamber [118], or cage implants [80, 97, 113, 119-121], have also

demonstrated reliable results regarding the interplay between direct and indirect material surface reactions. Cage implant models were shown [97, 119-121] to be useful to identify recruited and adherent cell types as well as macrophage fusion into FBGCs [80] and cytokine release [113] in response to implanted materials, either in rats [80, 97, 119, 120] or mice [113]. Additionally, with air pouch rat models it has been possible to accurately evaluate the oxidative stress experienced by leukocytes in the presence of implants [82, 116]. Moreover, the observation of leukocyte recruitment and accumulation was possible in a dorsal skin fold chamber [118], using an intra-vital fluorescence and avoiding the sacrifice of animals at different experimental time periods.

Despite the achievements using subcutaneous, intramuscular and intraperitoneal implantations, together with their particular variations, in the evaluation of host inflammatory/immune reactions to biomaterials, a major lack is still present. The understanding of the mechanisms involved on the transition from an acute to a chronic reaction, to which the existing animal models are not capable to answer, is a significant depletion of field.

Table 1.1: Overview of the animal models used to evaluate the host reaction to biomaterials

Animal	Model	Aims	Assessed parameters	References
Mouse	SC	Host reactions evaluation	Material/tissue interactions Foreign body reaction Fibrosis	29, 86, 87, 88, 91, 105*
	IP		Systemic reaction Inflammatory cells recruitment Fibrosis	108**, 92, 87, 91, 98
	Cage implant		Inflammatory cells recruitment	113
	SC air pouch		Inflammatory cells recruitment	117
Rat	SC		Material/tissue interactions Foreign body reaction Fibrosis	12, 30, 81, 89, 90, 93, 97, 100, 101, 107, 111, 115
	IP		Systemic reaction Inflammatory cells recruitment Fibrosis	81, 83, 94
	IM		Material/tissue interactions Foreign body reaction Fibrosis	30, 84, 85, 102
	Cage implant		Inflammatory cells recruitment	80, 114, 119, 120
	SC air pouch			82, 116

* Knockout mouse (KO); ** Transgenic mice.

1.5.2 – Models for Skin Regeneration

Although trauma and surgical procedures are the main causes for acute skin lesions, their healing mechanisms are not necessarily similar. Incisional wounds heal by primary intention, following the events described in section 2 [122]. This means that tissue loss is not extensive, inflammatory response is not exuberant and wound contraction is not a concerning issue. In contrast, skin excisions involve a higher tissue removal and thus a secondary intention healing process [123]. Inflammation as well as granulation tissue formation is abundant, resulting in a significant level of wound contraction.

Incisional full thickness wound rat [124-126] and mouse models [47, 127] have been used to evaluate the effect of biomaterials *per se*, or of locally releasing growth factors over healing rates, considering skin breaking strength [128] and bleeding cessation [129] in rat and mice, respectively. By its turn, excisional skin wound models are the most appropriate and the ones that have shown some usefulness [130] when testing biomaterials or tissue engineering constructs aiming to directly participate in the regeneration of the wounded skin. The depth of the wound and consequently the lesion of the skin epidermal or, if deeper, also the dermal component, are characteristic of respectively a partial or a full-thickness excisional acute wound model.

In partial-thickness skin excisions, the *panniculus carnosus*, the muscle beneath epidermis, is left intact and for that reason, this type of injuries heal from the wound bottom to the top. Due to the muscle contractile nature, wound contraction is a major concern in these models. By its turn, full-thickness models imply the ablation of the *panniculus carnosus* and the healing progresses from the uninjured margins of the wound. Thus, the regeneration of full-thickness wounds, contrarily to what is claimed in some works [131-135], is not efficiently supported only with dressing materials. These have proved to be capable of regenerate partial-thickness wound in different models [134, 136]. However, and in addition to the contraction observed with small animals, the adherence of the dressers [136] and the presence of dressing debris [134, 136] might compromise the aimed reepithelialisation by influencing the normal progress of the inflammatory/healing process. Full-thickness wound models are, contrarily to the partial-thickness, mandatory to demonstrate the direct role of materials [37, 124, 125, 127, 133, 134, 137, 138] and/or cells [139-141] over the healing mechanisms, which ultimately rely on the uninjured tissue at the margins of the wound.

When acute inflammatory reaction persists at the wound site, a chronic skin wound [130] with delayed healing [142, 143] develops. A major problem of chronic wounds with associated impaired healing relies on its different etiologies, such as diabetes, immunessupression, deficiencies in blood supply or nourishing, glucocorticoids administration and age [130, 142], which do not represent a localized deficiency. Frequently, the established models mimic delayed

wound healing and not the impaired wound healing observed in the clinical condition of chronic wounds. Therefore these models have been mainly used in order to try to understand the mechanisms underlying impaired healing in mice [144] and rats [145, 146], as the case of diabetes, instead of working as proper chronic wound models for testing skin regeneration systems. Particular characteristics of chronic wounds such as deficient vascularisation can be though mimicked with the porcine split-thickness skin wound model. Even not being a specific model of chronic wound formation, its impaired vascularisation allows to test the potential of modified polymeric structures such as collagen over dermal regeneration and vascularisation [138].

Additionally, rabbit [147] and murine [148] models of decubitus ulcers have been gaining an increased interest [149], especially on gathering further knowledge on the mechanisms of pressure ulcer development and on the assessment of healing mechanisms. Wound contraction and the fast healing rate observed in small animals, such as rodent compel researchers to adjust the rodent models or to substitute small animals by larger animals with skin characteristics closer to humans [150, 151]. The adjustment of the skin healing rate to values comparable to humans may include the administration of steroids to impair the animal wound healing [152]. An alternative approach to try to eliminate or minimise this factor would be to perform comparative studies using different excisional models [153]. In the guinea pig skin excision model, for example, wound contraction is almost absent and a parallel assessment with the classical mouse excisional model would allow the extrapolation of the results for humans. Nevertheless, Cahn and Kyriakides [153] considered that the residual degree of contraction observed in the guinea pig skin excision model significantly influenced the results and that extrapolation is not possible.

A major obstacle for proposing new strategies for improving skin regeneration is the dissimilarity between the human and other species skin [130]. The structural and functional differences are sufficient to quarrel about the relevance of the results obtained with some animal models for skin regeneration. Nonetheless, the resemblances between porcine and human skin, sustain the reliability of porcine models not only for testing skin tissue engineered constructs [138, 154, 155] but also to study therapeutic agents such as growth factors and topical antimicrobials aimed to human use [156].

Table 1.2: Overview of the animal models used to test materials for skin regeneration

Animal	Model		Aims	Assessed parameters	References
Mouse	Incisional		Wound dressing Skin healing	Scarring Inflammation	47, 127, 129
	Excisional	Full-thickness		Reepithelialisation Inflammatory infiltrate Scarring	139
Rat	Incisional			Scarring Inflammation	124-126, 128
	Excisional	Partial-thickness		Reepithelialisation Inflammatory infiltrate Scarring Wound contraction	135
		Full-thickness			37, 137
Pig	Excisional	Partial-thickness	Wound dressing Skin healing	Reepithelialisation Inflammatory infiltrate Scarring Wound contraction	131, 134, 136
		Full-thickness			138, 150, 151
Mouse	Decubitus ulcers		Skin healing and regeneration	Reepithelialisation Inflammatory infiltrate Scarring Wound contraction	148
Rabbit					147

1.5.3 - Models for Bone Tissue Engineering

The continuous developments in the tissue engineering field [157] have also guided the progress of the approaches that have been proposed for bone regeneration [158, 159]. However, the translation from bench to bedside is always a challenge and a delicate issue. In the particular case of bone tissue, its complexity both at the metabolic and functional levels, have somehow compromised further advances [160].

The establishment of valuable animal models capable to mimic, as much as possible, the clinical scenarios of bone lesions is of outmost interest [57, 161]. The metabolic differences observed between human and rodents are the main reason for some authors [57, 162, 163] to consider that rodents as not suitable models to assess bone formation/regeneration [163]. Nevertheless, rats [164, 165] and mice [64, 166, 167] are vastly used models for ectopic bone formation [166, 167] or orthotopic regeneration [164] and biomaterials integration evaluation. Additionally, despite all the controversy and the observed differences in bone macro and microstructure, composition and remodeling [163], Colnot and co-workers [167] showed that mice bones heal similarly to rats, rabbits, dogs, sheep, monkeys and humans, this is with intramembranous bone formation and without the transitional cartilage formation [167]. Orthotopic rabbit models [58, 77, 168] might be used as alternative models to rodents which not only facilitates the surgical handling but also

approximates the tissue features to humans and consequently a more reliable extrapolation of the results to a clinical scenario.

New bone formation is impaired in significant bone loss situations. Therefore, for the assessment of the outcome of a proposed bone tissue engineering approach it is imperative to use critical size bone defect models [160, 161]. Small-animal models have been extensively used to evaluate bone healing and new bone formation [58, 77, 165-167, 169], new bone colonization [164], and implant integration in critical size defects not only in long [64, 168] but also in flat [164, 170] bones.

Bone formation is highly dependent on the applied load [54, 55] and on particular bone healing mechanisms [63]. For this reason, long bones of large animals, in the opinion of many authors [61, 62, 66], are the most adequate to establish bone critical size defect models. However, flat bones critical size defects [58, 170-172], in particular calvaria defects, have been also extensively used. The ease handling, availability and cost effectiveness, especially provided by rodents comparatively to larger animals such as sheep or pig, render these models as suitable alternatives to long bones critical size defects.

Sheep tibia critical size defect models [61, 62, 66, 76, 173-175] have been widely used in order to assess the osteogenic potential of scaffolding materials for bone tissue engineering applications [62, 76, 173-175]. The role of key growth factors on bone tissue regenerations has been addressed in critical size defects of long bones in large animals [73]. Moreover, cell therapies based on the transplantation of mesenchymal stem cells aimed at bone regeneration were also studied using these models [62, 175-177]. A goat iliac crest critical size defect model was created to understand the healing rate of bone grafts donor sites since autografts are still the most used strategy for bone regeneration [178]. The consistency of the results obtained with these and other works [176, 177, 179] justify in a great extent that long bone segmental defects animal models are the pre-clinical gold standard models for bone regeneration [161].

Bone biomechanics also determine the need for maxillofacial bone regeneration models to evaluate the different approaches proposed for the regeneration of those defects. Different models have been providing insights and deeper knowledge on useful strategies for maxillofacial reconstruction. A mini-pig mandibular critical size defect model was used to assess the capacity of autologous tooth deciduous stem cells to sustain new bone formation and regenerate the created defect [180]. Major achievements have also been reached after testing the effect of BMP-7 [181, 182] or human recombinant osteogenic protein-1 (rhOP-1) [183] release *in vivo* in a critical size mandibular sheep defect model. Moreover, and despite all the ethical controversy, a

baboon maxillary critical size defect was used [184] to compare the performance of a demineralised freeze-dried bone allograft and tendonous collagen as bone fillers.

Although mandibular bone belongs to the long bones set, the load-bearing to which it is subjected is very much different from the limb long bones. This justifies the widespread use of mandibular defects in big animals, including baboons, whose maxillofacial bones are anatomically very similar to humans.

Recently a new spinal fusion model was established in both rabbits [169] and rats [165] to assess the osteoconductive behaviour of collagen combined with osteogenic protein-1 (OP-1) [169] and the effect of recombinant bone morphogenic protein-2 [165] over bone healing. These models are giving insights to an emergent clinical situation in which surgeons are obliged to fuse vertebras [185] to correct instability due to infections or tumours resection, spinal deformities, fractures, hernias or to alleviate pain.

Bone healing and regeneration is highly reliant on its biomechanical stimulation and on the load-bearing situation of the affected bone [54, 55]. For these reasons, and despite the numerous works [64, 166, 167] testing new bone formation in ectopic models, it is of outmost importance to corroborate the obtained information in orthotopic models in which the micro-environment actually simulates the clinical sets.

Besides the mandatory development of reliable, reproducible and standardized segmental bone defect models in large animals [161] the rational in the choice of the animal model has to be always in accordance to the target clinical setting.

Table 1.3: Overview of the animal models used to test materials for bone tissue regeneration

Animal	Model		Aims	Assessed parameters	References
Rat	Ectopic	SC	New bone formation	Mineralization of the surrounding tissue	67
		IM			67, 166
	Orthotopic	Flat bone	Bone regeneration	Mineralization of bone/material interface *Callus* formation	74, 171, 172
		Long bone			65, 164
		Spinal fusion			165
		Mandible bone			166
Sheep	Orthotopic				181, 182, 183
		Long bone			61, 62, 66, 76, 173, 174, 175
Rabbit	Orthotopic	Flat bone		Mineralization of bone/material interface *Callus* formation	58, 70
		Spinal fusion			169
		Long bone			69, 75, 164
Babbon					73, 168
		Mandible bone			184
Guinea pig		Flat bone			170
Goat					178
		Long bone			176, 177
Pig					179
		Mandible			180

1.6 Final Remarks

The shape and size of the biomaterial to be tested, as well as its final application, are important features to have into consideration when choosing an animal model. The final intended use and function of the implanted biomaterial is also related with degradability issues. In some cases is

not the biomaterial itself that induces a specific reaction, but rather the degradation products resulting from the concomitant action of the cells in the device. Host reaction models are very useful to evaluate those issues. However, when considering tissue engineering applications the information obtained with these models has a relative relevance. In fact, the incorporation of other elements such as cells and/or growth factors into a scaffolding material completely changes the microenvironment and therefore the obtained response. For this reason and due to the specific anatomical and physiological features of each tissue, significant information that can be extrapolated to humans and to a particular clinical situation has to be obtained with animal models that closely mimic those properties. The confidence in the obtained data also results from a statistically representative approach, not only in the number of samples, but also in the number of tested animals. This is however contrary to the increased discussion regarding the limitation of the number of animals used in research. Alternative models making use of bioluminescence and transgenic animals represent a valuable combination that permits an analysis along the time avoiding the sacrifice of the animals at the intermediate time points. However, the currently available models are still far from ideal and the pursued accuracy with *in vivo* tests rely on choosing a model which allows the most precise answers to the experimental questions, as well as a correct extrapolation to human clinics.

References

1. Mikos, A.G., et al., *Host response to tissue engineered devices.* Adv Drug Deliv Rev, 1998. **33**(1-2): p. 111-139.
2. Hunt, J.A., *Inflammation*, in *Encyclopedia of Materials: Science and Technology*. 2001, Elsevier Science Ltd. p. 4068-4075.
3. Stevens, A., J.S. Lowe, and B. Young, *Wheater's Basic Histopathology: A Colour Atlas and Text*. Fourth Edition ed. 2002, Edinburgh: Churchill Livingstone. 295.
4. Williams, D.F., *Biocompatibility Principles*, in *Encyclopedia of Materials: Science and Technology*. 2001, Elsevier Science Ltd. p. 542-548.
5. Fantone, J. and P. Ward, *Inflammation*, in *Pathology*, E. Rubin and J. Farber, Editors. 1999, Lippincott-Raven.
6. Atkinson, J.P. and T. Farries, *Separation of self from non-self in the complement system* Immunol. Today, 1987. **8**(7-8): p. 212-215

7. Mollnes, T.E., *Biocompatibility: complement as mediator of tissue damage and as indicator of incompatibility.* Exp Clin Immunogenet, 1997. **14**(1): p. 24-9.
8. Gorbet, M.B. and M.V. Sefton, *Biomaterial-associated thrombosis: roles of coagulation factors, complement, platelets and leukocytes.* Biomaterials, 2004. **25**(26): p. 5681-703.
9. Nilsson, B., et al., *The role of complement in biomaterial-induced inflammation.* Mol Immunol, 2007. **44**(1-3): p. 82-94.
10. Bellingan, G.J., et al., *In vivo fate of the inflammatory macrophage during the resolution of inflammation: inflammatory macrophages do not die locally, but emigrate to the draining lymph nodes.* J Immunol, 1996. **157**(6): p. 2577-85.
11. Anderson, J.M., *Multinucleated giant cells.* Curr Opin Hematol, 2000. **7**(1): p. 40-7.
12. Lickorish, D., et al., *An in-vivo model to interrogate the transition from acute to chronic inflammation.* Eur Cell Mater, 2004. **8**: p. 12-9; discussion 20.
13. Goldsby, R.A., T.J. Kindt, and B.A. Osborne, *Kuby Immunology*. 2000, USA: W. H. Freeman and Company.
14. Griffiths, M.M., J.J. Langone, and M.M. Lightfoote, *Biomaterials and Granulomas.* Methods, 1996. **9**(2): p. 295-304.
15. Anderson, J.M., A. Rodriguez, and D.T. Chang, *Foreign body reaction to biomaterials.* Semin Immunol, 2008. **20**(2): p. 86-100.
16. Kasper, C.S. and P.J. Chandler, Jr., *Talc deposition in skin and tissues surrounding silicone gel-containing prosthetic devices.* Arch Dermatol, 1994. **130**(1): p. 48-53.
17. Houpt, K.R. and R.D. Sontheimer, *Autoimmune connective tissue disease and connective tissue disease-like illnesses after silicone gel augmentation mammoplasty.* J Am Acad Dermatol, 1994. **31**(4): p. 626-42.
18. Ossoff, R.H., et al., *Difficulties in endoscopic removal of Teflon granulomas of the vocal fold.* Ann Otol Rhinol Laryngol, 1993. **102**(6): p. 405-12.
19. Mitnick, J.S., et al., *Fine needle aspiration biopsy in patients with augmentation prostheses and a palpable mass.* Ann Plast Surg, 1993. **31**(3): p. 241-4.
20. Hess, J.A., J.A. Molinari, and P.J. Mentag, *Two cases of incompatibility to carbon-coated subperiosteal implants.* Oral Surg Oral Med Oral Pathol, 1982. **54**(5): p. 499-505.
21. Joosten, L.A., M.M. Helsen, and W.B. van den Berg, *Accelerated onset of collagen-induced arthritis by remote inflammation.* Clin Exp Immunol, 1994. **97**(2): p. 204-11.
22. Kaiser, W. and J. Zazgornik, *[Late reactions following implantation of silicone prostheses].* Urologe A, 1991. **30**(5): p. 302-5.

23. Overholt, M.A., J.A. Tschen, and R.L. Font, *Granulomatous reaction to collagen implant: light and electron microscopic observations.* Cutis, 1993. **51**(2): p. 95-8.
24. Wu, C.A., et al., *Responses in vivo to purified poly(3-hydroxybutyrate-co-3-hydroxyvalerate) implanted in a murine tibial defect model.* J Biomed Mater Res A, 2008.
25. Anderson, J.M., *Biological responses to materials.* Annual Review of Materials Research, 2001. **31**: p. 81-110.
26. Wynn, T.A., *Cellular and molecular mechanisms of fibrosis.* J Pathol, 2008. **214**(2): p. 199-210.
27. Martinez-Hernandez, A., *Repair, Regeneration, and Fibrosis*, in *Pathology*, E. Rubin and J. Farber, Editors. 1999, Lippincott-Raven.
28. Tang, L. and J.W. Eaton, *Inflammatory responses to biomaterials.* Am J Clin Pathol, 1995. **103**(4): p. 466-71.
29. Haisch, A., et al., *Creating artificial perichondrium by polymer complex membrane macroencapsulation: immune protection and stabilization of subcutaneously transplanted tissue-engineered cartilage.* Eur Arch Otorhinolaryngol, 2005. **262**(4): p. 338-44.
30. Rhodes, N.P., C.D. Bartolo, and J.A. Hunt, *Analysis of the cellular infiltration of benzyl-esterified hyaluronan sponges implanted in rats.* Biomacromolecules, 2007. **8**(9): p. 2733-8.
31. Harrrist, T., et al., *The Skin*, in *Pathology*, E. Rubin and J. Farber, Editors. 1999, Lippincott-Raven.
32. Martin, P. and S.J. Leibovich, *Inflammatory cells during wound repair: the good, the bad and the ugly.* Trends Cell Biol, 2005. **15**(11): p. 599-607.
33. Eming, S.A., T. Krieg, and J.M. Davidson, *Inflammation in wound repair: molecular and cellular mechanisms.* J Invest Dermatol, 2007. **127**(3): p. 514-25.
34. Paddock, H.N., G.S. Schultz, and B.A. Mast, *Methods in Reepithelialization: A Porcine Model of Partial-Thickness Wounds*, in *Wound Healing: Methods and Protocols*, L.A. DiPietro and A.L. Burns, Editors. 2003, Humana Press Inc.: Totowa, New Jersey. p. 17-36.
35. Theoret, C.L., *The pathophysiology of wound repair.* Vet Clin North Am Equine Pract, 2005. **21**(1): p. 1-13.
36. Stewart, C.J., et al., *Kinetics of blood flow during healing of excisional full-thickness skin wounds in pigs as monitored by laser speckle perfusion imaging.* Skin Research and Technology, 2006. **12**(4): p. 247-253.

37. Noorjahan, S.E. and T.P. Sastry, *An in vivo study of hydrogels based on physiologically clotted fibrin-gelatin composites as wound-dressing materials.* J Biomed Mater Res B Appl Biomater, 2004. **71**(2): p. 305-12.
38. Yang, Z., et al., *D-glucosamine-based supramolecular hydrogels to improve wound healing.* Chem Commun (Camb), 2007(8): p. 843-5.
39. Hantash, B.M., et al., *Adult and fetal wound healing.* Front Biosci, 2008. **13**: p. 51-61.
40. Metcalfe, A.D. and M.W. Ferguson, *Tissue engineering of replacement skin: the crossroads of biomaterials, wound healing, embryonic development, stem cells and regeneration.* J R Soc Interface, 2007. **4**(14): p. 413-37.
41. Whitby, D.J. and M.W. Ferguson, *Immunohistochemical localization of growth factors in fetal wound healing.* Dev Biol, 1991. **147**(1): p. 207-15.
42. Whitby, D.J. and M.W. Ferguson, *The extracellular matrix of lip wounds in fetal, neonatal and adult mice.* Development, 1991. **112**(2): p. 651-68.
43. Mori, R., T.J. Shaw, and P. Martin, *Molecular mechanisms linking wound inflammation and fibrosis: knockdown of osteopontin leads to rapid repair and reduced scarring.* J Exp Med, 2008. **205**(1): p. 43-51.
44. Valls, M.D., B.N. Cronstein, and M.C. Montesinos, *Adenosine receptor agonists for promotion of dermal wound healing.* Biochem Pharmacol, 2009. **77**(7): p. 1117-24.
45. Wagner, W. and M. Wehrmann, *Differential cytokine activity and morphology during wound healing in the neonatal and adult rat skin.* J Cell Mol Med, 2007. **11**(6): p. 1342-51.
46. Steiling, H., et al., *Different types of ROS-scavenging enzymes are expressed during cutaneous wound repair.* Exp Cell Res, 1999. **247**(2): p. 484-94.
47. Repertinger, S.K., et al., *EGFR enhances early healing after cutaneous incisional wounding.* J Invest Dermatol, 2004. **123**(5): p. 982-9.
48. Han, D., et al., *Wound healing activity of gamma-aminobutyric Acid (GABA) in rats.* J Microbiol Biotechnol, 2007. **17**(10): p. 1661-9.
49. Schafer, M. and S. Werner, *Oxidative stress in normal and impaired wound repair.* Pharmacol Res, 2008. **58**(2): p. 165-71.
50. Azad, A.K., et al., *Chitosan membrane as a wound-healing dressing: characterization and clinical application.* J Biomed Mater Res B Appl Biomater, 2004. **69**(2): p. 216-22.
51. Bao, L., et al., *Agar/collagen membrane as skin dressing for wounds.* Biomed Mater, 2008. **3**(4): p. 44108.

52. Rhinelander, F.W., *The normal microcirculation of diaphyseal cortex and its response to fracture.* J Bone Joint Surg Am, 1968. **50**(4): p. 784-800.
53. Junqueira, L.C. and J. Carneiro, *Basic Histology: text & atlas*. 2005, New York: McGraw-Hill.
54. Gurley, A. and S. Roth, *Bone*, in *Histology for Pathologists*, S. Sternberg, Editor. 1992, Raven Press: New York. p. 61-80.
55. Schiller, A. and S. Teitelbaun, *Bones and Joints*, in *Pathology*, E. Rubin and J. Farber, Editors. 1999, Lippincott-Raven.
56. Wheater, P., H. Burkitt, and V. Daniels, *Functional Histology: A Text and Colour Atlas*. 1979, Edinburgh: Churchill Livingstone.
57. Liebschner, M.A., *Biomechanical considerations of animal models used in tissue engineering of bone.* Biomaterials, 2004. **25**(9): p. 1697-714.
58. Schopper, C., et al., *Mineral apposition rates provide significant information on long-term effects in BMP-induced bone regeneration.* Journal of Biomedical Materials Research Part A, 2009. **89A**(3): p. 679-686.
59. Shapiro, F., *Bone development and its relation to fracture repair. The role of mesenchymal osteoblasts and surface osteoblasts.* Eur Cell Mater, 2008. **15**: p. 53-76.
60. Guichet, J.M., et al., *Gradual femoral lengthening with the Albizzia intramedullary nail.* J Bone Joint Surg Am, 2003. **85-A**(5): p. 838-48.
61. Rozen, N., et al., *Transplanted blood-derived endothelial progenitor cells (EPC) enhance bridging of sheep tibia critical size defects.* Bone, 2009. **45**(5): p. 918-24.
62. Niemeyer, P., et al., *Xenogenic transplantation of human mesenchymal stem cells in a critical size defect of the sheep tibia for bone regeneration.* Tissue Eng Part A, 2009.
63. Einhorn, T.A., *The cell and molecular biology of fracture healing.* Clin Orthop Relat Res, 1998(355 Suppl): p. S7-21.
64. Fu, Y.C., et al., *Optimized bone regeneration based on sustained release from three-dimensional fibrous PLGA/HAp composite scaffolds loaded with BMP-2.* Biotechnol Bioeng, 2008. **99**(4): p. 996-1006.
65. Stevenson, S., et al., *The effect of osteogenin (a bone morphogenetic protein) on the formation of bone in orthotopic segmental defects in rats.* J Bone Joint Surg Am, 1994. **76**(11): p. 1676-87.
66. Pluhar, G.E., et al., *A comparison of two biomaterial carriers for osteogenic protein-1 (BMP-7) in an ovine critical defect model.* J Bone Joint Surg Br, 2006. **88**(7): p. 960-6.

67. Forslund, C. and P. Aspenberg, *CDMP-2 induces bone or tendon-like tissue depending on mechanical stimulation.* J Orthop Res, 2002. **20**(6): p. 1170-4.

68. Seeherman, H. and J.M. Wozney, *Delivery of bone morphogenetic proteins for orthopedic tissue regeneration.* Cytokine Growth Factor Rev, 2005. **16**(3): p. 329-45.

69. Beck, L.S., et al., *Combination of bone marrow and TGF-beta1 augment the healing of critical-sized bone defects.* J Pharm Sci, 1998. **87**(11): p. 1379-86.

70. McKinney, L. and J.O. Hollinger, *A bone regeneration study: transforming growth factor-beta 1 and its delivery.* J Craniofac Surg, 1996. **7**(1): p. 36-45.

71. Toung, J.S., et al., *Insulinlike growth factor 1- and 2-augmented collagen gel repair of facial osseous defects.* Arch Otolaryngol Head Neck Surg, 1999. **125**(4): p. 451-5.

72. Murakami, S., et al., *Recombinant human basic fibroblast growth factor (bFGF) stimulates periodontal regeneration in class II furcation defects created in beagle dogs.* J Periodontal Res, 2003. **38**(1): p. 97-103.

73. Radomsky, M.L., et al., *Novel formulation of fibroblast growth factor-2 in a hyaluronan gel accelerates fracture healing in nonhuman primates.* J Orthop Res, 1999. **17**(4): p. 607-14.

74. Lee, Y.M., et al., *The bone regenerative effect of platelet-derived growth factor-BB delivered with a chitosan/tricalcium phosphate sponge carrier.* J Periodontol, 2000. **71**(3): p. 418-24.

75. Nash, T.J., et al., *Effect of platelet-derived growth factor on tibial osteotomies in rabbits.* Bone, 1994. **15**(2): p. 203-8.

76. Sarkar, M.R., et al., *Bone formation in a long bone defect model using a platelet-rich plasma-loaded collagen scaffold.* Biomaterials, 2006. **27**(9): p. 1817-23.

77. Chang, S.H., et al., *Fabrication of pre-determined shape of bone segment with collagen-hydroxyapatite scaffold and autogenous platelet-rich plasma.* Journal of Materials Science-Materials in Medicine, 2009. **20**(1): p. 23-31.

78. Hunt, J.A., P.J. McLaughlin, and B.F. Flanagan, *Techniques to investigate cellular and molecular interactions in the host response to implanted biomaterials.* Biomaterials, 1997. **18**(22): p. 1449-59.

79. Hunt, J.A. and D.F. Williams, *Quantifying the soft tissue response to implanted materials.* Biomaterials, 1995. **16**(3): p. 167-70.

80. Kao, W.J. and D. Lee, *In vivo modulation of host response and macrophage behavior by polymer networks grafted with fibronectin-derived biomimetic oligopeptides: the role of RGD and PHSRN domains.* Biomaterials, 2001. **22**(21): p. 2901-9.

81. Azab, A.K., et al., *Biocompatibility evaluation of crosslinked chitosan hydrogels after subcutaneous and intraperitoneal implantation in the rat.* J Biomed Mater Res A, 2007. **83**(2): p. 414-22.

82. Krause, T.J., F.M. Robertson, and R.S. Greco, *Measurement of intracellular hydrogen peroxide induced by biomaterials implanted in a rodent air pouch.* J Biomed Mater Res, 1993. **27**(1): p. 65-9.

83. Christenson, L., L. Wahlberg, and P. Aebischer, *Mast cells and tissue reaction to intraperitoneally implanted polymer capsules.* J Biomed Mater Res, 1991. **25**(9): p. 1119-31.

84. Mendez, J.A., et al., *Injectable self-curing bioactive acrylic-glass composites charged with specific anti-inflammatory/analgesic agent.* Biomaterials, 2004. **25**(12): p. 2381-92.

85. Meinel, L., et al., *The inflammatory responses to silk films in vitro and in vivo.* Biomaterials, 2005. **26**(2): p. 147-55.

86. Kamath, S., et al., *Surface chemistry influences implant-mediated host tissue responses.* J Biomed Mater Res A, 2008. **86**(3): p. 617-26.

87. Tang, L., T.A. Jennings, and J.W. Eaton, *Mast cells mediate acute inflammatory responses to implanted biomaterials.* Proc Natl Acad Sci U S A, 1998. **95**(15): p. 8841-6.

88. Spargo, B.J., A.S. Rudolph, and F.M. Rollwagen, *Recruitment of tissue resident cells to hydrogel composites: in vivo response to implant materials.* Biomaterials, 1994. **15**(10): p. 853-8.

89. Marques, A.P., R.L. Reis, and J.A. Hunt, *An in vivo study of the host response to starch-based polymers and composites subcutaneously implanted in rats.* Macromol Biosci, 2005. **5**(8): p. 775-85.

90. Kim, M.S., et al., *An in vivo study of the host tissue response to subcutaneous implantation of PLGA- and/or porcine small intestinal submucosa-based scaffolds.* Biomaterials, 2007. **28**(34): p. 5137-43.

91. De Souza, R., et al., *Biocompatibility of injectable chitosan-phospholipid implant systems.* Biomaterials, 2009. **30**(23-24): p. 3818-24.

92. Tomazic-Jezic, V.J., K. Merritt, and T.H. Umbreit, *Significance of the type and the size of biomaterial particles on phagocytosis and tissue distribution.* J Biomed Mater Res, 2001. **55**(4): p. 523-9.

93. van Luyn, M.J., et al., *Repetitive subcutaneous implantation of different types of (biodegradable) biomaterials alters the foreign body reaction.* Biomaterials, 2001. **22**(11): p. 1385-91.

94. Schlosser, M., et al., *Immunogenicity of polymeric implants: long-term antibody response against polyester (Dacron) following the implantation of vascular prostheses into LEW.1A rats.* J Biomed Mater Res, 2002. **61**(3): p. 450-7.

95. DeLustro, F., et al., *Immune responses to allogeneic and xenogeneic implants of collagen and collagen derivatives.* Clin Orthop Relat Res, 1990(260): p. 263-79.

96. Hung, W.S., et al., *Cytotoxicity and immunogenicity of SACCHACHITIN and its mechanism of action on skin wound healing.* J Biomed Mater Res, 2001. **56**(1): p. 93-100.

97. Rodriguez, A., et al., *T cell subset distributions following primary and secondary implantation at subcutaneous biomaterial implant sites.* J Biomed Mater Res A, 2008. **85**(2): p. 556-65.

98. Tang, L. and J.W. Eaton, *Fibrin(ogen) mediates acute inflammatory responses to biomaterials.* J Exp Med, 1993. **178**(6): p. 2147-56.

99. Hickey, T., et al., *In vivo evaluation of a dexamethasone/PLGA microsphere system designed to suppress the inflammatory tissue response to implantable medical devices.* J Biomed Mater Res, 2002. **61**(2): p. 180-7.

100. Hetrick, E.M., et al., *Reduced foreign body response at nitric oxide-releasing subcutaneous implants.* Biomaterials, 2007. **28**(31): p. 4571-80.

101. Khouw, I.M., et al., *Enzyme and cytokine effects on the impaired onset of the murine foreign-body reaction to dermal sheep collagen.* J Biomed Mater Res, 2001. **54**(2): p. 234-40.

102. Ravin, A.G., et al., *Long- and short-term effects of biological hydrogels on capsule microvascular density around implants in rats.* J Biomed Mater Res, 2001. **58**(3): p. 313-8.

103. Anderson, J.M. and K.M. Miller, *Biomaterial biocompatibility and the macrophage.* Biomaterials, 1984. **5**(1): p. 5-10.

104. Kao, W.J., *Evaluation of protein-modulated macrophage behavior on biomaterials: designing biomimetic materials for cellular engineering.* Biomaterials, 1999. **20**(23-24): p. 2213-21.

105. Keselowsky, B.G., et al., *Role of plasma fibronectin in the foreign body response to biomaterials.* Biomaterials, 2007. **28**(25): p. 3626-31.

106. Schmidt, D.R. and W.J. Kao, *The interrelated role of fibronectin and interleukin-1 in biomaterial-modulated macrophage function.* Biomaterials, 2007. **28**(3): p. 371-82.

107. Rhodes, N.P., J.A. Hunt, and D.F. Williams, *Macrophage subpopulation differentiation by stimulation with biomaterials.* J Biomed Mater Res, 1997. **37**(4): p. 481-8.

108. Busuttil, S.J., et al., *A central role for plasminogen in the inflammatory response to biomaterials.* J Thromb Haemost, 2004. **2**(10): p. 1798-805.

109. van Wachem, P.B., et al., *In vivo biocompatibility of carbodiimide-crosslinked collagen matrices: Effects of crosslink density, heparin immobilization, and bFGF loading.* J Biomed Mater Res, 2001. **55**(3): p. 368-78.

110. Vogt, J.C., et al., *A comparison of different nanostructured biomaterials in subcutaneous tissue.* J Mater Sci Mater Med, 2008. **19**(7): p. 2629-36.

111. Romanos, G.E., et al., *Extracellular matrix interactions during the in vivo degradation of collagen membranes in the rat skin: immunohistochemical distribution of collagen types IV, V, and VI.* J Biomed Mater Res, 1995. **29**(9): p. 1121-7.

112. Lozano, F.S., et al., *Systemic inflammatory response induced by dacron graft and modulation by antimicrobial agents: experimental study.* J Surg Res, 2002. **107**(1): p. 7-13.

113. Brodbeck, W.G., et al., *In vivo leukocyte cytokine mRNA responses to biomaterials are dependent on surface chemistry.* J Biomed Mater Res A, 2003. **64**(2): p. 320-9.

114. Schutte, R.J., et al., *In vivo cytokine-associated responses to biomaterials.* Biomaterials, 2009. **30**(2): p. 160-8.

115. Robitaille, R., et al., *Inflammatory response to peritoneal implantation of alginate-poly-L-lysine microcapsules.* Biomaterials, 2005. **26**(19): p. 4119-27.

116. Hooper, K.A., et al., *Characterization of the inflammatory response to biomaterials using a rodent air pouch model.* J Biomed Mater Res, 2000. **50**(3): p. 365-74.

117. Wooley, P.H., et al., *Inflammatory responses to orthopaedic biomaterials in the murine air pouch.* Biomaterials, 2002. **23**(2): p. 517-26.

118. Laschke, M.W., et al., *New experimental approach to study host tissue response to surgical mesh materials in vivo.* J Biomed Mater Res A, 2005. **74**(4): p. 696-704.

119. Brodbeck, W.G., et al., *Biomaterial adherent macrophage apoptosis is increased by hydrophilic and anionic substrates in vivo.* Proc Natl Acad Sci U S A, 2002. **99**(16): p. 10287-92.

120. Marchant, R., et al., *In vivo biocompatibility studies. I. The cage implant system and a biodegradable hydrogel.* J Biomed Mater Res, 1983. **17**(2): p. 301-25.

121. Marchant, R.E., *The cage implant system for determining in vivo biocompatibility of medical device materials.* Fundam Appl Toxicol, 1989. **13**(2): p. 217-27.

122. Gamelli, R.L. and L.-K. He, *Incisional Wound Healing: Model and Analysis of Wound Breaking Strength*, in *Wound Healing: Methods and Protocols*, L.A. DiPietro and A.L. Burns, Editors. 2003, Humana Press Inc.: Totowa, New Jersey. p. 37-54.

123. Frank, S. and H. Kaempfer, *Excisional Wound Healing: An Experimental Approach*, in *Wound Helaing: Methods and Protocols*, L.A. DiPietro and A.L. Burns, Editors. 2003, Humana Press Inc.: Totowa, New Jersey. p. 3-15.

124. Cho, Y.W., et al., *Water-soluble chitin as a wound healing accelerator.* Biomaterials, 1999. **20**(22): p. 2139-45.

125. Hu, M., et al., *Three-dimensional hyaluronic acid grafts promote healing and reduce scar formation in skin incision wounds.* J Biomed Mater Res B Appl Biomater, 2003. **67**(1): p. 586-92.

126. Ono, I., et al., *Local administration of hepatocyte growth factor gene enhances the regeneration of dermis in acute incisional wounds.* Journal of Surgical Research, 2004. **120**(1): p. 47-55.

127. Ishihara, M., et al., *Acceleration of wound contraction and healing with a photocrosslinkable chitosan hydrogel.* Wound Repair Regen, 2001. **9**(6): p. 513-21.

128. Wu, L., et al., *Effects of electrically charged particles in enhancement of rat wound healing.* J Surg Res, 1999. **85**(1): p. 43-50.

129. Ishihara, M., et al., *Photocrosslinkable chitosan as a dressing for wound occlusion and accelerator in healing process.* Biomaterials, 2002. **23**(3): p. 833-40.

130. Davidson, J.M., *Animal models for wound repair.* Arch Dermatol Res, 1998. **290 Suppl**: p. S1-11.

131. Khan, T.A. and K.K. Peh, *A preliminary investigation of chitosan film as dressing for punch biopsy wounds in rats.* J Pharm Pharm Sci, 2003. **6**(1): p. 20-6.

132. Mi, F.L., et al., *Fabrication and characterization of a sponge-like asymmetric chitosan membrane as a wound dressing.* Biomaterials, 2001. **22**(2): p. 165-73.

133. Sugihara, A., et al., *Promotive effects of a silk film on epidermal recovery from full-thickness skin wounds.* Proc Soc Exp Biol Med, 2000. **225**(1): p. 58-64.

134. Suzuki, Y., et al., *In vivo evaluation of a novel alginate dressing.* J Biomed Mater Res, 1999. **48**(4): p. 522-7.

135. Yusof, N.L., et al., *Flexible chitin films as potential wound-dressing materials: wound model studies.* J Biomed Mater Res A, 2003. **66**(2): p. 224-32.

136. Agren, M.S., *Four alginate dressings in the treatment of partial thickness wounds: a comparative experimental study.* Br J Plast Surg, 1996. **49**(2): p. 129-34.

137. Choi, Y.S., et al., *Studies on gelatin-based sponges. Part III: A comparative study of cross-linked gelatin/alginate, gelatin/hyaluronate and chitosan/hyaluronate sponges and their application as a wound dressing in full-thickness skin defect of rat.* J Mater Sci Mater Med, 2001. **12**(1): p. 67-73.

138. Markowicz, M.P., et al., *Enhanced dermal regeneration using modified collagen scaffolds: Experimental porcine study.* International Journal of Artificial Organs, 2006. **29**(12): p. 1167-1173.

139. Altman, A.M., et al., *IFATS collection: Human adipose-derived stem cells seeded on a silk fibroin-chitosan scaffold enhance wound repair in a murine soft tissue injury model.* Stem Cells, 2009. **27**(1): p. 250-8.

140. Inoue, H., et al., *Bioimaging assessment and effect of skin wound healing using bone-marrow-derived mesenchymal stromal cells with the artificial dermis in diabetic rats.* J Biomed Opt, 2008. **13**(6): p. 064036.

141. Markowicz, M., et al., *Human bone marrow mesenchymal stem cells seeded on modified collagen improved dermal regeneration in vivo.* Cell Transplantation, 2006. **15**(8-9): p. 723-732.

142. Menke, N.B., et al., *Impaired wound healing.* Clin Dermatol, 2007. **25**(1): p. 19-25.

143. Schultz, G.S. and A. Wysocki, *Interactions between extracellular matrix and growth factors in wound healing.* Wound Repair Regen, 2009. **17**(2): p. 153-62.

144. Brown, D.L., W.W. Kao, and D.G. Greenhalgh, *Apoptosis down-regulates inflammation under the advancing epithelial wound edge: delayed patterns in diabetes and improvement with topical growth factors.* Surgery, 1997. **121**(4): p. 372-80.

145. Komesu, M.C., et al., *Effects of acute diabetes on rat cutaneous wound healing.* Pathophysiology, 2004. **11**(2): p. 63-67.

146. Chen, C., et al., *Molecular and mechanistic validation of delayed healing rat wounds as a model for human chronic wounds.* Wound Repair Regen, 1999. **7**(6): p. 486-94.

147. Niitsuma, J., H. Yano, and T. Togawa, *Experimental study of decubitus ulcer formation in the rabbit ear lobe.* J Rehabil Res Dev, 2003. **40**(1): p. 67-73.

148. Wassermann, E., et al., *A chronic pressure ulcer model in the nude mouse.* Wound Repair Regen, 2009. **17**(4): p. 480-4.

149. Salcido, R., A. Popescu, and C. Ahn, *Animal models in pressure ulcer research.* J Spinal Cord Med, 2007. **30**(2): p. 107-16.

150. Ma, L., et al., *In vitro and in vivo biological performance of collagen-chitosan/silicone membrane bilayer dermal equivalent.* J Mater Sci Mater Med, 2007. **18**(11): p. 2185-91.

151. Middelkoop, E., et al., *Porcine wound models for skin substitution and burn treatment.* Biomaterials, 2004. **25**(9): p. 1559-1567.

152. Saulis, A. and T.A. Mustoe, *Models of wound healing in growth factor studies*, in *Surgery Research*, W.W. Souba and D.W. Wilmore, Editors. 2001, Academic Press. p. 857-874.

153. Cahn, F. and T.R. Kyriakides, *Generation of an artificial skin construct containing a non-degradable fiber mesh: a potential transcutaneous interface.* Biomed Mater, 2008. **3**(3): p. 034110.

154. Maas, C.S., et al., *Evaluation of expanded polytetrafluoroethylene as a soft-tissue filling substance: an analysis of design-related implant behavior using the porcine skin model.* Plast Reconstr Surg, 1998. **101**(5): p. 1307-14.

155. Okabayashi, R., et al., *Efficacy of polarized hydroxyapatite and silk fibroin composite dressing gel on epidermal recovery from full-thickness skin wounds.* J Biomed Mater Res B Appl Biomater, 2009. **90**(2): p. 641-6.

156. Sullivan, T.P., et al., *The pig as a model for human wound healing.* Wound Repair Regen, 2001. **9**(2): p. 66-76.

157. Yarlagadda, P.K., M. Chandrasekharan, and J.Y. Shyan, *Recent advances and current developments in tissue scaffolding.* Biomed Mater Eng, 2005. **15**(3): p. 159-77.

158. Mistry, A.S. and A.G. Mikos, *Tissue engineering strategies for bone regeneration.* Adv Biochem Eng Biotechnol, 2005. **94**: p. 1-22.

159. Stylios, G., T. Wan, and P. Giannoudis, *Present status and future potential of enhancing bone healing using nanotechnology.* Injury, 2007. **38 Suppl 1**: p. S63-74.

160. Cancedda, R., P. Giannoni, and M. Mastrogiacomo, *A tissue engineering approach to bone repair in large animal models and in clinical practice.* Biomaterials, 2007. **28**(29): p. 4240-50.

161. Reichert, J.C., et al., *The challenge of establishing preclinical models for segmental bone defect research.* Biomaterials, 2009. **30**(12): p. 2149-63.

162. Egermann, M., J. Goldhahn, and E. Schneider, *Animal models for fracture treatment in osteoporosis.* Osteoporos Int, 2005. **16 Suppl 2**: p. S129-38.

163. Pearce, A.I., et al., *Animal models for implant biomaterial research in bone: a review.* Eur Cell Mater, 2007. **13**: p. 1-10.

164. Le Guehennec, L., et al., *Small-animal models for testing macroporous ceramic bone substitutes.* J Biomed Mater Res B Appl Biomater, 2005. **72**(1): p. 69-78.

165. Alanay, A., et al., *The adjunctive effect of a binding peptide on bone morphogenetic protein enhanced bone healing in a rodent model of spinal fusion.* Spine (Phila Pa 1976), 2008. **33**(16): p. 1709-13.

166. Lattanzi, W., et al., *Ex vivo-transduced autologous skin fibroblasts expressing human Lim mineralization protein-3 efficiently form new bone in animal models.* Gene Ther, 2008. **15**(19): p. 1330-43.

167. Colnot, C., et al., *Molecular analysis of healing at a bone-implant interface.* Journal of Dental Research, 2007. **86**(9): p. 862-867.

168. Ronold, H.J. and J.E. Ellingsen, *The use of a coin shaped implant for direct in situ measurement of attachment strength for osseointegrating biomaterial surfaces.* Biomaterials, 2002. **23**(10): p. 2201-2209.

169. Qian, Y., et al., *Natural Bone Collagen Scaffold Combined with OP-1 for Bone Formation Induction In Vivo.* Journal of Biomedical Materials Research Part B-Applied Biomaterials, 2009. **90B**(2): p. 778-788.

170. Taga, M.L., et al., *Healing of critical-size cranial defects in guinea pigs using a bovine bone-derived resorbable membrane.* Int J Oral Maxillofac Implants, 2008. **23**(3): p. 427-36.

171. Fowler, E.B., et al., *Evaluation of pluronic polyols as carriers for grafting materials: study in rat calvaria defects.* J Periodontol, 2002. **73**(2): p. 191-7.

172. Park, S.S., et al., *Osteogenic activity of the mixture of chitosan and particulate dentin.* J Biomed Mater Res A, 2008. **87**(3): p. 618-23.

173. Gugala, Z. and S. Gogolewski, *Regeneration of segmental diaphyseal defects in sheep tibiae using resorbable polymeric membranes: a preliminary study.* J Orthop Trauma, 1999. **13**(3): p. 187-95.

174. Viateau, V., et al., *A technique for creating critical-size defects in the metatarsus of sheep for use in investigation of healing of long-bone defects.* Am J Vet Res, 2004. **65**(12): p. 1653-7.

175. Viateau, V., et al., *Long-bone critical-size defects treated with tissue-engineered grafts: a study on sheep.* J Orthop Res, 2007. **25**(6): p. 741-9.

176. Liu, G., et al., *Repair of goat tibial defects with bone marrow stromal cells and beta-tricalcium phosphate.* J Mater Sci Mater Med, 2008. **19**(6): p. 2367-76.

177. Zhu, L., et al., *Tissue-engineered bone repair of goat-femur defects with osteogenically induced bone marrow stromal cells.* Tissue Eng, 2006. **12**(3): p. 423-33.

178. Krijnen, M.R., et al., *PLDLA mesh and 60/40 biphasic calcium phosphate in iliac crest regeneration in the goat.* J Biomed Mater Res B Appl Biomater, 2009. **89**(1): p. 9-17.

179. Jian, Y.K., et al., *Properties of deproteinized bone for reparation of big segmental defect in long bone.* Chin J Traumatol, 2008. **11**(3): p. 152-6.

180. Zheng, Y., et al., *Stem cells from deciduous tooth repair mandibular defect in swine.* J Dent Res, 2009. **88**(3): p. 249-54.

181. Ayoub, A., et al., *Use of a composite pedicled muscle flap and rhBMP-7 for mandibular reconstruction.* Int J Oral Maxillofac Surg, 2007. **36**(12): p. 1183-92.

182. Kontaxis, A., et al., *Mechanical testing of recombinant human bone morphogenetic protein-7 regenerated bone in sheep mandibles.* Proc Inst Mech Eng H, 2004. **218**(6): p. 381-8.

183. Abu-Serriah, M., et al., *The role of ultrasound in monitoring reconstruction of mandibular continuity defects using osteogenic protein-1 (rhOP-1).* Int J Oral Maxillofac Surg, 2003. **32**(6): p. 619-27.

184. Kohles, S.S., et al., *A morphometric evaluation of allograft matrix combinations in the treatment of osseous defects in a baboon model.* Calcif Tissue Int, 2000. **67**(2): p. 156-62.

185. Sandhu, H.S. and S.N. Khan, *Recombinant human bone morphogenetic protein-2: use in spinal fusion applications.* J Bone Joint Surg Am, 2003. **85-A Suppl 3**: p. 89-95.

Chapter II
Materials and Methods

2.1 Experimental approach and research rationalization

The research work presented in this thesis was developed with the purpose of gaining further understanding on the host reaction to the implantation of natural-based biomaterials aimed for skin wound healing and bone regeneration, making use of different animal models. The specific aims included:

- Investigate the effect of chitosan-based membranes over the activation of human inflammatory cells.
- Understand the influence of chitosan in the host reaction elicited by soy-based biomaterials.
- Assess the suitability of newly developed chitosan/soy-based membranes as wound dressing material.
- Compare the inflammatory response induced by the implantation of starch-based scaffolds in two rat implantation models, subcutaneous and intramuscular.
- Evaluate the host reaction elicited by different starch-based tissue engineering constructs aimed for bone tissue engineering.

The work was divided in two major sections having in consideration the experimental approach/methodology. The first section studied the *in vitro* response of human specific inflammatory cells in direct contact with different types of chitosan-based membranes (Chapter III). The second part of the research work intended to address key issues regarding *in vivo* inflammatory host reaction and material's performance when implanted in different animal models, specifically: i) elicited inflammation provoked by chitosan- and soy-based materials (Chapter IV); ii) evaluation of the suitability of chitosan/soy-based membranes as wound dressing materials (Chapter V); iii) assessment of different host reaction to starch-based materials, depending on the site of implantation (Chapter VI); and iv) inflammatory reaction induced by starch-based Tissue Engineering (TE) constructs (Chapter VII).

2.2 Materials

2.2.1 Reagents

Reagent grade chitosan (Cht) with a deacetylation degree of 85% was obtained from Sigma, USA, Soy protein isolate from Loders Crocklaan BV, The Netherlands, and tetraethyl orthosilicate (TEOS) from Aldrich, USA.

2.2.2 - Soybean protein isolate (SI-P) and chitosan (Cht-P) powders

Soybean protein biomaterials have demonstrated quite interesting properties for bone regeneration purposes [1-5], nonetheless few studies [6-8] have in fact investigated its suitability within the field. It was demonstrated [9] that soybean-based biomaterials promote osteoblast-like cells' differentiation *in vitro* without inducing activation of human macrophages [9]. However, additional studies are required to further elucidate the potential of these materials in the biomedical field.

In contrast to soybean protein, chitosan has been extensively proposed in the biomedical arena for bone-[10-14], cartilage-[11, 15, 16] and skin-related [11, 17, 18] applications. The promotion of osteoblast proliferation and activity characterized by an up-regulated expression of bone-related proteins and mineral rich matrix deposition, directed by chitosan-based structures, has been well demonstrated [13, 14]. Concerning cartilage-related applications, the structural similarity of chitosan with various glycosaminoglycans (GAGs) found in articular cartilage has burst the investigations. Besides playing a role in modulating chondrocyte morphology, differentiation and function [16], chitosan was shown to act on the growth of epiphyseal cartilage and wound healing of articular cartilage [15]. The successful role of chitosan in the skin wound healing mechanisms has been successively confirmed [17-19]. Although it was observed that chitosan does not directly accelerate extracellular matrix (ECM) production by fibroblast-like cells [20], it was proven that chitosan-based materials have the capacity to promote the production of growth factors, such as transforming growth factors (TGF)-β1 and platelet-derived growth factor (PDGF) by macrophages [19] which, in turn, induce and/or enhance ECM production [18, 19]. Moreover, these materials accelerate the infiltration of polymorphonuclear neutrophils (PMNs) at the early stage of wound healing that is followed by the production of collagen by fibroblasts [17].

Despite all the promising results in the use of chitosan for the biomedical field, studies from different groups [19, 21, 22] have shown controversial results after implanting chitosan-based materials. An adverse inflammatory response showing extensive macrophage activation after

subcutaneous implantation of, either lyophilized chitosan [19] or collagen-chitosan-hydroxyapatite hydrogels in rats [21] was detected. Conversely, other authors showed that chitosan hydrogels induce mild acute and chronic inflammatory responses, identical to the typical wound healing cascade, after subcutaneous [23] and intraperitoneal implantations in rats [22].

Nevertheless the significance of chitosan within the biomedical field is unquestionable since the observed differences on the response of cells and tissues to the different chitosan-based materials may be attributed or influenced by the source of the raw material or by the shape of the biomaterial. Chitosan has also been one of the most used materials to improve the biological performance of other materials such as metals [24-27] and other biodegradable polymers [7, 14, 28]. Recent studies demonstrated that neonatal rat calvaria osteoblasts proliferate at higher rates on titanium surfaces coated with chitosan [24], which also promote better adhesion of osteoblast-like cells [25]. In the same way, the hydrophobic surface of poly(L-lactide) (PLLA) matrices coated with chitosan displayed a different wetability and enhanced cell affinity [26]. In a rabbit tibia defect model [27] it was showed that the coating of titanium pins with chitosan induced minimal inflammatory response and a typical healing sequence of fibrous woven bone formation followed by the development of lamellar bone. This is indicative for the role of the chitosan-coatings in the osseointegration of orthopaedic implants [27]. When blended with synthetic polymers, such as polycaprolactone [14] or poly(butylene succinate) [28], chitosan have shown to exert a synergistic effect of on the blend. While the synthetic polyester promoted the adhesion of osteoblast-like cells, the presence of chitosan significantly enhanced their osteoblastic activity [14, 28]. Chitosan-soy based membranes have also demonstrated improved *in vitro* biological performance in comparison to unblended soy-based materials [7]. Additionally, *in vitro* analysis of the potential of chitosan/soy-based membranes to stimulate immune system cells showed that they did not elicit the activation of human polymorphonuclear neutrophils freshly isolated from circulating blood [29]. Despite the *in vitro* promising results, *in vivo* validation of the improved biological behaviour of the soy-based materials after blended with chitosan is needed, since the organism includes a very complex immune system.

Soybean protein isolate and chitosan powders were used as received.

2.2.3 - Preparation of the Chitosan/Soy (Cht/Soy)-based and Soybean Isolate (SI) membranes

Chitosan-soy based membranes have also demonstrated improved *in vitro* biological performance in comparison to unblended soy-based materials [7]. These new systems combine

the blending of natural polymers, such as chitosan and soy [7, 30], in order to develop hybrid materials for tissue engineering and regenerative medicine.

Chitosan (Cht) and chitosan/soy protein (Cht/Soy) blended membranes were prepared by means of solvent casting, as previously reported [7]. By its turn, the chitosan-soy protein hybrid membranes (Cht/Soy-TEOS) were produced by means of a combination of a sol-gel method and solvent casting [31]. Firstly, a 4 wt% chitosan solution was prepared by dissolving chitosan in 0.2 M acetic acid solution. Secondly, a 1 wt% soy suspension (water/glycerol (10 % w/v)) was also prepared and the pH adjusted to 8.0 ± 0.3 with 1 M sodium hydroxide solution. Then, the dispersion was heated in a water bath at 50ºC for 30 min. The blend was prepared by means of mixing the solutions (75/25 wt% chitosan-soy protein) under constant agitation for the period of 1 hour. Finally, the cross-linking agent TEOS and 0.5 M chloridric acid (HCl) solution in the molar ratio (TEOS:HCl) of 1:0.1 wt% were added to the blend, under constant stirring for 24 hours. Finally, the sol-gel was poured into a Petri dish and allowed to dry at room temperature for several days, followed by neutralisation using a 0.1 M sodium hydroxide solution, as described elsewhere [31].

The Soybean Isolate (SI) membranes were prepared by solvent casting, according to a previously reported procedure [30]. Briefly, SI was suspended in distilled water (10%w/v) at room temperature under gentle stirring in order to avoid protein denaturation and consequently, foam formation. Glycerol was added to this suspension (1g per 5g of SI), which was then poured into moulds, directly in the drying place. The moulds were not moved until complete drying in order to assure that the insoluble part of SI was uniformly distributed. Drying was performed at room temperature and relative humidity. Alternatively, denaturated SI (dSI) membranes were prepared by heating the referred SI suspensions at 100ºC during 2h. After denaturation, the obtained viscous solution was casted as described above.

2.2.4 - Preparation of the Starch-based (SPCL) scaffolds

Natural-origin biomaterials have been considered for many years as a way to improve, in comparison to synthetic polymers, in vivo biofunctionality and to modulate/avoid a harmful host response due to its similarities with biological molecules. Starch-based scaffolds, processed using several methodologies aiming at different TE applications [32-39], have been demonstrating a great potential in the field. Very promising results for bone tissue regeneration have been particularly obtained with a blend of starch and poly-caprolactone (SPCL) [33-36, 38, 40-43]. SPCL scaffolds, with adequate physicochemical and mechanical properties for bone TE [32, 35] and adequate degradability rate [37, 38, 44], have shown support mesenchymal stem

cells growth and differentiation [32, 33] and to be excellent supporting structures for endothelial cells [35, 36, 45, 46]. Consequently, a lacuna is still present concerning the *in vivo* reaction to SPCL-based scaffolds.

Starch-based scaffolds were produced from a blend of Starch with ε-Polycaprolactone (30:70%) (SPCL), by two different methodologies described elsewhere: wet spinning (SPCL-WS) [39] and fibre-bonding (SPCL-FB) [35]. Briefly, for the production of SPCL-WS scaffolds, the polymer was dissolved in chloroform at a concentration of 40% (w/v) in order to obtain a polymer solution with proper viscosity. The polymer solution was loaded into a syringe, placed in a syringe pump (World Precision Instruments, UK) and a certain amount of polymer solution was subsequently extruded into a methanol coagulation solution. The fibre mesh structure was formed during the processing by the random movement of the precipitation container. The formed scaffolds were then dried overnight at room temperature to allow any remaining solvents to evaporate. For the fabrication of the SPCL-FB scaffolds, fibre-meshes previously obtained by a meltspinning methodology were placed in a glass mould and heated in an oven at 150ºC. Immediately after removing the moulds from the oven, the fibres were slightly compressed by a Teflon cylinder and then cooled at −15ºC. All samples were cut into discs of 5mm diameter and approximately 1mm thickness.

All samples were sterilized by ethylene oxide, at 45ºC with a moisture level of 50%, in a cycle time of 14h and within a chamber pressure of 50 kPa [47].

2.3. *In Vitro* methodologies

2.3.1 Reagents

Dextran, Histopaque 1077, phosphate buffer saline (PBS) with and without Ca^{2+} and Mg^{2+}, *Micrococcus lysodeikticus*, phorbol 12-myristate 13-acetate (PMA), lucigenin and luminal were obtained from Sigma, St. Louis, USA. Formyl-methionyl-leucyl-phenylalanine (fMLP) was purchased from Fluka, St. Louis, USA. Lipofectamine™2000 was obtained from Invitrogen, UK, Ham's F-12 cell culture medium was purchased to Sigma-Aldrich, Germany, and the two-component FS Tisseel VH was a kindly offer from Baxter AG, Vienna, Austria.

2.3.2 Cells and Growth factors

2.3.2.1 PMNs

Inflammation triggers the influx of circulating inflammatory cells to the injury site, in a first phase, PMNs. Within 24 hours, macrophages also begin to migrate to the site of injury and two or three days following the beginning of the inflammatory process, lymphocytes begin to enter the

damaged area. Together with this influx, other inflammatory cells, such as mast cells and eosinophils will orchestrate the ongoing of the inflammatory response to the implanted device.

It is well known that PMNs are crucial early in the development of an inflammatory response [48-50]. Neutrophils also have the capacity to dictate the progression of the host immune system reaction by their capacity to produce cytokines, such as interleukins -12 and -10 (IL-12 and IL-10) among others [50-52]. PMNs have a high capacity to act as phagocytes of foreign bodies, nevertheless, the great majority of biomaterials comprises a range of dimensions incompatible with phagocytosis, leading PMNs to "frustrated phagocytosis" [53], resulting in the release of hydrolytic enzymes [54, 55], known as an oxygen-independent mechanism [56]. Lysozyme, present in both primary and secondary granules of PMNs, is one of the most important enzymes released during the inflammatory response [54, 55]. The importance of its role in the foreign body reaction to biodegradable biomaterials is further supported by its capacity to degrade polymers such as chitosan [57].

Another defence approach that is potentially deleterious for the implanted device occurs simultaneously to degranulation and is commonly designated as respiratory burst. This PMNs oxygen-dependent mechanism of defence, involve the consumption of oxygen (O_2) by the activation of the Nicotinamide Adenine Dinucleotide Phosphate (NADPH) oxidase system, leading to the production of oxygen radicals and their reaction products - Reactive Oxygen Species (ROS) which are known to induce tissue destruction [56].

Human polymorphonuclear neutrophils (PMN) were isolated from heparinized fresh peripheral blood. Each 10 ml of heparinized blood was placed in 10 ml of Dextran (6% solution in PBS without Ca^{2+} and Mg^{2+}). After 20 minutes the top layer was removed with a glass pipette and about 6 ml were carefully added to 4 ml of Histopaque 1077 (Sigma, St. Louis, USA). After a 25 minutes centrifugation at 21ºC and 2400rpm, the cloudy layer was firstly removed and then the others, keeping the bottom red pellet to resuspend it with 5 ml of PBS without Ca^{2+} and Mg^{2+}. The tube was filled up with PBS (about 12 ml). A centrifugation for 25 minutes at 21ºC and 2400rpm was performed and the supernatant was removed. One ml of distilled water was added, triturated 3 times with the glass pipette and shacked gently for 35 seconds, in order to lyse erythrocytes. The tube was quickly filled up with PBS without Ca^{2+} and Mg^{2+}. The cells were washed by centrifugation, for 25 minutes at 21ºC and 2400rpm, the supernatant was removed as well as the top red pellet, very carefully, without touching the white pellet in the bottom. The tube was filled up again with PBS without Ca^{2+} and Mg^{2+} and centrifuged for 25 minutes at 21ºC and 2400rpm. The supernatant was removed and the volume needed of PBS without Ca^{2+} and Mg^{2+} was added

to count the number of cells after resuspension. The cell suspension was kept at 4ºC until perform the assays, within a maximum of 2 hours.

The cell suspensions used were of $1.3X10^6$ cells/ml for the ROS assay and 100 µl of cell suspension per well, and $5X10^5$ cells/ml and 1.0 ml of cell suspension per well for the Lysozyme assay.

2.3.2.2 Adipose Derived Stem Cells (ASCs)

Adipose tissue-derived stem cells have been proved to differentiate into osteogenic lineage [58]. Additionally, they are able to adhere and proliferate when seeded on 3D natural-based structures [59]. These features made them optimal candidates to use in a starch-based construct aimed for bone TE.

2.3.2.3 - Transfection of the ASCs

It was previously reported [60] that human adipose tissue derived stem cells (ASCs) were successfully transfected with two different protocols. The relatively easy protocol to follow permitted that the cells remain viable and with a normal proliferation rate [60]. Additionally, after injected in the backs of mice it was possible to track their dislocation within the animal, with the course of time [60].

In other to trace the human Adipose-derived Stem Cells (hASCs) after implantation in TE assembled constructs, cells were prior transfected with a luciferase plasmid using Lipofectamine™2000. Cell transfection was carried out according to the manufacturer's recommendations. Briefly, luciferase DNA (plasmid) and lipofectamine was separately diluted in 50µl of Ham's F-12 cell culture medium, without foetal calf serum (FCS), complemented with 1% L-Glutamin and antibiotics, and gently mixed. The two solutions were mixed and incubated for 20 minutes at room temperature in order to allow the formation of "lipo-complexes". After the incubation period, the mixture was added to the cells in culture and left for 4 hours, after which the medium was changed to fresh cell culture medium. The cells were ready to be used approximately 20 hours after the transfection procedure.

2.3.3 - In vitro *detection of human leukocytes activation*

2.3.3.1 – Lysozyme quantification

Lysozyme, present in both primary and secondary granules of PMNs, is one of the most important enzymes released during the inflammatory response [54, 55]. The importance of its role in the foreign body reaction to biodegradable biomaterials is further supported by its capacity to degrade polymers such as chitosan [57].

A bacterial (*Micrococcus lysodeikticus*) suspension of 1.5 mg/ml was prepared. The isolated PMN were resuspended in PBS with Ca^{2+} and Mg^{2+} (to promote cell attachment) at a final concentration of $5X10^5$ cells/ml. Each sample material was incubated with 1ml of the previous cell suspension (in PBS with Ca^{2+} and Mg^{2+}), for the three pre-determined time periods of reaction (30 min., 1 and 2 hours), at 37ºC and in an humid atmosphere with 5% CO_2 and non-adherent 24-well plates. Three samples with the cell suspension alone were incubated for the same periods of reaction, acting as negative controls.

After each incubation period, 0.5 ml of the supernatant were transferred to new wells and 0.5 ml/well of the bacterial suspension previously prepared was added. The new wells with the lysozyme of the PMN (released when in contact with the materials) and the bacterial suspension were incubated for 30 min., at 37ºC and in a humid atmosphere with 5% CO_2. After incubation, the optical density (OD) was recorded at 541nm. After the absorbance reading of the samples, controls and the standards, the lysozyme secreted form the PMN after the contact with the materials, was quantified normalizing the OD values to a calibration curve of known concentrations of lysozyme.

2.3.3.2 – Reactive Oxygen Species Quantification

Another defence approach that is potentially deleterious for the implanted device occurs simultaneously to degranulation and is commonly designated as respiratory burst. This PMNs oxygen-dependent mechanism of defence, involve the consumption of oxygen (O_2) by the activation of the Nicotinamide Adenine Dinucleotide Phosphate (NADPH) oxidase system, leading to the production of oxygen radicals and their reaction products - Reactive Oxygen Species (ROS) - which are known to induce tissue destruction [56].

For the quantification of lysozyme, the considered incubation periods were of 30 minutes, 1 and 2 hours. For the reactive oxygen species detection a kinetic study were performed from the time point zero to a maximum of 2 hours, without previous incubation.

The isolated PMN were resuspended in PBS with Ca^{2+} and Mg^{2+} at a final concentration of $1.3X10^6$ cells/ml. A mixture of cells (100 µl), with or without cell stimulants (phorbol 12-myristate 13-acetate (PMA), 8 µg/ml in PBS or formyl-methionyl-leucyl-phenylalanine (fMLP), 10 µg/ml in PBS (100 l each), with luminol 1.5 Mm in PBS and lucigenin, 5.4X10-5 M in PBS (100 µl each), and with or without materials were made in the wells of a white opaque 96-well plate. In this step, the cells, the reagents and the plate were kept on ice. The chemiluminescence was read in a microplate reader (Sinergy HT, BioTech). The results were obtained in terms of number of counts per time period.

2.4 Assembling of the TE constructs

The challenges of bone TE rely not only on finding the ideal material to stimulate bone new formation, but also on finding the appropriate cells able to differentiate and induce bone regeneration. Moreover, the addition of key growth factors, such as the ones able to enhance vascularisation, is useful to assemble a reliable construct for bone TE. For these reasons, the study of the assembled was mandatory.

For the cell tracking experiments the two types of SPCL scaffolds were seeded with the transfected hASCs in a concentration of $1.33x10^4$ cells/scaffold in cell culture medium supplemented with 10% FCS and 1% antibiotics (penicillin/streptomycin), and incubated for 24 hours at 37ºC and 5% CO_2 in a humidified environment.

The assembling of the TE constructs to implant in the Vascular Endothelial Growth Factor Receptor-2 (VEGF-R2) transgenic mice was performed as follows: each type of SPCL scaffold was mixed with the 2.0mL two-component FS Tisseel VH, growth factors (VEGF and FGF-2), and hASCs. The sealer protein component (Fibrinogen 75–115mg/ml) was reconstituted with a fibrinolysis inhibitor solution (Aprotinin 3,000 KIU/ml) and spiked either with VEGF (200 ng/ml) or FGF-2 (200 ng/ml). The thrombin component (500 IU/ml) was reconstituted with $CaCl_2$ (40-mmol/ml) and diluted to 4 IU/ml [61]. Scaffolds, cells ($1.5x10^4$ cells/scaffold/50µl) and growth factors, which were added to the fibrinogen component, were then mixed with the thrombin component (1:1), in a total volume of 75µl, at 37ºC. The clot was allowed to form for 15 minutes, at 37ºC and 5% CO_2 after which 300µl of cell culture medium was added. Constructs were kept overnight at 37ºC and 5% CO_2.

2.5 Animal Models

This research work involved the use of different animal models for the evaluation of the host reaction elicited by the implantation of several natural-based biomaterials, as well as related assembled TE constructs. Hence, the used animal models depended on the final intended use of the developed materials and on the material shape. Additionally, different implantation site were considered to compare the host response to the biomaterials. Moreover, as the TE constructs were assembled, specific transgenic mice models were used to address the constructs behaviour considering inflammation and vascularisation.

All animal experiments were performed according to the standard operating procedures required from the national authorities and after their respective approval.

2.5.1 - Reagents

Phosphate buffer saline (PBS) was obtained from Sigma-Aldrich, USA, pentobarbital from CEVA Santé Animale, France, ketamine hydrochloride was purchased to Schoeller Chemie Produkte, Vienna, Austria, xylazine hydrochloride to Bayer AG, Leverkussen, Germany and methylprednisolone acetate was obtained from Depo-Medrol®, Pfizer. Monoclonal mouse anti-human CD3 antibody was purchased to Dako, Denmark, monoclonal mouse anti-rat CD18 antibody to Serotec, UK and monoclonal mouse anti-human phosphoinositide 3-Kinase (Pi3K) antibody obtained from BD, Belgium.

2.5.2 - Animals

Wistar Han rats were purchased to Charles River, Spain, Sprague-Dawley rats were obtained from the Himberg breeding institute, Austria, Balb/c nu/nu *nude* mice were purchased to Harlan Laboratories, Germany and FVB/N-Tg(VEGF-r2–luc)Xen mice obtained from in house breeding.

2.5.3 - Rat Intraperitoneal injection model

Intraperitoneal injection models allow the injection of powder suspensions. Besides, these types of models are suitable to evaluate the recruitment of inflammatory cells in response to the implanted materials, since the recovery of the cell exudate is very easy.

Phosphate buffer saline (PBS - 0.01M) suspensions of the powders with different concentrations (0.1% and 1% SI; and 0.1%, 1% and 2% chitosan) were injected into the intraperitoneal (IP) cavity of the rats (1 mL per animal). Three animals per concentration and per time period (16 hours, 3 days, 7 days and 15 days) were used. One animal per each concentration and per time period was injected with sterile PBS as control. The animals had access to food and water *ad libitum* during the entire observation period.

2.5.4 – Rat Subcutaneous implantation model

The subcutaneous implantation reveals appropriate for the implantation of compact or scaffold materials. The main objective for using this model is to achieve information on the host reaction after the implantation of the material or TE construct. Thus, it is possible to evaluate the adherent and infiltrating cells into the materials, as wells as the reaction of the surrounding tissue to the implanted material.

5.4.1 Subcutaneous implantation of the SI membranes

For the implantation of the SI-M and the dSI-M, the Wistar Han rats were anaesthetized by an intraperitoneal injection of 2.5% pentobarbital. The interscapular region was shaved and disinfected with 70% ethanol, a full thickness skin longitudinal incision (about 1.5 cm) was performed in each animal and one cranial oriented subcutaneous pocket was created by blunt

dissection. A membrane (12 mm diameter) was positioned into each pocket and the incision was carefully sutured. Three animals were used per each time period of implantation (3, 7, 15 and 30 days), and per type of membrane. For each time period of implantation a control animal, with an empty subcutaneous pocket, was set. The animals were kept in single cages with food and water *ad libitum* during all experimentation time.

2.5.4.2 Subcutaneous implantation of the chit/soy membranes

Four male Sprague-Dawley rats (2 for 1 week and 2 for 2 weeks of implantation) were anesthetized prior to surgery by intramuscular injection of 90 mg/kg ketamine hydrochloride and 5 mg/kg xylazine hydrochloride. For the subcutaneous implantation of the Cht/Soy-M, 2 medial full thickness skin incisions were performed on the dorsum of the rats. Two craniolateral oriented pockets per each incision one to the left and one to the right were subcutaneously created by blunt dissection, and the membranes were inserted into these pockets (4 membranes/animal). The animals were kept in single cages with food and water *ad libitum* during all experimentation time.

2.5.4.3 Subcutaneous implantation of the starch-based scaffolds

Six male Sprague-Dawley rats weighting between 350g and 380g (3 for each implantation time of 1 and 2 weeks), were used. Each test animal was anaesthetized with an intramuscular injection of 90 mg/Kg ketamine hydrochloride and 5 mg/Kg xylazine hydrochloride and 2 medial and ventral incisions of approximately 2 cm containing the subcutis and the *Panniculus Carnosus* were performed in the dorsum of the rats. Craniolateral oriented pockets (2 per incision) were subcutaneously created by blunt dissection. The scaffolds (4 scaffolds per animal), previously embedded into a sterile saline solution, were introduced into the pockets and the *Panniculus carnosus* and the skin were carefully sutured. The animals were kept in single cages with food and water *ad libitum* during all time of implantation. During the first week, the animals received daily 200 µg/g of body weight of metamizole sodium in drinking water *ad libitum*.

For a long term reaction, six male Sprague Dawley rats, 3 for each implantation time, and weighting between 280g and 340g were used for the subcutaneous implantation of the SPCL scaffolds. The surgical procedure followed was the same as above mentioned for the subcutaneous implantation.

2.5.5 - Rat Intramuscular implantation model

The intramuscular implantation model is very similar to the subcutaneous model regarding the objectives and the obtained information. However, a major difference resides in the type of surrounding tissue that reacts with the implanted material. The muscle, being highly vascularised, allows an easier recruitment of circulating inflammatory cells and thus, the inflammatory reaction

induced by intramuscular implantations is likely to be slightly intense in comparison with the subcutaneous implantation of the same material or TE construct.

Six male Sprague Dawley rats weighting between 380g and 400g (3 for each implantation time) were used. Each animal was anaesthetized with an intramuscular injection of 90 mg/Kg ketamine hydrochloride and 5 mg/Kg xylazine hydrochloride. After shaving and disinfecting the back of the animals, 4 paraventral skin incisions, of approximately 2 cm containing the subcutis and the *Panniculus Carnosus*, were performed under surgical sterile conditions. An incision on the fascia of the back muscle was performed and craniolateral oriented muscle-pockets were created by blunt dissection. After introducing the scaffolds (4 scaffolds per animal), previously embedded into a sterile saline solution, the fascia, the *Panniculus carnosus* and finally the skin were carefully sutured. The animals were kept in single cages with food and water *ad libitum* during all time of implantation. During the first week, the animals received daily 200 µg/g of body weight of metamizole sodium in drinking water *ad libitum*.

2.5.6 - Rat skin excision model

Despite the different healing capacities between rats and humans, rat model of partial-thickness skin wound can be used, under impaired healing conditions, to test wound dressers. In partially-thickness wounds the large amount of granulation tissue formed results in wound contraction and re-epithelialisation which closes the wounded area allowing the regeneration of the epidermis with its different layers and annexes [62, 63]. Furthermore, as the subcutaneous tissue with the portion of the *panniculus carnosus* muscle in the backs of the animals is left intact [64], the re-epithelialisation of the wound will start not only from the margins of the wound containing healthy and intact skin, but also from the wound bed [62, 64].

Twenty male Sprague Dawley rats weighting between 230 g and 280 g were used for the study. Three groups were investigated: membranes (wound directly covered with the cht/soy-based (CS75) membranes); positive control (wound directly covered with Epigard® - Biovision GmbH, Germany); and a negative control (no direct coverage of the wound). Epigard® is composed of a non-textile outer layer of polytetrafluorethylene and an inner layer of soft elastic polyurethane that forms an open matrix to which adsorbs the wound exudate from the wound bed. This dressing was chosen as positive control because it is extensively used in the clinical practice as a short term wound dressing [65].

Each animal was anaesthetized with an intramuscular injection of 90 mg/kg of ketamine combined with 5 mg/kg xylazine after induction with 3-3.5% isofluorane and 7 L/minute of air for 2-3 minutes. After shaving the skin, the back of the animals was disinfected and 2 paravertebral wounds (17 mm in diameter) were created by excision, leaving the skin smooth muscle layer

(*panniculus carnosus*) intact. The test conditions were randomly distributed among the animals. After dressing (except in the negative control), the wounds were protected with Bactigras® and then covered with Opsite Flexigrid®. Bactigras® is a paraffin gauze dressing containing 0.5% of chlorhexidine acetate; being soothing and non-adhesive it allows the wound to drain freely into an absorbent secondary dressing [66]. Opsite Flexigrid®, a vapour permeable adhesive film dressing which is the standard in moist wound healing [67] was used as a secondary dressing. The whole abdomen of each animal was protected with stretching bandages to prevent the removal of the whole set of dressings by scratching and biting (Fig. 1). At days 0 (surgery day) and 7, methylprednisolone acetate (Depo-Medrol®, Pfizer) was subcutaneously injected (20 mg/kg BW) to impair wound healing [68] and inhibit hair growth.

The animals were kept separately and received daily analgesia with metamizole sodium (200µg/g BW) and sedation with diazepam (2.5mg/125ml water) in drinking water.

The bandages were changed every 3-4 days.

2.5.7 - Nude Mice Subcutaneous implantation model

Nude mice have a hair absence which is a secondary effect from its major deficiency. These animals do not possess thymus, the organ responsible for T lymphocytes maturation. Thus, *nude* mice are immunossupressed animals which allow exogenous cells transplantation.

The *in vivo* fate of the *in vitro* transfected hASCs seeded onto SPCL scaffolds was followed in *nude* mice. Thirteen female Balb/c nu/nu *nude* mice, with an average weight of 21.6g±1.2 were used: 6 animals to implant the SPCL-WS scaffolds, 6 animals to implant the SPCL-FB scaffolds and one animal as control. All surgical procedures were performed under sterile conditions in a vertical laminar flow hood. Each animal was intraperitoneally (IP) anaesthetized with ketamine (60 mg/kg) and xylazine (7.5 mg/kg). Subsequently, the skin of the mice was disinfected with betaisodona and two lateral incisions of approximately 0.5 cm, containing the subcutis and *Panniculus carnosus*, were performed in the back of the animals. Two caudal-lateral oriented pockets were created in each animal by blunt dissection, where the TE constructs with the transfected ASCs were inserted. After implantation, the *Panniculus carnosus* and the skin of the animals were carefully sutured.

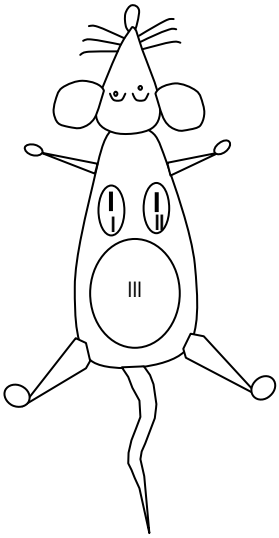

Figure 2.1: Schematic representation of a *nude* mouse with the areas considered for the capture of the luminescence signal emitted by the transfected cells seeded on the SPCL-based scaffolds: I and II correspond to the implantation sites; III corresponds to the dorsum (back) of the animals to where the cells eventually migrate.

2.5.8 - Transgenic Mice Subcutaneous implantation model

VEGFR2-luc transgenic mouse model was established [69] using the murine VEGFR2 promoter to direct the expression of the luciferase reporter. It is used to assess the expression of VEGFR2 under particular conditions. It is well reported that VEGFR2 mediates most of the mitogenic, cell survival, and vascular permeability effects of VEGF [70, 71]. Moreover, as VEGFR2 plays an important role in many aspects of blood vessel growth, an *in vivo* monitoring of the *VEGFR2* gene expression, with non-invasive techniques was found useful to achieve its real time function in angiogenesis [72].

Thirty eight FVB/N-Tg(VEGF-r2–luc)Xen mice (VEGFR2-LUC) [69], with an average weight of 33.8 g±3.6 were used to assess the effect of the addition of VEGF, FGF-2, hASCs or fibrin sealant to the SPCL scaffolds for vascularisation. These mice carry a transgene that contains a 4.5 kb murine VEGF-R2 promoter fragment that drives the expression of a firefly luciferase reporter protein.

Six test groups were established per type of scaffold (table 2.1): a) untreated control to measure endogenous expression of VEFG-R2 due to surgical procedure; b) scaffold group to measure expression of VEFG-R2 due to scaffold implantation (SPCL-WS and SPCL-FB); c) scaffold plus FS to measure the expression of VEGF-R2 due to the use of FS (SPCL-WS+FS and SPCL-FB+FS); d) scaffold plus FS and hASCs group, to measure the expression of VEGF-R2 due to the presence of hASCs (SPCL-WS+FS+hASCs and SPCL-FB+FS+hASCs); e) scaffold plus FS, hASCs and VEGF (200 ng/mL) to measure the expression of VEGF-R2 induced by the VEGF

delivery (SPCL-WS+FS+hASCs+VEGF and SPCL-FB+FS+hASCs+VEGF); and f) scaffold plus FS, ASCs and FGF-2 (200 ng/mL), to measure the expression of VEGF-R2 induced by the FGF-2 delivery (SPCL-WS+FS+hASCs+FGF-2 and SPCL-FB+FS+hASCs+FGF-2).

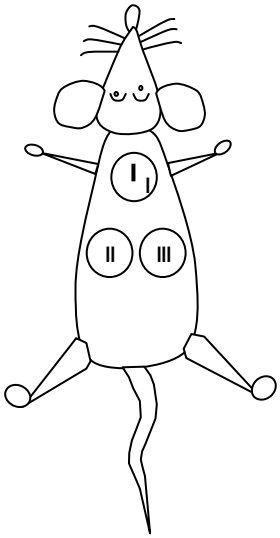

Figure 2.2: Schematic representation of a transgenic VEGFR2-LUC mouse with the areas considered for the capture of the luminescence signal emitted by the transfected cells seeded on the SPCL-based TE constructs: I corresponds to incision area; II and III correspond to the left and right implant sites (pockets).

Each animal was anaesthetized using 3% isoflurane for induction and maintaining with an i.p. injection of ketamine (60 mg/kg) and xylazine (7.5 mg/kg). Mice were injected subcutaneously with luciferin (150 mg/kg) and imaged with the *in vivo* imaging system (VivoVisions IVISs, Xenogen, Alameda, CA) to acquire the background image signal corresponding to the pre-surgical activity, set to 100%) as reported below. After this, each animal's dorsum was then shaved and disinfected, and a 1 cm incision at the caudal aspect of the neck was made. For the subcutaneous implantation, a caudal lateral access to each flank was bluntly subcutaneously created through this incision, forming 2 pockets per animal. Into each pocket, the construct was inserted accordingly to the different test groups. Subsequent measurements in the pre-determined areas were referenced to the pre-surgical baseline and obtained immediately after surgery and on days 3, 6, 9 and 13 after implantation, as well as 15 minutes after luciferin injection.

Table 2.1: Distribution of the test groups for the in vivo implantation on the transgenic FVB/N-Tg(VEGF-r2–luc)Xen mice.

Group	Condition	
a	Control – subcutaneous pockets without any implant	
b	SPCL-WS	SPCL-FB
c	SPCL-WS+FS	SPCL-FB+FS
d	SPCL-WS+FS+hASCs	SPCL-FB+FS+hASCs
e	SPCL-WS+FS+hASCs+VEGF	SPCL-FB+FS+hASCs+VEGF
f	SPCL-WS+FS+hASCs+FGF	SPCL-FB+FS+hASCs+FGF

2.6 Post-implant Analysis

2.6.1 - Macroscopic Evaluation

The skin wounds of the animals from the rat skin excision model were periodically verified. Macroscopic analysis of the wounds was carried out at days 3, 7 and 14 and the images taken used for the planimetric evaluation of the healing process. The evaluation was performed with the LUCIA software by two independent researchers blinded to the experimental condition.

2.6.2 - Cytological preparations

The kinetics of the inflammatory reaction induced by the injected suspensions (made from the Cht and SI powders) was assessed by analysis of the peritoneal exudate. The animals were anaesthetized with a subcutaneous injection of 2.5% pentobarbital and sacrificed with an intracardial overdose of anaesthetic. The abdominal area of each animal was disinfected with 70% ethanol and an incision in the abdominal skin and the linea alba was performed, in order to expose the external abdominal wall as most as possible to the subsequent lavage. Thirty five mL of sterile PBS solution were injected into the intraperitoneal cavity, and the abdomen was massaged in order to recover the inflammatory cells adherent to the abdominal organs and peritoneal cavity. The peritoneal exudate was collected in a syringe and stored on ice until further analysis. The total number of leukocytes was counted using a haemocytometer and cytospins of $1x10^6$ cells were performed by cytocentrifugation (5 minutes at 1000 rpm). Cells were then gently washed in tap water and fixed in formaldehyde-ethanol (50/50 (v/v) – formaldehyde 3.7% and absolute ethanol) for 45 seconds. The Wright's staining for blood samples (Hemacolor, Merck, Germany) was performed and after being dried, each slide was observed in an optical microscope. A minimum of 300 cells per sample was counted in different areas of the cytospin and the different types of leukocytes distinguished.

2.6.3 – Explants

The animals with subcutaneously implanted SI-M, dSI-M and Cht/Soy-M were anaesthetized, at the end of each implantation period, respectively with an intraperitoneal injection of 2.5% pentobarbital or with an intramuscular injection of 90 mg/kg ketamine hydrochloride and 5 mg/kg xylazine hydrochloride, and sacrificed with an intracardial overdose of anaesthetic. The implanted membranes, the respective surrounding tissue and the lymph nodes of the rats with Cht/Soy-M were explanted

2.6.4 - Histological preparations

Histological preparations are obtained from fixed animal tissues. The samples follow a series of procedures to an ultimate goal of having thin (2-5μm) paraffin embedded sections of the samples. The histological sections should illustrate the tissue with all its components in order to understand some interactions and to recognize microscopical structures. For that, sections have to be stained.

2.6.4.1 Haematoxylin and Eosin (HE) Staining

HE staining is a standard protocol to identify, microscopically the basic morphology of the cells in the tissues, formalin fixed and paraffin embedded. Haematoxylin is directed to the nucleus providing it with a dark blue colour. By its turn, eosin stains the cytoplasm of the cell with a pink colour. Thus, the main cell structures are easily indentified.

At the end point times (1, 2, 8 and 12 weeks), the animals with the SPCL scaffolds subcutaneously implanted were intramuscularly anaesthetized and sacrificed with an intracardial overdose of 90 mg/Kg ketamine hydrochloride and 5 mg/Kg xylazine hydrochloride. From each animal the 4 implanted scaffolds and surrounding tissue, as well as the axillary and inguinal lymph nodes, were explanted. The explanted samples were either fixed in 3.7% formalin for histological evaluation, or frozen for posterior molecular biology analysis.

Two weeks after the implantation), the animals with the SPCL scaffolds intramuscularly implanted were IP anaesthetized and subsequently sacrificed with an intracardial overdose of ketamine (60 mg/kg) and xylazine (7.5 mg/kg). The scaffolds and surrounding tissue were explanted and, half of the sample was fixed in 3.7% formalin for histological analysis, and the other half was snap frozen for molecular biology evaluation. Histology was performed according to existing standard protocols for HE.

In the rat skin excision model, at each end time point (1 and 2 weeks), the animals were anaesthetized with isofluorane and then euthanized by and intracardial overdose of ketamin/xylazine. The wound region and the surrounding healthy skin were explanted. Central

wound cross-sections were fixed for histological analysis, in 3.7% formalin, and then paraffin embedded, sectioned and stained according to a routine HE protocol.

The histological samples were analysed using an Axioplan Imager Z1 microscope (Zeiss, Germany). The histological analysis also included the measurement of the length of the wound, which permitted to establish a correlation with the planimetric assessment of the wound areas. The length of the wounds was measured, using the standard microscope scale, after the composition of multiple standardized histological pictures including the full wounded area and the healthy margins.

2.6.4.2 - Massson Goldner Trichrome Staining

Masson Trichrome staining is used to identify collagen fibres within the tissue structure. Similarly to haematoxylin and eosin staining, is used in formalin fixed and paraffin embedded sections. The overall image provided by this staining is such: collagen fibres stained in bluish-green, nuclei in dark blue-black and the remaining background in red.

2.6.4.3 Immunohistochemistry

Immunohistochemistry is based on a highly specific reaction antigen-antibody. An antibody is directed against the specific antigen aimed to be identified. In the situation of having formalin fixed and paraffin embedded sections, the most used protocol involves the use of an enzyme-conjugated secondary antibody with specificity to the primary antibody used. The enzyme from the secondary antibody reacts with a specific protein (avidin or streptavidin) which, by its turn will be revealed by a die, such as horseradish peroxidise (HRP). Thus, the localisation of a specific antibody is detected by the brownish-reddish labelling.

In this particular work, immunohistochemistry was performed in formalin fixed and paraffin embedded sections and the antibodies used were: monoclonal mouse anti-human CD3 antibody (Dako, Denmark) with cross reactivity for rat T lymphocytes, a monoclonal mouse anti-rat CD18 antibody (Serotec, UK) for Integrin β2 chain of recruited leukocytes, and a monoclonal mouse anti-human phosphoinositide 3-Kinase (Pi3K) antibody (BD, Belgium) with cross reactivity for rat activated and proliferating lymphocytes, following standard protocols.

2.6.5 - Molecular Biology Analysis

The samples recovered from the animals subcutaneously and intramuscularly implanted with the SPCL scaffolds and SPCL-based TE constructs, were processed for reverse transcriptase polymerase chain reaction (RT-PCR). The procedure was performed according standard established RNA extraction, cDNA synthesis and amplification, as well as agarose gel detection protocols.

For the SPCL scaffolds subcutaneously and intramuscularly implanted in rats, the detection of the expression of IL-1α, IL-18, IL-10, IL-13, IFN-γ and MHC class II genes was carried out. The used primers sequences and amplification conditions are referred in table 2.2.

Table 2.2: Forward and Reverse seuences of the genes detected by RT-PCR on rat samples.

Function	Gene	Sequences	Tm (ºC)	Bp
Housekeeping gene	GAPDH	Sense - GGTGATGCTGGTGCTGAGTA	59.4	81
		Antisense - GGATGCAGGGATGATGTTCT	57.3	
Pro-inflammatory	IL-18	Sense - AGATGTGGAACTGGCAGAGG	59.4	220
		Antisense - CCCATTTGGGAACTTCTCCT	57.3	
	IL-1α	Sense –GCAAAGCCTAGTGGAACCAG	59.4	244
		Antisense -GCAGAAGGTGCACAGTGAGA	59.4	
Anti-inflammatory	IL-10	Sense - GAATTCCCTGGGAGAGAAGC	59.4	219
		Antisense - CCGGGTGGTTCAATTTTTCAT	55.9	
	IL-13	Sense - ATCGAGGAGCTGAGCAACAT	57.3	189
		Antisense - CGAGGCCTTTTGGTTACAGA	57.3	
	IFN-γ	Sense - GCCCTCTCTGGCTGTTACTG	61.4	221
		Antisense - CTGATGGCCTGGTTGTCTTT	57.3	
	MHC class II	Sense - TCCCAGATACACAGCAGCAG	59.4	320
		Antisense - CATGCGAAGGTTCTCCAGTT	57.3	

For the SPCL-based TE constructs subcutaneously implanted in nude and transgenic mice, the expression of vascularisation and inflammation specific genes was performed with the primers and amplification conditions from table 2.3.

Table 2.3: Forward and Reverse sequences of the genes detected by RT-PCR on mice samples.

Function	Gene	Sequences	Tm (ºC)	Bp
Vascularisation	VEGF-α	Sense - CCGAAACCATGAACTTTCT	55.19	604
		Antisense - CGTTCGTTTAACTCAAGCTG	56.31	
	VEGF-R1	Sense - GAGGGATAACAGGCAATTC	54.59	960
		Antisense - CCCAGCAAGATCGTATAGTC	54.91	
Inflammation	IL-4	Sense - TCATCCTGCTCTTCTTTCTC	54.67	325
		Antisense - GATGTGGACTTGGACTCATT	54.82	
	IFN-γ	Sense - CTACCTTCTTCAGCAACAGC	55.36	568
		Antisense - TGTAGACATCTCCTCCCATC	54.92	
	TNF-α	Sense - GTCTCAGCCTCTTCTCATTC	54.03	654
		Antisense - CAGAGTAAAGGGGTCAGAG	54.57	

2.6.6 - In vivo *luminescence*

One of the aims of the *in vivo* luminescence technique used in this particular work was to identify, in the living organism, the movement of luciferase transfected cells after seeded into starch-based scaffolds and after subcutaneous implantation in *nude* mice. The other objective of the study to use *in vivo* luminescence was to identify the expression of VEGF-R2 after implantation of starch-based TE constructs, after subcutaneous implantation into FVB/N-Tg(VEGF-r2–luc)Xen mice (VEGFR2-LUC).

2.6.6.1 Nude mice luminescence

The bioluminescence signal, from the *in vivo* luciferase activity that identifies the location of the transfected cells, was quantified (emitted photon counts per second) using the Live Image Software (Xenogen®). Specific areas for the signal detection, considering the original location of the implants and possible migration of the cells from the constructs, were pre-determined (Fig.1A): I and II correspond to the left and right implant sites; III corresponds to the dorsum of the animals, the most probable migration localization. Bioluminescence images were collected immediately after surgery and on days 1, 3, 6, 9, and 13. The luciferase activity was measured 15 minutes after luciferin subcutaneous injection and normalised to the respective areas for further graphical representation.

2.6.6.2 Transgenic mice luminescence

Prior to surgical procedure, specific areas for the bioluminescence detection were established. One correspondent to the incision area and other two correspondents to the left and right implant

sites (pockets). The signal detected at the incision site correlates with the expression of the *VEGFR2* gene with the ongoing inflammatory process as the incision heals. After the surgical implantation procedure, subsequent measurements in the pre-determined areas were referenced to the pre-surgical baseline and obtained immediately after surgery and on days 3, 6, 9 and 13 after implantation, as well as 15 minutes after luciferin injection.

2.7 Statistical Analysis

All the obtained data, obtained from the quantification experiments [73], was analysed by a single factor ANOVA test and the significance value was set at $p<0.05$.

References

1. Vaz, C.M., et al., *Effect of crosslinking, thermal treatment and UV irradiation on the mechanical properties and in vitro degradation behavior of several natural proteins aimed to be used in the biomedical field.* J Mater Sci Mater Med, 2003. **14**(9): p. 789-96.
2. Vaz, C.M., et al., *Casein and soybean protein-based thermoplastics and composites as alternative biodegradable polymers for biomedical applications.* J Biomed Mater Res A, 2003. **65**(1): p. 60-70.
3. Vaz, C.M., et al., *Controlled delivery achieved with bi-layer matrix devices produced by co-injection moulding.* Macromol Biosci, 2004. **4**(8): p. 795-801.
4. Vaz, C.M., et al., *Soy matrix drug delivery systems obtained by melt-processing techniques.* Biomacromolecules, 2003. **4**(6): p. 1520-9.
5. Silva, G.A., et al., *In vitro degradation and cytocompatibility evaluation of novel soy and sodium caseinate-based membrane biomaterials.* J Mater Sci Mater Med, 2003. **14**(12): p. 1055-66.
6. Silva, R.M., et al., *Preparation and characterisation in simulated body conditions of glutaraldehyde crosslinked chitosan membranes.* J Mater Sci Mater Med, 2004. **15**(10): p. 1105-12.
7. Silva, S.S., et al., *Physical properties and biocompatibility of chitosan/soy blended membranes.* J Mater Sci Mater Med, 2005. **16**(6): p. 575-9.

8. Silva, S.S., et al., *Physicochemical Characterization of Novel Chitosan-Soy Protein/TEOS Porous Hybrids for Tissue Engineering Applications.* Materials Science Forum, 2006. **514-516**: p. 1000-1004.
9. Santin, M., et al., *A new class of bioactive and biodegradable soybean-based bone fillers.* Biomacromolecules, 2007. **8**(9): p. 2706-2711.
10. Tuzlakoglu, K., et al., *Production and characterization of chitosan fibers and 3-D fiber mesh scaffolds for tissue engineering applications.* Macromol Biosci, 2004. **4**(8): p. 811-9.
11. Kim, I.Y., et al., *Chitosan and its derivatives for tissue engineering applications.* Biotechnol Adv, 2008. **26**(1): p. 1-21.
12. Di Martino, A., M. Sittinger, and M.V. Risbud, *Chitosan: a versatile biopolymer for orthopaedic tissue-engineering.* Biomaterials, 2005. **26**(30): p. 5983-90.
13. Zhang, Y., et al., *Calcium phosphate-chitosan composite scaffolds for bone tissue engineering.* Tissue Eng, 2003. **9**(2): p. 337-45.
14. Wu, H., et al., *Response of rat osteoblasts to polycaprolactone/chitosan blend porous scaffolds.* J Biomed Mater Res A, 2009.
15. Lu, J.X., et al., *Effects of chitosan on rat knee cartilages.* Biomaterials, 1999. **20**(20): p. 1937-44.
16. Yamane, S., et al., *Feasibility of chitosan-based hyaluronic acid hybrid biomaterial for a novel scaffold in cartilage tissue engineering.* Biomaterials, 2005. **26**(6): p. 611-9.
17. Ueno, H., et al., *Accelerating effects of chitosan for healing at early phase of experimental open wound in dogs.* Biomaterials, 1999. **20**(15): p. 1407-14.
18. Cho, Y.W., et al., *Water-soluble chitin as a wound healing accelerator.* Biomaterials, 1999. **20**(22): p. 2139-45.
19. Peluso, G., et al., *Chitosan-mediated stimulation of macrophage function.* Biomaterials, 1994. **15**(15): p. 1215-20.
20. Ueno, H., et al., *Evaluation effects of chitosan for the extracellular matrix production by fibroblasts and the growth factors production by macrophages.* Biomaterials, 2001. **22**(15): p. 2125-30.
21. Rucker, M., et al., *Angiogenic and inflammatory response to biodegradable scaffolds in dorsal skinfold chambers of mice.* Biomaterials, 2006. **27**(29): p. 5027-38.
22. Azab, A.K., et al., *Biocompatibility evaluation of crosslinked chitosan hydrogels after subcutaneous and intraperitoneal implantation in the rat.* J Biomed Mater Res A, 2007. **83**(2): p. 414-22.

23. Hong, Y., et al., *Covalently crosslinked chitosan hydrogel formed at neutral pH and body temperature.* J Biomed Mater Res A, 2006. **79**(4): p. 913-22.
24. Cai, K., et al., *Surface modification of titanium thin film with chitosan via electrostatic self-assembly technique and its influence on osteoblast growth behavior.* J Mater Sci Mater Med, 2008. **19**(2): p. 499-506.
25. Bumgardner, J.D., et al., *Chitosan: potential use as a bioactive coating for orthopaedic and craniofacial/dental implants.* J Biomater Sci Polym Ed, 2003. **14**(5): p. 423-38.
26. Lee, J.Y., et al., *Enhanced bone formation by controlled growth factor delivery from chitosan-based biomaterials.* J Control Release, 2002. **78**(1-3): p. 187-97.
27. Bumgardner, J.D., et al., *The integration of chitosan-coated titanium in bone: an in vivo study in rabbits.* Implant Dent, 2007. **16**(1): p. 66-79.
28. Coutinho, D.F., et al., *The effect of chitosan on the in vitro biological performance of chitosan-poly(butylene succinate) blends.* Biomacromolecules, 2008. **9**(4): p. 1139-45.
29. Santos, T.C., et al., *In vitro evaluation of the behaviour of human polymorphonuclear neutrophils in direct contact with chitosan-based membranes.* J Biotechnol, 2007. **132**(2): p. 218-26.
30. Silva, R.M., et al., *Influence of beta-radiation sterilisation in properties of new chitosan/soybean protein isolate membranes for guided bone regeneration.* J Mater Sci Mater Med, 2004. **15**(4): p. 523-8.
31. Silva, S.S., et al., *Physicochemical Characterization of Novel Chitosan-Soy Protein/TEOS Porous Hybrids for Tissue Engineering Applications.* Materials Science Forum, 2006. **514-516**: p. 1000-1004

32. Gomes, M.E., et al., *A new approach based on injection moulding to produce biodegradable starch-based polymeric scaffolds: morphology, mechanical and degradation behaviour.* Biomaterials, 2001. **22**(9): p. 883-889.
33. Gomes, M.E., et al., *In vitro localization of bone growth factors in constructs of biodegradable scaffolds seeded with marrow stromal cells and cultured in a flow perfusion bioreactor.* Tissue Eng, 2006. **12**(1): p. 177-188.
34. Salgado, A.J., et al., *In vivo response to starch-based scaffolds designed for bone tissue engineering applications.* Journal of Biomedical Materials Research Part A, 2007. **80A**(4): p. 983-989.

35. Gomes, M.E., et al., *Starch-poly(epsilon-caprolactone) and starch-poly(lactic acid) fibre-mesh scaffolds for bone tissue engineering applications: structure, mechanical properties and degradation behaviour.* J Tissue Eng Regen Med, 2008. **2**(5): p. 243-252.

36. Santos, M.I., et al., *Endothelial cell colonization and angiogenic potential of combined nano- and micro-fibrous scaffolds for bone tissue engineering.* Biomaterials, 2008. **29**(32): p. 4306-4313.

37. Azevedo, H.S. and R.L. Reis, *Encapsulation of alpha-amylase into starch-based biomaterials: An enzymatic approach to tailor their degradation rate.* Acta Biomater, 2009.

38. Martins, A.M., et al., *The Role of Lipase and alpha-Amylase in the Degradation of Starch/Poly(varepsilon-Caprolactone) Fiber Meshes and the Osteogenic Differentiation of Cultured Marrow Stromal Cells.* Tissue Eng Part A, 2009. **15**(2): p. 295-305.

39. Tuzlakoglu, K., et al., *A new route to produce starch-based fiber mesh scaffolds by wet spinning and subsequent surface modification as a way to improve cell attachment and proliferation.* Journal of Biomedical Materials Research Part A *in press*, 2009.

40. Marques, A.P., et al., *Effect of starch-based biomaterials on the in vitro proliferation and viability of osteoblast-like cells.* Journal of Materials Science-Materials in Medicine, 2005. **16**(9): p. 833-842.

41. Alves, C.M., et al., *Modulating bone cells response onto starch-based biomaterials by surface plasma treatment and protein adsorption.* Biomaterials, 2007. **28**(2): p. 307-315.

42. Balmayor, E.R., et al., *A novel enzymatically-mediated drug delivery carrier for bone tissue engineering applications: combining biodegradable starch-based microparticles and differentiation agents.* J Mater Sci Mater Med, 2008. **19**(4): p. 1617-1623.

43. Martins, A.M., et al., *Natural origin scaffolds with in situ pore forming capability for bone tissue engineering applications.* Acta Biomater, 2008. **4**(6): p. 1637-1645.

44. Azevedo, H.S., F.M. Gama, and R.L. Reis, *In vitro assessment of the enzymatic degradation of several starch based biomaterials.* Biomacromolecules, 2003. **4**(6): p. 1703-1712.

45. Santos, M.I., et al., *Crosstalk between osteoblasts and endothelial cells co-cultured on a polycaprolactone-starch scaffold and the in vitro development of vascularization.* Biomaterials, 2009. **30**(26): p. 4407-15.

46. Santos, M.I., et al., *Response of micro- and macrovascular endothelial cells to starch-based fiber meshes for bone tissue engineering.* Biomaterials, 2007. **28**(2): p. 240-8.

47. Reis, R.L., et al., *Processing and in vitro degradation of starch/EVOH thermoplastic blends.* Polym Int, 1997. **43**: p. 347.

48. Marques, A.P., R.L. Reis, and J.A. Hunt, *An in vivo study of the host response to starch-based polymers and composites subcutaneously implanted in rats.* Macromol Biosci, 2005. **5**(8): p. 775-85.

49. Chander, C.L., et al., *Myofibroblasts in cotton-induced granulation tissue and the bovine adrenal capsule: morphological aspects.* Int J Tissue React, 1989. **11**(4): p. 161-3.

50. Stevens, A., J.S. Lowe, and B. Young, *Wheater's Basic Histopathology: A Colour Atlas and Text*. Fourth Edition ed. 2002, Edinburgh: Churchill Livingstone. 295.

51. Martin, P. and S.J. Leibovich, *Inflammatory cells during wound repair: the good, the bad and the ugly.* Trends Cell Biol, 2005. **15**(11): p. 599-607.

52. Marques, A.P., R.L. Reis, and J.A. Hunt, *Cytokine secretion from mononuclear cells cultured in vitro with starch-based polymers and poly-L-lactide.* J Biomed Mater Res, 2004. **71A**(3): p. 419-29.

53. Liu, L., et al., *Surface-related triggering of the neutrophil respiratory burst. Characterization of the response induced by IgG adsorbed to hydrophilic and hydrophobic glass surfaces.* Clin Exp Immunol, 1997. **109**(1): p. 204-10.

54. Mutasa, H.C., *Analysis of human neutrophil granule protein composition in chronic myeloid leukaemia by immuno-electron microscopy.* Cell Tissue Res, 1989. **258**(1): p. 111-7.

55. Rice, W.G., J.M. Kinkade, Jr., and R.T. Parmley, *High resolution of heterogeneity among human neutrophil granules: physical, biochemical, and ultrastructural properties of isolated fractions.* Blood, 1986. **68**(2): p. 541-55.

56. Segal, A.W., *How neutrophils kill microbes.* Annu Rev Immunol, 2005. **23**: p. 197-223.

57. Etienne, O., et al., *Degradability of polysaccharides multilayer films in the oral environment: an in vitro and in vivo study.* Biomacromolecules, 2005. **6**(2): p. 726-33.

58. Rada, T., R.L. Reis, and M.E. Gomes, *Adipose Tissue-Derived Stem Cells and Their Application in Bone and Cartilage Tissue Engineering.* Tissue Eng Part B Rev, 2009.

59. Mauney, J.R., et al., *Engineering adipose-like tissue in vitro and in vivo utilizing human bone marrow and adipose-derived mesenchymal stem cells with silk fibroin 3D scaffolds.* Biomaterials, 2007. **28**(35): p. 5280-90.

60. Wolbank, S., et al., *Labelling of human adipose-derived stem cells for non-invasive in vivo cell tracking.* Cell Tissue Bank, 2007. **8**(3): p. 163-77.

61. Goessl, A. and H. Redl, *Optimized thrombin dilution protocol for a slowly setting fibrin sealant in surgery.* European Surgery, 2005. **37**: p. 43-51.

62. Laplante, A.F., et al., *Mechanisms of wound reepithelialization: hints from a tissue-engineered reconstructed skin to long-standing questions.* FASEB J, 2001. **15**(13): p. 2377-89.

63. Davidson, J.M., *Animal models for wound repair.* Arch Dermatol Res, 1998. **290 Suppl**: p. S1-11.

64. Saulis, A. and T.A. Mustoe, *Models of wound healing in growth factor studies*, in *Surgery Research*, W.W. Souba and D.W. Wilmore, Editors. 2001, Academic Press. p. 857-874.

65. Stone, H.A., R.D. Edelman, and J.J. McGarry, *Epigard: a synthetic skin substitute with application to podiatric wound management.* J Foot Ankle Surg, 1993. **32**(2): p. 232-8.

66. Azad, A.K., et al., *Chitosan membrane as a wound-healing dressing: characterization and clinical application.* J Biomed Mater Res B Appl Biomater, 2004. **69**(2): p. 216-22.

67. Yusof, N.L., et al., *Flexible chitin films as potential wound-dressing materials: wound model studies.* J Biomed Mater Res A, 2003. **66**(2): p. 224-32.

68. Wicke, C., et al., *Effects of steroids and retinoids on wound healing.* Arch Surg, 2000. **135**(11): p. 1265-70.

69. Zhang, N., et al., *Tracking angiogenesis induced by skin wounding and contact hypersensitivity using a Vegfr2-luciferase transgenic mouse.* Blood, 2004. **103**(2): p. 617-626.

70. Millauer, B., et al., *High affinity VEGF binding and developmental expression suggest Flk-1 as a major regulator of vasculogenesis and angiogenesis.* Cell, 1993. **72**(6): p. 835-846.

71. Rissanen, T.T., et al., *Expression of vascular endothelial growth factor and vascular endothelial growth factor receptor-2 (KDR/Flk-1) in ischemic skeletal muscle and its regeneration.* Am J Pathol, 2002. **160**(4): p. 1393-1403.

72. Mittermayr, R., et al., *Sustained (rh)VEGF(165) release from a sprayed fibrin biomatrix induces angiogenesis, up-regulation of endogenous VEGF-R2, and reduces ischemic flap necrosis.* Wound Repair Regen, 2008. **16**(4): p. 542-550.

73. Kirkwood, B. and J. Sterne, *Essential Medical Statistics*. 2nd Edition ed. 2003: Wiley. 512.

Chapter III

In vitro evaluation of the behaviour of human polymorphonuclear neutrophils in direct contact with chitosan-based membranes

3.1 Abstract

Several novel biodegradable materials have been proposed for wound healing applications in the past few years. Taking into consideration the biocompatibility of chitosan-based biomaterials, and that they promote adequate cell adhesion, this work aims at investigating the effect of chitosan-based membranes, over the activation of human polymorphonuclear neutrophils (PMNs). The recruitment and activation of polymorphonuclear neutrophils (PMNs) reflects a primary reaction to foreign bodies. Activation of neutrophils results in the production of reactive oxygen species (ROS) such as O_2^- and HO^- and the release of hydrolytic enzymes which are determinant factors in the inflammatory process, playing an essential role in the healing mechanisms.

PMNs isolated from human peripheral blood of healthy volunteers were cultured in the presence of chitosan or chitosan/soy newly developed membranes. The effect of the biomaterials on the activation of PMNs was assessed by the quantification of lysozyme and ROS.

The results showed that PMNs, in the presence of the chitosan-based membranes secrete similar lysozyme amounts, as compared to controls (PMNs without materials) and also showed that the materials do not stimulate the production of either O_2^- or HO^-. Moreover, PMNs incubated with the biomaterials when stimulated with phorbol 12-myristate 13-acetate (PMA) or formyl-methionyl-leucyl-phenylalanine (fMLP) showed a chemiluminescence profile with a slightly lower intensity, to that observed for positive controls (cells without materials and stimulated with PMA), which reflects the maintenance of their stimulation capacity.

Our data suggests that the new biomaterials studied herein do not elicit activation of PMNs, as assessed by the low lysozyme activity and by the minor detection of ROS by chemiluminescence. These findings reinforce previous statements supporting the suitability of chitosan-based materials for wound healing applications.

***This chapter is based on the following publication:**

T. C. Santos, A. P. Marques, S. S. Silva, J. M. Oliveira, J. F. Mano, A. G. Castro, R. L. Reis, In vitro *evaluation of the behaviour of human polymorphonuclear neutrophils in direct contact with chitosan-based membranes*, **2007. Journal of Biotechnology, 132:218-226**.

3.2 Introduction

In the past few years a huge effort has been made to create the ideal wound dressing and skin substitutes to respond to the increasing needs of mankind. Several research groups suggested that chitosan is a promising material for regenerative medicine [1-4]. Chitosan-based membranes were shown to promote the proliferation of human skin fibroblasts and keratinocytes *in vitro* [3] and the application of a chitosan-based hydrogel in mice wounds had proved to accelerate wounding [5]. Furthermore it was demonstrated that wounds in human skin heal better if covered with chitosan-based membranes [6, 7], beyond its proven antimicrobial properties [8, 9].

After implantation of a medical device, the tissue will inevitably be traumatized by the implantation procedure [10-13] triggering an inflammatory response. This response to trauma and to the implantation of biomaterials is associated to the secretion of a variety of mediators [10-13]. Their action results in the recruitment of certain populations of cells that, if not properly regulated, can cause tissue damage and ultimately lead to the rejection of the implant [13]. The concomitant increased vascular permeability in the inflammatory response allows the influx of circulating inflammatory cells to the implantation site, in a first phase, polymorphonuclear neutrophils (PMNs). Within 24 hours, macrophages also begin to migrate to the site of injury and two or three days following the beginning of the inflammatory process, lymphocytes begin to enter the damaged area. Together with this influx, other inflammatory cells, such as mast cells and eosinophils will orchestrate the ongoing of the inflammatory response to the implanted device.

It is well known that PMNs are crucial early in the development of an inflammatory response [12, 14, 15]. Neutrophils also have the capacity to dictate the progression of the host immune system reaction by their capacity to produce cytokines, such as interleukin -12 and -10 (IL-12 and IL-10) among others [12, 16, 17]. PMNs have a high capacity to act as phagocytes of foreign bodies, nevertheless, the great majority of biomaterials comprises a range of dimensions incompatible with phagocytosis, leading PMNs to “frustrated phagocytosis” [18] resulting in the release of hydrolytic enzymes [19, 20], known as an oxygen-independent mechanism [21]. Lysozyme, present in both primary and secondary granules of PMNs, is one of the most important enzymes released during the inflammatory response [19, 20]. The importance of its role in the foreign body reaction to biodegradable biomaterials is further supported by its capacity to degrade polymers such as chitosan [22].

Another defence approach that is potentially deleterious for the implanted device occurs simultaneously to degranulation and is commonly designated as respiratory burst. This PMNs oxygen-dependent mechanism of defence, involve the consumption of oxygen (O_2) by the activation of the Nicotinamide Adenine Dinucleotide Phosphate (NADPH) oxidase system,

leading to the production of oxygen radicals and their reaction products - Reactive Oxygen Species (ROS) which are known to induce tissue destruction [21].

The aim of this study was to gain further knowledge on the biological reactions to chitosan and chitosan/soy based membranes meant for wound healing applications. Reis and his group have shown previously that [23], chitosan-based membranes were non cytotoxic and support mouse fibroblast cell adhesion and spreading. These new systems combine the blending of natural polymers, such as chitosan and soy [23, 24], in order to develop hybrid materials for tissue engineering and regenerative medicine. In fact, chitosan based systems have been proposed by the same group for several different applications within the tissue and regenerative field [24-26]. Therefore the present study intended to focus on the effect of the presence of the newly developed chitosan-based membranes over the *in vitro* response of PMNs isolated from human blood. The considered newly developed biomaterials are the chitosan/soy blends, thus the membranes of chitosan blended with soy in two forms, one comprehending simply the blend of chitosan with soy (Cht/Soy), and the other which is the same blend but cross-linked with TEOS (Cht/Soy/TEOS). PMNs degranulation was addressed by quantification of the granular hydrolytic enzyme lysozyme while the respiratory burst mechanisms were followed by a chemiluminescence assay [27, 28] knowing that PMNs can be stimulated *in vitro* with phorbol 12-myristate 13-acetate (PMA) [29, 30] or formyl-methionyl-leucyl-phenylalanine (fMLP) [27, 30, 31].

3.3 Materials and Methods

3.3.1 Materials tested

Reagent grade chitosan (Cht, Sigma, USA) with a deacetylation degree of 85% and viscosimetric molecular weight of about 700 KDa, Soy protein isolate (Loders Crocklaan, The Netherlands) and tetraethyl orthosilicate (TEOS, Aldrich, USA) were used on the preparation of the different membranes. All other reagents were also analytical grade and used as received.

Chitosan, chitosan/soy protein blended membranes (Cht) were prepared by means of solvent casting, as previously reported by the group of Reis [23]. By its turn, the chitosan-soy protein hybrid membranes (Cht/Soy) were produced by means of a combination of a sol-gel method and solvent casting [32]. Firstly, a 4 wt% chitosan solution was prepared by dissolving chitosan in 0.2 M acetic acid solution. Secondly, a 1 wt% soy suspension (water/glycerol (10 % w/v)) was also prepared and the pH adjusted to 8.0 ± 0.3 with 1 M sodium hydroxide solution. Then, the dispersion was heated in a water bath at 50ºC for 30 min. The blend was prepared by means of mixing the solutions (75/25 wt% chitosan-soy protein) under constant agitation for the period of 1 hour. The cross-linking agent TEOS and 0.5 M chloridric acid (HCl) solution in the molar ratio

(TEOS:HCl) of 1:0.1 wt% were added to the blend to Cht: TEOS ratio of 10:0.1wt% , under constant stirring for 24 hours. Following the solvent casting methodology, the blended solutions was poured into a Petri dish and allowed to dry at room temperature for several days, followed by neutralisation using a 0.1 M sodium hydroxide solution, as described elsewhere [32].

The referred to chitosan-based membranes were considered for the studies: chitosan membranes (Cht), membranes of chitosan blended with soy in two forms, one comprehending simply the blend of chitosan with soy (Cht/Soy), and the other which is the same blend but cross-linked with TEOS, i.e. hybrid membranes (Cht/Soy/TEOS). Three samples of each different membrane were tested and four repetitions of each test were performed. The samples were sterilized by ethylene oxide (EtO) in conditions that have been described previously [33].

For the quantification of lysozyme the considered incubation periods were of 30 minutes, 1 hour and 2. For the reactive oxygen species detection a kinetic study were performed from the time point zero to a maximum of 2 hours, without previous incubation.

3.3.2 Cells

Human polymorphonuclear neutrophils (PMN) were isolated from heparinized fresh peripheral blood. Each 10 ml of heparinized blood was placed in 10 ml of Dextran (Sigma, St. Louis, USA) (6% solution in phosphate buffer saline (PBS) without Ca^{2+} and Mg^{2+} – Sigma, St. Louis, USA). After 20 minutes, about 6 ml of the top layer was removed with a glass pipette and carefully added to 4 ml of Histopaque 1077 (Sigma, St. Louis, USA). After a 25 minutes centrifugation at 21ºC and 2400rpm, the cloudy layer was firstly removed and then the others, keeping the bottom red pellet to resuspend it with 5 ml of PBS without Ca^{2+} and Mg^{2+}. The tube was filled up with PBS (about 12 ml). A centrifugation for 25 minutes at 21ºC and 2400rpm was performed and the supernatant was removed. One ml of distilled water was added, triturated 3 times with the glass pipette and shacked gently for 35 seconds, in order to lyse erythrocytes. The tube was quickly filled up with PBS without Ca^{2+} and Mg^{2+}. The cells were washed by centrifugation, for 25 minutes at 21ºC and 2400rpm, the supernatant was removed as well as the top of the red pellet, very carefully, without touching the white pellet in the bottom. The tube was filled up again with PBS without Ca^{2+} and Mg^{2+} and centrifuged for 25 minutes at 21ºC and 2400rpm. The supernatant was removed and the volume needed of PBS without Ca and Mg was added to count the number of cells after resuspension. The cell suspension was kept at 4ºC until perform the assays, within a maximum of 2 hours.

The cell suspensions used were of $1.3X10^6$ cells/ml for the Reactive Oxygen Species assay and 100 µl of cell suspension per well, and $5X10^5$ cells/ml and 1.0 ml of cell suspension per well for the Lysozyme assay.

3.3.4 Lysozyme Quantification

A bacterial (*Micrococcus lysodeikticus* – Sigma, St. Louis, USA) suspension of 1.5 mg/ml was prepared. The isolated PMN were resuspended in PBS with Ca and Mg (Sigma, St. Louis, USA) (to promote cell attachment) at a final concentration of $5X10^5$ cells/ml. Each sample material (14 mm diameter) was incubated with 1ml of the previous cell suspension (in PBS with Ca^{2+} and Mg^{2+}), for the three pre-determined time periods of reaction (30 min., 1 and 2 hours), at 37ºC and in an humid atmosphere with 5% CO_2 and non-adherent 24-well plates. Three wells with the cell suspension alone were incubated for the same periods of reaction, acting as negative controls.

After each incubation period, 0.5 ml of the supernatant were transferred to new wells and 0.5 ml/well of the bacterial suspension previously prepared was added. The new wells with the lysozyme of the PMN (released when in contact with the materials) and the bacterial suspension were incubated for 30 min., at 37ºC and in an humid atmosphere with 5% CO_2. After incubation, the optical density (OD) was recorded at 541nm. The concentration of the viable cells in the bacterial suspension is quantified by the changes in the turbidity of the bacterial suspension. The cell wall of the bacteria acts as a substrate for lysozyme, leading to the cleavage and consequent lysis of the cell. The intact bacterial suspension is characteristically opaque, but after incubation with a lysozyme solution, the turbidity decreases with the increasing bacterial lysis [34]. After the absorbance reading of the samples, controls and the standards, the lysozyme secreted form the PMN after the contact with the materials, was quantified normalizing the OD values to a calibration curve of known concentrations of lysozyme.

3.3.5 Reactive Oxygen Species Quantification

The isolated PMN were resuspended in PBS with Ca^{2+} and Mg^{2+} at a final concentration of $1.3X10^6$ cells/ml. A mixture of cells (100 µl), with or without cell stimulants (phorbol 12-myristate 13-acetate (PMA) (Sigma, St. Louis, USA), 8 µg/ml in PBS or formyl-methionyl-leucyl-phenylalanine (fMLP) (Fluka, , St. Louis, USA), 10 µg/ml in PBS (100 µl each), with luminol (Sigma, St. Louis, USA) 1.5 Mm in PBS and lucigenin (Sigma, St. Louis, USA), 5.4X10-5 M in PBS (Sigma, St. Louis, USA) (100 µl each), and with or without materials were made in the wells of a white opaque 96-well plate. In this step, the cells, the reagents and the plate were kept on

ice. The chemiluminescence was read in a microplate reader (Sinergy HT, BioTech). The results were obtained in terms of number of counts per time period.

3.4 Results and Discussion

3.4.1 Lysozyme Secretion

Wound healing is a very complex process involving a number of cells, mediators and molecules that, if not properly regulated, may lead to severe damage of the surrounding tissues. If the wounded tissue is the skin, the inflammatory response is accompanied by re-epithelialization, formation of granulation tissue and contraction of connective tissue [16]. Neutrophils play an important role in the development of the inflammatory response and, in the particular situation of a skin wound they can dictate the progression of the healing. PMNs can be activated by multiple mechanisms [35] resulting in an increased phagocytic activity as well as in the release of hydrolytic enzymes, such as lysozyme, from their cytoplasmic granules [20, 36]. When activated neutrophils phagocytose necrotic tissue debris [12] but also try to phagocytose the damaging material which is promoted by a coating of immunoglobulins and proteins of the complement system [12]. The attempt to eliminate the harmful agent is endorsed by the lytic enzymes, including lysozyme that can be released during the process of frustrated phagocytosis, when the material is too large to be internalized, or in association with the respiratory burst [11]. Nevertheless, the lytic activity of neutrophils is limited by their inability to regenerate lysosomal enzymes and, after the "respiratory burst", neutrophils degenerate [12, 21].

In the present work, the lysozyme secreted by the PMNs in direct contact with the Chitosan-based membranes was quantified by a spectrophotometric assay. The amount of lysozyme secreted by PMNs after 30 minutes of incubation with the chitosan (Cht), chitosan and soy (Cht/Soy) and Cht/soy cross-linked with TEOS (Cht/Soy/TEOS) membranes was similar (Fig. 3.1). Moreover, it was not observed a significant difference from the values obtained for the negative control, where the cells were incubated with Tissue Culture Polystyrene (TCPS). Increasing incubation times (1 and 2 hours) revealed that the peak of lysozyme secretion occurred at 1 hour and that after that time the amount of enzyme produced by the cells reached the values of the earlier time point. However, as the same profile was observed for all the tested conditions, it can be concluded that the amount of lysozyme secreted at each time point was comparable for the 3 types of chitosan-based membranes and the negative control and that there were no significant differences along the assay.

The lysozyme quantification data suggest that the membranes of Cht, Cht/soy and Cht/Soy/TEOS were able to activate the PMNs in a comparable degree as the TCPS. Therefore the developed chitosan-based membranes did not have any significant effect on PMNs degranulation.

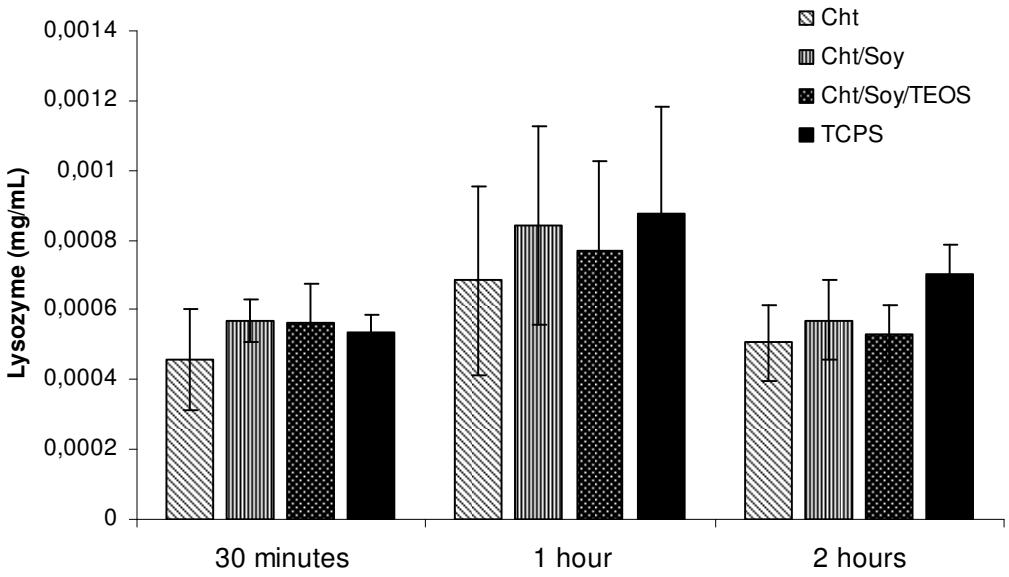

Figure 3.1: Amount of lysozyme secreted by the PMN after 30, 60 and 120 minutes in direct contact with Chitosan-based membranes. No statistical difference was detected when comparing the lysozyme secretion profile between the Chitosan-based membranes and the Tissue Culture Polystyrene (TCPS).

3.4.2 Chemiluminescence

The increased metabolism of activated neutrophils is translated in the so called "respiratory burst", which results in the generation of superoxide anions (O_2^-), hydrogen peroxide (H_2O_2), singlet oxygen ($^1O_2$) and hydroxyl radicals (OH^-) [12, 13, 21]. Despite the apoptotic self destruction mechanism of PMNs once they finish their functions at the wound site and their rapid recognition and clearance by macrophages [37], the accumulation of PMNs at injury sites is not unusual to occur. This gathering of PMNs at the site of implantation or injury, specially in the cases of chronic wounds, blitz the environment with free radicals that kill healthy host cells [16]. In fact, it is well known that the respiratory burst of neutrophils has harmful effects on themselves and on surrounding healthy tissues [38, 39]. Therefore, it is imperative to gain further knowledge on the *in vitro* behaviour of PMNs in direct contact with newly developed materials to predict, as much as possible, their role in the *in vivo* inflammatory reaction.

The assessment of the effect of the chitosan-based membranes on PMN activation was further achieved by the quantification of the produced ROS using a chemiluminescence assay [30], in

the presence and absence of cell stimulants (PMA and fMLP). This two cell stimulants were chosen due to their different mechanisms of action; PMA activates neutrophils directly at the level of Protein Kinase C [35, 40] while fMLP activates NADPH-oxidase [35] thus allowing to conclude about the signalling pathways activated by the contact with the materials studied.

As previously reported [41], the developed chitosan based membranes used in this work showed the following features: (i) higher surface roughness (7.0 μm) of the Cht/Soy/TEOS membranes in comparison to Cht and Cht/Soy membranes (4.6 and 2.5 μm, respectively); (ii) contact angles values between 80° and 117° and thus an hydrophobic nature, and (iii) increasing of surface energy of the blended membranes in comparison to Cht membranes. All resulting changes are related to both incorporation of soy protein and inorganic phase (TEOS). More details about the characterization of the membranes can be found elsewhere [41].

The kinetics of PMN activation induced by PMA and fMLP was determined under the same conditions as the assays performed in the presence of the materials in study and represents the maximum capacity of the cells to be activated under the defined conditions (Fig. 3.2). Superoxide anion (O_2^-) generation was detected by the oxidation of lucigenin while the generation of the hydroxyl anion (HO^-) was detected from the oxidation of luminol. In the tested conditions, PMA was able to stimulate human neutrophils for the production of either O_2^- or HO^-. The stimulation with PMA induced the cells to start to produce HO^- after 10 min. of incubation. This stimulation was prolonged for approximately 1h12min., reaching its peak around minute 25 after the beginning of the stimulation with PMA.

The production of O_2^-, represents a later and prolonged defence mechanism compared to the production of HO^-, once it started 15 min. after the incubation with PMA and reached a maximum value approximately 1h after. The stimulation with fMLP induced the PMNs to produce either O_2^- or HO^- at similar periods of time which started around minute 15, lasted for 1h 20min and showed a maximum stimulation after 30min of the beginning of stimulation. Nevertheless, the O_2^- production was lower than the production of HO^- and the amount of these ROS was much lower in the fMLP stimulation compared to the stimulation with PMA.

The chemiluminescence results show that the chitosan-based membranes did not stimulate PMNs to produce HO^- (Figs. 3.3A, 3.4A and 3.5A) and represent a weak stimulus for the production of O_2^- (Figs. 3.3B, 3.4B and 3.5B). In fact, the luminol oxidation signals presented outlines comparable to the observed for the negative controls where the cells were incubated with PBS. Nevertheless, since PMNs were able to produce HO^- or $O2^-$ when stimulated with PMA or fMLP in direct contact with the chitosan-based membranes, their activation capacity was retained. Additionally, the majority of the kinetic profiles of the response of PMNs to the cell stimulants in

the presence of the chitosan-based membranes were different from the controls. The intensity of the luminescence peak related to the production of HO^- and O_2^- by cells stimulated with PMA and in direct contact with the chitosan-membranes was lower than in the control conditions (PMNs only in the presence of the stimulants – Fig. 3.2) and shifted in time. This means that the PMA-stimulated HO^- and O_2^- production was slightly diminished and delayed in the presence of the chitosan-based membranes. An interesting and distinct behaviour was found for the fMLP-stimulated PMNs in the presence of the developed membranes. While the fMLP-stimulated production of O_2^- was both diminished and delayed in the presence of the three tested materials (Figs. 3.3B, 3.4B and 3.5B), the fMLP-stimulated HO^- production was only lower and delayed in the presence of the chitosan/soy (Fig. 3.4A) and of the hybrid membranes (Fig. 3.5A). In fact fMLP-stimulated PMNs presented comparable HO^- production kinetic profiles when in the control conditions (Fig. 3.2) and in the presence of the chitosan membranes, meaning that the chitosan membranes did not induce a lower and delayed response of PMNs (Fig. 3.3A).

The comparison of the chemiluminescence data from the different materials revealed that the PMA-stimulated HO^- and O_2^- production in the presence of the chitosan/soy and hybrid membranes did not present significant differences. This similarity was also found for the fMLP-stimulated HO^- production but not for the fMLP-stimulated O_2^- production in which the hybrid membranes induced a less significant effect than the chitosan/soy membranes in comparison to the control. Moreover, the chitosan membranes while exerting a more pronounced effect on stimulating PMNs over the PMA-stimulated HO^- production in comparison with the control conditions and with the two other chitosan-based membranes, showed to induce comparable fMLP-stimulated HO^- production to control and lower effect than the chitosan/soy and hybrid membranes also over the PMA and fMLP-stimulated O_2^- production.

It was demonstrated that the human neutrophils were successfully stimulated by PMA, with a maximum production of HO^- between 20 min. and 30 min. and O_2^- and a maximum production of O_2^- between 55 min. and 65 min. (Fig. 3.2). The stimulation for the secretion of HO^- started earlier and was slightly stronger than the stimulation for the release of O_2^-, but the O_2^--elicited oxidation of lucigenin lasted longer. The HO^- and O_2^- maximum production by fMLP-stimulated neutrophils was shown to occur between minutes 20 and 50 however, the intensity of those peaks was significantly lower when compared with the production of HO^- and O_2^- by PMA-stimulated PMNs.

McPhail and colleagues [35] demonstrated that modifications in the cytoplasmic membranes of neutrophils lead to cells that respond to stimuli such as PMA with normal O_2^- production, but are unable to respond normally to fMLP stimulation.

In contact with all the tested chitosan-based membranes, the PMNs were not stimulated for the release of HO^- and represent a weak stimulus for the production of O_2^-. Despite the differences assessed in the surface of the chitosan-based membranes [32], the cells showed a similar behaviour in terms of activation. These observations indicate that the characteristics of those surfaces were inert for PMNs, corroborate the already assessed biocompatibility [23]. Nonetheless, if the cells were simultaneously, in direct contact with the chitosan-based membranes and stimulated with PMA or fMLP, they showed capacity to produce both HO^- and O_2^-, meaning that the contact with the chitosan-membranes did not eliminate their capacity to respond to those stimuli, although responding differently from the control conditions. This may indicate an *in vivo* anti-inflammatory/anti-oxidant potential of the chitosan-based membranes. In fact, the intensity of the chemiluminescence peaks resulting from PMA and fMLP stimulation in the presence of the materials is lower than in the control and was shifted in time which indicates a decrease in the amount of detected ROS and a delaying in the response of the cells to the stimuli. Thus the maximum activation capacity of the PMNs in the presence of the materials was either affected or the chitosan-based membranes have the capacity to react with the produced ROS, which can explain the lower intensity and consequently the lower amount of ROS detected.

Furthermore, the alteration in time of the signal measured might be a consequence of the cell-material interactions that occur at the surface of the different membranes. In fact, the response obtained in the presence of the chitosan membranes was different from the observed for the Cht/soy and hybrid membranes. The PMNs stimulated with PMA and in contact with chitosan membranes, showed an intensity of the chemiluminescence peak resultant from the oxidation of luminol by HO^-, lower than the observed for the control and for the two other chitosan-based membranes. In contrast, chitosan membranes showed to induce comparable fMLP-stimulated HO^- production to control and higher PMA and fMLP-stimulated O_2^- production than the other materials.

The *in vivo* biological acceptance of an implanted biomaterial always involves inflammation and wound healing, without which the body would only tolerate the biomaterial instead of get it into a functional and long-term association [11].

The chitosan/soy blended membranes were obtained by combination of chitosan and soy protein. In a previous study [23], the chemical cross-linking of this two components was performed with glutaraldehyde in order to increase their interaction reducing the immiscibility [42].

Despite the fact that the chitosan-based membranes presented a rougher surface and higher surface energy and siloxane bonds when comparing to chitosan membrane alone [41], the results showed that is not possible to establish a direct correlation with the PMN's activation in direct

contact with the membranes and without chemical stimulants (PMA and fMLP). Nonetheless, they still retain their capacity of activation and it is imperative to consider that the stimulation and activation of these cells is highly influenced by the type of molecules or mediators adsorbed to the surface of materials [43, 44] once they are implanted *in vivo*. PMNs that are activated mainly in response to the wound healing process subsequent to the injury produced by the implantation procedure, at least, are not directly activated by the chitosan/soy membranes *in vitro*, as it was proved by the poor activation demonstrated by the production of ROS. Even though, it is possible that, *in vivo*, the response elicited by the same membranes could differ. The present results show that the chitosan/soy membranes, *in vitro*, were not able to stimulate human PMNs neither for the release of lysozyme nor for the production of ROS found in the "respiratory burst". Nonetheless, the *in vivo* activation of PMNs by the implantation of any medical device for tissue engineering purposes is required at controlled levels, since their function in wound hound healing precedes the adaptive changes if the tissue recovers from injury and returns to normal function. The low *in vitro* stimulation of the PMNs induced by these chitosan/soy-based membranes seems to be a good indicator for the development of a normal wound healing process, when implanted *in vivo*, as well as the normal restoration of the tissue function.

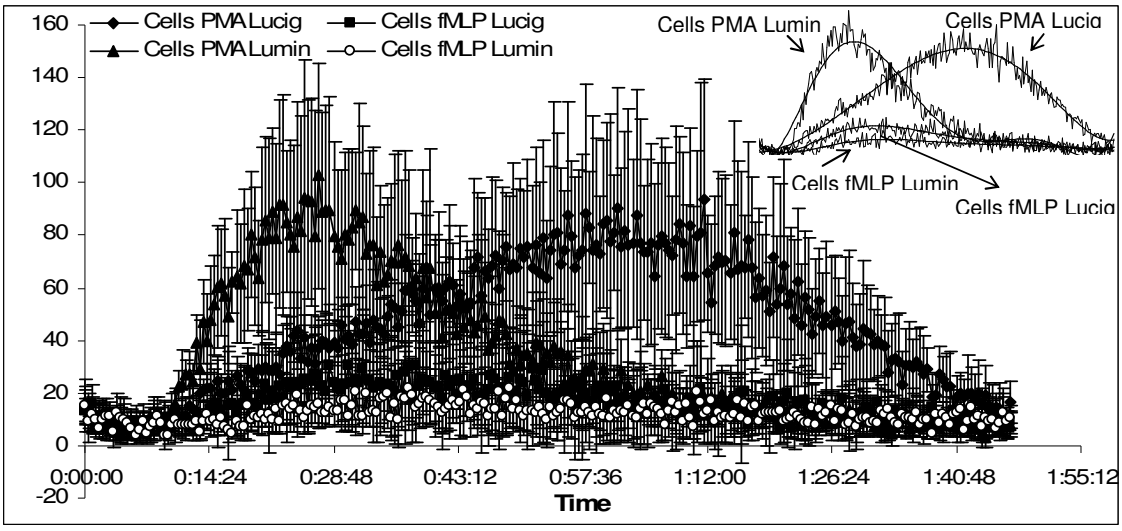

Figure 3.2: PMA and fMLP-stimulated chemiluminescence profiles for polymorphonuclear neutrophils incubated for 107 minutes at 37°C. Superoxide anion generation was detected by the oxidation of lucigenin while the generation of the hydroxyl anion was detected after the oxidation of luminol. In the tested conditions, PMA was able to stimulate human neutrophils for the production of either O_2^- or HO^-, but fMLP was not able to stimulate neutrophils to produce neither O_2^- nor HO^-. The figure shows representative data of five separate experiments. Schematic representation of graph A.

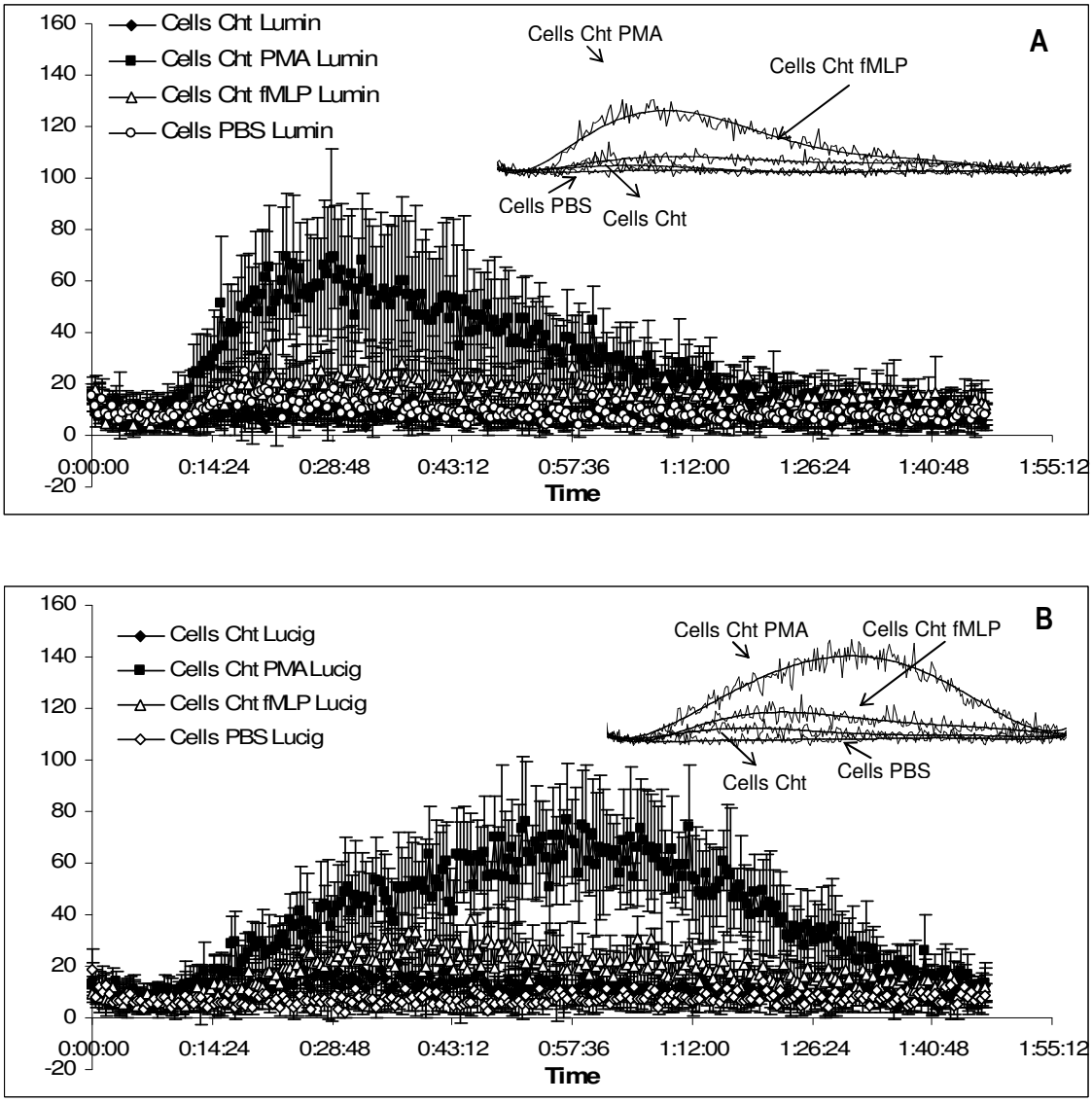

Figure 3.3: Influence of chitosan membranes on the production of HO^- (A) and O_2^- (B) by polymorphonuclear neutrophils with and without PMA and fMLP stimulation. In the presence of the chitosan membranes, unstimulated PMNs and fMLP-stimulated cells did not have the ability to produce neither O2$^-$ nor HO^-. Contrarily, PMA-stimulated PMNs in contact with the chitosan membranes produced either O_2^- or HO^-. Schematic representation of graph A.

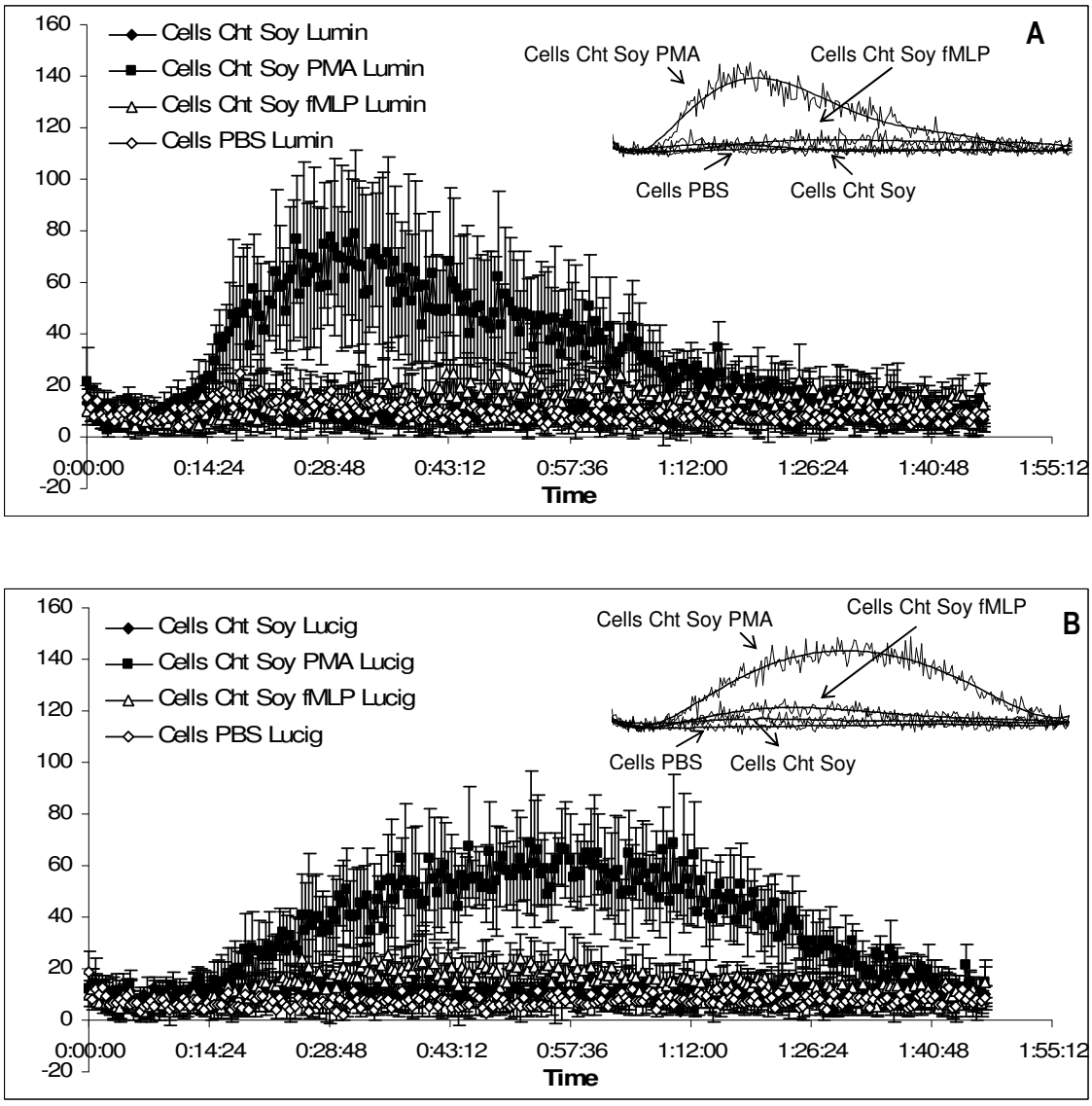

Figure 3.4: Influence of chitosan/soy membranes on the production of HO^- (A) and O_2^- (B) by polymorphonuclear neutrophils with and without PMA and fMLP stimulation. In the presence of the chitosan/soy membranes, unstimulated PMNs and fMLP-stimulated cells did not have the ability to produce neither O2$^-$ nor HO^-. Contrarily, PMA-stimulated PMNs in contact with the chitosan membranes produced either O_2^- or HO^-. Schematic representation of graph A.

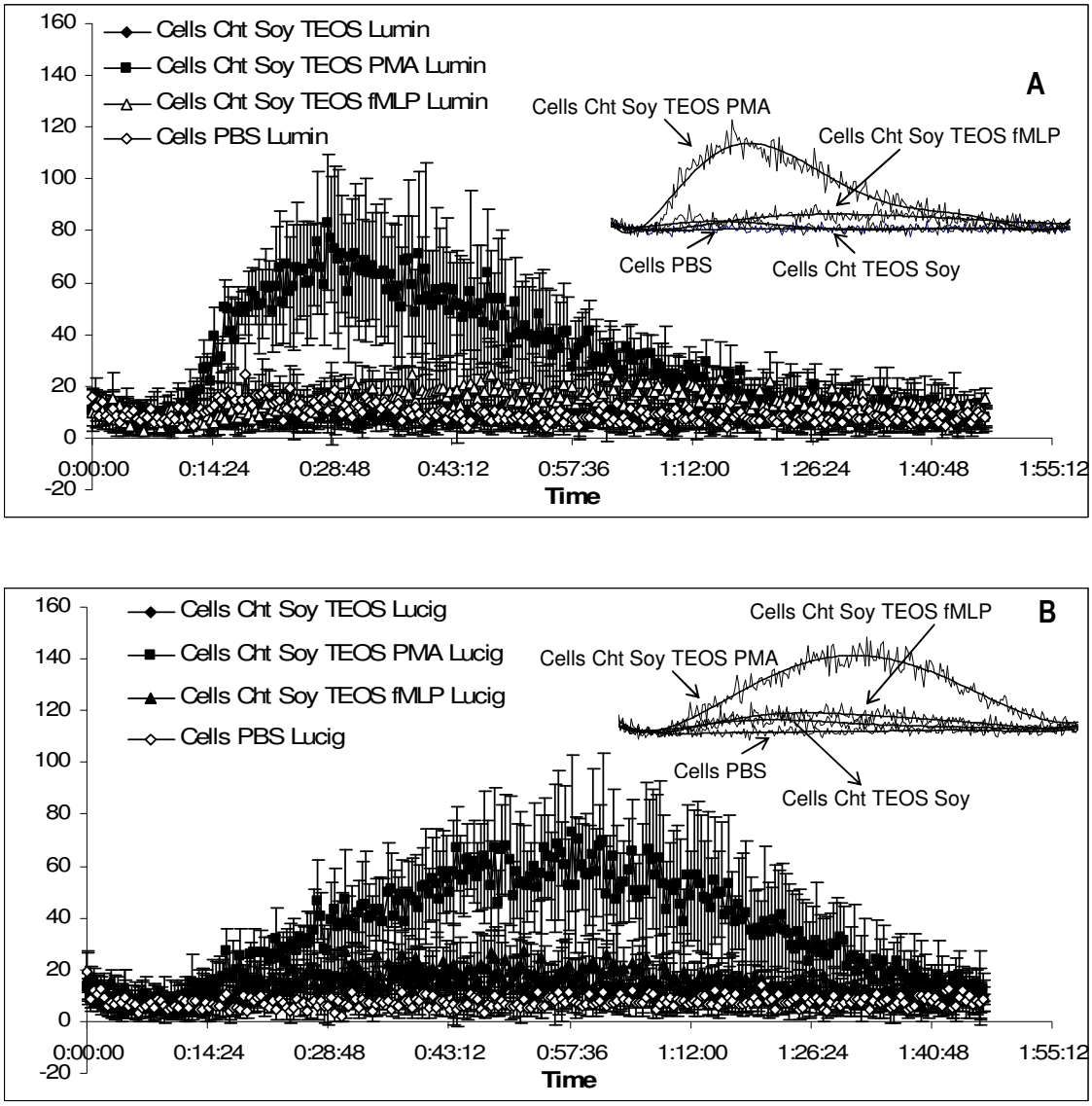

Figure 3.5: Influence of hybrid membranes on the production of HO^- (A) and O_2^- (B) by polymorphonuclear neutrophils with and without PMA and fMLP stimulation. In the presence of the TEOS-crosslinked chitosan/soy membranes, unstimulated PMNs and fMLP-stimulated cells did not have the ability to produce neither $O2^-$ nor HO^-. Contrarily, PMA-stimulated PMNs in contact with the chitosan membranes produced either O_2^- or HO^-. Schematic representation of graph A.

Acknowledgments

This work was carried out under the scope of the European NoE EXPERTISSUES (NMP3-CT-2004-500283) and partially supported by the European STREP Project HIPPOCRATES (NMP3-CT-2003-505758).

References

1. Shi, C., et al., *Therapeutic Potential of Chitosan and Its Derivatives in Regenerative Medicine.* J Surg Res, 2006.
2. Marreco, P.R., et al., *Effects of different sterilization methods on the morphology, mechanical properties, and cytotoxicity of chitosan membranes used as wound dressings.* J Biomed Mater Res, 2004. **71B**(2): p. 268-77.
3. Azad, A.K., et al., *Chitosan membrane as a wound-healing dressing: characterization and clinical application.* J Biomed Mater Res B Appl Biomater, 2004. **69**(2): p. 216-22.
4. Khor, E. and L.Y. Lim, *Implantable applications of chitin and chitosan.* Biomaterials, 2003. **24**(13): p. 2339-49.
5. Ishihara, M., et al., *Acceleration of wound contraction and healing with a photocrosslinkable chitosan hydrogel.* Wound Repair Regen, 2001. **9**(6): p. 513-21.
6. Howling, G.I., et al., *The effect of chitin and chitosan on the proliferation of human skin fibroblasts and keratinocytes in vitro.* Biomaterials, 2001. **22**(22): p. 2959-66.
7. Wedmore, I., et al., *A special report on the chitosan-based hemostatic dressing: experience in current combat operations.* J Trauma, 2006. **60**(3): p. 655-8.
8. Burkatovskaya, M., et al., *Use of chitosan bandage to prevent fatal infections developing from highly contaminated wounds in mice.* Biomaterials, 2006. **27**(22): p. 4157-64.
9. Singla, A.K. and M. Chawla, *Chitosan: some pharmaceutical and biological aspects--an update.* J Pharm Pharmacol, 2001. **53**(8): p. 1047-67.
10. Mikos, A.G., et al., *Host response to tissue engineered devices.* Adv Drug Deliv Rev, 1998. **33**(1-2): p. 111-139.
11. Hunt, J.A., *Inflammation*, in *Encyclopedia of Materials: Science and Technology*, K.H.J. Buschow, et al., Editors. 2001, Elsevier Science Ltd. p. 40068-4075.
12. Stevens, A., J.S. Lowe, and B. Young, *Wheater's Basic Histopathology: A Colour Atlas and Text*. Fourth Edition ed. 2002, Edinburgh: Churchill Livingstone. 295.
13. Williams, D.F., *Biocompatibility Principles*, in *Encyclopedia of Materials: Science and Technology*, K.H.J. Buschow, et al., Editors. 2001, Elsevier Science Ltd. p. 542-548.
14. Marques, A.P., R.L. Reis, and J.A. Hunt, *An in vivo study of the host response to starch-based polymers and composites subcutaneously implanted in rats.* Macromol Biosci, 2005. **5**(8): p. 775-85.
15. Chander, C.L., et al., *Myofibroblasts in cotton-induced granulation tissue and the bovine adrenal capsule: morphological aspects.* Int J Tissue React, 1989. **11**(4): p. 161-3.

16. Martin, P. and S.J. Leibovich, *Inflammatory cells during wound repair: the good, the bad and the ugly.* Trends Cell Biol, 2005. **15**(11): p. 599-607.
17. Marques, A.P., R.L. Reis, and J.A. Hunt, *Cytokine secretion from mononuclear cells cultured in vitro with starch-based polymers and poly-L-lactide.* J Biomed Mater Res, 2004. **71A**(3): p. 419-29.
18. Liu, L., et al., *Surface-related triggering of the neutrophil respiratory burst. Characterization of the response induced by IgG adsorbed to hydrophilic and hydrophobic glass surfaces.* Clin Exp Immunol, 1997. **109**(1): p. 204-10.
19. Mutasa, H.C., *Analysis of human neutrophil granule protein composition in chronic myeloid leukaemia by immuno-electron microscopy.* Cell Tissue Res, 1989. **258**(1): p. 111-7.
20. Rice, W.G., J.M. Kinkade, Jr., and R.T. Parmley, *High resolution of heterogeneity among human neutrophil granules: physical, biochemical, and ultrastructural properties of isolated fractions.* Blood, 1986. **68**(2): p. 541-55.
21. Segal, A.W., *How neutrophils kill microbes.* Annu Rev Immunol, 2005. **23**: p. 197-223.
22. Etienne, O., et al., *Degradability of polysaccharides multilayer films in the oral environment: an in vitro and in vivo study.* Biomacromolecules, 2005. **6**(2): p. 726-33.
23. Silva, S.S., et al., *Physical properties and biocompatibility of chitosan/soy blended membranes.* J Mater Sci Mater Med, 2005. **16**(6): p. 575-9.
24. Silva, R.M., et al., *Influence of beta-radiation sterilisation in properties of new chitosan/soybean protein isolate membranes for guided bone regeneration.* J Mater Sci Mater Med, 2004. **15**(4): p. 523-8.
25. PP, B.M., et al., *Chitosan particles agglomerated scaffolds for cartilage and osteochondral tissue engineering approaches with adipose tissue derived stem cells.* J Mater Sci Mater Med, 2005. **16**(12): p. 1077-85.
26. Tuzlakoglu, K., et al., *Production and characterization of chitosan fibers and 3-D fiber mesh scaffolds for tissue engineering applications.* Macromol Biosci, 2004. **4**(8): p. 811-9.
27. Robinson, J.P., *Oxygen and Nitrogen Reactive Metabolites and Phagocytic Cells*. Phagocyte Function: A Guide for Research and Clinical Evaluation, ed. J.P.R.a.G.F. Babcock. 1998: Wiley-Liss, Inc. 217-252.
28. Li, Y., et al., *Validation of lucigenin (bis-N-methylacridinium) as a chemilumigenic probe for detecting superoxide anion radical production by enzymatic and cellular systems.* J Biol Chem, 1998. **273**(4): p. 2015-23.

29. Azadniv, M., et al., *Neutrophils in lung inflammation: Which reactive oxygen species are being measured?* Inhal Toxicol, 2001. **13**(6): p. 485-95.
30. Marques, A.P., R.L. Reis, and J.A. Hunt, *Evaluation of the potential of starch-based biodegradable polymers in the activation of human inflammatory cells.* J Mater Sci Mater Med, 2003. **14**(2): p. 167-73.
31. Lee, Y.-T., et al., *Effects of phenolic acid esters and amides on stimulus-induced reactive oxygen species production in human neutrophils.* Clinica Chimica Acta, 2005. **352**: p. 135-141.
32. Silva, S.S., et al., *Physicochemical Characterization of Novel Chitosan-Soy Protein/TEOS Porous Hybrids for Tissue Engineering Applications.* Materials Science Forum, 2006. **514-516**: p. 1000-1004
33. Reis, R.L., et al., *Processing and in vitro degradation of starch/EVOH thermoplastic blends.* Polym Int, 1997. **43**: p. 347.
34. Salton, M.R., *The properties of lysozyme and its action on microorganisms.* Bacteriol Rev, 1957. **21**(2): p. 82-100.
35. McPhail, L.C., P.M. Henson, and R.B. Johnston, Jr., *Respiratory burst enzyme in human neutrophils. Evidence for multiple mechanisms of activation.* J Clin Invest, 1981. **67**(3): p. 710-6.
36. Borregaard, N. and J.B. Cowland, *Granules of the human neutrophilic polymorphonuclear leukocyte.* Blood, 1997. **89**(10): p. 3503-21.
37. Schwartz, B.R., et al., *A novel beta 1 integrin-dependent mechanism of leukocyte adherence to apoptotic cells.* J Immunol, 1999. **162**(8): p. 4842-8.
38. Fadeel, B., et al., *Involvement of caspases in neutrophil apoptosis: regulation by reactive oxygen species.* Blood, 1998. **92**(12): p. 4808-18.
39. Tuo, J., S. Loft, and H.E. Poulsen, *Enhanced benzene-induced DNA damage in PMA-stimulated cells in vitro and in LPS-treated animals.* Free Radic Biol Med, 1999. **26**(7-8): p. 801-8.
40. Melloni, E., et al., *The involvement of calpain in the activation of protein kinase C in neutrophils stimulated by phorbol myristic acid.* J Biol Chem, 1986. **261**(9): p. 4101-5.
41. Silva, S.S., et al., *Development of novel chitosan/soy protein based hybrid membranes prepared by means of an in situ cross-linking process.* 2007.
42. Silva, S.S., et al., *Morphology and miscibility of chitosan/soy protein blended membranes. Carbohydrate polymers* 2007.

43. Jackson, J.K., et al., *Neutrophil activation by plasma opsonized polymeric microspheres: inhibitory effect of pluronic F127.* Biomaterials, 2000. **21**(14): p. 1483-91.

44. Nimeri, G., et al., *The influence of plasma proteins and platelets on oxygen radical production and F-actin distribution in neutrophils adhering to polymer surfaces.* Biomaterials, 2002. **23**(8): p. 1785-95.

Chapter IV

Chitosan improves the biological performance of soy-based biomaterials

4.1 Abstract

Soybean protein has been proposed for distinct applications within nutritional, pharmaceutical, and cosmetic industries among others. More recently, soy-based biomaterials have also demonstrated promising properties for biomedical applications. However, although many reports within other fields exist, the inflammatory/immunogenic potential of those materials is still poorly understood and therefore can hardly be controlled. On the contrary, chitosan has been well explored in the biomedical field, either by itself or combined with synthetic or other natural-based polymers. Therefore, the combination of chitosan with soybean protein is foreseen as a suitable approach to control the biological behaviour of soy-based biomaterials. Under this context this work was designed to try to understand the influence of chitosan in the host response elicited by soy-based biomaterials.

Soybean isolate protein (SI-P) and chitosan (Cht-P) were injected as suspension into the intraperitoneal cavity of rats. SI-P induced the recruitment of higher numbers of leukocytes compared to the Cht-P during the entire observation period. In this sense, SI-P elicited a considerable reaction from the host comparing to the Cht-P, which elicited leukocyte recruitment similar to the negative control.

After subcutaneous implantation of the soybean and denaturated membranes (SI-M and dSI-M) a severe host inflammatory reaction was observed. Conversely chitosan/soy-membranes (Cht/Soy-M) showed the induction of a normal host response after subcutaneous implantation in rats which allowed concluding that the addition of chitosan to the soy-based membranes improved their *in vivo* performance. Thus, the presented results assert the improvement of the host response, considering inflammatory cells recruitment and overall inflammatory reaction, when chitosan is combined to soybean. Together with previous results that reported their promising physicochemical characteristics and their inability to activate human PMNs *in vitro*, the herein presented conclusions reinforce the usefulness of the cht/soy-based membranes and justify the pursue for a specific application within the biomedical field.

Key Words: chitosan-based materials; soy-based materials; host response; leukocyte kinetics; *in vivo* inflammatory reaction

***This chapter is based on the following publication:**

T. C. Santos, A. P. Marques, S. S. Silva, J. M. Oliveira, J. F. Mano, A. G. Castro, M. van Griensven, R. L. Reis, *Chitosan improves the biological performance of soy-based biomaterials*, **2009. *Submitted*.**

4.2 Introduction

Soybean protein biomaterials have demonstrated quite interesting properties for bone regeneration purposes [1-5], nonetheless few studies [6-8] have in fact investigated its suitability within the field. Santin et al. [9] showed that soybean-based biomaterials promote osteoblast-like cells' differentiation *in vitro* without inducing activation of human macrophages [9]. However, additional studies are required to further elucidate the potential of these materials in the biomedical field. Moreover, despite the wide use of soy products in nutritional, pharmaceutical, cosmetic and many other industries [10] numerous allergic reactions, from skin, gastrointestinal and respiratory tract up to anaphylaxis [10, 11] have been attributed to the soy Gly m 4 protein, homologous of the major birch pollen allergen, Bet v 1 [11].

In contrast to soybean protein, chitosan has been extensively proposed in the biomedical arena for bone-[12-16], cartilage-[13, 17, 18] and skin-related [13, 19, 20] applications. The promotion of osteoblast proliferation and activity characterized by an up-regulated expression of bone-related proteins and mineral rich matrix deposition, directed by chitosan-based structures, has been well demonstrated [15, 16]. Concerning cartilage-related applications, the structural similarity of chitosan with various glycosaminoglycans (GAGs) found in articular cartilage has burst the investigations. Besides playing a role in modulating chondrocyte morphology, differentiation and function [18], chitosan was shown to act on the growth of epiphyseal cartilage and wound healing of articular cartilage [17]. The successful role of chitosan in the skin wound healing mechanisms has been successively confirmed [19-21]. Although it was observed that chitosan does not directly accelerate extracellular matrix (ECM) production by fibroblast-like cells [22], it was proven that chitosan-based materials have the capacity to promote the production of growth factors, such as transforming growth factors (TGF)-β1 and platelet-derived growth factor (PDGF) by macrophages [21] which, in turn, induce and/or enhance ECM production [20, 21]. Moreover, these materials accelerate the infiltration of polymorphonuclear neutrophils (PMNs) at the early stage of wound healing that is followed by the production of collagen by fibroblasts [19].

Despite all the promising results in the use of chitosan for the biomedical field, studies from different groups [21, 23, 24] have shown controversial results after implanting chitosan-based materials. An adverse inflammatory response showing extensive macrophage activation after subcutaneous implantation of, either lyophilized chitosan [21] or collagen-chitosan-hydroxyapatite hydrogels in rats [23] was detected. Conversely, other authors showed that chitosan hydrogels induce mild acute and chronic inflammatory responses, identical to the typical wound healing cascade, after subcutaneous [25] and intraperitoneal implantations in rats [24].

Nevertheless the significance of chitosan within the biomedical field is unquestionable since the observed differences on the response of cells and tissues to the different chitosan-based materials may be attributed or influenced by the source of the raw material or by the shape of the biomaterial. Chitosan has also been one of the most used materials to improve the biological performance of other materials such as metals [26-29] and other biodegradable polymers [7, 16, 30]. Recent studies demonstrated that neonatal rat calvaria osteoblasts proliferate at higher rates on titanium surfaces coated with chitosan [26], which also promote better adhesion of osteoblast-like cells [27]. In the same way, the hydrophobic surface of poly(L-lactide) (PLLA) matrices coated with chitosan displayed a different wetability and enhanced cell affinity [28]. In a rabbit tibia defect model, Bumgardner and co-workers [29] showed that the coating of titanium pins with chitosan induced minimal inflammatory response and a typical healing sequence of fibrous woven bone formation followed by the development of lamellar bone. This is indicative for the role of the chitosan-coatings in the osseointegration of orthopaedic implants [29]. When blended with synthetic polymers, such as polycaprolactone [16] or poly(butylene succinate) [30], chitosan have shown to exert a synergistic effect of on the blend. While the synthetic polyester promoted the adhesion of osteoblast-like cells, the presence of chitosan significantly enhanced their osteoblastic activity [16, 30]. Chitosan-soy based membranes have also demonstrated improved *in vitro* biological performance in comparison to unblended soy-based materials [7]. Additionally, *in vitro* analysis of the potential of chitosan/soy-based membranes to stimulate immune system cells showed that they did not elicit the activation of human polymorphonuclear neutrophils freshly isolated from circulating blood [31]. Despite the *in vitro* promising results, *in vivo* validation of the improved biological behaviour of the soy-based materials after blended with chitosan is needed, since the organism includes a very complex immune system. Therefore, the aim of this study was to test the influence of chitosan in the host response provoked by soy-based biomaterials. The response to the raw materials soybean protein isolate (SI-P) and chitosan (Cht-P) in the form of powder was assessed after injection in the intraperitonial cavity of rats. The *in vivo* reaction to soybean protein isolate (SI) and chitosan-soy (Cht/Soy) membranes was compared after subcutaneous implantation of the biomaterials. The results from the different models and the comparison of the performance of the SI and the chitosan blended membranes allowed to conclude about the effect of the chitosan over the *in vivo* behaviour of soy-based membranes.

4.3 Materials and Methods

4.3.1 Materials

The tested materials were: **p**owders of i) soybean protein isolate (SI-P) and ii) chitosan (cht-P); and **m**embranes of iii) soybean protein isolate (SI-M) and chitosan/soy (Cht/Soy-M). Soybean protein isolate (SI) was provided by *Loders Crocklaan BV* (The Netherlands) and the reagent grade chitosan, with a deacetylation degree of 85% and viscosimetric molecular weight of about 700 KDa, by Sigma (USA). The SI membranes were prepared by solvent casting, according to a previously reported procedure [32]. Briefly, SI was suspended in distilled water (10%w/v) at room temperature under gentle stirring in order to avoid protein denaturation and consequently, foam formation. Glycerol was added to this suspension (1g per 5g of SI), which was then poured into moulds, directly in the drying place. The moulds were not moved until complete drying in order to assure that the insoluble part of SI was uniformly distributed. Drying was performed at room temperature and relative humidity. Alternatively, denaturated SI (dSI) membranes were prepared by heating the referred SI suspensions at 100ºC during 2h. After denaturation, the obtained viscous solution was casted as described above. Chitosan/soy protein blended membranes (CS) (average thickness of 84 μm and 17 mm of diameter) were prepared by solvent casting according to a procedure described elsewhere [7]. Briefly, chitosan was dissolved in an aqueous acetic acid 2% (v/v) solution at a concentration of 4wt%. A soy suspension (1wt%) was prepared by slowly dispersing the soy protein powder, under constant stirring, in distilled water with glycerol. After adjusting the pH to 8.0±0.3 with 1M sodium hydroxide, the dispersion was heated in a water bath at 50ºC for 30 min. The Cht and the SI solutions were mixed at a weight ratio of 75/25% chitosan/soy (CS75). After homogenization, the CS75 solution was casted into Petri dishes and dried at room temperature for 6 days. The neutralization of the membranes was obtained by immersion in 0.1 M sodium hydroxide for about 10 min. Membranes were washed with distilled water to remove all traces of alkali and again the membranes were dried at room temperature. The materials were sterilized under standard conditions by ethylene oxide [33].

4.3.2.Animals

Twenty four male Wistar Han rats (Charles River, Spain) weighting 420-450g were used for the subcutaneous implantation of SI-M and dSI-M, as well as for the intraperitoneal injection of SI-P and Cht-P. Four male Sprague-Dawley rats (Himberg breeding institute, Austria) weighting 320-470g were used for the subcutaneous implantation of the Cht/Soy-M. Animal experimentation was performed according to the standard operating procedures required from the national authorities and after their respective approval.

4.3.4 Intraperitoneal injection of SI and chitosan powders

Phosphate buffer saline (PBS) (0.01M – Sigma-Aldrich, USA) suspensions of the powders with different concentrations (0.1% and 1% SI; and 0.1%, 1% and 2% chitosan) were injected into the intraperitoneal (IP) cavity of the rats (1 mL per animal). Three animals per concentration and per time period (16 hours, 3 days, 7 days and 15 days) were used. One animal per each concentration and per time period was injected with sterile PBS as control. The animals had access to food and water *ad libitum* during the entire observation period.

4.3.5.Subcutaneous implantation of membranes

Subcutaneous implantation of the SI membranes

For the implantation of the SI-M and the dSI-M, the Wistar Han rats were anaesthetized by an intraperitoneal injection of 2.5% pentobarbital (CEVA Santé Animale, France). The interscapular region was shaved and disinfected with 70% ethanol, a full thickness skin longitudinal incision (about 1.5 cm) was performed in each animal and one cranial oriented subcutaneous pocket was created by blunt dissection. A membrane (12mm diameter) was positioned into each pocket and the incision was carefully sutured. Three animals were used per each time period of implantation (3, 7, 15 and 30 days), and per type of membrane. For each time period of implantation a control animal, with an empty subcutaneous pocket, was set. The animals were kept in single cages with food and water *ad libitum* during all experimentation time.

Subcutaneous implantation of the Chit/Soy membranes

Male Sprague-Dawley rats were anesthetized prior to surgery by intramuscular injection of 90 mg/kg ketamine hydrochloride (Schoeller Chemie Produkte, Vienna, Austria) and 5 mg/kg xylazine hydrochloride (Bayer AG, Leverkussen, Germany). For the subcutaneous implantation of the Cht/Soy-M, 2 medial full thickness skin incisions were performed on the dorsum of the rats. Two craniolateral oriented pockets per each incision one to the left and one to the right were subcutaneously created by blunt dissection, and the membranes were inserted into these pockets (4 membranes/animal). The animals were kept in single cages with food and water *ad libitum* during all experimentation time.

4.3.6 Cytological preparations

The kinetics of the inflammatory reaction induced by the injected suspensions (made from the powders) was assessed by analysis of the peritoneal exudate. The animals were anaesthetized with a subcutaneous injection of 2.5% pentobarbital and sacrificed with an intracardial overdose of anaesthetic. The abdominal area of each animal was disinfected with 70% ethanol and an incision in the abdominal skin and the linea alba was performed, in order to expose the external abdominal wall as most as possible to the subsequent lavage. Thirty five mL of sterile PBS

solution were injected into the intraperitoneal cavity, and the abdomen was massaged in order to recover the inflammatory cells adherent to the abdominal organs and peritoneal cavity. The peritoneal exudate was collected in a syringe and stored on ice until further analysis. The total number of leukocytes was counted using a haemocytometer and cytospins of $1x10^6$ cells were performed by cytocentrifugation (5 minutes at 1000 rpm). Cells were then gently washed in tap water and fixed in formaldehyde-ethanol (50/50 (v/v) – formaldehyde 3.7% and absolute ethanol) for 45 seconds. The Wright's staining for blood samples (Hemacolor, Merck, Germany) was performed and after being dried, each slide was observed in an optical microscope. A minimum of 300 cells per sample was counted in different areas of the cytospin and the different types of leukocytes distinguished.

4.3.7 Histological preparations

The animals with the implanted SI-M, dSI-M and Cht/Soy-M were anaesthetized, at the end of each implantation period, respectively with an intraperitoneal injection of 2.5% pentobarbital or with an intramuscular injection of 90 mg/kg ketamine hydrochloride and 5 mg/kg xylazine hydrochloride, and sacrificed with an intracardial overdose of anaesthetic. The implanted membranes, the respective surrounding tissue and the lymph nodes of the rats with Cht/Soy-M were explanted and prepared for histological analysis using H&E staining and subsequently analyzed using an Axioplan Imager Z1 microscope (Zeiss, Germany). Inflammatory reaction, integration of the membranes in the host tissue and *in vivo* degradation were the assessed parameters

Statistical Analysis

Mean values and standard deviations are reported for the measurements [34] of the leukocyte kinetics. Data was analysed by a single factor ANOVA test and the significance value was set at $p<0.05$.

4.4 Results

4.4.1 Leukocyte recruitment kinetics

The intraperitoneal injection of a suspension of SI powders allowed creating, after counting the existing sub-populations, the kinetic of leukocyte recruitment into in the intraperitoneal cavity subsequent to its injection which is reported in table 4.1.

The number PMNs, expected to be the firstly recruited cell type, was neglectful in the negative control, showing that the injection of the saline solution did not elicit a significant recruitment of those cells. Few PMNs were found at 16 hours after the saline solution injection which is expected as a normal reaction to the injection.

Conversely, PMNs were extensively recruited early after injection of the SI-P suspensions. The number of recruited PMNs reached a peak 16 hours post-injection of the 0.1% SI-P suspension and decreased to values similar to the control from that time point onward. After injection of the higher concentration of SI-P (1%), higher numbers of PMNs were detected up to 3 days while consecutively decreasing.

Concerning the number of PMNs after the injection of the chitosan suspensions, a recruitment pattern similar to the negative control was observed at all times. A higher, but not statistically significant (p>0.05) number of PMNs was recruited in the presence of the higher concentration of Cht-P (2%) 16 hours post-injection. This number decreased afterwards to comparable values to the observed for lower concentrations of Cht-P and for the control.

Macrophages (MO), either tissue resident or recruited from the bloodstream, are the most abundant cells into the intraperitoneal cavity at physiological conditions. Therefore, the constant number of MO observed for the control along the time was expected and attributed to resident cells. Sixteen hours after the injection of the SI-P, the number of detected MO was higher than for the negative control (p>0.05) and associated, together with the PMNs reaction, to an expected inflammatory reaction to any implantation procedure. MO recruitment reached a maximum between days 3 and 7 (p>0.05), and between 7 and 14 days (p>0.05) respectively for 0.1% and 1% of SI-P. The number of MO started to decrease from that day onward although a significantly higher number, compared to the negative control, was detected at day 15 for 1% SI-P.

Regarding the number of MO present in the peritoneal cavity of the animals injected with the three different concentrations of Cht-P, no significant differences (p>0.05) were observed between them and in comparison to the negative control at all time points.

In the context of a chronic inflammation, it is expected that lymphocytes, the type of cells that correlates with the onset of the reaction, start to migrate from circulation around the day 7 after the inflammatory challenge. Nonetheless, lymphocytes are also resident cells into the peritoneal cavity. The presence of lymphocytes was in fact noticed in the negative control at earlier time points. An increase (p>0.05) in the number of lymphocytes was observed after the injection of the SI-P. The percentage of SI-P and the time of reaction did not induce significant changes over the recruitment kinetics except for 0.1% SI-P at day 3 that presented a value significantly different from the control. As for the PMNs and MO, the number of recruited lymphocytes to the peritoneal cavity in the animals injected with the three different concentrations of Cht-P, was comparable to the negative control at all time points.

The recruitment of eosinophils and mast cells, which are mostly related with allergic reactions, was neglectful after the injection of the saline solution (negative control). The same profile was

observed for all of the concentrations of Cht-P and SI-P during the observation time. An exception was detected for the 0.1% SI-P solution which induced a maximum of eosinophil and mast cell exudation at day 3, although the increase was not statistically significant ($p>0.05$). From that time period onward the number of these cells decreased reaching levels comparable to the other tested concentration and the negative control.

Table 4.1: Number of leukocytes present in the peritoneal cavity of Wistar Han rats, 16 hours, 3, 7 and 15 days after the injection of the different solutions of chitosan and soybean isolate powders.

		Neutrophils ± SD (x10^5)				Macrophages ± SD (x10^5)				Lymphocytes ± SD (x10^5)				Eosinophils ± SD (x10^5)				Mast Cells ± SD (x10^5)			
Time		16h	3d	7d	15d	16h	3d	7d	15d	16h	3d	7d	15d	16h	3d	7d	15d	16h	3d	7d	15d
Chitosan Powders	0.1%	13.8 ±4.8	2.7 ±0.53	0.0 ±0.0	0.0 ±0.0	245 ±125	194 ±25.0	134 ±19.4	176 ±35.5	17.0 ±15.1	3.01 ±0.97	1.36 0.39	5.50 ±4.17	49.9 ±8.48	22.5 ±1.21	16.8 ±2.35	35.1 ±10.6	6.77 ±5.52	7.88 ±4.18	8.49 ±1.03	8.45 ±4.24
	1%	20.1 ±14.2	2.43 ±1.70	0.0 ±0.0	0,19 ±0.054	177 ±51.4	199 ±17.7	179 ±45.4	108 ±87.1	4.73 ±1.14	4.80 ±1.05	4.25 ±2.58	3.26 ±2.80	23.5 ±9.24	46.1 ±18.2	38.1 ±5.71	5.52 ±2.86	1.57 ±0.80	2.31 ±0.93	1.52 ±1.29	5.06 ±7.11
	2%	77.0 ±16.3	3.54 ±4.46	4.94 ±4.71	0.0 ±0.0	323 ±86.1	220 ±79.8	235 ±39.6	85.1 ±1.32	6.39 ±1.40	4.01 ±3.85	7.64 ±4.79	3.16 ±2.55	19.7 ±11.1	39.8 ±19.1	36.1 ±35.1	15.9 ±3.58	0.67 ±1.15	1.87 ±0.58	0.0 ±0.0	22.0 ±1.64
Soybean Powders	0.1%	207 ±120	108 ±143	8.18 ±4.28	0.0 ±0.0	664 ±153	1390 ±459	1110 ±193	797 ±150	71,7 ±47.0	92.3 ±10.3	46.5 ±28.8	18.1 ±3.87	74.3 ±59.7	428 ±222	218 ±55.3	158 ±62.1	49.3 ±19.2	75.9 ±15.7	53.2 ±46.2	6.69 ±2.75
	1%	237 ±49.5	643 ±359	44.4 ±40.1	0.0 ±0.0	914 ±402	1160 ±223	1330 ±686	886 ±38.4	99 ±36.5	60.3 ±12.2	81.7 ±52.3	84.8 ±17.0	9.30 ±5.27	78.5 ±37.5	75.8 ±25.3	135 ±66.1	11.7 ±3.64	0.0 ±0.0	0.0 ±0.0	4.33 ±7.50
Control		26.2	0.0	0.0	4.03	349	369	385	540	19.3	41.2	6.26	36.2	24.9	122	141	94.6	19.3	25.8	14.1	8.05

4.4.2 Histological analysis

SI-M and dSI-M degradation and tissue inflammatory response

Animals did not show any surgical complications during the post-operative period. The explantation of SI-M, dSI-M and the respective surrounding tissue, was performed at 3, 7, 14 and 30 days after the subcutaneous implantation and processed for histological analysis. Inflammatory reaction, integration of the membranes in the host tissue and *in vivo* degradation were the assessed parameters.

The obtained histological sections revealed that, after 3 days of implantation, the SI-M maintained its integrity (Figs. 4.1A-B) compared to the dSI-M (Figs. 4.1C-D) which lost some of its integrity. Additionally, the extension of the observed inflammatory infiltrate was higher in the dSI-M (Figs. 4.1C-D) than in the SI-M (Figs. 4.1A-B) demonstrating that the dSI-M elicited higher recruitment of inflammatory cells in comparison to the SI-M. The histological examination at day 3 of implantation revealed the physical separation between the membranes and the adjacent tissue, resulting from the processing procedure. However, it was possible to notice a more evident detachment of the SI-M (Fig. 4.1A) from the inflammatory infiltrate in contrast to the dSI-M (Fig. 4.1C) in which attached inflammatory cells were easily identified. A detailed observation of the histological sections showed that the inflammatory infiltrate is mainly constituted of PMNs, characterized by multi-lobulated nuclei, recruited from circulation in response to either the SI-M (Fig. 4.1B) or the dSI-M (Fig. 4.1D). Nonetheless, some mononuclear cells, presenting a smaller cytoplasm and a round shaped nucleus, were also observed in both situations.

After 7 days of the subcutaneous implantation of the SI-M and the dSI-M, the density of the inflammatory infiltrate increased (Figs. 4.1E and 4.1G). The degradation of both types of membranes was obvious after 7 days of implantation (Figs. 4.1E-H), although more noticeable, like at 3 days of implantation, for the dSI-M. Moreover, a network of fibrotic tissue was observable surrounding the inflammatory infiltrate, again characterized by the presence of PMNs, which seem to be attempting to phagocyte the polymeric material, and mononuclear cells. In the tissue surrounding the dSI-M, the inflammatory infiltrate was denser and early signs of oedema formation and necrosis with the exteriorization of cell cytoplasm, the presence of cell debris and picnotic nucleus were clearly identified (Fig. 4.1H).

After 14 days of implantation, the expected resolution of a normal inflammatory process was not occurring. In the case of the SI-M, the PMNs persisted (Figs. 4.2A-B). Additionally, cell apoptosis and necrosis are evident (Fig. 4.2B) and seem to increase in comparison to 7 days of implantation. These observations were even more evident for the dSI-M; the density of the inflammatory infiltrate was higher and the signs of necrosis were even clearer (Figs. 4.2C-D). At

this stage, the degradation of the dSI-M was also more pronounced, both compared to the SI-M and to the first 7 days of implantation of the dSI-M.

After 30 days of subcutaneous implantation of the SI-M and dSI-M, the degradation of the membranes, the oedema and necrosis evidently increased more in comparison with the previous implantation periods (Figs. 4.2E-H).

Cht/Soy membranes degradation and tissue inflammatory response

The Cht/Soy-M were subcutaneously implanted in rats for 7 and 14 days. During the post-implantation period no signals of systemic or regional surgical complications were detected for any of the animals. The local and systemic host responses to the implanted materials were analysed after histological processing of the explants comprising the implanted Cht/Soy-M and respective surrounding tissue, and of the axillary and inguinal lymph nodes.

Local reaction to the Cht/Soy-M after 7 days of implantation comprised an inflammatory infiltrate formed by recruited PMNs (Fig. 4.3A). Additionally, some matrix started to be deposited around resident and inflammatory cells present in the subcutaneous tissue. Furthermore, blood vessels and adipocytes were also observed in the surroundings of the implantation site (Fig. 4.3B). Concerning the systemic host response, the analysis of the neighbouring lymph nodes revealed its reactive state characterised by a higher cell density of the germinal centres compared to the medullar region (Fig. 4.3C).

After 14 days of implantation, the progress of the inflammatory reaction was noticed; the inflammatory infiltrate was concentrated a few microns from the membrane and the newly developed vascularisation of connective tissue was evident (Figs. 4.3D-E). The presence of mononuclear cells that typically appear 2 weeks after the implantation of the material, and the absence of persistent PMNs were detected. Moreover foreign body giant cells (Fig. 4.3E) were not observed. Similarly to what was observed for day 7 of implantation, the neighbouring lymph nodes showed comparable signs of reactivity (Fig. 4.3F).

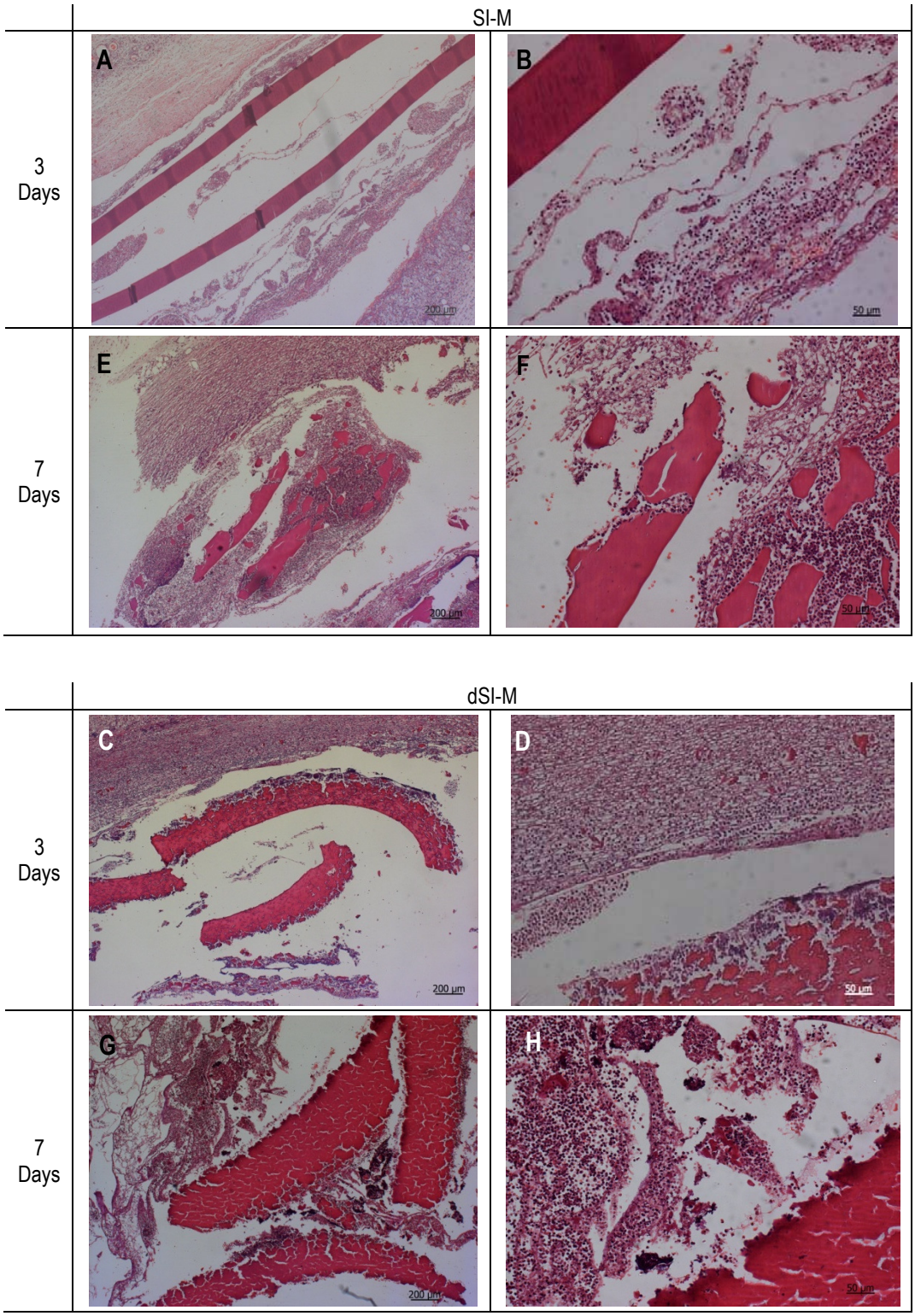

Figure 4.1: Microscopic images obtained from the explanted Soy Isolate Protein Membrane (SI-M) and denaturated SI-M (dSI-M) and surrounding tissue, subcutaneously implanted for 3 and 7 days in rats.

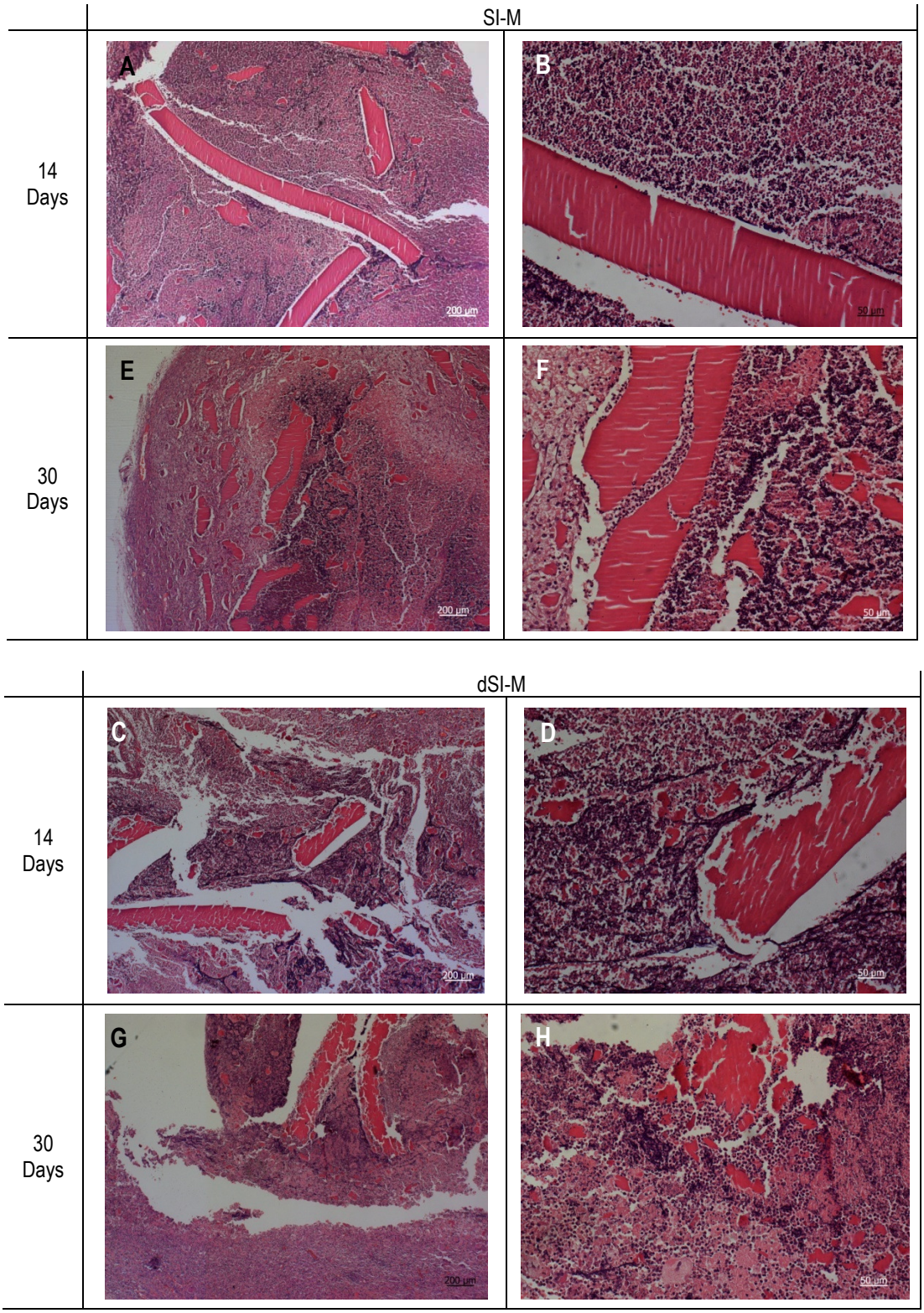

Figure 4.2: Microscopic images obtained from the explanted Soy Isolate Protein Membrane (SI-M) and denaturated SI-M (dSI-M) and surrounding tissue, subcutaneously implanted for 14 and 30 days in rats.

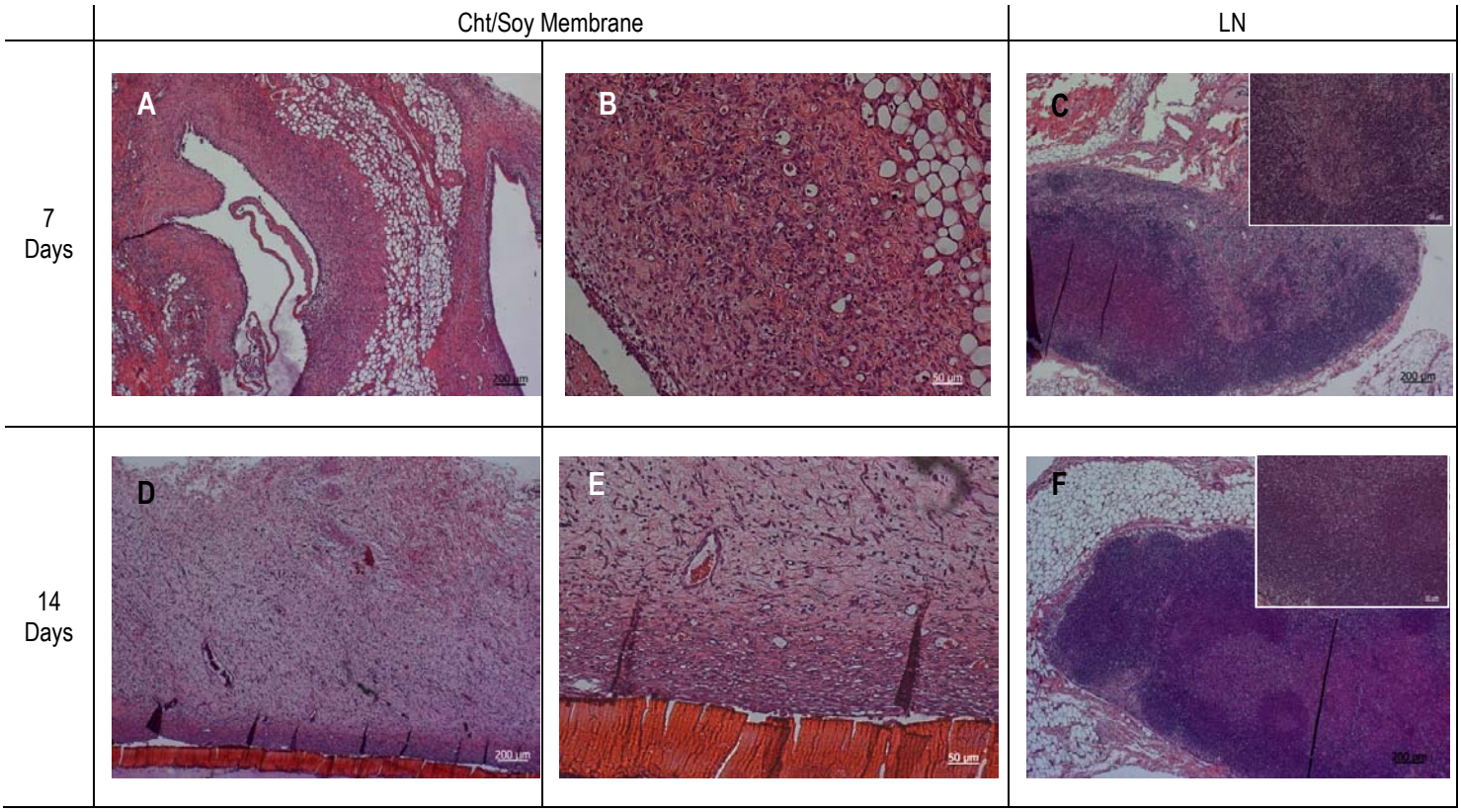

Figure 4.3: Microscopic images obtained from the explanted Chitosan/Soy-based Membranes and surrounding tissue, subcutaneously implanted for 7 and 14 days in rats, as well as the nearby lymph nodes (LN).

4.5 Discussion

The combination of one of the most used natural materials, chitosan [6, 13, 14, 35], with a rather promising one, soy [5, 36], has recently shown to possess very interesting features [7, 8, 31, 32] that should be explored within the context of potential biomedical applications. Following these recent findings, and considering that there is a significant number of reports in the literature that highlight soy's inflammatory and allergic character [11, 37], the evaluation of the *in vivo* behaviour of those materials was missing. Therefore, this study aimed to investigate the *in vivo* host reaction of these materials.

One of the most relevant features of biodegradable biomaterials that determine a successful performance refers to its degradation rate and subsequent degradation products. The direct reaction to these as well as the inability of the host to deal with those products has been frequently reported as the major cause of implant failure [38]. Thus, the testing of chitosan and

soy materials was considered relevant for a first assessment of the inflammatory and allergic potential of the materials in study. The host tissue response to both chitosan and soy suspensions was monitored by investigating the intraperitoneal leukocyte kinetics at 4 different periods of time (3, 7, 14 and 30 days). The basal level of reaction, induced by the procedure, was established with the injection of a saline solution and showed the typical population of inflammatory cells present in the rat peritoneal cavity in a physiological condition of minor trauma due to injection [39]. Macrophages, the intraperitoneal tissues resident cells, were the most evident type of cells detected. Although not at significant numbers, lymphocytes can also be present in the tissues [40], which justify the obtained values for the control.

Concerning leukocyte recruitment by the injection of soybean isolate protein and chitosan as suspensions from the powders into the intraperitoneal cavity of rats, SI-P elicited the recruitment of higher cell numbers compared to Cht-P at all times studied. In this sense, SI-P was considered more reactive to the host comparing to the Cht-P, which independently of the concentration elicited leukocyte recruitment comparable to the negative control. Although it would be expected that a direct effect exists that increasing the concentration of the suspension results in an increase in intensity of the provoked reaction. This was not observed for the cht-P which is in consonance with previous studies with chitosan-based materials, showing a typical inflammatory reaction induced by its implantation [41] .

The observed host response also did not seem to directly correlate with the different concentrations of the tested SI-P. Soybean isolate protein induced a persistent recruitment of all inflammatory cell types in comparison with the chitosan powders and negative control, since mononuclear cells (macrophages and lymphocytes), the hallmark of a chronic inflammation, were extensively present at the latter stage of reaction (14 days). These results seem to be in accordance with the observed reaction after the subcutaneous implantation of the membranes. Despite the absence of physiologic signs of inflammation or infection, the histological analysis of the explants revealed a severe host inflammatory reaction. Comparing the SI-M and the dSI-M, it was possible to observe that the reaction to dSI-M was more intense. The extension of the inflammatory infiltrate was representative of an acute persistent reaction characterised by the presence of PMNs at longer implantation periods (14 and 30 days) that undergo frustrated phagocytosis. The higher degradation rate of the dSI-M, in comparison to SI-M and subsequent presence of smaller fragments of the membrane might be responsible for the stronger reaction since a higher surface area is available for PMNs to respond to. The metabolites secreted by the PMNs in this situation lead to the decrease of the physiological pH and to the apoptosis and necrosis of neighbouring cells, evident at later stages of implantation. Other studies [21, 42, 43]

suggested that surface properties such as hydrophilicity and surface charge determine inflammatory cells apoptosis and necrosis. Nevertheless, a typical foreign body reaction [44] was not observed.

The results of the leukocyte kinetics, where the SI-P induced a severe and persistent recruitment of inflammatory cells in the intraperitoneal cavity of the rats after injection, were indicative of the expected subcutaneous response and could be extrapolated from previous reports of inflammation caused by soy products [11, 37].

The addition of chitosan to the soy-based membranes improved, as expected, the host response which showed the features of a typical inflammatory response to implanted materials [19-21, 24]. Moreover, the integration of the membranes within the surrounding tissue was revealed by the presence of matrix [38] after 2 weeks of implantation. These results are in agreement with the results of other researchers, reporting the *in vitro* inhibition of anti-inflammatory cytokines by chitosan, such as IL-6, IL-8 and TNF-α [45, 46], which tend to prolong the acute inflammatory response, instead of allowing the host to progress to the resolution of inflammation [44]. The non-activated state of the lymph nodes after Cht/Soy-M implantation indicates that the implanted materials were not able to induce a more systemic host reaction and no debris or molecules of the materials were transported through circulation to induce a remote response of the related lymphatic tissues.

The presented results assert the improvement of the host response, considering inflammatory cells recruitment and overall of the inflammatory reaction, when chitosan is added to soybean. Having in consideration previous indications on the behaviour of PMNs after stimulation with Cht/Soy-based membranes [31], the present results may assert the influence of chitosan on masking specific soy reactive epitopes or even on suppressing leukocyte activation, namely PMNs. The Cht/Soy-based membranes showed the induction of a normal inflammatory reaction and the features characterizing this reaction are crucial for the integration of the implanted material, as well as for the ongoing process of wound healing and tissue regeneration. Together with previous results that reported their promising physicochemical characteristics and their inability to activate human PMNs *in vitro* [31], the herein presented conclusions reinforce the usefulness of the cht/soy-based membranes and justify the pursue for a specific application within the biomedical field.

References

1. Vaz, C.M., et al., *Effect of crosslinking, thermal treatment and UV irradiation on the mechanical properties and in vitro degradation behavior of several natural proteins aimed to be used in the biomedical field.* J Mater Sci Mater Med, 2003. **14**(9): p. 789-96.
2. Vaz, C.M., et al., *Casein and soybean protein-based thermoplastics and composites as alternative biodegradable polymers for biomedical applications.* J Biomed Mater Res A, 2003. **65**(1): p. 60-70.
3. Vaz, C.M., et al., *Controlled delivery achieved with bi-layer matrix devices produced by co-injection moulding.* Macromol Biosci, 2004. **4**(8): p. 795-801.
4. Vaz, C.M., et al., *Soy matrix drug delivery systems obtained by melt-processing techniques.* Biomacromolecules, 2003. **4**(6): p. 1520-9.
5. Silva, G.A., et al., *In vitro degradation and cytocompatibility evaluation of novel soy and sodium caseinate-based membrane biomaterials.* J Mater Sci Mater Med, 2003. **14**(12): p. 1055-66.
6. Silva, R.M., et al., *Preparation and characterisation in simulated body conditions of glutaraldehyde crosslinked chitosan membranes.* J Mater Sci Mater Med, 2004. **15**(10): p. 1105-12.
7. Silva, S.S., et al., *Physical properties and biocompatibility of chitosan/soy blended membranes.* J Mater Sci Mater Med, 2005. **16**(6): p. 575-9.
8. Silva, S.S., et al., *Physicochemical Characterization of Novel Chitosan-Soy Protein/TEOS Porous Hybrids for Tissue Engineering Applications.* Materials Science Forum, 2006. **514-516**: p. 1000-1004.
9. Santin, M., et al., *A new class of bioactive and biodegradable soybean-based bone fillers.* Biomacromolecules, 2007. **8**(9): p. 2706-2711.
10. L'Hocine, L. and J.I. Boye, *Allergenicity of soybean: new developments in identification of allergenic proteins, cross-reactivities and hypoallergenization technologies.* Crit Rev Food Sci Nutr, 2007. **47**(2): p. 127-43.
11. Mittag, D., et al., *Soybean allergy in patients allergic to birch pollen: clinical investigation and molecular characterization of allergens.* J Allergy Clin Immunol, 2004. **113**(1): p. 148-54.
12. Tuzlakoglu, K., et al., *Production and characterization of chitosan fibers and 3-D fiber mesh scaffolds for tissue engineering applications.* Macromol Biosci, 2004. **4**(8): p. 811-9.

13. Kim, I.Y., et al., *Chitosan and its derivatives for tissue engineering applications.* Biotechnol Adv, 2008. **26**(1): p. 1-21.
14. Di Martino, A., M. Sittinger, and M.V. Risbud, *Chitosan: a versatile biopolymer for orthopaedic tissue-engineering.* Biomaterials, 2005. **26**(30): p. 5983-90.
15. Zhang, Y., et al., *Calcium phosphate-chitosan composite scaffolds for bone tissue engineering.* Tissue Eng, 2003. **9**(2): p. 337-45.
16. Wu, H., et al., *Response of rat osteoblasts to polycaprolactone/chitosan blend porous scaffolds.* J Biomed Mater Res A, 2009.
17. Lu, J.X., et al., *Effects of chitosan on rat knee cartilages.* Biomaterials, 1999. **20**(20): p. 1937-44.
18. Yamane, S., et al., *Feasibility of chitosan-based hyaluronic acid hybrid biomaterial for a novel scaffold in cartilage tissue engineering.* Biomaterials, 2005. **26**(6): p. 611-9.
19. Ueno, H., et al., *Accelerating effects of chitosan for healing at early phase of experimental open wound in dogs.* Biomaterials, 1999. **20**(15): p. 1407-14.
20. Cho, Y.W., et al., *Water-soluble chitin as a wound healing accelerator.* Biomaterials, 1999. **20**(22): p. 2139-45.
21. Peluso, G., et al., *Chitosan-mediated stimulation of macrophage function.* Biomaterials, 1994. **15**(15): p. 1215-20.
22. Ueno, H., et al., *Evaluation effects of chitosan for the extracellular matrix production by fibroblasts and the growth factors production by macrophages.* Biomaterials, 2001. **22**(15): p. 2125-30.
23. Rucker, M., et al., *Angiogenic and inflammatory response to biodegradable scaffolds in dorsal skinfold chambers of mice.* Biomaterials, 2006. **27**(29): p. 5027-38.
24. Azab, A.K., et al., *Biocompatibility evaluation of crosslinked chitosan hydrogels after subcutaneous and intraperitoneal implantation in the rat.* J Biomed Mater Res A, 2007. **83**(2): p. 414-22.
25. Hong, Y., et al., *Covalently crosslinked chitosan hydrogel formed at neutral pH and body temperature.* J Biomed Mater Res A, 2006. **79**(4): p. 913-22.
26. Cai, K., et al., *Surface modification of titanium thin film with chitosan via electrostatic self-assembly technique and its influence on osteoblast growth behavior.* J Mater Sci Mater Med, 2008. **19**(2): p. 499-506.
27. Bumgardner, J.D., et al., *Chitosan: potential use as a bioactive coating for orthopaedic and craniofacial/dental implants.* J Biomater Sci Polym Ed, 2003. **14**(5): p. 423-38.

28. Lee, J.Y., et al., *Enhanced bone formation by controlled growth factor delivery from chitosan-based biomaterials.* J Control Release, 2002. **78**(1-3): p. 187-97.
29. Bumgardner, J.D., et al., *The integration of chitosan-coated titanium in bone: an in vivo study in rabbits.* Implant Dent, 2007. **16**(1): p. 66-79.
30. Coutinho, D.F., et al., *The effect of chitosan on the in vitro biological performance of chitosan-poly(butylene succinate) blends.* Biomacromolecules, 2008. **9**(4): p. 1139-45.
31. Santos, T.C., et al., *In vitro evaluation of the behaviour of human polymorphonuclear neutrophils in direct contact with chitosan-based membranes.* J Biotechnol, 2007. **132**(2): p. 218-26.
32. Silva, R.M., et al., *Influence of beta-radiation sterilisation in properties of new chitosan/soybean protein isolate membranes for guided bone regeneration.* J Mater Sci Mater Med, 2004. **15**(4): p. 523-8.
33. Reis, R.L., et al., *Processing and in vitro degradation of starch/EVOH thermoplastic blends.* Polym Int, 1997. **43**: p. 347.
34. Kirkwood, B. and J. Sterne, *Essential Medical Statistics*. 2nd Edition ed. 2003: Wiley. 512.
35. Shi, C., et al., *Therapeutic potential of chitosan and its derivatives in regenerative medicine.* J Surg Res, 2006. **133**(2): p. 185-92.
36. Santin, M. and L. Ambrosio, *Soybean-based biomaterials: preparation, properties and tissue regeneration potential.* Expert Rev Med Devices, 2008. **5**(3): p. 349-58.
37. Steinman, H.A., *"Hidden" allergens in foods.* J Allergy Clin Immunol, 1996. **98**(2): p. 241-50.
38. Williams, D.F., *On the mechanisms of biocompatibility.* Biomaterials, 2008. **29**(20): p. 2941-53.
39. Goldsby, R.A., T.J. Kindt, and B.A. Osborne, *Kuby Immunology*. 2000, USA: W. H. Freeman and Company.
40. Rajakariar, R., et al., *Novel biphasic role for lymphocytes revealed during resolving inflammation.* Blood, 2008. **111**(8): p. 4184-92.
41. Malafaya, P.B., et al., *Morphology, mechanical characterization and in vivo neo-vascularization of chitosan particle aggregated scaffolds architectures.* Biomaterials, 2008. **29**(29): p. 3914-26.
42. Brodbeck, W.G., et al., *Biomaterial adherent macrophage apoptosis is increased by hydrophilic and anionic substrates in vivo.* Proc Natl Acad Sci U S A, 2002. **99**(16): p. 10287-92.

43. Mori, T., et al., *Mechanism of macrophage activation by chitin derivatives.* J Vet Med Sci, 2005. **67**(1): p. 51-6.

44. Anderson, J.M., A. Rodriguez, and D.T. Chang, *Foreign body reaction to biomaterials.* Semin Immunol, 2008. **20**(2): p. 86-100.

45. Kim, M.S., et al., *Water-soluble chitosan inhibits the production of pro-inflammatory cytokine in human astrocytoma cells activated by amyloid beta peptide and interleukin-1beta.* Neurosci Lett, 2002. **321**(1-2): p. 105-9.

46. Kim, M.S., et al., *Inhibitory effect of water-soluble chitosan on TNF-alpha and IL-8 secretion from HMC-1 cells.* Immunopharmacol Immunotoxicol, 2004. **26**(3): p. 401-9.

Chapter V

In vivo performance of chitosan/soy-based membranes as wound dressing devices for acute skin wounds

5.1 Abstract

Wound management represents a major clinical challenge when it comes to enhance healing and control pain. Thus, the selection of an appropriate dressing plays an important role both in the complete recovery (regeneration) and in the aesthetic appearance of the regenerated tissue. A wide range of dressings and bandages, adaptable to various types of wounds, are nowadays available in the wound care market. Even though, the increasing interest in the use of natural-based products for biomedicine applications is leading the progress of the field.

In this work, a rat wound dressing model of partial-thickness skin wounds was used to assess the suitability of newly developed chitosan/soy-based (Cht/Soy) membranes as wound dressing material. Healing and tissue regeneration of non-dressed, chitosan/soy membranes and Epigard® dressed wounds were followed macroscopically and histologically for 1 and 2 weeks. Chitosan/soy membranes were found to perform better as compared to the controls, promoting not only a faster, but most importantly, functional regeneration of the chitosan/soy dressed wounds. The re-epithelisation, already observed one week after wounding, was followed by the cornification of the outermost epidermal layer indicating a functional recovery of the excised tissue.

These new Cht/Soy-based membranes possess the desired features in terms of healing stimulation, ease of handling and final aesthetic appearance which are considered to be useful features as wound dressing material. Therefore, these Cht/Soy-based membranes include one of the most promising natural-based materials in the skin healing and regeneration field.

***This chapter is based on the following publication:**

T. C. Santos, B. Höring, K. Reise, A. P. Marques, S. S. Silva, J. M. Oliveira, J. F. Mano, A. G. Castro, R. L. Reis, M. van Griensven, In vivo *performance of chitosan/soy-based membranes as wound dressing devices for acute skin wounds*. **2009. *Submitted*.**

5.2 Introduction

Tissue trauma and pain are two main considerations of wound management. Thus, the appropriate dressing selection plays an important role both in the complete regeneration and in the aesthetic appearance of the injured tissue [1]. A wide range of dressings and bandages, adaptable to various types of wounds, are nowadays available in the wound care market and many currently applied in the clinics. The traditional wound dressing that simply covered and protected the wound [2, 3] were replaced by alternatives that may allow control wound moist [4-7] and more recently to dressings with an (bio-)active role in the healing environment [8, 9]. Nonetheless, further developments that can facilitate the healing process or address issues such as the control of the chemical environment and bacterial infection are still required and desired. In fact, most of the existing products need to be changed every few days after their application and, in some cases, there is the need to substitute the material to maintain/accelerate the ongoing healing process [10].

Indiscriminately, synthetic [11-14], natural [8, 15, 16] or biological materials [10, 17, 18] have been presented along the years as the key elements for controlling/modulating the healing mechanisms and the outcomes of wound healing upon dressing [10]. Among the recently proposed natural-based materials, such as collagen [2, 9, 19, 20], chitosan [21-25] and silk [26, 27] occupy a central. These have been proposed as alternatives to the commercially available products for wound dressing, as they might present improved performance.

The positive impact of chitosan, a deacetylated derivative from chitin, concerning the healing mechanisms, including the inflammatory process, is well documented. Chitosan powders showed to enhance healing and re-epithelialisation of full thickness skin wound in rats [28]. In a clinical trial, Azab et al. [29] have shown a positive effect of chitosan both on the re-epithelialisation and regeneration of the granular layer of the skin where chitosan-dressed wounds healed faster as compared to controls. This data is in agreement with other studies demonstrating that chitosan induce the migration of polymorphonuclear neutrophils (PMN) at the early stage of wound healing, when treating open skin wounds in dogs, enhancing the formation of granulation tissue and production of collagen by fibroblasts [30]. Furthermore a reduction of the influx of activated tissue macrophages, which in turn diminishes the subsequent events such as angiogenesis, fibroplasia, and connective tissue deposition was also attributed to chitosan [31]. Chitosan also displays haemostatic properties, preventing bleeding [31], as well as antibacterial activity when applied in skin wounds [23, 25, 32].

Chitosan/Soy membranes were previously proposed for biomedical applications based on the observations of both *in vitro* capacity to enhance either the proliferation of fibroblasts [33] and the

impaired ability to activate polymorphonuclear neutrophils [34], and normal host immune reaction after subcutaneous and intraperitoneal implantation in rats [35]. Other important features of these chitosan/soy membranes that are critical for wound dressings are its practical manipulation and its transparency. In this context and on the worldwide recognized potential of chitosan for skin wounds regeneration, the aim of this study was to evaluate the suitability of the newly developed chitosan/soy-based membranes as dressings for partial thickness skin wounds. Among the many different animal models to study wound healing and skin regeneration, excision of skins portions is the model widely used [8, 17, 23, 36-41]. Despite the different healing capacities between rats and humans, a wound dressing rat model of partial-thickness skin wound, under impaired healing conditions, was used to assess the suitability of the chitosan/soy membranes to promote wound healing. Comparatively, Epigard®, a clinically accepted wound dresser was used as control.

5.3 Materials and Methods

5.3.1 Materials

Chitosan (Cht), with a deacetylation degree of about 85% was purchased from Sigma (Germany) and the soy protein isolate (SI) was provided by Loders Crocklaan (The Netherlands). All other reagents were analytical grade and used as received. Chitosan/soy protein blended membranes (average thickness of 84 μm and 17mm of diameter) were prepared by solvent casting according to a procedure described elsewhere [33]. Briefly, chitosan was dissolved in an aqueous acetic acid 2% (v/v) solution at a concentration of 4wt%. A soy suspension (1wt%) was prepared by slowly dispersing the soy protein powder, under constant stirring, in distilled water with glycerol. After adjusting the pH to 8.0±0.3 with 1M sodium hydroxide, the dispersion was heated in a water bath at 50ºC for 30 min. The Cht and the SI solutions were mixed at a weight ratio of 75/25% chitosan/soy (CS75). After homogenization, the CS75 solution was casted into Petri dishes and dried at room temperature for 6 days. The neutralization of the membranes was obtained by immersion in 0.1 M sodium hydroxide for about 10 min. Membranes were washed with distilled water to remove all traces of alkali and again the membranes were dried at room temperature. The materials were sterilized under standard conditions under ethylene oxide atmosphere [42].

5.3.2 Animals

Twenty male Sprague Dawley rats weighting between 230g and 280g were used for the study. Three groups were investigated: membranes (wound directly covered with the Cht/Soy-based membranes); positive control (wound directly covered with Epigard® - Biovision GmbH, Germany); and a negative control (no direct coverage of the wound). Epigard® is composed of a

non-textile outer layer of polytetrafluorethylene and an inner layer of soft elastic polyurethane that forms an open matrix to which adsorbs the wound exudate from the wound bed. This dressing was chosen as positive control because it is extensively used in the clinical practice as a short term wound dressing [12].

Each animal was anaesthetized with an intramuscular injection of 90 mg/kg of ketamine combined with 5 mg/kg xylazine after induction with 3-3.5% isofluorane and 7 L/minute of air for 2-3 minutes. After shaving the skin, the back of the animals was disinfected and 2 paravertebral wounds (17 mm in diameter) were created by excision, leaving the skin smooth muscle layer (*panniculus carnosus*) intact. The test conditions were randomly distributed among the animals. After dressing (except the negative control), the wounds were protected with Bactigras® and then covered with Opsite Flexigrid®. Bactigras® is a paraffin gauze dressing containing 0.5% of chlorhexidine acetate; being soothing and non-adhesive it allows the wound to drain freely into an absorbent secondary dressing [29]. Opsite Flexigrid®, a vapour permeable adhesive film dressing which is the standard in moist wound healing [43] was used as a secondary dressing. The whole abdomen of each animal was protected with stretching bandages to prevent the removal of the whole set of dressings by scratching and biting (Fig. 5.1). At days 0 (surgery day) and 7, methylprednisolone acetate (Depo-Medrol®, Pfizer) was subcutaneously injected (20 mg/kg BW) to impair wound healing [44] and inhibit hair growth.

The animals were kept separately and received daily analgesia with metamizole sodium (200µg/g BW) and sedation with diazepam (2.5 mg/125ml water) in drinking water.

The bandages were changed every 3-4 days. Macroscopic analysis of the wounds was carried out at days 3, 7 and 14 and the images taken used for the planimetric evaluation of the healing process. The evaluation was performed with the LUCIA software by two independent researchers blinded to the experimental condition.

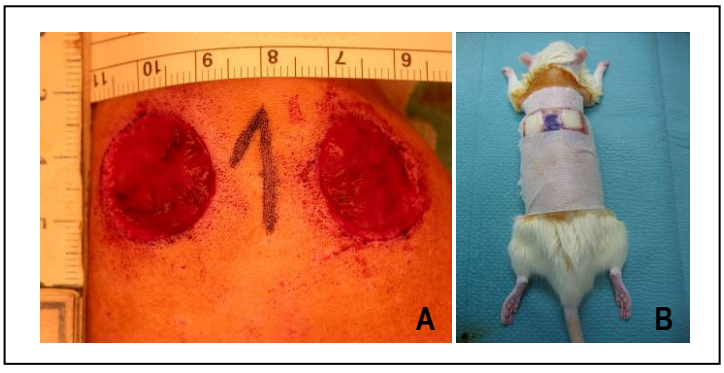

Figure 5.1: Macroscopic appearance of the wounds created by skin excision and before dressing (A). Set of dressings and bandages used to treat the animals (B).

At each end time point (1 and 2 weeks), the animals were anaesthetized with isofluorane and then euthanized by and intracardial overdose of ketamin/xylazine. The wound area and the surrounding healthy skin were explanted. Central wound cross-sections were fixed for histological analysis, in 3.7% formalin, and then paraffin embedded, sectioned and stained according to a routine haematoxylin and eosin (HE) protocol.

The histological samples were analysed using an Axioplan Imager Z1 microscope (Zeiss, Germany). The histological analysis also included the measurement of the length of the wound, which permitted to establish a correlation with the planimetric assessment of the wound areas. The length of the wounds was measured, using the standard microscope scale, after the composition of multiple standardized histological pictures including the full wounded area and the healthy margins.

5.3.3 Statistical analysis

Data from the planimetry and from the wound length measurements [45] were analysed by a single factor Anova test and the significance value was set at $p<0.05$.

5.4 Results

5.5.1 Macroscopic analysis

Despite some scratching of the secondary bandages after 7 days of dressing no signs of infection were detected for all the test groups and dressing times (Fig. 5.2-A).

The macroscopic characterization of the wounds during the observation period was based on the planimetric analysis of wound area. The wound area significantly decreased from the operation day (OpD) until the final excision time point (14 days) in all the conditions, which is an indication of increasing epithelialisation and replacement of the wounded tissue (Figs. 5.2-A and B). A significant and consecutive reduction of the wound area was also observed for both negative and positive controls from time point to time point. In respect to the Cht/Soy membrane-dressed wounds, a significantly smaller wounded area was observed at day 3 as compared to OpD (Figs. 5.2-A and B). Non significant changes were observed from day 3 to day 7. By comparing the results from day 7 to day 14, it was possible to observe a significant reduction of the wound area (Figs. 5.2-A and B).

At day 3 after wounding and dressing, clear macroscopic differences between the groups were observed (Fig. 5.2-A). The Cht/Soy membrane-dressed wounds showed a significant infiltration of granulation tissue that allowed membrane lifting and wound observation. Conversely, the non-dressed wounds (negative control) showed bleeding, which is a sign of impaired healing.

Epigard® (positive control) was completely adhered to the wound bed making it impossible to remove without wounding again (Fig. 5.2-A). The planimetric analysis revealed that the area of the negative control and the Cht/Soy membrane-dressed wounds were not significantly different ($p>0.05$) in contrast to that using Epigard® (Fig. 5.2-B). By comparing the negative and the positive controls, the wounded area of the negative control was significantly smaller ($p<0.05$) (Fig. 5.2-B). The higher wound dimensions observed for the Epigard®, only statistically different in comparison to the negative control ($p<0.05$) (Fig. 5.2-B), can be attributed to the adhesion of the Epigard® to the wound bed that did not permit its removal. In the same manner, the wounds dressed with the Cht/Soy membrane presented a reduced area compared to the positive controls ($p<0.05$) (Fig. 5.2-B).

After 7 days of dressing, in the Cht/Soy membranes-dressed wounds the granulation tissue started to be replaced by new epithelial tissue and the membranes were easily lifted from the wound bed. An improved healing, with new epithelial tissue was observed for the Cht/Soy membrane-covered wounds, compared to the negative control where some granulation tissue was still present (Fig. 5.2-A). Additionally, no bleeding was observed after the removal of the Cht/Soy membranes or negative control bandages. Moreover, the limits of the wounds dressed with the Cht/Soy membranes were smoother than the observed for the negative and positive controls (Fig. 5.2-A). Despite the smaller wound area of the Cht/Soy membrane group, the planimetric evaluation did not reveal significant differences as compared to both negative and positive controls ($p>0.05$) (Fig. 5.2-B).

Comparing the contour and dimensions of the wounds at day 14 (Figs. 5.2-A and B), it was evident that the re-epithelialisation and healing was more efficient on the wounds dressed with the cht/soy-based membranes. As observed for the membrane-dressed wounds, the negative control did not bleed at the removal of the bandages but some granulation tissue was still present on the wound bed (Fig. 5.2-A). In the case of the wounds dressed with Epigard® (positive control), the material completely adhere to the wound bed, impeding the new epidermis. In fact, in an attempt to remove it, the wound started to bleed extensively (Fig. 5.2-A). Compared to the negative and positive controls, the wound dressed with the Cht/Soy membranes showed thinner margins with an almost complete healing and regeneration of all the layers of the excised epidermis (Fig. 5.2-A). Thus, at the last end point of the experiment the Epigard®-dressed wounds showed a significantly delayed wound closure, as compared to the other test groups (Fig. 5.2-A). A smaller wounded area was observed for the chit/soy membrane group indicating a significantly faster healing of the wound (Fig. 5.2-B).

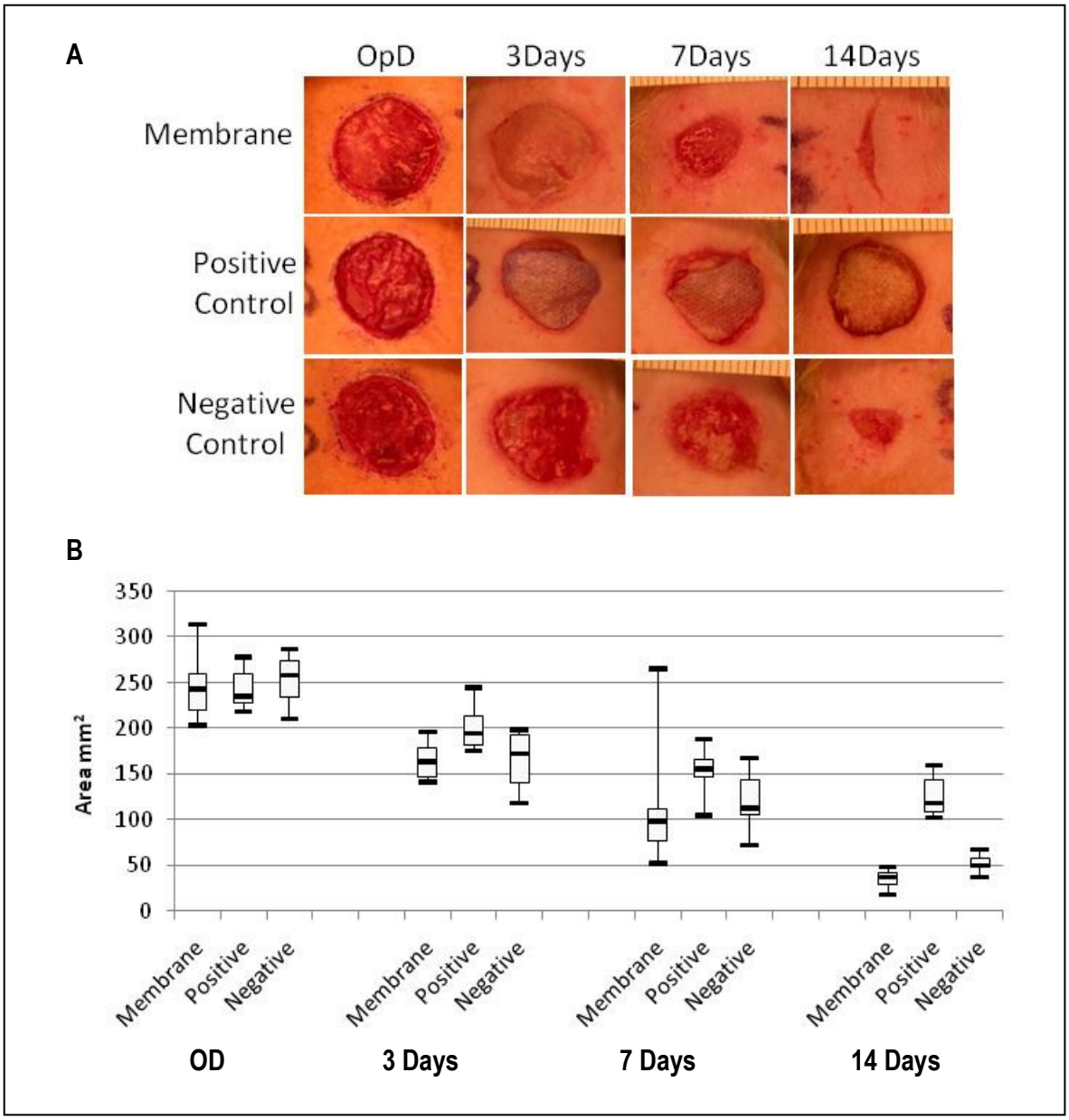

Figure 5.2: Representative images of the macroscopic aspect of the excisional wounds at the Operation Day (OpD) and subsequent healing at days 3, 7 and 14 after dressing with the chitosan/soy-based membranes, and in comparison with the negative and positive controls (A). Follow up of the wound area determined by planimetric analysis (B).

5.5.2 Histological analysis

After each time point the wounds and surrounding healthy skin were excised, together with the attached dressing in the case of the positive controls, and prepared for histological analysis. As during the process of sectioning and staining, the adherent Epigard® did not detach from the wound bed, the analysis of the explants included, in this case, its integration with the regenerating tissue.

One week after dressing, the Cht/Soy-based membranes seemed to enhance the formation of granulation tissue, in comparison to the negative control (undressed wounds) (Fig. 5.3-A). Furthermore, the margins of the Cht/Soy membrane-dressed wounds presented a continuity of the regenerating tissue that was not observed in the wound margins of the positive and negative controls (Figs. 5.3-A, B and C). At this stage of healing, it was already possible to identify some stratification of the tissue in the membrane-dressed wounds that increased in complexity from the healthy skin to the centre of the wound (Figs. 5.3-A and 5.4-A). These features were not detectable either in the positive (Fig. 5.3-B) or in the negative controls (Fig. 5.3-C). A disorganised mesh of cells, including a large amount of inflammatory cells, some fibroblasts and collagen fibres were observed in these both groups. Furthermore, while some necrosis was detected in the non-dressed wounds (negative controls) (Figs. 5.3-C and 5.4-C), in the Epigard® dressed wounds, no necrosis was observed. In fact, the material adhered to the wound bed forming an intimate network composed by the polymer matrix and the regenerating cells. This network started to vascularise, which is an indication of good integration of the material into the wound bed (Figs.3-D and 5.4-D). During the first week of healing the formation of foreign body giant cells was not detected in all groups.

At the second week of dressing, the healing of the wounds covered by the Cht/Soy membranes is enhanced as compared to the negative and positive controls. The wounds decreased in size, the margins were thinner and the granulation tissue previously observed was replaced by a more stratified regenerated epidermis (Fig. 5.3-D). Cornification of the outermost epidermal layer, although still near the margin of the wound was observed (Figs. 5.3-D and 5.4-B), demonstrating clear signs of re-epithelialisation. The negative controls (non-dressed wounds) showed a severe macerating effect of the epidermis translated in extensive necrosis of the tissue (Fig. 5.3-F). In respect to Epigard®-dressed wounds, the matrix network detected at the first week of healing was still present and a higher colonization of cells was observed (Fig. 5.3-E). Underneath the network, a significant layer of muscle and collagen fibres was observed (Fig. 5.3-E).

The microscopic measurement of the obtained histological samples among the groups showed not significant statistical differences ($p>0.05$) in the length of the wounds after 1 and 2 weeks (Fig. 5.5). At the first week of healing the wounds dressed with the Cht/Soy membranes showed a significant decrease in length, as compared either with the negative or the positive controls ($p<0.05$) (Fig. 5.5). Conversely, both controls did not significantly differ in the length of the wounds ($p>0.05$) (Fig. 5.5). Two weeks after healing, the positive and negative controls showed to have significantly different wound lengths ($p<0.05$) (Fig. 5.5). On the contrary, the Cht/Soy

membranes-dressed wounds had lengths comparable to the negative and positive controls (p>0.05) (Fig.5).

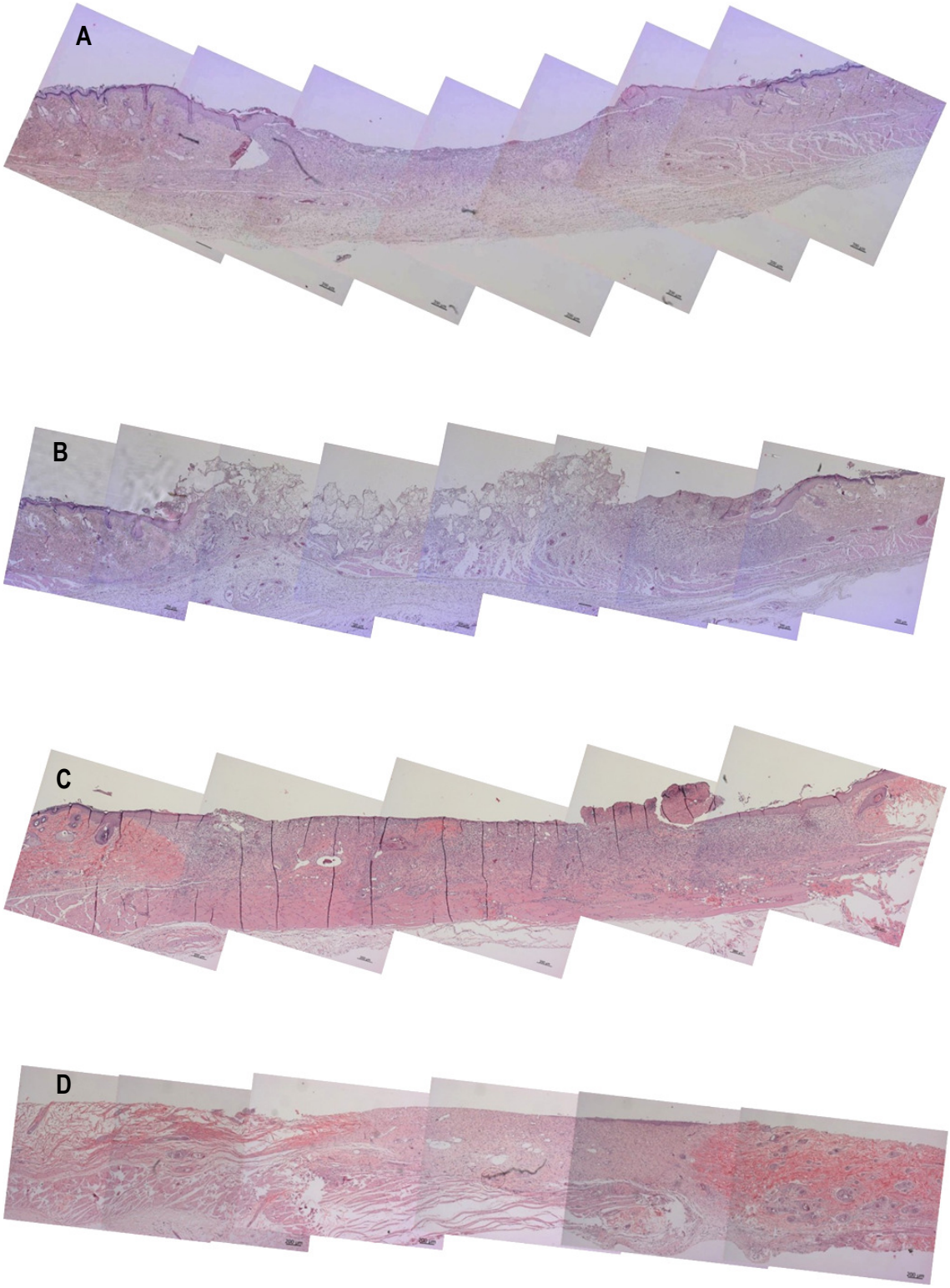

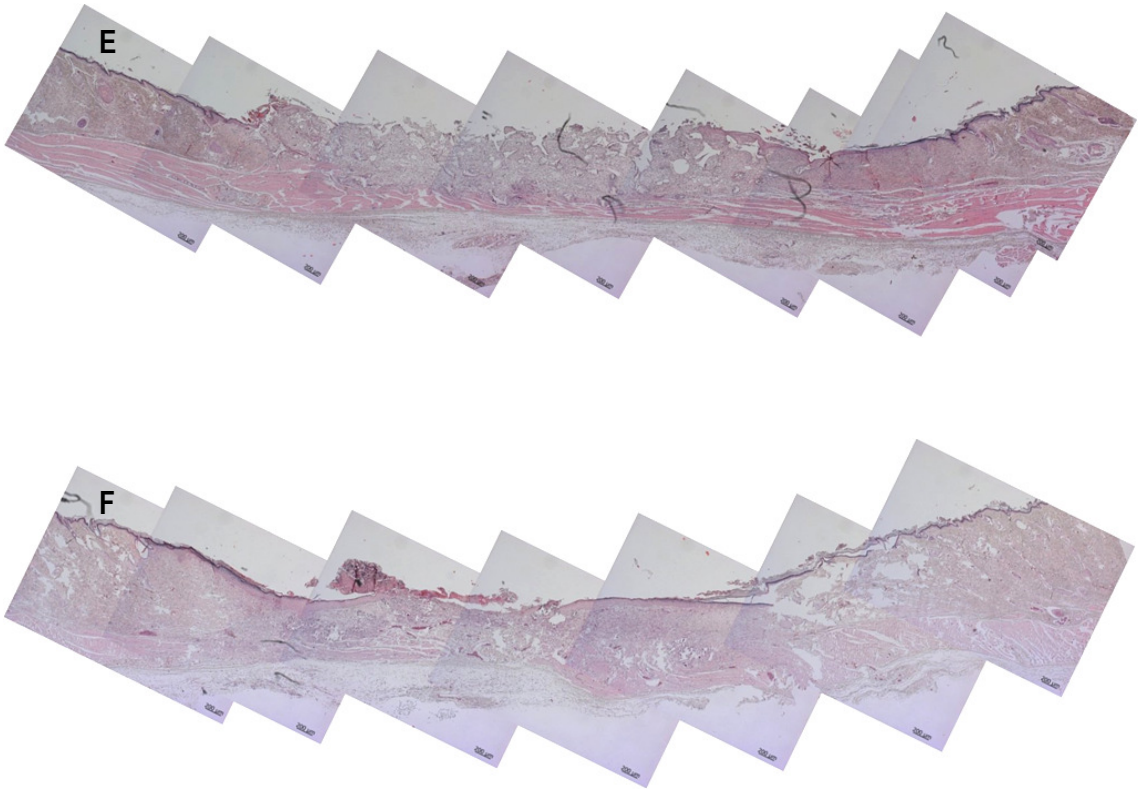

Figure 5.3: Representative composition of the histological micrographs of the wounded skin 1 (A,B,C) and 2 (D,E,F) weeks after dressing with the Cht/Soy Membrane (A, D), the Eppigard® (positive control) (B,E) and left undressed (negative control) (C,F).

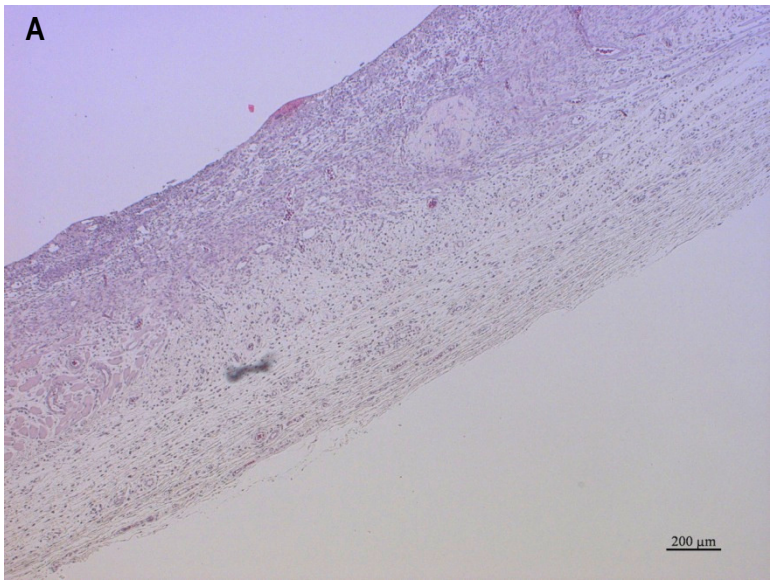

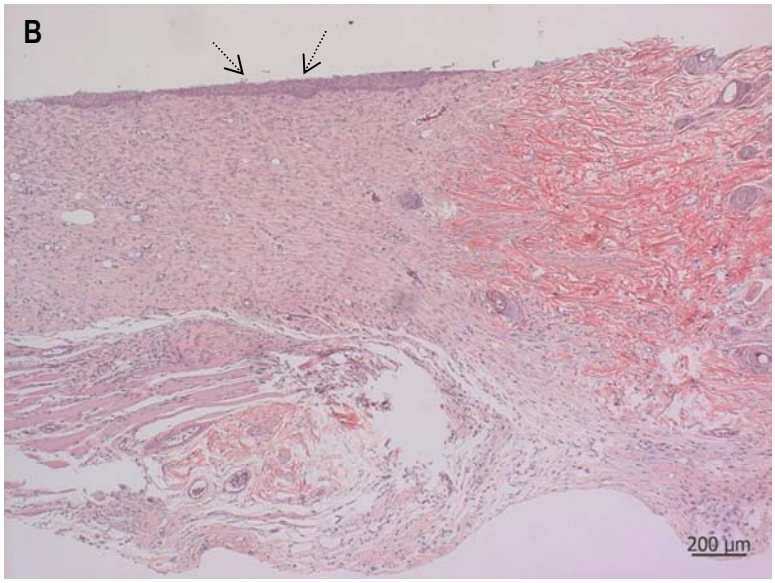
B
200 µm

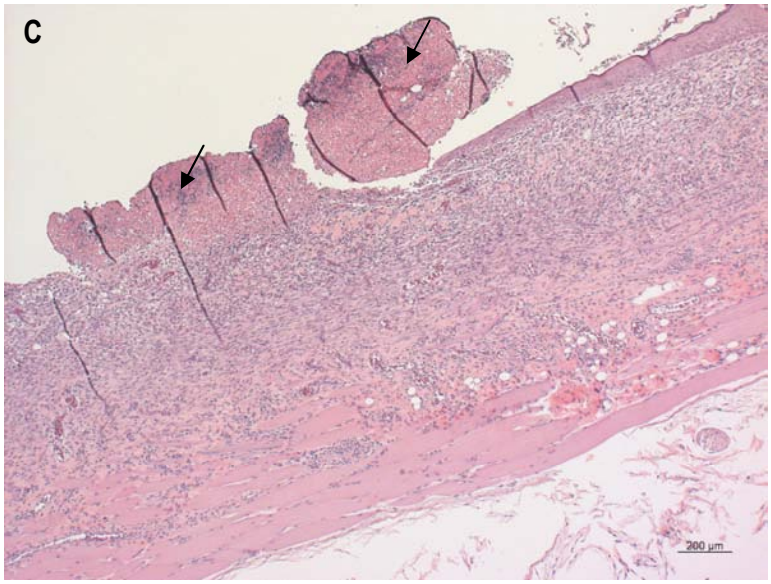
C
200 µm

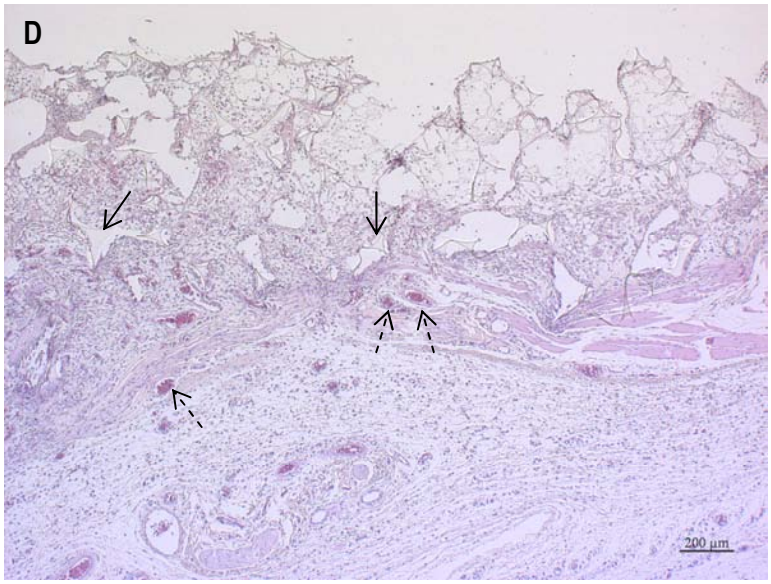
D
200 µm

Figure 5.4: Histological micrographs of the wound bed representing the stratification of the regenerated tissue (A) and the epidermal cornification (→) (B) respectively one and two weeks after dressing with the Cht/Soy Membrane. In contrast necrotic tissue (→) was observed in the undressed wound (negative control) (C). In the positive control it was perceived the integration of the Eppigard® (→) and the formation of blood vessels (-≫) one week onward after wounding (D).

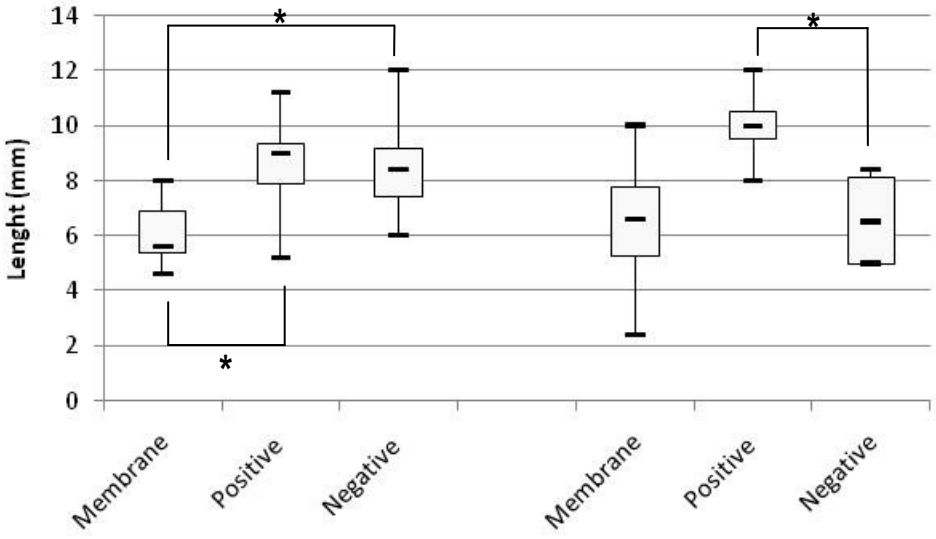

Figure 5.5: Representation of the length of the wound one and two weeks after dressing with the Cht/Soy Membrane (Membrane), the Eppigard® (Positive) and undressed (Negative). Measurements were obtained from the histological micrographs of the wounded region of the skin. * - differences statistically significant (p<0.05).

5.5 Discussion

Excisional wound animal models are the most frequently used models to investigate the performance of skin wound dressings [46]. These types of wounds are useful to assess re-epithelialisation after implantation of different devices when considerable volume of skin is removed. Such examples are wound dressings, topical formulations and growth factors [46]. Many research groups have reported the successful use of different types of chitosan-based materials for wound dressing applications [29, 43, 47-49]. Following some of those reports and previous knowledge on the behaviour of cht/soy-based membranes [34], a wound dressing rat model of partial-thickness skin wound was used to assess the suitability of these membranes as wound dressings. It is well known that (young) rodents possess a very fast and easy healing capacity thus, in such *in vivo* models, it is mandatory to simulate human condition of wound healing, since humans have an impaired healing compared with rodents [50]. This study demonstrates that the Cht/Soy membranes, under impaired healing conditions as induced by

corticosteroid treatment, are suitable wound dressings as they permit the progress of a normal healing path and a faster regeneration of the excised epidermis as compared to an undressed wound (negative control). The presence of granulation tissue at earlier stages of healing was representative of an accelerated tissue reaction [51]. In contrast, an early inflammatory stage and bleeding were observed in the negative control. In fact, for both negative and positive controls, a disorganised mesh of cells, a large amount of inflammatory cells, some fibroblasts and collagen fibres were observed at the first week of healing. At this stage, the inflammation subsequent to wounding should be resolved and the expected tissue would be granulation tissue [51] as evidenced in the Cht/Soy membrane-dressed wounds (Figs. 5.3-A, B and C).

In partially-thickness wounds the large amount of granulation tissue formed results in wound contraction and re-epithelialisation which closes the wounded area allowing the regeneration of the epidermis with its different layers and annexes [39, 46]. Furthermore, as the subcutaneous tissue with the portion of the *panniculus carnosus* muscle in the backs of the animals is left intact [50], the re-epithelialisation of the wound will start not only from the margins of the wound containing healthy and intact skin, but also from the wound bed [39, 50]. After one week, in the wounds dressed with the Cht/Soy membrane, some stratification of the wound was already detected that increased in complexity from the healthy skin to the centre of the wound. The smaller wound area and the thinner margins, with an almost complete healing and regeneration of all the layers of the excised epidermis after 14 days of dressing with the Cht/Soy membrane, confirmed the normal progress of re-epithelialisation and a better healing (Figs. 5.3-D, E and F).

The fact that the Cht/Soy membrane was completely loose on the wound seemed to facilitate the spatial and increased progression of the newly formed epithelium. Therefore, these membranes appear not only to be able to regulate the wound moist, which at extreme levels would impair epidermis regeneration, but also to provide the adequate coverage that does not physically constrain the formation of new tissue.

Despite the decreased area of the undressed wounds, severe necrosis and no signs of re-epithelialisation were detected. According to a previous report [34], polymorphonuclear neutrophils (PMNs) did not secrete reactive oxygen species (ROS) after direct contact with Cht/Soy membranes. Furthermore, the membranes exerted an anti-inflammatory effect by inhibiting the PMNs to produce ROS when stimulated with phorbol 12-myristate 13-acetate (PMA) or formyl-methionyl-leucyl-phenylalanine (fMLP) [34]. Bearing this in mind, it is possible to consider that the inflammatory cells present at the wound bed of undressed wounds are secreting ROS. These can be responsible for destroying the surrounding cells and tissues, which may explain the observed necrosis at the wound bed. On the contrary, Cht/Soy membranes exerted

their anti-inflammatory potential by inhibiting the activation of the inflammatory cells and avoiding a toxic environment in the wound bed, which lead to normal wound healing process and tissue regeneration. Moreover, the observed necrosis at the wound bed of the negative controls may be explained as a consequence of the lack of stimulation of the wound bed tissue to regenerate. In fact it is well known that, as the growth from the wound margins is slower, the absence of nutrients in the wound bed leads to cell death.

In this study, an unexpected reaction, independently of the time periods tested, was observed for the Epigard® since its clinical use as a wound dressing did not predict the observed impaired regeneration. Conversely to the Cht/Soy membranes that were easily detached from the wounds without additional trauma and without removing the granular tissue, the Epigard® integrated within the wound tissue thus delaying the resolution of the inflammatory process. This behaviour can be explained by the different healing rates between rats and humans; the faster metabolism of rats, although in impaired wound conditions, lead to an exacerbated reaction thus, leading to the formation of a vascularised network of cell-embedded matrix. The continued presence of the Epigard® within the wound for the longer time period showed that the host is still combating the foreign body and thus is able to proceed with the re-epithelisation and the closure of the wound. Nevertheless, a good integration within the wound bed and with the regenerating tissue was observed.

However, further studies of wound dressing, including the cellular and molecular mechanisms involved in skin wound healing, as well as studies in advanced wound healing models, such as excisional skin wounds in pigs could improve the knowledge on these cht/soy-based membranes.

5.6 Conclusions

The present work allows to conclude that the newly developed cht/soy-based membranes produced by solvent casting methodology, that had proven to promote low *in vitro* activation of human PMNs isolated from circulating blood, decrease the healing time period of partial-thickness skin wounds in rats. Moreover, these cht/soy-based membranes showed an enhanced performance as compared to the negative and positive controls, inducing re-epithelialisation. The new cht/soy-based membranes can be considered for further studies of wound dressing, including the cellular and molecular mechanisms involved in skin wound healing, as well as for studies in advanced wound healing models, such as excisional skin wounds in pigs.

References

1. White, R. and C. Morris, *Mepitel: a non-adherent wound dressing with Safetac technology.* Br J Nurs, 2009. **18**(1): p. 58-64.
2. Alvarez, O.M., P.M. Mertz, and W.H. Eaglstein, *The effect of occlusive dressings on collagen synthesis and re-epithelialization in superficial wounds.* J Surg Res, 1983. **35**(2): p. 142-8.
3. Nathan, P., B.G. MacMillan, and I.A. Holder, *In situ production of a synthetic barrier dressing for burn wounds in rats.* Infect Immun, 1975. **12**(2): p. 257-60.
4. Geronemus, R.G. and P. Robins, *The effect of two new dressings on epidermal wound healing.* J Dermatol Surg Oncol, 1982. **8**(10): p. 850-2.
5. James, J.H. and A.C. Watson, *The use of Opsite, a vapour permeable dressing, on skin graft donor sites.* Br J Plast Surg, 1975. **28**(2): p. 107-10.
6. Wood, R.A. and L.E. Hughes, *Silicone foam sponge for pilonidal sinus: a new technique for dressing open granulating wounds.* Br Med J, 1975. **4**(5989): p. 131-3.
7. Tavis, M.J., et al., *Graft adherence to de-epithelialized surfaces: a comparative study.* Ann Surg, 1976. **184**(5): p. 594-600.
8. Damour, O., et al., *A dermal substrate made of collagen--GAG--chitosan for deep burn coverage: first clinical uses.* Clin Mater, 1994. **15**(4): p. 273-6.
9. Burget, A., et al., *The effect of a collagen dressing on contaminated surgical wounds in rats.* Langenbecks Arch Chir, 1976. **343**(1): p. 69-73.
10. Ovington, L.G., *Advances in wound dressings.* Clin Dermatol, 2007. **25**(1): p. 33-8.
11. Nathan, P., B.G. Macmillan, and I.A. Holder, *Effect of a synthetic dressing formed on a burn wound in rats: a comparison of allografts, collagen sheets, and polyhydroxyethylmethacrylate in the control of wound infection.* Appl Microbiol, 1974. **28**(3): p. 465-8.
12. Stone, H.A., R.D. Edelman, and J.J. McGarry, *Epigard: a synthetic skin substitute with application to podiatric wound management.* J Foot Ankle Surg, 1993. **32**(2): p. 232-8.
13. Szycher, M. and S.J. Lee, *Modern wound dressings: a systematic approach to wound healing.* J Biomater Appl, 1992. **7**(2): p. 142-213.
14. Nathan, P., et al., *A new biomaterial for the control of infection in the burn wound.* Trans Am Soc Artif Intern Organs, 1976. **22**: p. 30-41.
15. Fulton, J.E., Jr., *The stimulation of postdermabrasion wound healing with stabilized aloe vera gel-polyethylene oxide dressing.* J Dermatol Surg Oncol, 1990. **16**(5): p. 460-7.

16. Okamoto, Y., et al., *Evaluation of chitin and chitosan on open would healing in dogs.* J Vet Med Sci, 1995. **57**(5): p. 851-4.
17. King, W.W., et al., *Evaluation of artificial skin (Integra) in a rodent model.* Burns, 1997. **23 Suppl 1**: p. S30-2.
18. Leipziger, L.S., et al., *Dermal wound repair: role of collagen matrix implants and synthetic polymer dressings.* J Am Acad Dermatol, 1985. **12**(2 Pt 2): p. 409-19.
19. Norton, L. and M. Chvapil, *Comparison of newer synthetic and biological wound dressings.* J Trauma, 1981. **21**(6): p. 463-8.
20. Chen, J.P., G.Y. Chang, and J.K. Chen. *Electrospun collagen/chitosan nanofibrous membrane as wound dressing*. in *Asian Conference on Nanoscience and Nanotechnology (AsiaNANO 2006)*. 2006. Busan, SOUTH KOREA.
21. Keong, L.C. and A.S. Halim, *In vitro models in biocompatibility assessment for biomedical-grade chitosan derivatives in wound management.* Int J Mol Sci, 2009. **10**(3): p. 1300-13.
22. Wang, W., et al., *Acceleration of diabetic wound healing with chitosan-crosslinked collagen sponge containing recombinant human acidic fibroblast growth factor in healing-impaired STZ diabetic rats.* Life Sciences, 2008. **82**(3-4): p. 190-204.
23. Wang, C.C., C.H. Su, and C.C. Chen, *Water absorbing and antibacterial properties of N-isopropyl acrylamide grafted and collagen/chitosan immobilized polypropylene nonwoven fabric and its application on wound healing enhancement.* Journal of Biomedical Materials Research Part A, 2008. **84A**(4): p. 1006-1017.
24. Qin, Y.M., *The preparation and characterization of chitosan wound dressings with different degrees of acetylation.* Journal of Applied Polymer Science, 2008. **107**(2): p. 993-999.
25. Ong, S.Y., et al., *Development of a chitosan-based wound dressing with improved hemostatic and antimicrobial properties.* Biomaterials, 2008. **29**(32): p. 4323-4332.
26. Okabayashi, R., et al., *Efficacy of polarized hydroxyapatite and silk fibroin composite dressing gel on epidermal recovery from full-thickness skin wounds.* J Biomed Mater Res B Appl Biomater, 2009.
27. Schneider, A., et al., *Biofunctionalized electrospun silk mats as a topical bioactive dressing for accelerated wound healing.* Acta Biomater, 2008.
28. Cho, Y.W., et al., *Water-soluble chitin as a wound healing accelerator.* Biomaterials, 1999. **20**(22): p. 2139-45.

29. Azad, A.K., et al., *Chitosan membrane as a wound-healing dressing: characterization and clinical application.* J Biomed Mater Res B Appl Biomater, 2004. **69**(2): p. 216-22.
30. Ueno, H., et al., *Accelerating effects of chitosan for healing at early phase of experimental open wound in dogs.* Biomaterials, 1999. **20**(15): p. 1407-14.
31. Diegelmann, R.F., et al., *Analysis of the effects of chitosan on inflammation, angiogenesis, fibroplasia, and collagen deposition in polyvinyl alcohol sponge implants in rat wounds.* Wound Repair Regen, 1996. **4**(1): p. 48-52.
32. Deng, C.M., et al., *Biological properties of the chitosan-gelatin sponge wound dressing.* Carbohydrate Polymers, 2007. **69**(3): p. 583-589.
33. Silva, S.S., et al., *Physical properties and biocompatibility of chitosan/soy blended membranes.* J Mater Sci Mater Med, 2005. **16**(6): p. 575-9.
34. Santos, T.C., et al., *In vitro evaluation of the behaviour of human polymorphonuclear neutrophils in direct contact with chitosan-based membranes.* J Biotechnol, 2007. **132**(2): p. 218-26.
35. Santos, T.C., et al., *Chitosan improves the biological performance of soy-based biomaterials, Submitted.* 2009.
36. Hong, H.J., et al., *Accelerated wound healing by smad3 antisense oligonucleotides-impregnated chitosan/alginate polyelectrolyte complex.* Biomaterials, 2008. **29**(36): p. 4831-4837.
37. Burkatovskaya, M., et al., *Effect of chitosan acetate bandage on wound healing in infected and noninfected wounds in mice.* Wound Repair and Regeneration, 2008. **16**(3): p. 425-431.
38. Noorjahan, S.E. and T.P. Sastry, *An in vivo study of hydrogels based on physiologically clotted fibrin-gelatin composites as wound-dressing materials.* J Biomed Mater Res B Appl Biomater, 2004. **71**(2): p. 305-12.
39. Laplante, A.F., et al., *Mechanisms of wound reepithelialization: hints from a tissue-engineered reconstructed skin to long-standing questions.* FASEB J, 2001. **15**(13): p. 2377-89.
40. Kweon, D.K., S.B. Song, and Y.Y. Park, *Preparation of water-soluble chitosan/heparin complex and its application as wound healing accelerator.* Biomaterials, 2003. **24**(9): p. 1595-601.
41. Burkatovskaya, M., et al., *Use of chitosan bandage to prevent fatal infections developing from highly contaminated wounds in mice.* Biomaterials, 2006. **27**(22): p. 4157-64.

42. Reis, R.L., et al., *Processing and in vitro degradation of starch/EVOH thermoplastic blends.* Polym Int, 1997. **43**: p. 347.
43. Yusof, N.L., et al., *Flexible chitin films as potential wound-dressing materials: wound model studies.* J Biomed Mater Res A, 2003. **66**(2): p. 224-32.
44. Wicke, C., et al., *Effects of steroids and retinoids on wound healing.* Arch Surg, 2000. **135**(11): p. 1265-70.
45. Kirkwood, B. and J. Sterne, *Essential Medical Statistics*. 2nd Edition ed. 2003: Wiley. 512.
46. Davidson, J.M., *Animal models for wound repair.* Arch Dermatol Res, 1998. **290 Suppl**: p. S1-11.
47. Ishihara, M., et al., *Photocrosslinkable chitosan as a dressing for wound occlusion and accelerator in healing process.* Biomaterials, 2002. **23**(3): p. 833-40.
48. Khan, T.A. and K.K. Peh, *A preliminary investigation of chitosan film as dressing for punch biopsy wounds in rats.* J Pharm Pharm Sci, 2003. **6**(1): p. 20-6.
49. Ueno, H., T. Mori, and T. Fujinaga, *Topical formulations and wound healing applications of chitosan.* Adv Drug Deliv Rev, 2001. **52**(2): p. 105-15.
50. Saulis, A. and T.A. Mustoe, *Models of wound healing in growth factor studies*, in *Surgery Research*, W.W. Souba and D.W. Wilmore, Editors. 2001, Academic Press. p. 857-874.
51. Atala, A., et al., *Principles of Regenerative Medicine*. 2008: Academic Press. 1448.

Chapter VI

In vivo short and long term host reaction to starch-based scaffolds

6.1 Abstract

The implantation of biomaterials implies a host response to a foreign body that depends on the host and the implanted material. The aim of this study was to compare the inflammatory response induced by the implantation of starch-based scaffolds in two implantation rat models, subcutaneous (SC) and intramuscular (IM). Two methodologies, wet spinning (WS) and fibre bonding (FB), were used to prepare the scaffolds. The short term inflammatory/immune host reaction was assessed by SC and IM implantations in rats after 1 and 2 weeks and the long term host response was addressed after 8 and 12 weeks of SC implantation of both types of SPCL scaffolds in rats. After each time period, the scaffolds, surrounding tissue and nearby lymph nodes were explanted and used for histological analysis and molecular biology evaluation. The results showed that SPCL-WS scaffolds seem to induce a slight lower inflammatory/immune reaction in both types of implantation models. Nonetheless comparing the two models the IM implantation resulted in a slightly higher inflammatory response than the SC implantation with early activation of the lymph nodes. The overall data suggests a good integration of the materials in the host, independently of the tissue location with a normal progress of the reaction for all the conditions.

***This chapter is based on the following publication:**

T. C. Santos, A. P. Marques, B. Höring, A. R. Martins, K. Tuzlakoglu, A. G. Castro, M. van Griensven, R. L. Reis, In Vivo *Short and Long Term Host Reaction to Starch-based Scaffolds*. **2009. *Submitted*.**

6.2 Introduction

The constant biomaterials development in the Tissue Engineering (TE) field has been attempting to answer to the rising needs of the new tissue replacement/regeneration strategies. Nonetheless, the increasing complexity of the TE devices, comprising cells [1-6] and/or bioactive agents [7-10] within 3D scaffolding structures, comprises additional concerns regarding adverse host reactions to the implantable constructs [11]. A considerable number of studies [12-16] have been demonstrating the immunomodulatory properties of mesenchymal stem cells obtained from different sources which seem to circumvent a potential host rejection of the transplanted cells.

The incorporation of foreign growth factors, eventually considered as immunogenic, in TE constructs is nowadays a recurrent approach as researchers have laid their expectation in recombinant technology to produce recombinant bioactive molecules [8, 9, 17] with a key role in tissue regeneration.

It seems though that, despite all the investment in the research on stem cells technology, as well as in the identification of key mediators in inflammation/immune reaction and differentiation pathways, the role of support biomaterials in the host reaction has been neglected. Natural-origin biomaterials are considered for many years as a way to improve, in comparison to synthetic polymers, *in vivo* biofunctionality and to modulate/avoid a harmful host response due to its similarities with biological molecules. Starch-based scaffolds, processed using several methodologies aiming at different TE applications [18-25], have been demonstrating a great potential in the field. Very promising results for bone tissue regeneration have been particularly obtained with a blend of starch and poly-caprolactone (SPCL) [19-22, 24, 26-29]. SPCL scaffolds, with adequate physicochemical and mechanical properties for bone TE [18, 21] and adequate degradability rate [23, 24, 30], have shown support mesenchymal stem cells growth and differentiation [18, 19] and to be excellent supporting structures for endothelial cells [21, 22, 31, 32]. Consequently, a lacuna is still present concerning the *in vivo* reaction to SPCL-based scaffolds. A systematic study was carried out using two different rat implantation models, subcutaneous and intramuscular, aiming at primarily to understand the tissue reaction to two SPCL-based scaffolds produced by different methodologies, wet spinning [25] and fibre-bonding [21], both at short and long term implantation periods, and secondly, to identify eventual differences between the two models in terms of inflammatory/immune response elicited by the two different forms of SPCL-based scaffolds.

6.3 Materials and Methods

6.4.1 Materials

Starch-based scaffolds were produced from a blend of Starch with β-Polycaprolactone (30:70%) (SPCL), by two different methodologies described elsewhere: wet spinning (SPCL-WS) [25] and fibre-bonding (SPCL-FB) [21]. Briefly, for the production of SPCL-WS scaffolds, the polymer was dissolved in chloroform at a concentration of 40% (w/v) in order to obtain a polymer solution with proper viscosity. The polymer solution was loaded into a syringe, placed in a syringe pump (World Precision Instruments, UK) and a certain amount of polymer solution was subsequently extruded into a methanol coagulation solution. The fibre mesh structure was formed during the processing by the random movement of the precipitation container. The formed scaffolds were then dried overnight at room temperature to allow any remaining solvents to evaporate. For the fabrication of the SPCL-FB scaffolds, fibre-meshes previously obtained by a meltspinning methodology were placed in a glass mould and heated in an oven at 150ºC. Immediately after removing the moulds from the oven, the fibres were slightly compressed by a Teflon cylinder and then cooled at −15ºC. All samples were cut into discs of 5 mm diameter and approximately 1mm thickness and sterilized by a standard procedure with ethylene oxide [33].

6.4.1 Intramuscular implantation

Six male Sprague Dawley rats weighting between 380 g and 400 g (3 for each implantation time) were used. Each animal was anaesthetized with an intramuscular injection of 90 mg/Kg ketamine hydrochloride and 5 mg/Kg xylazine hydrochloride. After shaving and disinfecting the back of the animals, 4 paraventral skin incisions, of approximately 2 cm containing the subcutis and the *Panniculus Carnosus*, were performed under surgical sterile conditions. An incision on the fascia of the back muscle was performed and craniolateral oriented muscle-pockets were created by blunt dissection. After introducing the scaffolds (4 scaffolds per animal), previously embedded into a sterile saline solution, the fascia, the *Panniculus carnosus* and finally the skin were carefully sutured. The animals were kept in single cages with food and water *ad libitum* during all time of implantation. During the first week, the animals received daily 200 µg/g of body weight of metamizole sodium in drinking water *ad libitum*.

6.4.2 Subcutaneous implantation

Six male Sprague Dawley rats weighting between 350 g and 380 g (3 for each implantation time of 1 and 2 weeks), were used. Each test animal was anaesthetized with an intramuscular injection of 90 mg/Kg ketamine hydrochloride and 5 mg/Kg xylazine hydrochloride and 2 medial and ventral incisions of approximately 2 cm containing the subcutis and the *Panniculus Carnosus* were performed in the dorsum of the rats. Craniolateral oriented pockets (2 per incision) were

subcutaneously created by blunt dissection. The scaffolds (4 scaffolds per animal), previously embedded into a sterile saline solution, were introduced into the pockets and the *Panniculus carnosus* and the skin were carefully sutured. The animals were kept in single cages with food and water *ad libitum* during all time of implantation. During the first week, the animals received daily 200 µg/g of body weight of metamizole sodium in drinking water *ad libitum*.

For a long term reaction, six male Sprague Dawley rats, 3 for each implantation time, and weighting between 280g and 340g were used for the subcutaneous implantation of the SPCL scaffolds. The surgical procedure followed was the same as above mentioned for the subcutaneous implantation.

6.4.3 Post-implantation analysis

At the end point times (1, 2, 8 and 12 weeks), each animal was intramuscularly anaesthetized and sacrificed with an intracardial overdose of 90 mg/Kg ketamine hydrochloride and 5 mg/Kg xylazine hydrochloride. From each animal the 4 implanted scaffolds and surrounding tissue, as well as the axillary and inguinal lymph nodes, were explanted. The explanted samples were either fixed in 3.7% formalin for histological evaluation, or frozen for posterior molecular biology analysis. The histological analysis of cross-section samples was performed after Haematoxylin and Eosin (HE), and Masson Goldner Trichrome (MGT) staining and immunohistochemistry using a monoclonal mouse anti-human CD3 antibody (Dako, Denmark) with cross reactivity for rat T lymphocytes, a monoclonal mouse anti-rat CD18 antibody (Serotec, UK) for Integrin β2 chain of recruited leukocytes, and a monoclonal mouse anti-human phosphoinositide 3-Kinase (Pi3K) antibody (BD, Belgium) with cross reactivity for rat activated and proliferating lymphocytes, following standard protocols. Reverse transcriptase polymerase chain reaction (RT-PCR) to detect the expression of IL-1α, IL-18, IL-10, IL-13, IFN-γ and MHC class II genes was carried out (table 1). Image analysis of the histological sections of the 8 and 12 weeks explants, considering the scaffold and the inflammation areas, was performed with the Olympus CellP software (Olympus, Belgium) and an Olympus BX61 Microscope (Olympus, Belgium).

Table 6.1: Forward and Reverse sequences of the genes detected by RT-PCR on rat samples.

Function	Gene	Sequences	Tm (ºC)	Bp
Housekeeping gene	GAPDH	Sense - GGTGATGCTGGTGCTGAGTA	59.4	81
		Antisense - GGATGCAGGGATGATGTTCT	57.3	
Pro-inflammatory	IL-18	Sense - AGATGTGGAACTGGCAGAGG	59.4	220
		Antisense - CCCATTTGGGAACTTCTCCT	57.3	
	IL-1α	Sense –GCAAAGCCTAGTGGAACCAG	59.4	244
		Antisense -GCAGAAGGTGCACAGTGAGA	59.4	
Anti-inflammatory	IL-10	Sense - GAATTCCCTGGGAGAGAAGC	59.4	219
		Antisense - CCGGGTGGTTCAATTTTTCAT	55.9	
	IL-13	Sense - ATCGAGGAGCTGAGCAACAT	57.3	189
		Antisense - CGAGGCCTTTTGGTTACAGA	57.3	
	IFN-γ	Sense - GCCCTCTCTGGCTGTTACTG	61.4	221
		Antisense - CTGATGGCCTGGTTGTCTTT	57.3	
	MHC class II	Sense - TCCCAGATACACAGCAGCAG	59.4	320
		Antisense - CATGCGAAGGTTCTCCAGTT	57.3	

6.4.4 Statistical Analysis

Mean values and standard deviations are reported for the measurements [34] of the scaffold and the associated inflammation areas. Data was analysed by a single factor ANOVA test and the significance value was set for $p<0.05$.

6.4 Results

6.4.1 Intramuscular implantation

Macroscopic signs of inflammation, infection or swelling were absent after 1 and 2 weeks of intramuscular implantation of the different types of SPCL scaffolds (Fig.6.1).

The histological analysis of the explanted materials and respective surrounding tissue revealed the absence of oedema and necrosis both at 1 and 2 weeks of implantation (Figs. 6.2.1.A.C.E.F). At the first week of intramuscular implantation of SPCL-FB scaffolds, the inflammatory infiltrate around the scaffold fibres (Fig. 6.2.1A) was mainly constituted by polymorphonuclear neutrophils (PMNs), characterised by their multilobular nuclei. The presence of recruited leukocytes, CD18 positive cells, was confirmed by immunohistochemistry using the specific marker of β-2 integrin

(Fig. 6.2.2A). The analysis carried out for the SPCL-WS scaffolds implanted intramuscularly seemed to indicate the diminishment of the inflammatory infiltrate (Fig. 6.2.1C) in comparison to what was observed for the SPCL-FB. Although PMNs were also present at the surrounding area of the scaffold's fibres (Fig. 6.2.2C). At this early stage of implantation it was noticed that for both SPCL-WS and SPCL-FB scaffolds, some collagen network started to be deposited between the scaffold's fibres, as showed by the MGT staining (Figs. 6.2.1B and D).

At the second week of implantation, the nature of the observed inflammatory infiltrate in the tissue surrounding the SPCL-FB scaffolds implanted intramuscularly was different than the observed at the first week of implantation. Mononuclear cells (Fig. 6.2.1E), namely T lymphocytes, positive cells for the CD3 marker (Fig. 6.2.2E), were predominant. Similarly, T lymphocytes were also present in the tissue surrounding the SPCL-WS fibres (Fig. 6.2.2G). Additionally, some foreign body giant cells (FBGCs) appeared at the fibres interfaces of both the SPCL-WS and the SPCL-FB scaffolds (Figs. 6.2.1.E and G). In comparison to the first week of implantation, a denser network of collagen fibres was also observed two weeks after the intramuscular implantation of both types of SPCL scaffolds (Figs. 6.2.1F and H). After 2 weeks of implantation, a significant amount of blood vessels was also observed within the tissue surrounding the fibres of both SPCL scaffolds.

In order to evaluate an eventual systemic host response to the intramuscular implantation of the different types of SPCL scaffolds, the axillary and inguinal lymph nodes were analysed. The general structure of the lymph nodes, assessed after HE staining, revealed the presence of germinal centres (lighter area), populated mainly with activated B lymphocytes, and some plasma cells (Figs. 6.2.3 A and C) in the cortex of the nodes after one week of implantation of both SPCL scaffolds. Additionally, denser areas surrounding the germinal centres comprehending lymphocytes, which are characterised by the intense blue nuclei staining (Figs. 6.2.3 A and C), were observed. A specific assessment of cell proliferation was carried out by tracking the signal transduction molecule PI3K. Very few cells were positive for PI3K and no differences were observed between one and two weeks of implantation of the two types of SPCL scaffolds. At the second week of implantation, the explanted lymph nodes still revealed the presence of germinal centres, with no differences between the two different types of scaffolds (Figs. 6.2.3 E and G). Once more, the immunolabelling of PI3K showed a low number of positive cells for both types of SPCL scaffolds (Figs. 6.2.3 F and H).

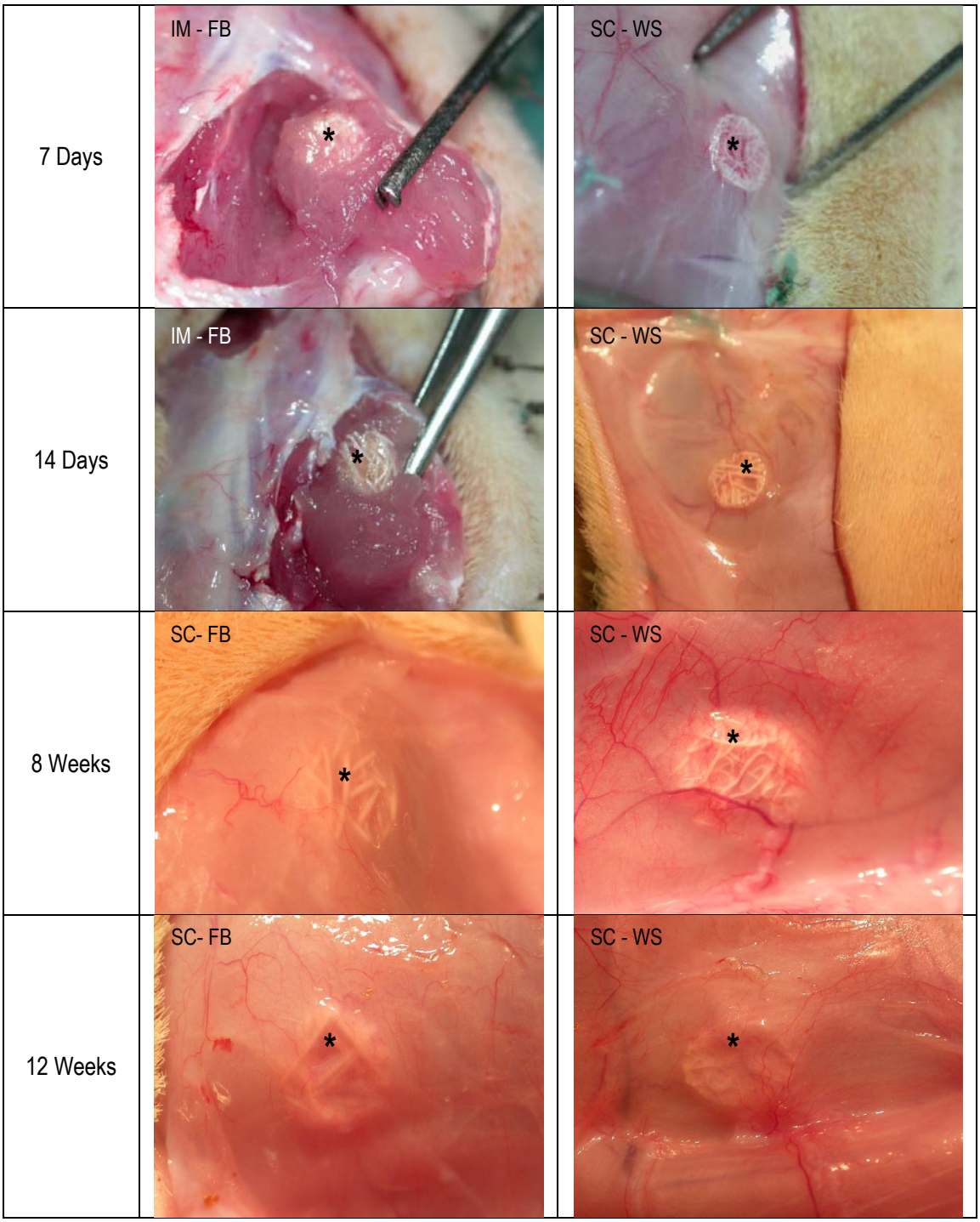

Figure 6.1: Photographs of the explanted fibre bonding (FB) and wet-spinning (WS) produced starch-based scaffolds, after one, two, eight and twelve weeks of intramuscular (IM) and subcutaneous (SC) implantations in rats. All scaffolds have 5mm diameter. * - SPCL scaffold.

The molecular biology analysis for specific genes of inflammation showed that, both after 1 and 2 weeks, the intramuscular implantation of SPCL-WS and SPCL-FB induced the expression of the inflammatory cytokines IL-18 and IL-1α as well as the anti-inflammatory cytokines IL-10 and IFN-γ (Fig. 6.4). In the same manner, the MHC class II was also expressed at both time periods of implantation and for the different types of SPCL scaffolds (Table 6.2). Concerning the other anti-

inflammatory cytokine IL-13, it was expressed in all conditions tested except after 2 weeks of implantation of the SPCL-FB scaffolds (Table 6.2).

Table 6.2: Results for the genes detected by RT-PCR on rat samples.

	GAPDH	IL-18	IL-1α	IL-10	IL-13	IFN-γ	MHC II
7D - SC - WS	+	-	+	-	-	-	-
7D - SC - FB	+	-	+	-	-	-	-
7D - IM - WS	+	+	+	+	-	+	+
7D - IM - FB	+	+	+	+	-	+	+
14D - SC - WS	+	-	+	-	-	-	-
							+
14D - SC - FB	+	-	+	-	-	-	-
14D - IM - WS	+	+	+	+	-	+	+
14D - IM - FB	+	+	+	+	+	+	+
8W - SC - WS	+	-	+	+	+	+	+
8W - SC - FB	+	+	+	+	+	+	+
	+				-	-	
12W - SC - WS	+	-	+	+	+	+	+
						-	
12W - SC - FB	+	-	+	-	+	-	-
						+	+

6.4.2 Subcutaneous implantation

Macroscopic signs of inflammation, infection or swelling were absent at the end points of the subcutaneous implantation of the SPCL-WS and SPCL-FB scaffolds, (Fig. 6.1). The nonexistence of oedema and necrosis was also histologically confirmed (Figs. 6.3.1.A.C.E.F) for all the conditions. A moderate inflammatory infiltrate, essentially characterised by the presence of PMNs (Figs. 6.3.1.A and C), was observed one week post subcutaneous implantation of both SPCL-WS and SPCL-FB scaffolds. However, the intensity of the observed inflammation appeared to be diminished in comparison to what was observed in the first week of intramuscular implantation, in particular for the SPCL-FB scaffold (Figs. 6.3.1.A and C and Figs. 6.3.1.A and C). The CD18 immunodetection confirmed the presence of mainly recruited PMNs, also identified by the multilobulated shape of the nuclei, at the first week of subcutaneous implantation of both types of

SPCL scaffolds (Figs. 6.3.2.A and C). Similarly to what was observed for the intramuscular implantation of SPCL scaffolds, at one week of reaction, a collagen network started to be deposited between the scaffold's fibres, although at an apparent lower density (Figs. 6.3.1.B and D).

Two weeks after the SPCL scaffolds being subcutaneously implanted, the nature of the inflammatory infiltrate changed in comparison to the first week of implantation. Some mononuclear cells and FBGCs were observed in the vicinity of the scaffold's fibres (Figs. 6.3.1.E and G). This tendency was observed for both SPCL-WS and SPCL-FB scaffolds, although the FBGCs density seemed to be greater at the SPCL-FB scaffold's interface (Figs. 6.3.1.G). Mononuclear cells were confirmed to be essentially T lymphocytes, positive for the CD3 marker, both in SPCL-WS and SPCL-FB (Figs. 6.3.2.E and G). At week 2, a higher amount of blood vessels, which seems to be enhanced in comparison to the intramuscular implantation of the SPCL scaffolds, was observed within the tissue surrounding the fibres of the subcutaneously implanted scaffolds. Like for the intramuscular implantation, the collagen network became more organized (Figs. 6.3.1.F and H) on the outline of the fibres 2 week after the subcutaneous implantation of both types of SPCL scaffolds.

In terms of systemic reaction, the overall observation of the lymph nodes structure revealed that, one week after subcutaneous implantation of both SPCL-WS and SPCL-FB, germinal centres (lighter area) were present in the cortex of the nodes (Fig. 6.3.3 A and C). Comparatively to the intramuscular implantation of SPCL scaffolds, denser areas surrounding the germinal centres of the lymph nodes comprehending lymphocytes (Fig. 6.3.3 A and C), were also observed. PI3K was not detected in the lymph nodes of the animals with SPCL-WS subcutaneously implanted for 1 week (Figs. 6.3.3.B, D, F and H). Although positive for the other conditions, only few positive cells were observed. Two week after implantation, the explanted lymph nodes still revealed the presence of germinal centres, with no differences between the animals implanted with the two types of scaffolds (Fig. 6.3.3 E and G). Again, PI3K signal was only present in a small number of cells in the nodes of the animals with both types of SPCL scaffolds implanted (Fig. 6.3.3 F and H).

The evaluation of a long term host response to the implantation of SPCL-FB and SPCL-WS scaffolds was performed after 8 and 12 weeks of subcutaneous implantation.

The macroscopic features observed at the end time points were similar to the ones found for the short term implantation. In fact, the implantation site did not show visible signs of inflammation, infection or swelling (Fig. 6.1). At 8 weeks of implantation the histological observation revealed a similar reaction for both SPCL scaffolds (Figs. 6.3.4A and C). The inflammatory infiltrate was

reduced in comparison to the short term subcutaneous implantation time periods (1 and 2 weeks). No significant differences were observed between 8 and 12 weeks of implantation of the two types of SPCL scaffolds (Figs. 6.3.4E and G).

The obtained results regarding the quantification of inflammation around the two types of SPCL scaffolds revealed to be identical. Therefore only the results for the SPCL-WS scaffolds are mentioned. The SPCL-WS scaffolds occupied an area which did not vary significantly from 8 to 12 weeks of implantation (Fig. 6.5). At 8 weeks of implantation the area of the inflammatory infiltrate was significantly lower than the area of the scaffolds (Fig. 6.5). However, the inflammation area notably increased from 8 to 12 weeks (Fig. 6.5) of implantation. Additionally, the inflammation area at 12 weeks of implantation was significantly higher compared with the area occupied by the implanted SPCL-WS scaffolds (Fig. 6.5).

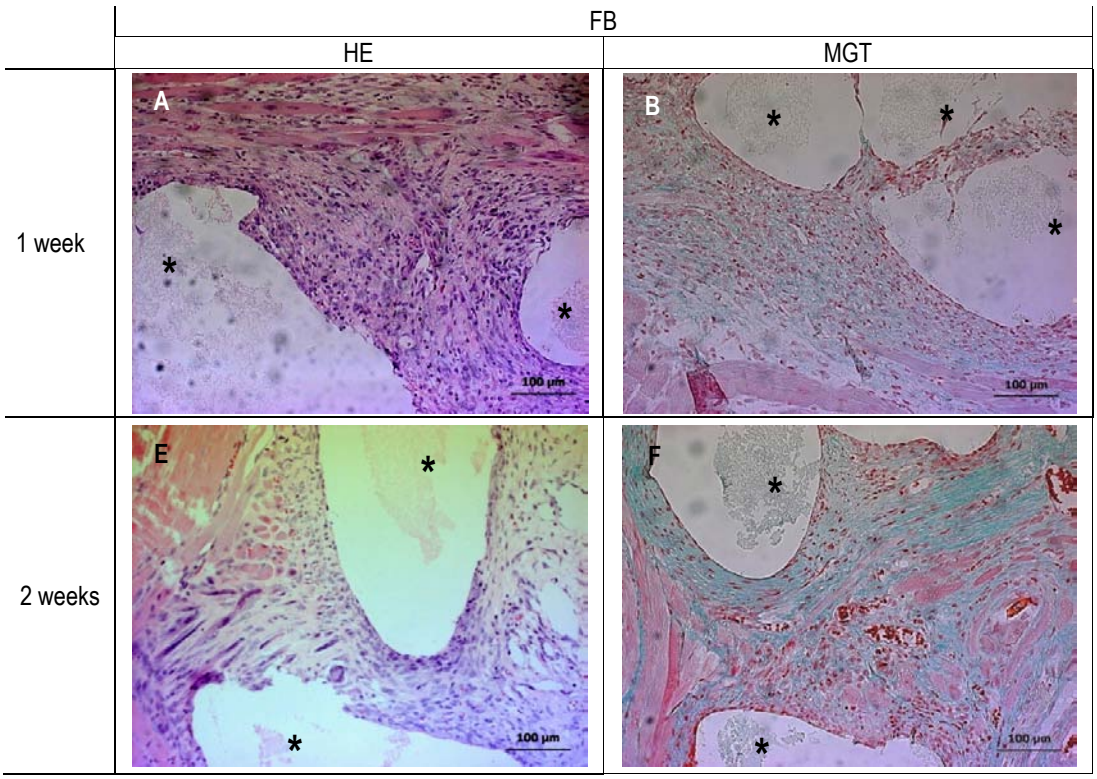

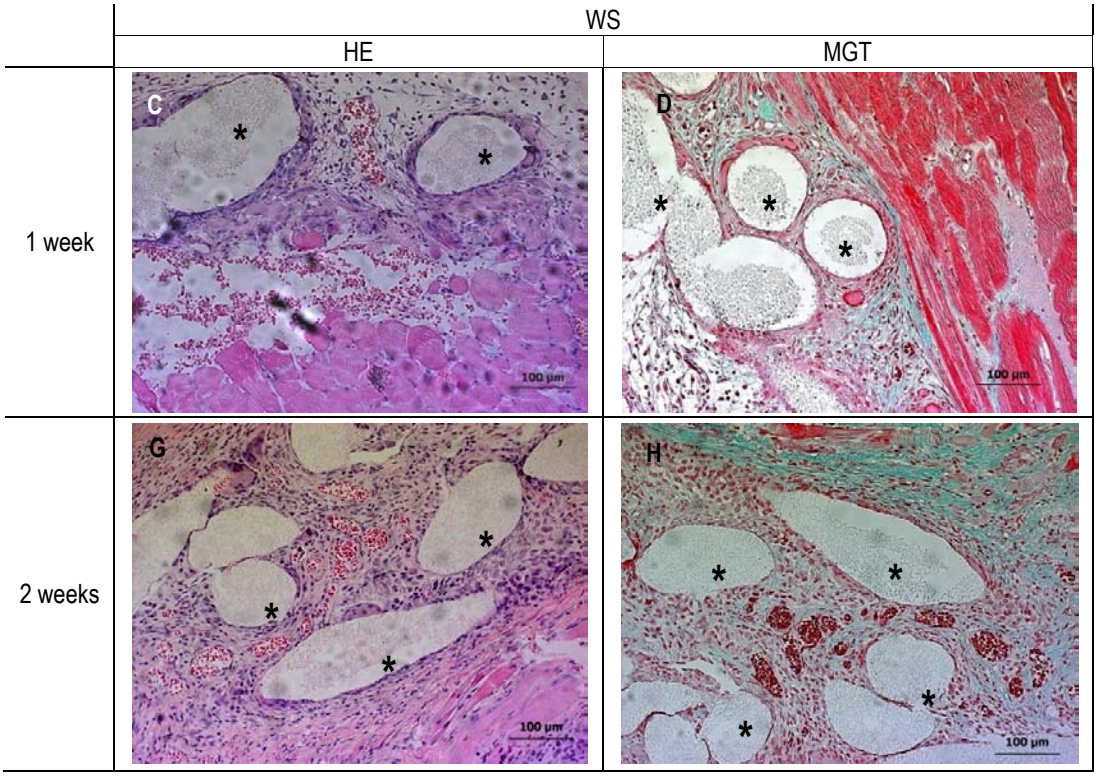

Figure 6.2.1: Micrographs of the sections of the explanted fibre bonding and wet-spinning produced starch-based scaffolds, after one (A-D) and two (E-H) weeks of intramuscular implantation in rats. Tissue was stained with Haematoxylin & Eosin (A, C, E, G) and Masson Goldner Trichrome (B, D, F, G). * - SPCL scaffold.

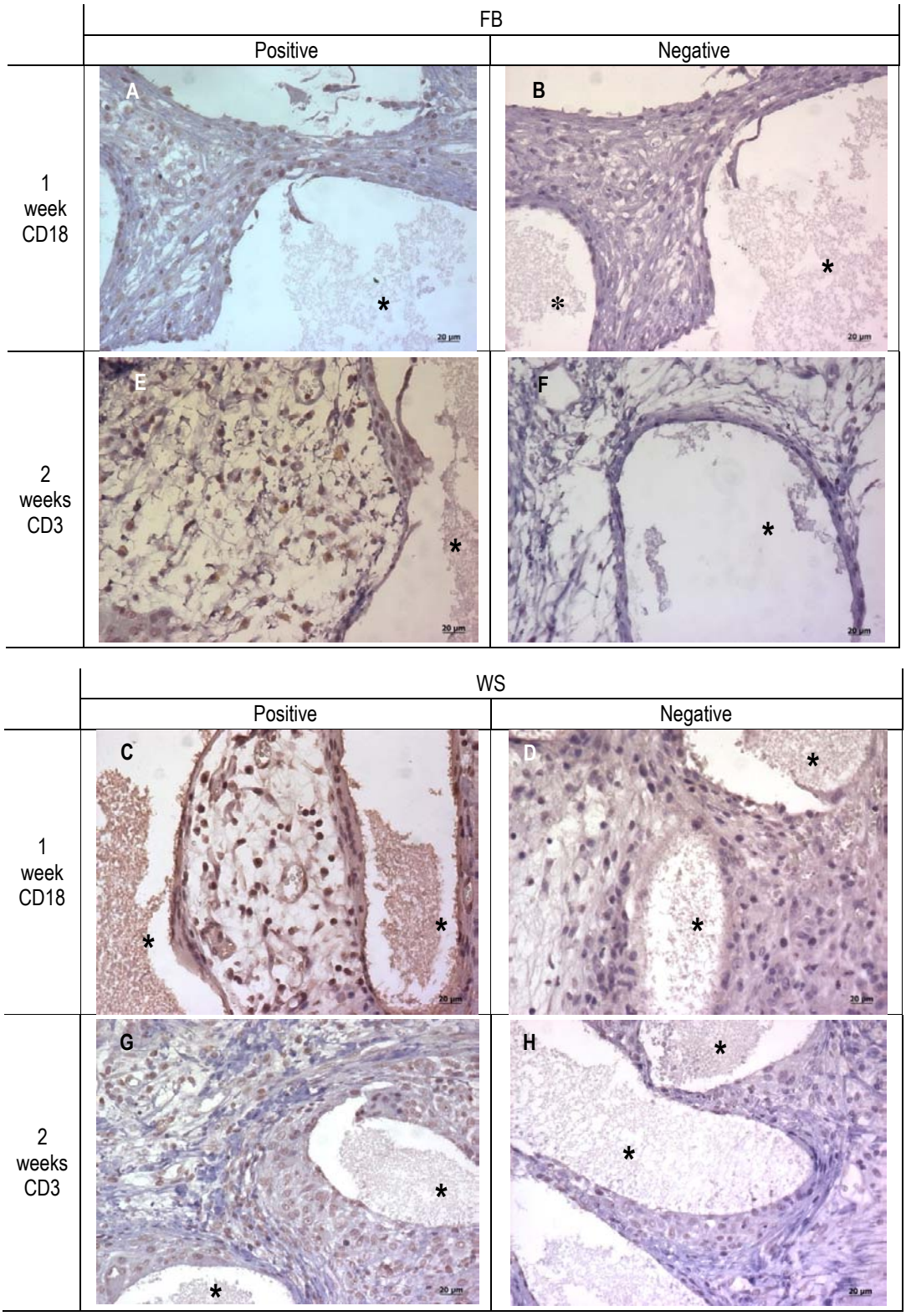

Figure 6.2.2: Micrographs of the sections of the explanted fibre bonding and wet-spinning produced starch-based scaffolds after one (A-D) and two (E-H) weeks of intramuscular implantation in rats. Tissue was immunohistochemically labelled for CD18 and CD3. * - SPCL scaffold.

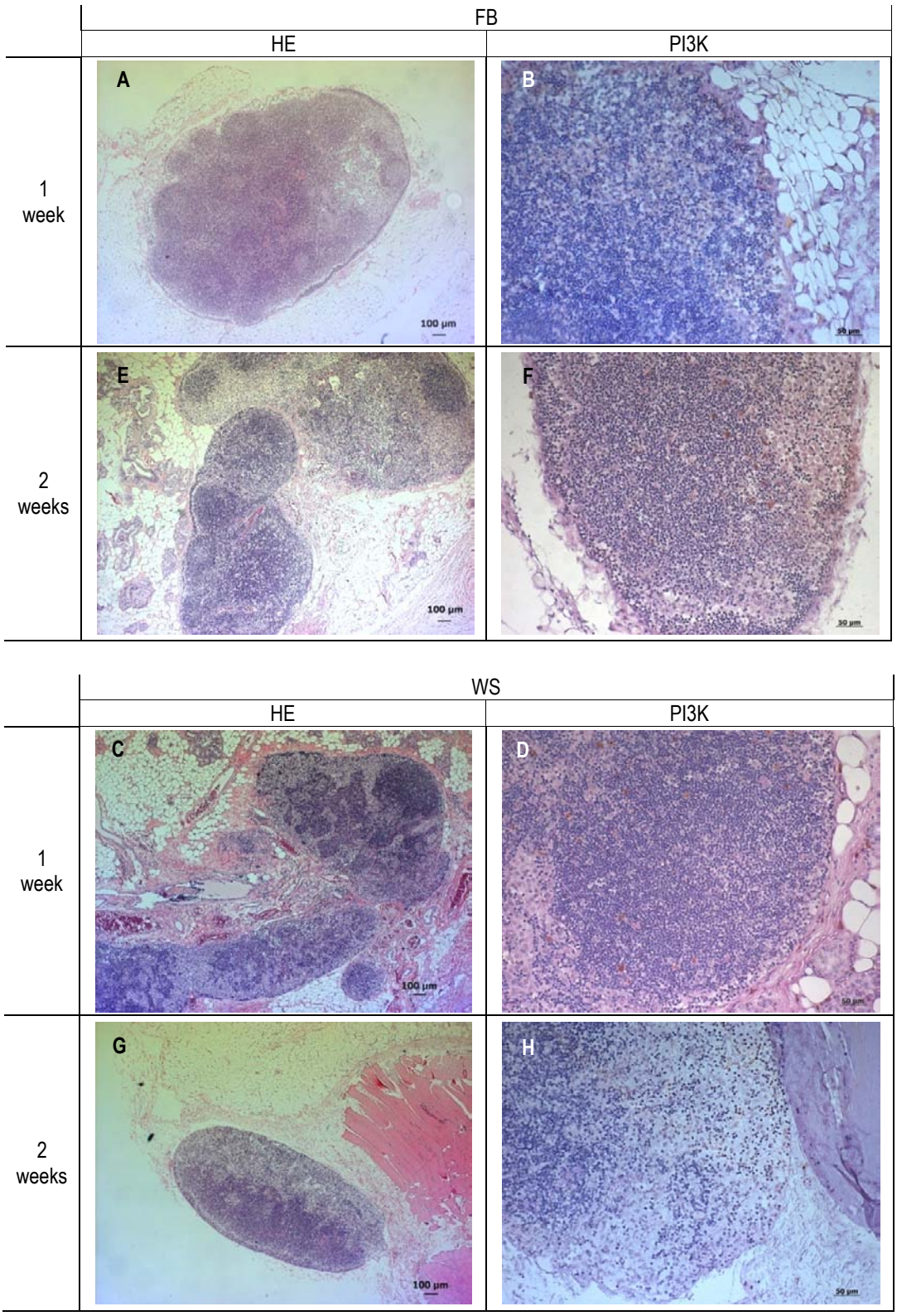

Figure 6.2.3: Micrographs of the sections of the explanted lymph nodes, after one (A-D) and two (E-H) weeks of intramuscular implantation in rats. Tissue was stained with Haematoxylin & Eosin (A, C, E, G) and immunohistochemically labelled for Pi3K (B, D, F, G).

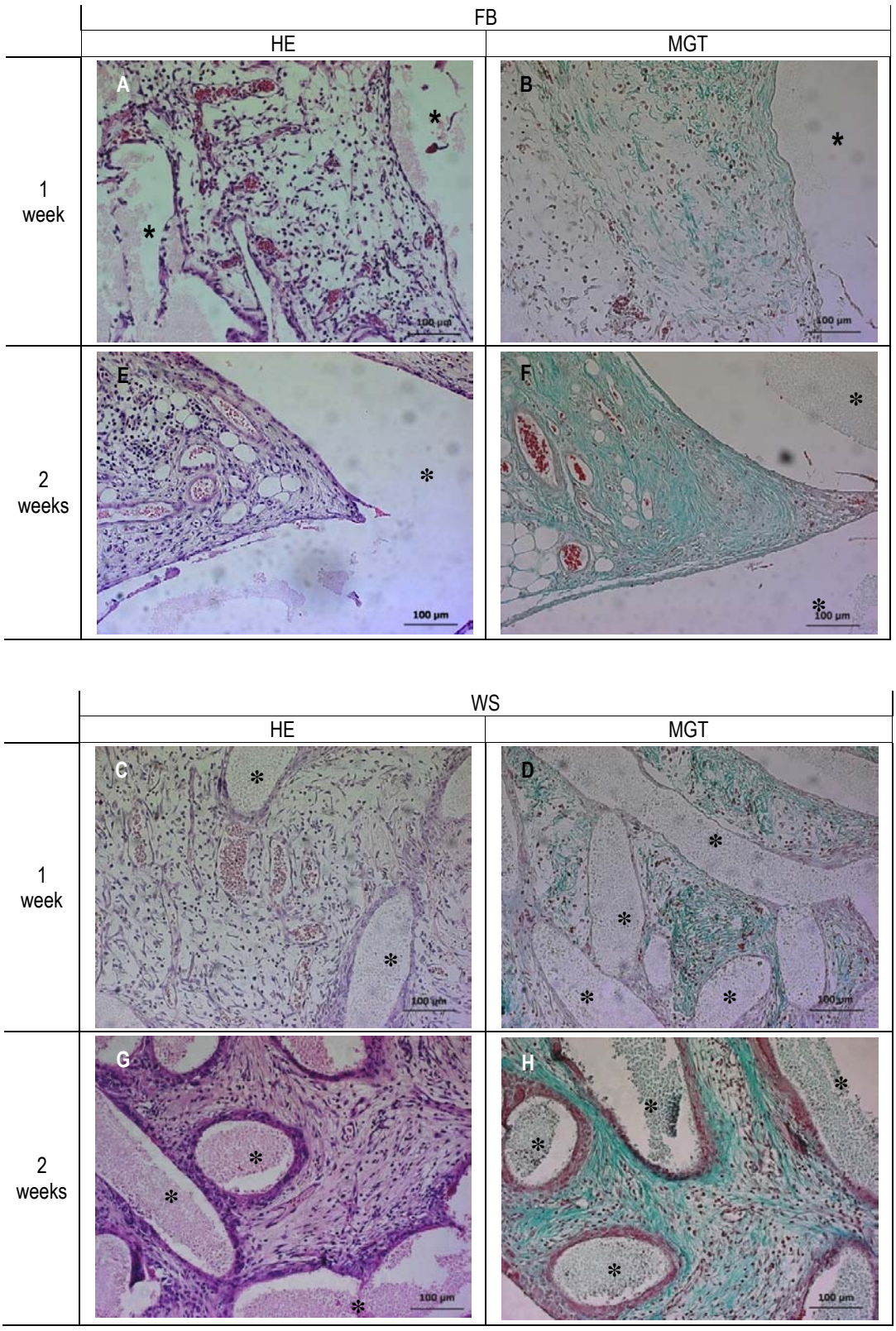

Figure 6.3.1: Micrographs of the sections of the explanted fibre bonding and wet-spinning produced starch-based scaffolds, after one (A-D) and two (E-H) weeks of subcutaneous implantation in rats. Tissue was stained with Haematoxylin & Eosin (A, C, E, G) and Masson Goldner Trichrome (B, D, F, G). * - SPCL scaffold.

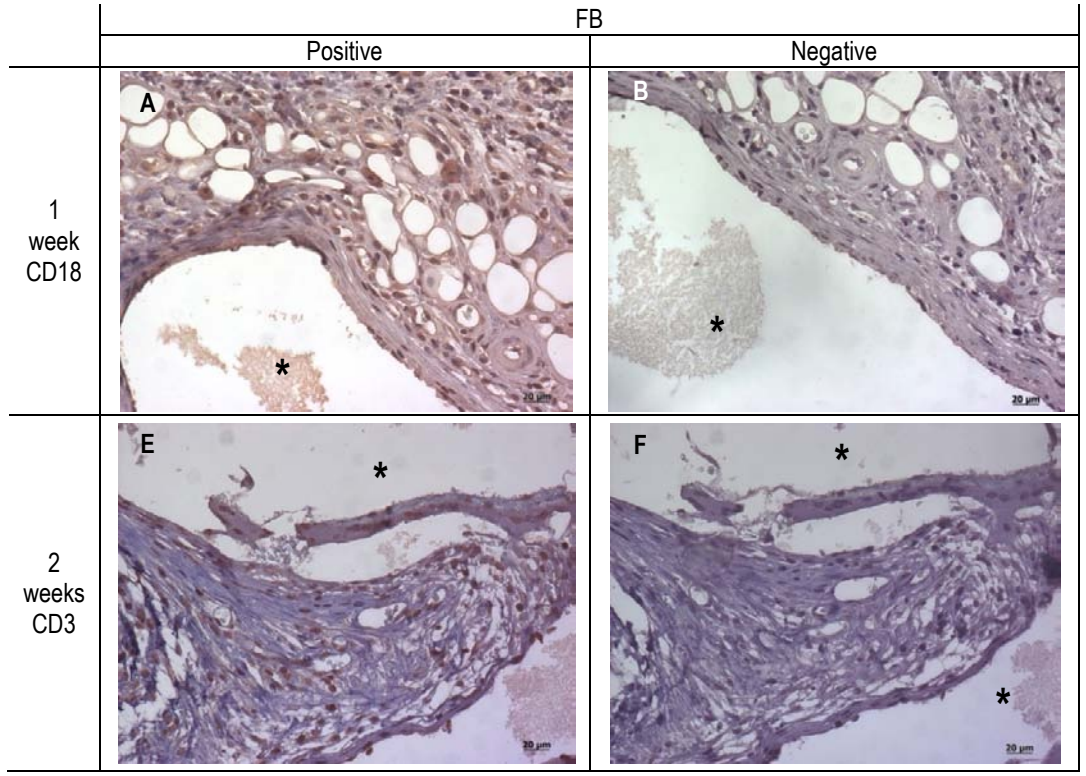

Figure 6.3.2: Micrographs of the sections of the explanted fibre bonding and wet-spinning produced starch-based scaffolds after one (A-D) and two (E-H) weeks of subcutaneous implantation in rats. Tissue was immunohistochemically labelled for CD18 and CD3. * - SPCL scaffold.

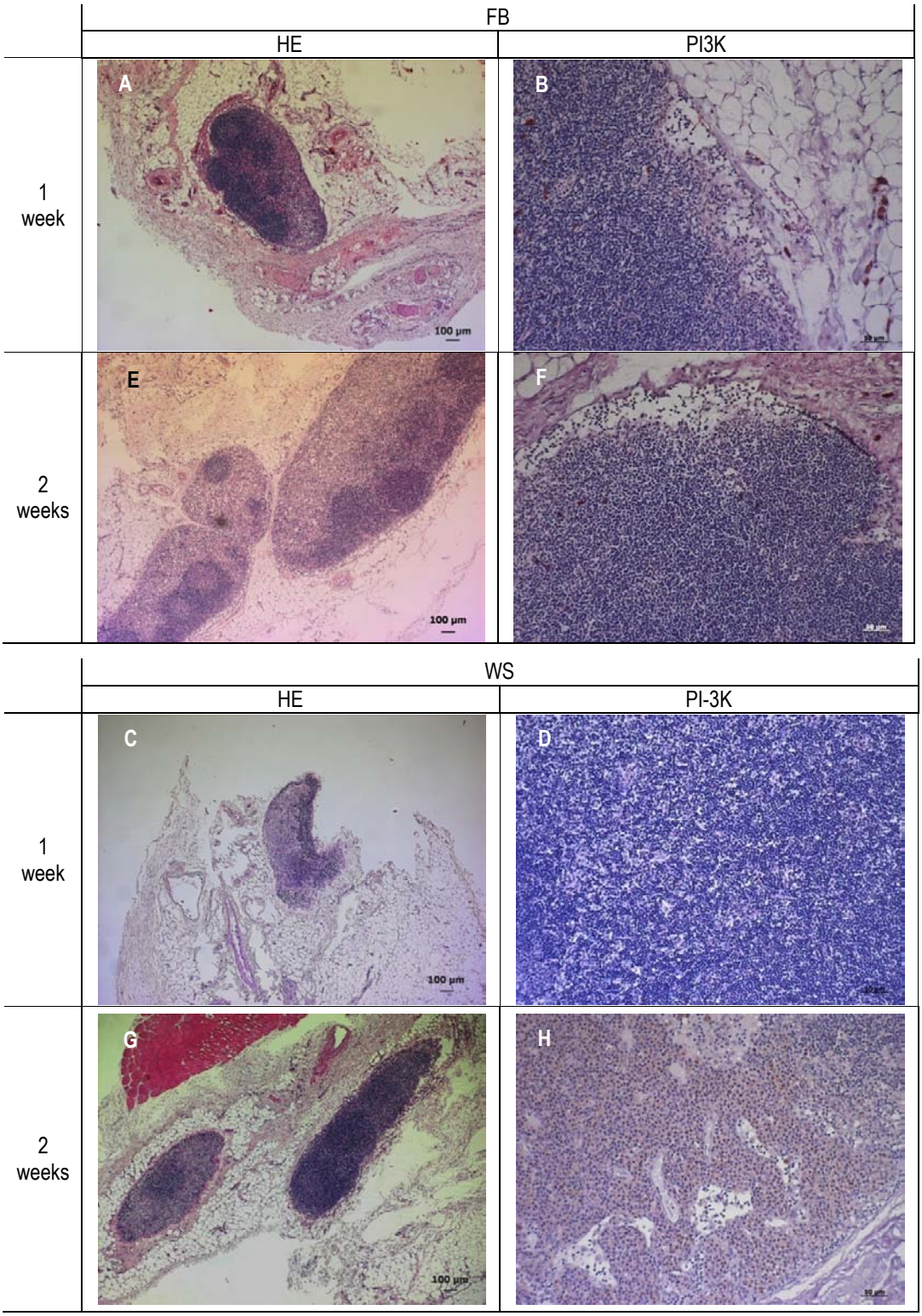

Figure 6.3.3: Micrographs of the sections of the explanted lymph nodes, after one (A-D) and two (E-H) weeks of subcutaneous implantation in rats. Tissue was stained with Haematoxylin & Eosin (A, C, E, G) and immunohistochemically labelled for Pi3K (B, D, F, G).

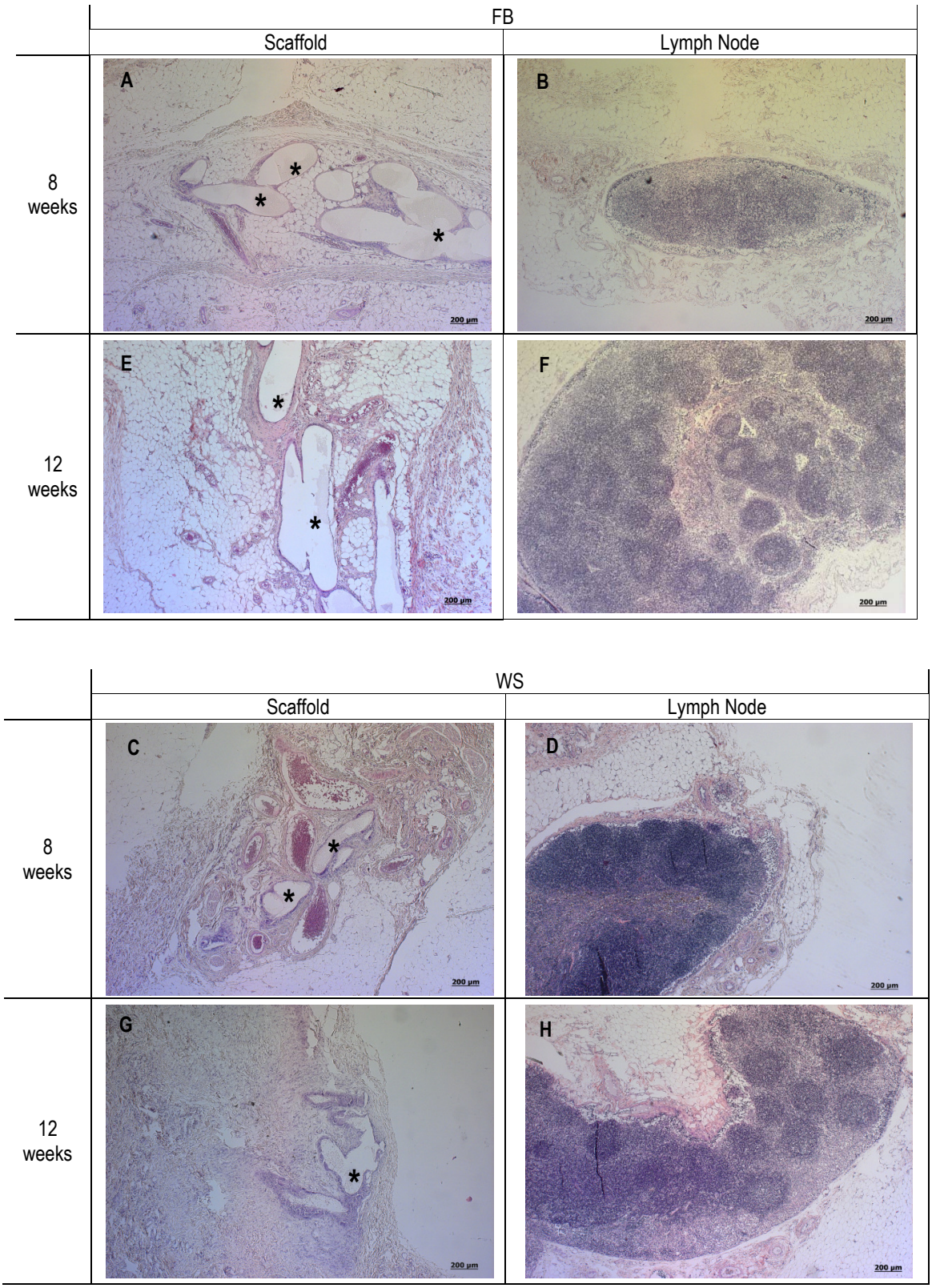

Figure 6.3.4: Micrographs of the sections of the explanted fibre bonding and wet-spinning produced starch-based scaffolds (A, E, C, G) and nearby lymph nodes (B, F, D, H), after 8 (A-D) and 12 (E-H) weeks of subcutaneous implantation in rats. * - SPCL scaffold.

Figure 6.4: Representative photograph of the electrophoresis gels reporting the results of the detected genes by PCR. This gel shows the results obtained for the IL-10 gene on the intramuscularly implanted SPCL scaffolds (1 to 6), and on the subcutaneously implanted SPCL scaffolds (7 to 13). Line 14 is the negative control and A is the cDNA marker.

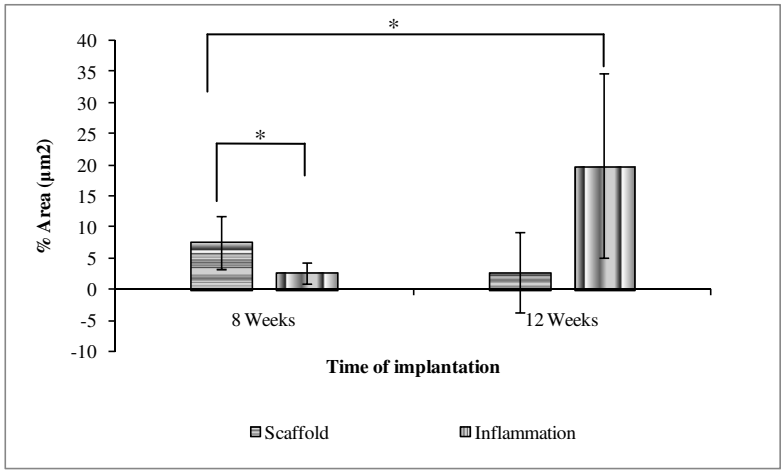

Figure 6.5: Areas occupied by the SPCL scaffolds and by the inflammatory infiltrate relatively to the total area quantified on the micrographs (Mean ± STD); * represent significant differences (p<0.05).

Concerning the molecular expression of specific genes of inflammation, the subcutaneous implantation of both SPCL-WS and SPCL-FB scaffolds induced the expression of IL-1α, but not IL-18, both at 1 and 2 weeks of implantation (Table 6.2). Regarding the anti-inflammatory cytokines IL-10, IL-13, IFN-γ and MHC class II, all tested conditions did not induce their expression. An exception was observed for the implantation of SPCL-WS for 14 days, which showed MHC II expression in half of the samples (Fig. 6.4 and Table 6.2).

In the long term host reaction, the molecular biology analysis showed that the inflammatory marker IL-1α was expressed both at 8 and 12 weeks of subcutaneous implantation of SPCL-WS and SPCL-FB scaffolds. Conversely IL-18 was not expressed in any condition, except for the SPCL-FB implanted for 8 weeks (Table 6.2). For a long term implantation reaction it was

expected the expression of a pro-wound healing pattern of cytokines, although that was not observed. Thus, after 8 weeks of subcutaneous implantation, both types of SPCL scaffolds induced the expression of IL-10, IL-13, IFN-γ and MHC II, although half of the SPCL-FB samples did not induce the expression of IL-13 and IFN-γ (Fig. 6.4 and Table 6.2). When SPCL-WS was implanted for 12 weeks, all the anti-inflammatory cytokines tested were expressed, albeit IFN-γ was not expressed in half of the samples (Table 6.2). For the same time of implantation, the SPCL-FB scaffolds induced the expression IL-13 in all samples, but IFN-γ and MHC II only in half of the samples (Table 6.2). On the contrary, IL-10 was not expressed after 12 weeks of SPCL-FB implantation (Fig. 6.4 and Table 6.2).

6.5 Discussion

The evaluation of the host reaction induced by the biomaterials aimed for TE application has been neglected, partly due to the increasing significance given to the other components of TE constructs, such as cells and growth factors [11]. This research work aimed to stress the influence and the relevance of the support material over the host reaction to an implanted TE construct, by addressing the response elicited by the implantation of two different types of SPCL scaffolds.

Microscopically, the subcutaneous implantation, considering the first 2 time periods, acute and onset of chronic inflammation respectively, showed a slight lower inflammatory reaction in comparison to the intramuscular implantation of both types of SPCL scaffolds. However, when the SPCL scaffolds were subcutaneously implanted for longer periods, the implant was perfectly integrated into the host tissue and the inflammatory process was resolving. In fact, the histological analysis at 8 and 12 weeks after SC implantation, showed the absence of fibrotic capsule, lower amounts of FBGCs and the total inflammation area was not significant in comparison to the area occupied by the scaffolds.

The presented results indicate that intramuscular implantation of biomaterials may be considered a more reactive implantation model to evaluate biomaterial-host interaction in terms of inflammatory/immune response, since the subcutaneous implantation showed a slight lower inflammatory/immune reaction to the SPCL scaffolds.

The present work showed that SPCL scaffolds induced the expression of IL-18 when intramuscularly implanted both for 7 and 14 days. This means that macrophages are activated at the implantation site [35]. The presented results revealed a associated expression of IL-18 and

IFN-γ, which is in accordance with previous a precious report demonstrating that IL-18 acts in T lymphocytes to induce the production of IFN-γ [35]. Conversely, the subcutaneous implantation of the SPCL scaffolds did not induce IL-18 expression and subsequent up-regulation of IFN-γ secretion by T lymphocytes. This may indicate that the inflammatory process is being resolved with PMNs apoptosis following activation [36]. However, IL-1α is expressed at all times of implantation and in both implantation models. It is well known that in the early stage of inflammation IL-1α is expressed by macrophages and endothelial cells which thus stimulate activation of B and T lymphocytes, and at latter inflammation phase is secreted by dendritic cells and B lymphocytes [35], which explains the detection of IL-1α at an early stage expressed by macrophages and at a later stage secreted by B lymphocytes and dendritic cells. Beezhold and Lause [37] demonstrated that macrophage interaction with fibronectin can lead to an increased release of IL-1 cytokines and increased IL-1 mRNA expression. This may also be a reason for the constant presence of IL-1α along all the implantation periods, meaning that macrophages were in contact with the fibronectin deposited on the SPCL scaffold's surface [27].

In the present work IL-10 was expressed in the intramuscular implantation at 7 and 14 days, as well as in the SC implantation for 8 weeks. Since IL-10 is secreted by T_H2 lymphocytes and acts on antigen presenting cells (APCs) by down-regulating MHC class II expression [35], our results showing the simultaneous IL-10 and MHC class II expression were not expected. A possible reason for the observed expression patterns of the MHC class II encoding genes is the close co-relation with IFN-γ expression, since it was previously reported that the inhibition of IFN-γ coincides with MCH class II inhibition [38].

At later time of implantation, SPCL scaffolds induced the expression of IL-13, an important regulator of inflammation and a pro-wounding cytokine [35]. This occurred as expected [39] and indicates that the surface chemistry of the SPCL scaffolds do not inhibit wound healing.

After 8 weeks of subcutaneous implantation of the SPCL scaffolds, the differences observed for the 2 different types of scaffolds were non considerable, indicating that resolution of inflammation took place with the integration of the scaffolds in the host tissue. At week 12 after implantation, the induced cytokine expression profile was typical of chronic inflammatory process and normal ongoing of inflammation provoked by the implantation of biodegradable biomaterials, although no fibrotic capsule was histologically observed surrounding the fibres of the scaffolds.

The present results show that SPCL scaffolds produced by two different methodologies, wet spinning [25] and fibre-bonding [21] do not induce a severe soft tissue inflammatory reaction. This could be observed by the low host reaction detected after subcutaneous and intramuscular

implantations of both types of SPCL scaffolds in rats for 1 and 2 weeks. Additionally, the a long-term implantation in the subcutaneous tissue of rats for 8 and 12 weeks showed a good integration of the SPCL scaffolds into the host tissue and a pro-wound healing cytokine profile expression.

6.6 Conclusions

The present work demonstrates that SPCL scaffolds produced by wet spinning (SPCL-WS) or by fibre bonding (SPCL-FB) methodologies induce a moderate inflammatory reaction after subcutaneous and intramuscular implantations. Nevertheless, SPCL-WS seemed to be less reactive, particularly when the cytokine profile was evaluated, showing an early resolution of the inflammatory process compared with the SPCL-FB scaffolds.

Additionally, it was shown that the intramuscular (IM) implantation of the same type of materials induces a slight intense inflammatory response in comparison to the subcutaneous (SC) model, which may indicate that IM implantation is a more sensitive model to address the inflammation and immune host response to biomaterial's implantation.

References

1. Rada, T., R.L. Reis, and M.E. Gomes, *Adipose Tissue-Derived Stem Cells and Their Application in Bone and Cartilage Tissue Engineering.* Tissue Eng Part B Rev, 2009.
2. Rombouts, W.J. and R.E. Ploemacher, *Primary murine MSC show highly efficient homing to the bone marrow but lose homing ability following culture.* Leukemia, 2003. **17**(1): p. 160-170.
3. Krebsbach, P.H., et al., *Repair of craniotomy defects using bone marrow stromal cells.* Transplantation, 1998. **66**(10): p. 1272-1278.
4. Bruder, S.P., et al., *Bone regeneration by implantation of purified, culture-expanded human mesenchymal stem cells.* J Orthop Res, 1998. **16**(2): p. 155-162.
5. Bruder, S.P., et al., *The effect of implants loaded with autologous mesenchymal stem cells on the healing of canine segmental bone defects.* J Bone Joint Surg Am, 1998. **80**(7): p. 985-996.
6. Bruder, S.P., et al., *Mesenchymal stem cells in osteobiology and applied bone regeneration.* Clin Orthop Relat Res, 1998(355 Suppl): p. S247-S256.

7. Uebersax, L., H.P. Merkle, and L. Meinel, *Insulin-like growth factor I releasing silk fibroin scaffolds induce chondrogenic differentiation of human mesenchymal stem cells.* J Control Release, 2008. **127**(1): p. 12-21.
8. Abarrategi, A., et al., *Chitosan film as rhBMP2 carrier: delivery properties for bone tissue application.* Biomacromolecules, 2008. **9**(2): p. 711-718.
9. Wei, G., et al., *The enhancement of osteogenesis by nano-fibrous scaffolds incorporating rhBMP-7 nanospheres.* Biomaterials, 2007. **28**(12): p. 2087-2096.
10. Jeon, O., et al., *Enhancement of ectopic bone formation by bone morphogenetic protein-2 released from a heparin-conjugated poly(L-lactic-co-glycolic acid) scaffold.* Biomaterials, 2007. **28**(17): p. 2763-2771.
11. Mikos, A.G., et al., *Host response to tissue engineered devices.* Adv Drug Deliv Rev, 1998. **33**(1-2): p. 111-139.
12. Aggarwal, S. and M.F. Pittenger, *Human mesenchymal stem cells modulate allogeneic immune cell responses.* Blood, 2005. **105**(4): p. 1815-1822.
13. Rasmusson, I., et al., *Mesenchymal stem cells inhibit lymphocyte proliferation by mitogens and alloantigens by different mechanisms.* Exp Cell Res, 2005. **305**(1): p. 33-41.
14. Glennie, S., et al., *Bone marrow mesenchymal stem cells induce division arrest anergy of activated T cells.* Blood, 2005. **105**(7): p. 2821-7.
15. Niemeyer, P., et al., *Comparison of immunological properties of bone marrow stromal cells and adipose tissue-derived stem cells before and after osteogenic differentiation in vitro.* Tissue Eng, 2007. **13**(1): p. 111-21.
16. Puissant, B., et al., *Immunomodulatory effect of human adipose tissue-derived adult stem cells: comparison with bone marrow mesenchymal stem cells.* Br J Haematol, 2005. **129**(1): p. 118-29.
17. Crouzier, T., et al., *Layer-by-layer films as a biomimetic reservoir for rhBMP-2 delivery: controlled differentiation of myoblasts to osteoblasts.* Small, 2009. **5**(5): p. 598-608.
18. Gomes, M.E., et al., *A new approach based on injection moulding to produce biodegradable starch-based polymeric scaffolds: morphology, mechanical and degradation behaviour.* Biomaterials, 2001. **22**(9): p. 883-889.
19. Gomes, M.E., et al., *In vitro localization of bone growth factors in constructs of biodegradable scaffolds seeded with marrow stromal cells and cultured in a flow perfusion bioreactor.* Tissue Eng, 2006. **12**(1): p. 177-188.

20. Salgado, A.J., et al., *In vivo response to starch-based scaffolds designed for bone tissue engineering applications.* Journal of Biomedical Materials Research Part A, 2007. **80A**(4): p. 983-989.
21. Gomes, M.E., et al., *Starch-poly(epsilon-caprolactone) and starch-poly(lactic acid) fibre-mesh scaffolds for bone tissue engineering applications: structure, mechanical properties and degradation behaviour.* J Tissue Eng Regen Med, 2008. **2**(5): p. 243-252.
22. Santos, M.I., et al., *Endothelial cell colonization and angiogenic potential of combined nano- and micro-fibrous scaffolds for bone tissue engineering.* Biomaterials, 2008. **29**(32): p. 4306-4313.
23. Azevedo, H.S. and R.L. Reis, *Encapsulation of alpha-amylase into starch-based biomaterials: An enzymatic approach to tailor their degradation rate.* Acta Biomater, 2009.
24. Martins, A.M., et al., *The Role of Lipase and alpha-Amylase in the Degradation of Starch/Poly(varepsilon-Caprolactone) Fiber Meshes and the Osteogenic Differentiation of Cultured Marrow Stromal Cells.* Tissue Eng Part A, 2009. **15**(2): p. 295-305.
25. Tuzlakoglu, K., et al., *A new route to produce starch-based fiber mesh scaffolds by wet spinning and subsequent surface modification as a way to improve cell attachment and proliferation.* Journal of Biomedical Materials Research Part A *in press*, 2009.
26. Marques, A.P., et al., *Effect of starch-based biomaterials on the in vitro proliferation and viability of osteoblast-like cells.* Journal of Materials Science-Materials in Medicine, 2005. **16**(9): p. 833-842.
27. Alves, C.M., et al., *Modulating bone cells response onto starch-based biomaterials by surface plasma treatment and protein adsorption.* Biomaterials, 2007. **28**(2): p. 307-315.
28. Balmayor, E.R., et al., *A novel enzymatically-mediated drug delivery carrier for bone tissue engineering applications: combining biodegradable starch-based microparticles and differentiation agents.* J Mater Sci Mater Med, 2008. **19**(4): p. 1617-1623.
29. Martins, A.M., et al., *Natural origin scaffolds with in situ pore forming capability for bone tissue engineering applications.* Acta Biomater, 2008. **4**(6): p. 1637-1645.
30. Azevedo, H.S., F.M. Gama, and R.L. Reis, *In vitro assessment of the enzymatic degradation of several starch based biomaterials.* Biomacromolecules, 2003. **4**(6): p. 1703-1712.
31. Santos, M.I., et al., *Crosstalk between osteoblasts and endothelial cells co-cultured on a polycaprolactone-starch scaffold and the in vitro development of vascularization.* Biomaterials, 2009. **30**(26): p. 4407-15.

32. Santos, M.I., et al., *Response of micro- and macrovascular endothelial cells to starch-based fiber meshes for bone tissue engineering.* Biomaterials, 2007. **28**(2): p. 240-8.
33. Reis, R.L., et al., *Processing and in vitro degradation of starch/EVOH thermoplastic blends.* Polym Int, 1997. **43**: p. 347.
34. Kirkwood, B. and J. Sterne, *Essential Medical Statistics*. 2nd Edition ed. 2003: Wiley. 512.
35. Goldsby, R.A., T.J. Kindt, and B.A. Osborne, *Kuby Immunology*. 2000, USA: W. H. Freeman and Company.
36. Kobayashi, S.D., et al., *Down-regulation of proinflammatory capacity during apoptosis in human polymorphonuclear leukocytes.* J Immunol, 2003. **170**(6): p. 3357-3368.
37. Beezhold, D.H. and D.B. Lause, *Stimulation of rat macrophage interleukin 1 secretion by plasma fibronectin.* Immunol Invest, 1987. **16**(5): p. 437-449.
38. Khouw, I.M., et al., *Inhibition of the tissue reaction to a biodegradable biomaterial by monoclonal antibodies to IFN-gamma.* J Biomed Mater Res, 1998. **41**(2): p. 202-210.
39. Brodbeck, W.G., et al., *In vivo leukocyte cytokine mRNA responses to biomaterials are dependent on surface chemistry*. J Biomed Mater Res A, 2003. **64**(2): p. 320-329.

Chapter VII

In vivo evaluation of the suitability of starch-based constructs for tissue engineering applications

7.1 Abstract

The ideal bone tissue engineering construct remains to be found, although daily discoveries significantly contribute to improvements in the field and certainly have valuable long term outcomes. In this work, different tissue engineering elements, aiming at bone tissue engineering applications, were assembled. Starch/polycaprolactone (SPCL) scaffolds, obtained by two different methodologies, were combined with fibrin sealant (Baxter®), human Adipose-derived Stem Cells (hASCs), and growth factors (Vascular Endothelial Growth Factor – VEGF or Fibroblast Growth Factor-2 – FGF-2), and implanted in vascular endothelial growth factor receptor-2 (*VEGFR2)-luc* transgenic mice. The performance of the designed constructs was followed using a luminescence device (Xenogen®) and at the end of observation (2 weeks) the explants were retrieved to perform histological analysis and RT-PCR for vascularisation (VEGF and VEGFR-1) and inflammatory (TNF-α, IL-4 and INF-γ) markers.

The results clearly showed that starch-based scaffolds obtained by wet spinning and by fibre bonding methodologies constitute a quite adequate support for ASCs. Furthermore it was demonstrated that the assembled TE constructs composed by fibrin sealant, ASCs, VEGF and FGF-2 induce only a mild inflammatory reaction after 2 weeks of implantation, and that the release of VEGF and FGF-2 from the constructs enhance the expression of VEGFR-2 as well as specific molecular markers of neovascularisation.

***This chapter is based on the following publication:**

T. C. Santos, T. Morton, M. Moritz, S. Pfeiffer, K. Reise, A. P. Marques, A. G. Castro, R. L. Reis, M. van Griensven, In vivo *evaluation of the suitability of starch-based constructs for tissue engineering applications*. **2009. *Submitted*.**

7.2 Introduction

The field of tissue engineering (TE) has achieved several successes within the recent past [1, 2]. Different biomaterials, cells, growth factors and stimulation conditions, as well as numerous combinations among them have been proposed by several research groups as potential routes to assemble the perfect bone TE construct [3-8]. Despite this, in bone TE, vascularisation remains a fairly large concern, not yet perfectly addressed. Besides the well known fact that bone is extremely dependent on a vascular network which provides nutrients, minerals and oxygen essential for cell survival [9], angiogenesis was shown to play a key role, not only in bone growth [9], but also in bone healing [10] and consequently in bone tissue regeneration. Numerous strategies [5, 11-13] have therefore emerged as a need to achieve the vascularisation of bone engineered constructs within a reasonable time, which contributes to attain functional tissue substitutes.

Noteworthy, works have been showing that endothelial cells, either in single culture or co-cultured with primary osteoblasts or stem cells, in 3D structures leads to the formation of vascular-like structures *in vitro* [14, 15] and improves vascularisation *in vivo* [11, 16-18]. Nevertheless, despite the developments in cell isolation and culture technologies, the variability of cell sources, as well as in culture conditions among the different studies is still a major issue and might jeopardize some of the conclusions drawn.

A valuable alternative to tackle the vascularisation of bone TE constructs relies on the incorporation in the construct of important mediators, such as vascular endothelial growth factor (VEGF) [6, 17-20] and fibroblast growth factor (FGF) [21, 22], that can be controlled released from the scaffolding material.

In fact the incorporation of VEGF and subsequent release has been achieved with microspheres [20], hydrogels [21, 22] and 3D scaffolds [17]. For all these systems VEGF release showed to promote *in vitro* and *in vivo* vascularisation [17, 20]. In the same context, FGF-2 showed increased *in vivo* neovascularisation after being released from a chitosan/heparinoid hydrogel after subcutaneous implantation [21, 22]. A combined approach, VEGF plus FGF incorporated into chitosan hydrogels was also attempted with confirmed release of both growth factors within the first day and with a significant stimulation of human umbilical vein endothelial cells (HUVEC) [23]. An uncertain issue is however the degradation rate of the carriers and subsequently the release profile and doses of the loaded factors which, if not controlled, might induce an unexpected reaction [23]. Considering this, a different cell-based strategy aiming at targeting not only the vascularization but also the regeneration of a vascularised tissue as bone, has been also proposed [7, 11]. The differentiation potential of several mesenchymal stem cells (MSCs) has

been taken into consideration when cell-seeded matrices are transplanted into several *in vivo* regeneration models expecting that the undifferentiated cells either undergo a commitment into the lineages of interest [5, 18] or significantly contribute to signalling host progenitor cells [16].

In this work it was hypothesised that the assembly of a complex tissue engineering construct, comprehending a well studied starch-based scaffold (SPCL) [3, 24, 25] and fibrin glue [26], human adipose-derived stem cells (hASCs) [27] and key growth factors (VEGF and FGF-2) [28, 29], would induce the vascularisation of the construct, compared to the scaffold by itself and with different, reduced combinations of the same factors.

Taking into consideration the features of the mentioned cells, growth factors and materials used in the last years of investigation in TE, as well as the results of the present research work, it will be possible to achieve a deeper knowledge on the role of specific mediators on the integration and performance of the assembled TE constructs. Particularly, with this work it was shown that SPCL-based scaffolds are an adequate support for ASCs transplantation into a host and that the SPCL-based TE constructs composed of fibrin sealant, ASCs, VEGF and FGF-2 induce a moderate inflammatory response typically observed for implanted devices. Additionally, the release of VEGF and FGF-2 from those TE constructs showed to enhance the expression of VEGFR-2, as well as important mediators in the vascularisation of newly formed tissue, such as VEGF and VEGFR-1.

7.3 Materials and Methods

7.3.1 Transfection of the ASCs

In other to trace the human Adipose-derived Stem Cells (hASCs) after implantation, cells were prior transfected with a luciferase plasmid using Lipofectamine™2000 (Invitrogen, UK). Cell transfection was carried out according to the manufacturer's recommendations. Briefly, luciferase DNA (plasmid) and lipofectamine was separately diluted in 50µl of Ham's F-12 cell culture medium (Sigma-Aldrich, Germany), without foetal calf serum (FCS), complemented with 1% L-Glutamin, and antibiotics (basal medium), and gently mixed. The two solutions were mixed and incubated for 20 minutes at room temperature in order to allow the formation of "lipo-complexes". After the incubation period, the mixture was added to the cells in culture and left for 4 hours after which the medium was changed to fresh basal medium. The cells were ready to be used approximately 20 hours after the transfection procedure.

7.3.2 Starch-based Scaffolds Production

Starch-based scaffolds were produced from a blend of Starch with Poly-ε-caprolactone (30:70%) (SPCL), by two different methodologies described elsewhere: wet spinning (SPCL-WS) [4] and

fibre-bonding (SPCL-FB) [3]. Briefly, for the production of SPCL-WS scaffolds, the polymer was dissolved in chloroform at a concentration of 40% (w/v) in order to obtain a polymer solution with proper viscosity. The polymer solution was loaded into a syringe, placed in a syringe pump (World Precision Instruments, UK) and the solution was subsequently extruded into a methanol coagulation solution. The fibre mesh structure was formed during the processing by the random movement of the precipitation container. The formed scaffolds were then dried overnight at room temperature to allow any remaining solvents to evaporate. For the fabrication of the SPCL-FB scaffolds, fibre-meshes previously obtained by a meltspinning methodology were placed in a glass mould and heated in an oven at 150ºC. Immediately after removing the moulds from the oven, the fibres were slightly compressed by a Teflon cylinder and then cooled at −15ºC [3]. All samples were cut into discs of 5mm diameter and approximately 1mm thickness and sterilized by a standard procedure with ethylene oxide [30].

7.3.3 Assembly of the tissue engineering constructs

For the cell tracking experiments the two types of SPCL scaffolds were seeded with the transfected hASCs in a concentration of $1.33x10^4$ cells/scaffold in basal medium supplemented with 10% FCS and 1% antibiotics (penicillin/streptomycin), and incubated for 24 hours at 37ºC and 5% CO_2 in a humidified environment.

The assembling of the TE constructs to implant in the VEGF-R2 transgenic mice was performed as follows: each type of SPCL scaffold was mixed with the 2.0 ml two-component FS Tisseel VH (Baxter AG, Vienna, Austria), growth factors (VEGF and FGF-2), and hASCs. The sealer protein component (Fibrinogen 75–115mg/ml) was reconstituted with a fibrinolysis inhibitor solution (Aprotinin 3,000 KIU/ml) and spiked either with VEGF (200 ng/ml) or FGF-2 (200 ng/ml). The thrombin component (500 IU/ml) was reconstituted with $CaCl_2$ (40-mmol/ml) and diluted to 4 IU/ml [31]. Scaffolds, cells ($1.5x10^4$ cells/scaffold/50µl) and growth factors, which were added to the fibrinogen component, were then mixed with the thrombin component (1:1), in a total volume of 75µl, at 37ºC. The clot was allowed to form for 15 minutes, at 37ºC and 5% CO_2 after which 300µl of cell culture medium was added. Constructs were kept overnight at 37ºC and 5% CO_2.

7.3.4 In vivo implantation

7.3.4.1 Nude Mice

All the animal experiments were previously approved by the local ethical authorities. The *in vivo* fate of the *in vitro* transfected hASCs seeded onto SPCL scaffolds was followed in *nude* mice. Thirteen female Balb/c nu/nu *nude* mice, with an average weight of 21.6g±1.2 were used: 6 animals to implant the SPCL-WS scaffolds, 6 animals to implant the SPCL-FB scaffolds and one animal as control. All surgical procedures were performed under sterile conditions in a vertical

laminar flow hood. Each animal was intraperitoneally (IP) anaesthetized with ketamine (60 mg/kg) and xylazine (7.5 mg/kg). Subsequently, the skin of the mice was disinfected with betaisodona and two lateral incisions of approximately 0.5 cm, containing the subcutis and *Panniculus carnosus*, were performed in the back of the animals. Two caudal-lateral oriented pockets were created in each animal by blunt dissection, where the TE constructs with the transfected ASCs were inserted. After implantation, the *Panniculus carnosus* and the skin of the animals were carefully sutured. The bioluminescence signal, from the *in vivo* luciferase activity that identifies the location of the transfected cells, was quantified (emitted photon counts per second) using the Live Image Software (Xenogen®). Specific areas for the signal detection, considering the original location of the implants and possible migration of the cells from the constructs, were pre-determined (Fig. 7.1A): I and II correspond to the left and right implant sites; III corresponds to the dorsum of the animals, the most probable migration localization. Bioluminescence images were collected immediately after surgery and on days 1, 3, 6, 9, and 13. The luciferase activity was measured 15 minutes after luciferin subcutaneous injection and normalised to the respective areas for further graphical representation.

7.3.4.2 Transgenic mice

Thirty eight FVB/N-Tg(VEGF-r2–luc)Xen mice (VEGFR2-LUC) [32], with an average weight of 33.8g±3.6 were used to assess the effect of the addition of VEGF, FGF-2, hASCs or fibrin sealant to the SPCL scaffolds for vascularisation. These mice carry a transgene that contains a 4.5 kb murine VEGF-R2 promoter fragment that drives the expression of a firefly luciferase reporter protein [32].

Six test groups were established per type of scaffold (Table 7.1): a) untreated control to measure endogenous expression of VEFG-R2 due to surgical procedure; b) scaffold group to measure expression of VEFG-R2 due to scaffold implantation (SPCL-WS and SPCL-FB); c) scaffold plus FS to measure the expression of VEGF-R2 due to the use of FS (SPCL-WS+FS and SPCL-FB+FS); d) scaffold plus FS and hASCs group, to measure the expression of VEGF-R2 due to the presence of hASCs (SPCL-WS+FS+hASCs and SPCL-FB+FS+hASCs); e) scaffold plus FS, hASCs and VEGF (200 ng/mL) to measure the expression of VEGF-R2 induced by the VEGF delivery (SPCL-WS+FS+hASCs+VEGF and SPCL-FB+FS+hASCs+VEGF); and f) scaffold plus FS, ASCs and FGF-2 (200 ng/mL), to measure the expression of VEGF-R2 induced by the FGF-2 delivery (SPCL-WS+FS+hASCs+FGF-2 and SPCL-FB+FS+hASCs+FGF-2).

Table 7.1: Distribution of the test groups for the *in vivo* implantation on the transgenic FVB/N-Tg(VEGF-r2–luc)Xen mice.

Group	Condition	
a	Control – subcutaneous pockets without any implant	
b	SPCL-WS	SPCL-FB
c	SPCL-WS+FS	SPCL-FB+FS
d	SPCL-WS+FS+hASCs	SPCL-FB+FS+hASCs
e	SPCL-WS+FS+hASCs+VEGF	SPCL-FB+FS+hASCs+VEGF
f	SPCL-WS+FS+hASCs+FGF	SPCL-FB+FS+hASCs+FGF

Each animal was anaesthetized using 3% isoflurane for induction and maintaining with an i.p. injection of ketamine (60 mg/kg) and xylazine (7.5 mg/kg). Mice were injected subcutaneously with luciferin (150 mg/kg) and imaged with the *in vivo* imaging system (VivoVisions IVISs, Xenogen, Alameda, CA) to acquire the background image signal corresponding to the pre-surgical activity, set to 100%). Specific areas for the bioluminescence detection were established (Fig. 7.2A): I corresponds to the incision area; II and III correspond to the left and right implant sites (pockets). The signal detected at the incision site correlates with the expression of the *VEGFR2* gene with the ongoing inflammatory process as the incision heals. Each animal's dorsum was then shaved and disinfected, and a 1 cm incision at the caudal aspect of the neck was made. For the subcutaneous implantation, a caudal lateral access to each flank was bluntly subcutaneously created through this incision, forming 2 pockets per animal. Into each pocket, the construct was inserted accordingly to the different test groups. Subsequent measurements in the pre-determined areas were referenced to the pre-surgical baseline and obtained immediately after surgery and on days 3, 6, 9 and 13 after implantation, as well as 15 minutes after luciferin injection.

7.3.5 Ex vivo analysis

At the end of observation (2 weeks), each animal was i.p. anaesthetized and subsequently sacrificed with an intracardial overdose of ketamine (60 mg/kg) and xylazine (7.5 mg/kg). The scaffolds and surrounding tissue were explanted and, half of the sample was fixed in 3.7% formalin for histological analysis, and the other half was snap frozen for molecular biology evaluation. Histology was performed according to existing standard protocols for haematoxylin and eosin staining (HE). Molecular biology was evaluated by reverse transcriptase polymerase chain reaction (RT-PCR) to detect the expression of vascularisation and inflammation (Table 7.2).

Table 7.2: Forward and Reverse sequences of the genes detected by RT-PCR.

Function	Gene	Sequences	Tm (ºC)	Bp
Vascularisation	VEGF-α	Sense - CCGAAACCATGAACTTTCT	55.19	604
		Antisense - CGTTCGTTTAACTCAAGCTG	56.31	
	VEGF-R1	Sense - GAGGGATAACAGGCAATTC	54.59	960
		Antisense - CCCAGCAAGATCGTATAGTC	54.91	
Inflammation	IL-4	Sense - TCATCCTGCTCTTCTTTCTC	54.67	325
		Antisense - GATGTGGACTTGGACTCATT	54.82	
	IFN-γ	Sense - CTACCTTCTTCAGCAACAGC	55.36	568
		Antisense - TGTAGACATCTCCTCCCATC	54.92	
	TNF-α	Sense - GTCTCAGCCTCTTCTCATTC	54.03	654
		Antisense - CAGAGTAAAGGGGTCAGAG	54.57	

7.3.6 Statistical analysis

Mean values and standard deviations are reported for the luminescence signal measurements [33] and represented graphically. Data was analysed by a single factor ANOVA test and the significance value was set at $p<0.05$.

7.4 Results

7.4.1 In vivo ASCs tracking

The luminescence emitted by the transfected cells was acquired with the Live Image Software (Xenogen®) and recorded as emitted photon counts per second.

Before the *in vivo* implantation of the tissue engineered constructs, a SPCL scaffold seeded with the transfected hASC for 24 hours, was placed into the dark chamber of the Xenogen® equipment to confirm the presence of luminescence-emitting cells on the scaffolds (data not shown).

The signal emitted from the transfected cells was similar in both types of SPCL scaffolds, and the peak of emitted signal was detected at day 6 after implantation (Fig. 7.1B). Either for SCPL-WS and for SPCL-FB scaffolds, the luminescence signal starts to increase from day 2 onward, reaching the maximum value at day 6 and decreases from this day until the end point of the experiment, 13 days (Fig. 7.1B). Nevertheless, for the control condition, to which to pockets were created without any implantation, the signal was similar to the luminescence emitted by the transfected hASCs seeded on the SPCL-based scaffolds (Fig. 7.1).

The transfected cells seem to migrate from the scaffolds very early, as can be observed by the significant higher signal (p<0.05) detected in the dorsum of the mice, either implanted with the SPCL-WS or with the SPCL-FB scaffolds (Fig. 7.1B). However, the kinetics of the emitted signal, during the implantation time, is similar for the implant sites in comparison to the dorsum of the animals (Fig. 7.1B).

A

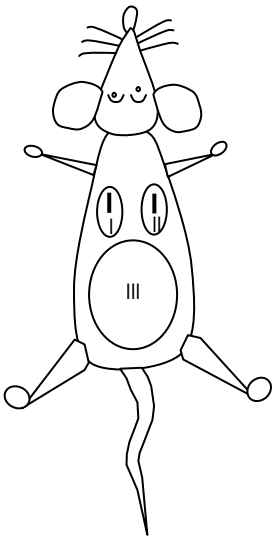

B

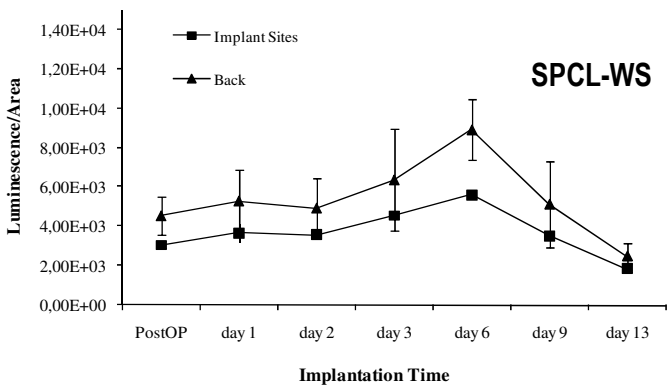

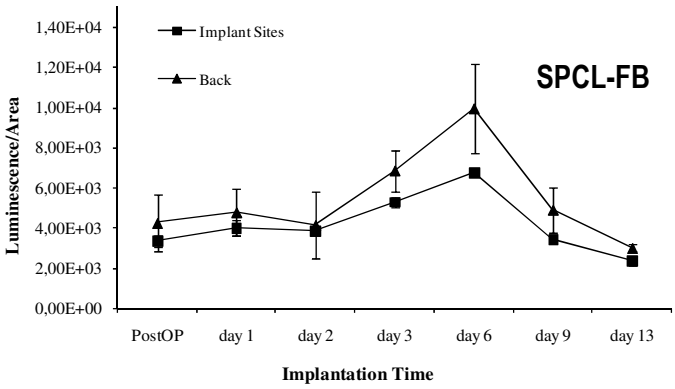

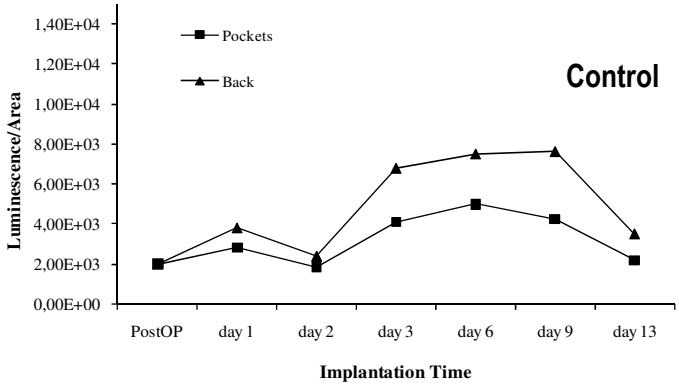

Figure 7.1: A) Schematic representation of a *nude* mouse with the areas considered for the capture of the luminescence signal emitted by the transfected cells seeded on the SPCL-based scaffolds: I and II correspond to the implantation sites; III corresponds to the dorsum (back) of the animals to where the cells eventually migrate. B) Graphical representation of the luminescence signal detected in the different areas, on the SPCL-WS and SPCL-FB implanted *nude* mice.

7.4.2 In vivo *induced neovascularisation potential*

7.4.2.1 VEGFR2 expression

After the assembly of the tissue engineering constructs combining the starch-based scaffolds, hASCs, fibrin sealant and growth factors (VEGF or FGF-2), the constructs were subcutaneously implanted in the back of transgenic VEGFR2-LUC mice. The emitted luminescence was detected with the *in vivo* imaging system (VivoVisions IVISs, Xenogen) and acquired with the Live Image Software (Xenogen®), in the pre-determined areas of incision and implant sites (Fig. 7.2A). The luminescence signal identified the expression of the murine *VEGFR2* gene 15 minutes after the subcutaneous injection of luciferin.

The analysis of the luminescence showed that either at the implantation sites or at the incision area, the luminescence signal increased from the surgery day until day 6 decreasing from that time points onward (Figs. 7.2B-C).

The expression of VEGFR2 at the SPCL-WS implantation sites was comparable ($p>0.05$) to the control for all time points except at the pre-implantation (Fig. 7.2B) time. In fact, the signal detected prior to implantation was significantly higher ($p<0.05$) than post-implantation which was similar ($p>0.05$) to the value at the end of observation.

When fibrin sealant was added to the SPCL-WS scaffolds, a different profile of VEGFR2 expression was observed in comparison to the scaffold alone (Fig. 7.2B). At day 3 of SPCL-WS+FS implantation, the expression of VEGFR2 was significantly lower ($p<0.05$), increasing from that day onward to comparable values to the SPCL-WS. Moreover, the VEGFR2 expression for the SPCL-WS+FS decreased ($p<0.05$) along the time until day 3 and reaches a significantly higher ($p<0.05$) value at day 6, comparable to the one obtained at day 13 ($p>0.05$). Despite the same pattern of VEGFR2 expression at implantation sites and incision, the signal detected at the incision where the SPCL-WS+FS scaffolds were implanted was lower ($p<0.05$) than the incision signal at day 6 where SPCL-WS scaffolds were implanted.

The VEGFR2 expression at the SPCL-FB implantation sites was higher ($p<0.05$) than the control for all the time points except post-implantation (Fig. 7.2C). This tendency was also observed at the incision site but only at days 9 and 13. Nonetheless, the increased expression along the time

of SPCL-FB implantation was only significantly different (p<0.05) from the time point post-implantation up to day 3.

The addition of fibrin sealant to the SPCL-FB scaffolds induced a decrease in VEGFR2 expression; despite the significantly lower (p<0.05) pre-implantation signal at the SPCL-FB+FS implantation sites in comparison to the SPCL-FB, major differences (p<0.05) were detected at days 6 and 9. However, as for the SPCL-FB, the increased expression along the time of SPCL-FB+FS implantation was only significantly different (p<0.05) from the post-implantation to day 3 (Fig. 7.2C).

A

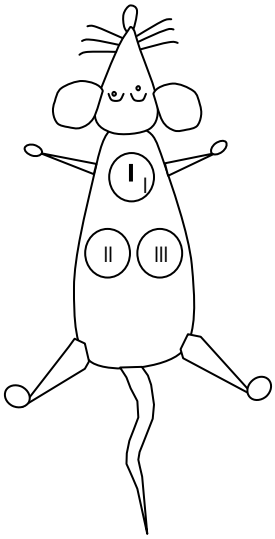

B

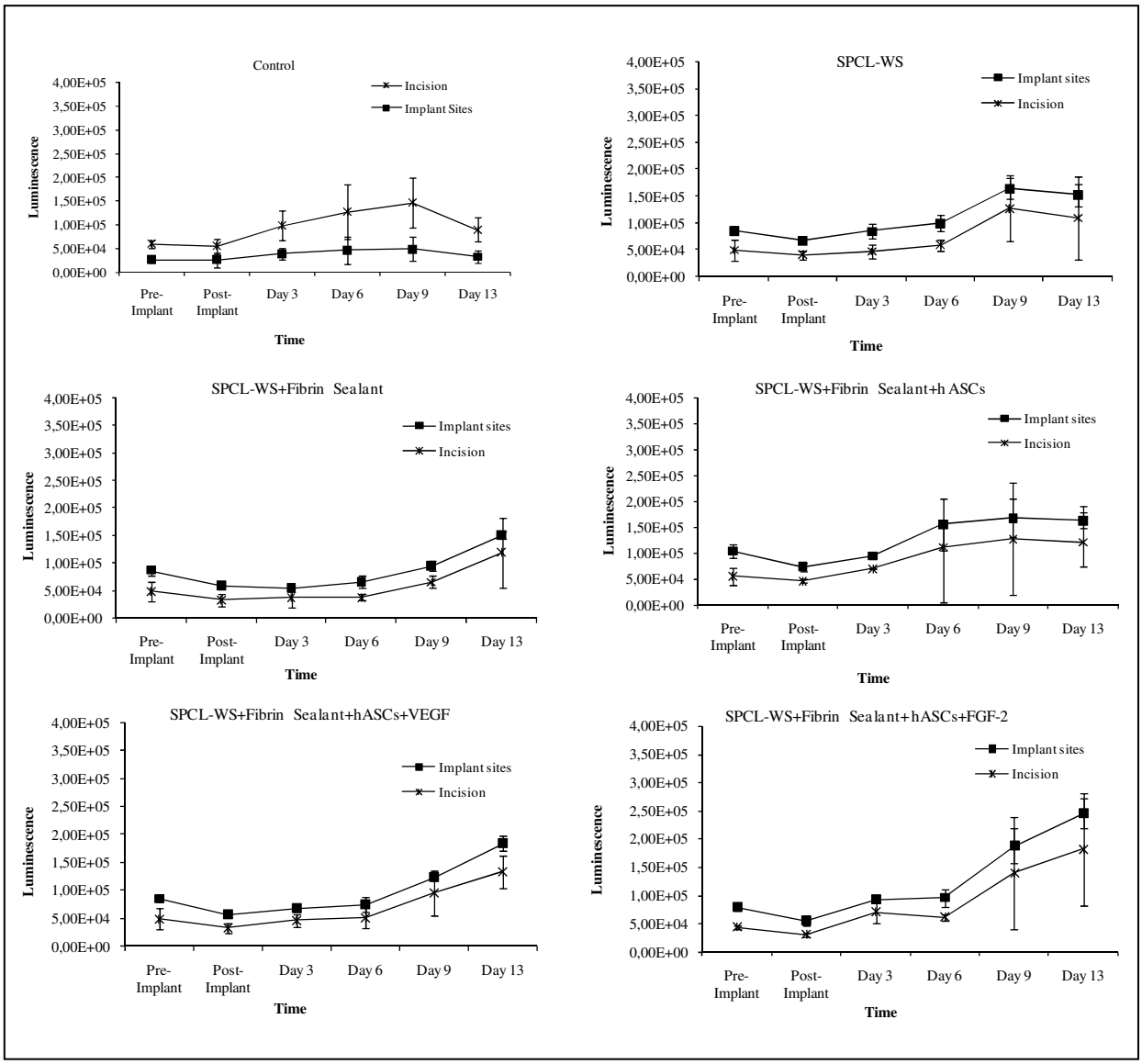
Control
Incision
Implant Sites
SPCL-WS
Implant sites
Incision
SPCL-WS+Fibrin Sealant
SPCL-WS+Fibrin Sealant+h ASCs
SPCL-WS+Fibrin Sealant+hASCs+VEGF
SPCL-WS+Fibrin Sealant+hASCs+FGF-2
Luminescence
4,00E+05
3,50E+05
3,00E+05
2,50E+05
2,00E+05
1,50E+05
1,00E+05
5,00E+04
0,00E+00
Pre-Implant
Post-Implant
Day 3
Day 6
Day 9
Day 13
Time

C

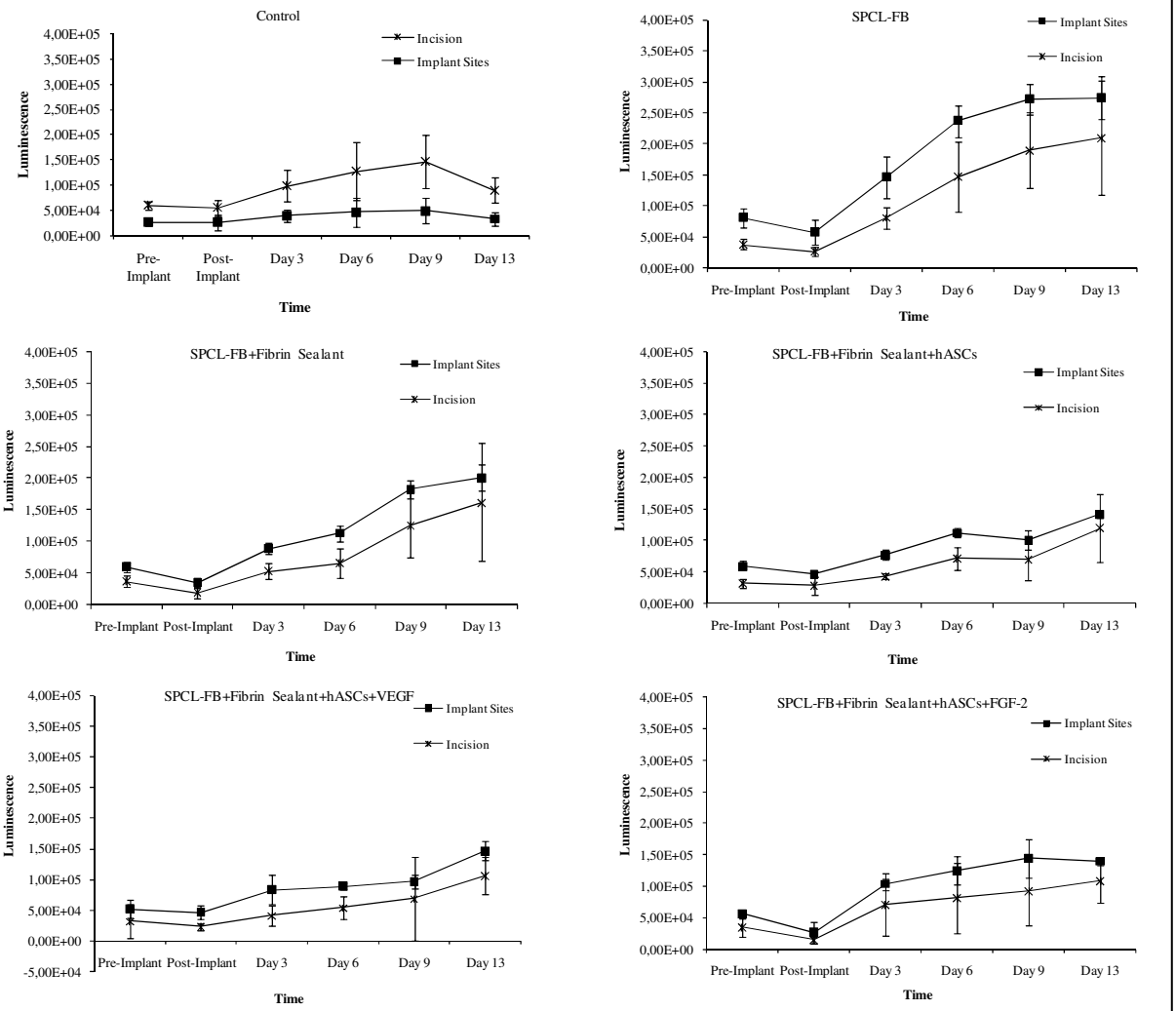

Figure 7.2: A) Schematic representation of a transgenic VEGFR2-LUC mouse with the areas considered for the capture of the luminescence signal emitted by the transfected cells seeded on the SPCL-based TE constructs: I corresponds to incision area; II and III correspond to the left and right implant sites (pockets). B) Graphical representation of the luminescence signal detected in the different areas, on the SPCL-WS assembled constructs. C) Graphical representation of the luminescence signal detected in the different areas, on the SPCL-FB assembled constructs.

When hASCs were added to the SPCL-WS+FS construct, the luminescence pattern detected at the implantation sites changed again. However, the VEGFR2 expression was similar at all times of SPCL-WS+FS+hASCs implantation in comparison to SPCL-WS+FS except at day 6 in the incision site (p<0.05). In addition, along the time of SPCL-WS+FS+hASCs implantation the VEGFR2 expression was similar, significantly decreasing (p<0.05) from pre- to post-implantation (Fig. 7.2C).

Contrarily to what was observed for the SPCL-WS+FS, the addition of hASCs to the SPCL-FB+FS construct did not induce significant differences in the detected luminescence (Fig. 7.2C). However, the decrease from the pre- to the post-implantation time and the subsequent increase of the detected signal until day 3 was statistically significant (p<0.05). Once more, the VEGFR2 expression pattern at the incision region, although at a lower level, was comparable to what was observed at the implantations sites (Fig. 7.2C).

The addition of either VEGF or FGF-2 to the SPCL-WS+FS+hASCs constructs changed the pattern of VEGFR2 expression (Fig. 7.2B) but the observed differences were not statistically significant except at the incision site, post-implanting the SPCL-WS+FS+hASCs+FGF-2 constructs (p<0.05) (Fig. 7.2C). However, the expression of VEGFR2 at the SPCL-WS+FS+hASCs+VEGF implantation site significantly decreased (p<0.05) from the pre- to the post-implantation time point and increased (p<0.05) from day 9 to day 13 reaching a significantly higher value (p<0.05) in comparison to the post-implantation time point. Apart from the enhanced VEGFR2 expression from day 9 to day 13, similar results were obtained along the time of implantation of the SPCL-WS+FS+hASCs+FGF-2 constructs.

In what concerns the incorporation of growth factors (VEGF and FGF-2) into the SPCL-FB+FS+hASCs constructs a significant decrease (p<0.05) was observed at the end of observation, day 13, at the implantation sites for both constructs and at the post-implantation time for the SPCL-FB+FS+hASCs+FGF-2 constructs (Fig. 7.2C). At the SPCL-FB+FS+hASCs+FGF-2 implantation site, the expression of VEGFR2 decreased (p<0.05) from the pre- to the post-implantation time point and subsequently increased (p<0.05) up to day 3. For both constructs an increased (p<0.05) VEGFR2 expression was observed when comparing the post-implantation and the end time point of implantation (Fig. 7.2C).

7.4.2.2 Inflammation and vascularisation

At the end of the experiment (2 weeks), the subcutaneously implanted tissue engineered constructs were explanted, along with the surrounding tissue, for histological and molecular biology analysis.

In terms of inflammatory reaction to the implantation of the TE constructs, the histological analysis allowed to observe that for all tested conditions neither the addition of hASCs or fibrin sealant from human origin, nor the release of VEGF or FGF-2 from the implanted constructs to the implantation site, elicited an exuberant inflammatory or rejection response from the transgenic VEGFR2-LUC mice (Fig. 7.3). The observed inflammatory reaction can be considered of moderate intensity and characterized by the presence of some polymorphonuclear neutrophils (PMNs), mononuclear cells (lymphocytes and macrophages) and some foreign body giant cells

(Fig. 7.3). These observations were complemented with the RT-PCR analysis that confirmed the expression of IL-4 and IFN-γ, two inflammatory cytokines, for all the tested conditions except when only the SPCL scaffolds were implanted (Fig. 7.4). In addition TNF-α expression was detected in all the test groups except the controls in which IL-4 and IFN-γ were also not detected. In fact in the control animals a residual inflammatory infiltrate, comprising PMNs and mononuclear cells was found as a reaction to the created pockets (Fig. 7.3).

Concerning the vascularisation specific markers, all the tested conditions, including the controls, expressed VEGF. Contrarily, VEGF-R1 expression was only detected in the tissues where the SPCL-WS+FS+ hASCs+FGF-2, the SPCL-FB +FS+hASCs+VEGF, and the SPCL-FB+FS+hASCs constructs were implanted (Fig. 7.4).

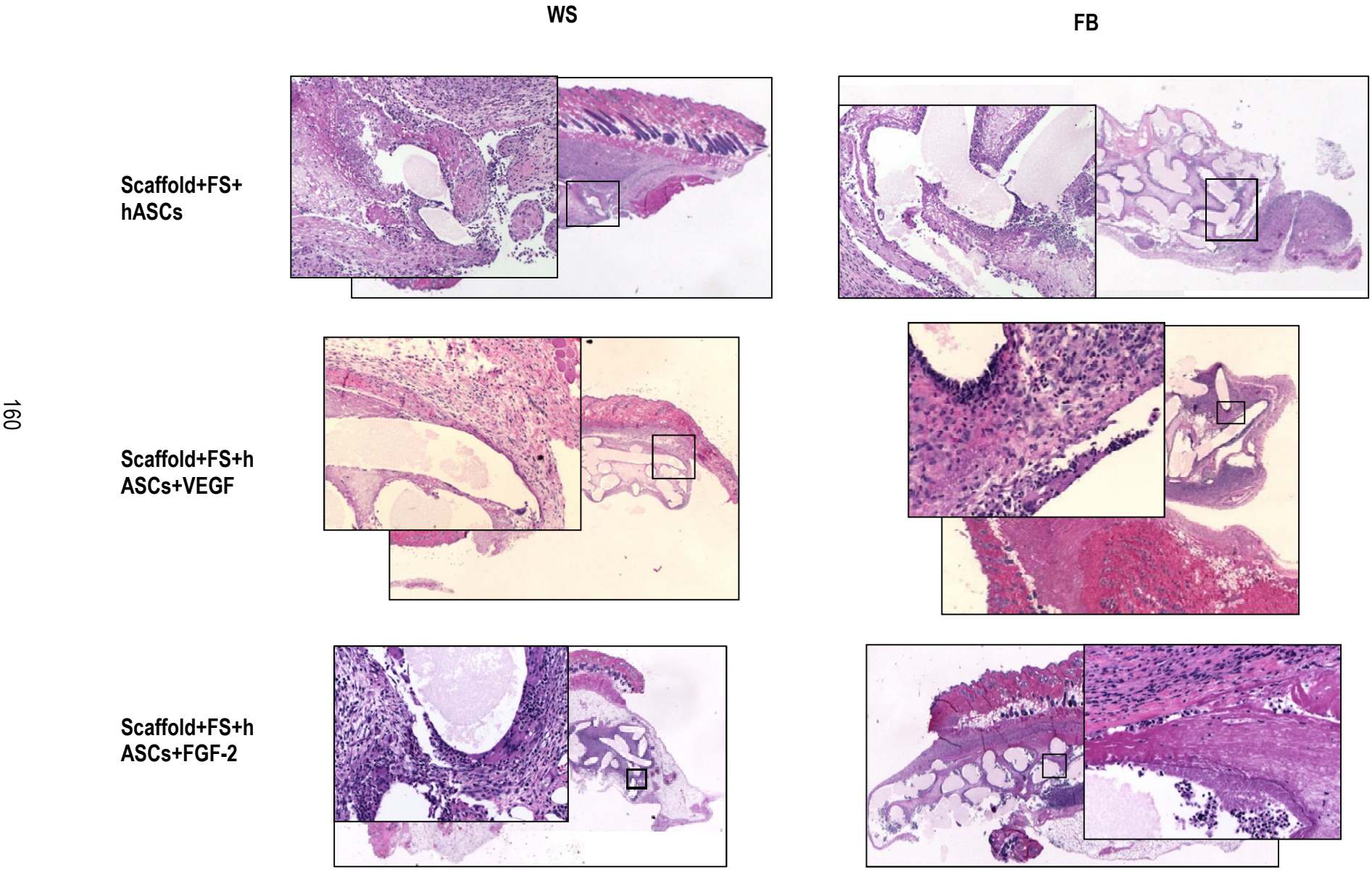
WS
FB
Scaffold+FS+ hASCs
Scaffold+FS+h ASCs+VEGF
Scaffold+FS+h ASCs+FGF-2

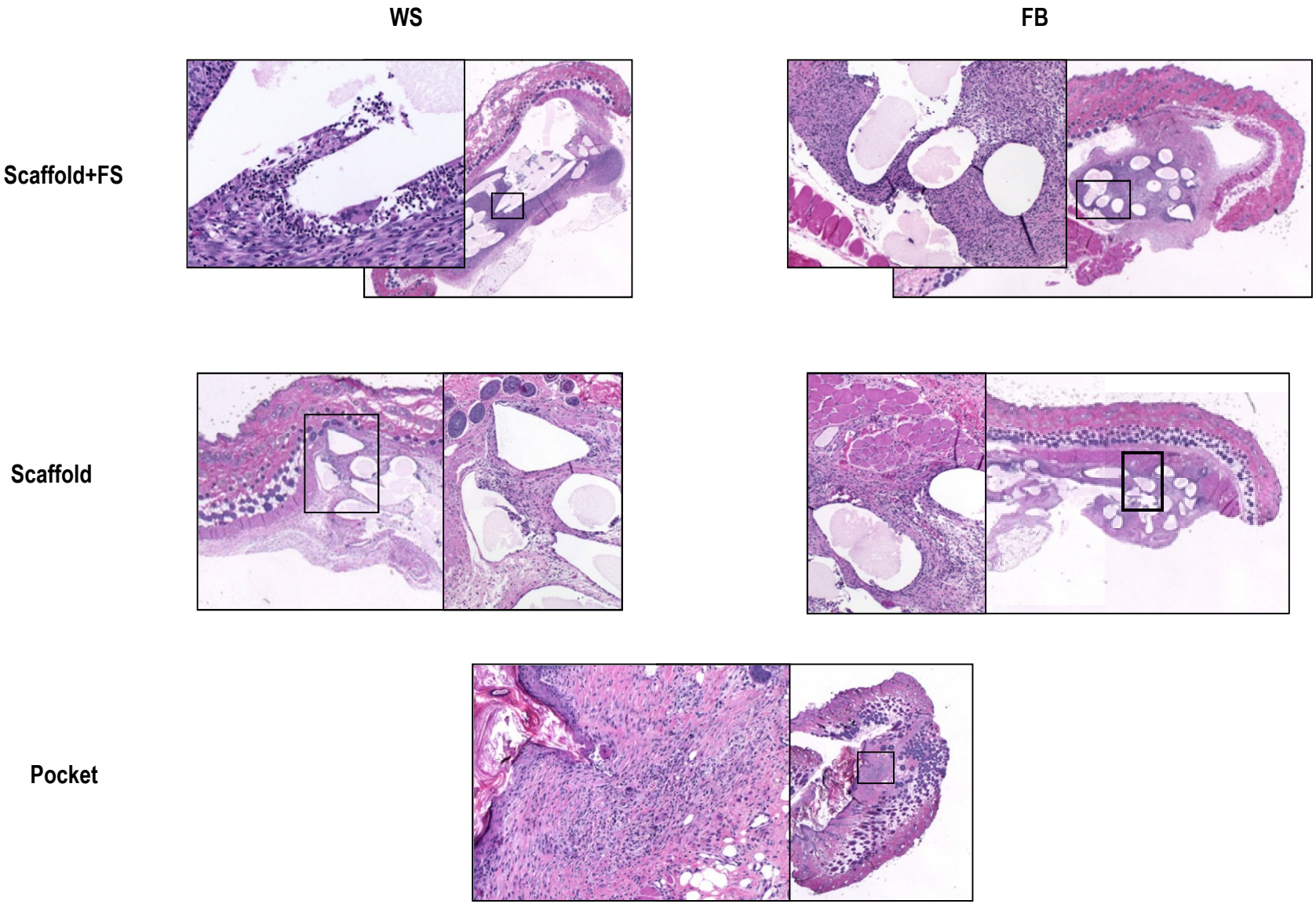
WS
FB
Scaffold+FS
Scaffold
Pocket

Figure 7.3: Micrographs obtained from the TE constructs and surrounding tissue explanted 13 days after implantation in the transgenic VEGFR2-LUC mice. SPCL-WS+FS+ASCs, SPCL-FB+FS+ASCs, SPCL-FB+FS+ASCs+VEGF, SPCL-FB+FS+ASCs+FGF-2 and SPCL-FB+FS with lower magnification of 12.5x and higher magnification of 200x; SPCL-WS+FS+ASCs+VEGF, SPCL-WS+FS+ASCs+FGF-2, SPCL-WS+FS, SPCL-WS, SPCL-FB and Pocket (control) with lower magnification of 12,5x and higher magnification of 100x.

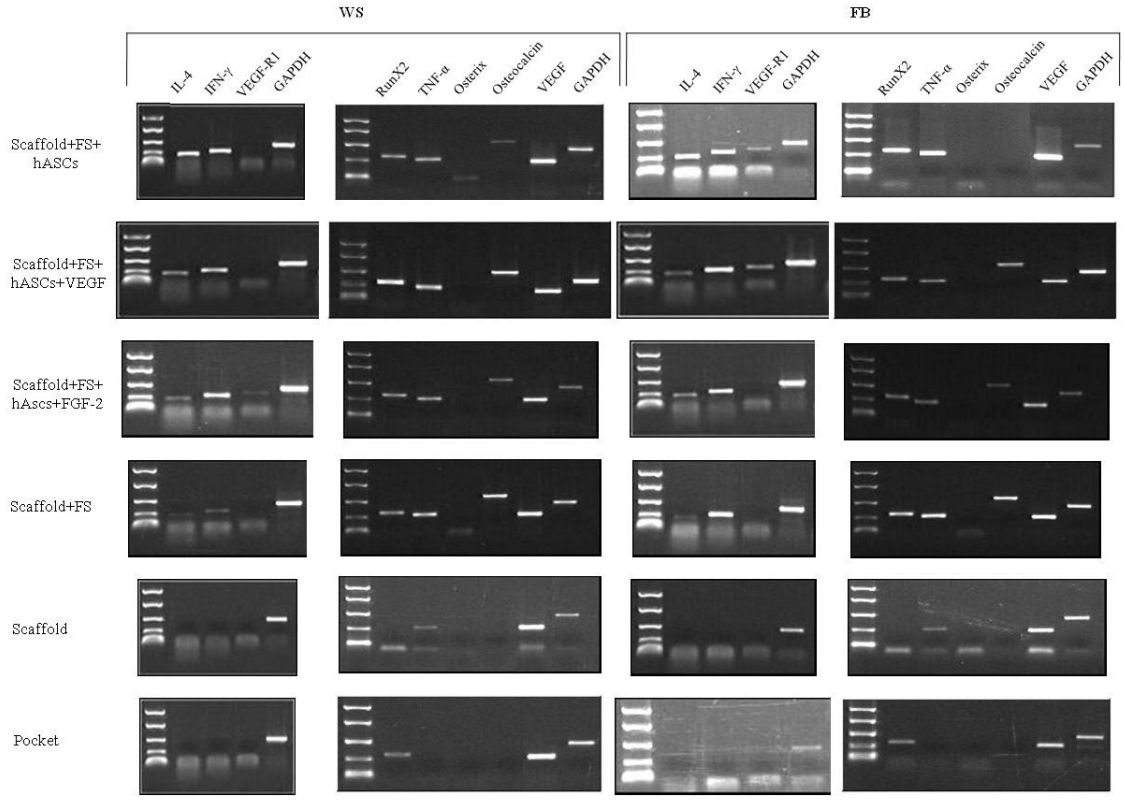

Figure 7.4: Electrophoresis gels of the PCR results showing the expression of inflammation, neovascularisation and osteogenic potential specific genes. The gene expression was assessed at the end time point of the experiment (2 weeks), on the implanted tissue engineering construct and respective surrounding tissue.

7.5 Discussion

Tissue engineering has been facing impairment of the development of suitable constructs, which is to promote the concomitant growing of new blood vessels as the tissue is healing and remodelling. Considerable steps have been taken towards new advances by co-culturing endothelial cells and osteoblasts [11, 14, 34] or stem cells within 3D matrices [16] or by controlled release relevant growth factors from those structures [21, 22] that can simultaneously support cell growth and ingrowth [5, 35]. Extensively studied starch-based scaffolds have shown great potential for bone tissue engineering not only demonstrated by their capacity to support osteogenic differentiation [36] and further bone matrix deposition/mineralization [12], but also to

bear the formation of vascular-like structures both *in vitro* [14, 37, 38] and *in vivo* [11]. Based on these, the main aim of this work was to assemble an improved bone tissue engineering construct, composed by starch/polycaprolactone-based scaffolds, angiogenic growth factors (VEGF and FGF-2) and hASCs and to assess the effect of each element overVEGFR2 expression.

A major concern with tissue engineered constructs is the fate and consequent role of the cells comprising the construct after transplantation. Cell transfection by lipofection has been shown to be a useful tool to trace cells either in an *in vitro* system [39-41] or in animal models [42, 43]. An immunosuppressed mouse model was used to implant the two types of SPCL scaffolds seeded with transfected hASCs in order to conclude about the effect of the processing methodology over cell fate within the host.

It is possible to conclude that the different types of methodologies to process the SPCL scaffolds do not induce differences on the migration of seeded cells. It was shown that the kinetic profile of emitted luminescence by the transfected cells seeded on the scaffolds is quite similar for the SPCL-WS and for the SPCL-FB scaffolds.

As the implants were introduced into the subcutaneous pockets of the *nude* mice, the transfected cells started to migrate from the scaffolds and moved to the dorsum of the animals. This was achieved from the observed higher luminescence signal emitted by the transfected cells in the dorsum area compared to the implantation areas. This is in accordance with previous works, showing an immediate release of ASCs from the substrate (unpublished data). Nevertheless, the presence of the scaffold at the implant site may interfere with the luminescence signal detected by the software. Therefore, it may be speculated that the luminescence signal detected at the implantation sites is not real and it is masked by the presence of the SPCL scaffolds. Since an increase of the signal was observed from day 2 after implantation, and a similar kinetics profile is noticed both for the implantation sites and for the dorsum of the animals, it means that the cells are proliferating in both sites. The decrease on the emitted signal observed from day 6 onward indicates that the cells are losing the plasmid, as expected after 2 weeks of transfection (unpublished data).

A VEGFR2-luc transgenic mouse model previously established [32], using the murine VEGFR2 promoter to direct the expression of the luciferase reporter, was used to assess the expression of VEGFR2 under the studied conditions. It is well reported that VEGFR2 mediates most of the mitogenic, cell survival, and vascular permeability effects of VEGF [44, 45]. Moreover, as VEGFR2 plays an important role in many aspects of blood vessel growth, an *in vivo* monitoring of the *VEGFR2* gene expression, with non-invasive techniques was found useful to achieve its real time function in angiogenesis [46].

While SPCL scaffolds, seeded with bone marrow mesenchymal cell have clearly proved to be suitable for bone tissue engineering applications [8, 12, 36], concomitantly demonstrating that support the formation of vascular-like structures [11, 37, 38], the potential of hASCs together with these materials was still to be addressed. This study was designed in order to assess the influence of hASCs seeded onto the SPCL scaffolds, as well as the incorporation and subsequent delivery of VEGF and FGF-2, in vascularisation. In this context, it was possible to achieve important cues from the VEGFR2-luc transgenic mouse model with implanted starch-based tissue engineering constructs.

Wound healing involves the induction of pro-inflammatory cytokines, such as IL-6, IL-8 and TNF-α, and various growth factors necessary for this process [47]. Among those factors is the VEGF for endothelial cells [48] and critically involved in angiogenesis, also an important part of wound healing [49].

The presented results shown that all conditions established with the assembled bone TE constructs induced the expression of VEGF gene by the tissues hosting the implants, as well as the control tissues where nothing was implanted. Although on the control animals none implant was placed, the creation of the pocket induced an inflammatory reaction, exactly as in the animals where the implants were placed. In both situations, the host tissue had to recover from the injury and restore the damaged tissue and associated vasculature. In this sense, it is possible to substantiate the expression of VEGF in all conditions, including the controls.

Higher levels of VEGF-R2 expression were detected in the animals where SPCL-FB scaffolds were implanted. At the molecular level, it was shown that when the SPCL scaffolds, either SPCL-WS or SPCL-FB, were implanted as simple materials, did not elicit the expression of the specific markers of inflammation, IL-4, IFN-γ and TNF-α. In addition, VEGF but not VEGFR-1 expression was also detected after SPCL-WS and SPCL-FB implantation. The histological analysis also confirms a residual inflammatory infiltrate in the vicinity of the SPCL scaffolds. All together these results demonstrate that SPCL possess a low inflammatory potential very unusual for a biodegradable scaffold, and that the detected VEGFR2 expression in the luminescence experiments are certainly related to the produced VEGF since VEGF-R2 is the major receptor for that growth factor [50]. However, although it has been reported that inflammatory cells, namely macrophages, express VEGF-R1 in response to VEGF stimulation [50-52], in this study was not possible to establish this correlation.

An interesting finding was the lower expression of the VEGFR2 in the SPCL-FB+FS in comparison with the SPCL-FB scaffold. This may be due to the incorporation of fibrin sealant which might be minimizing an eventual physical aggression of the subcutaneous tissue and

consequent inflammation with the release of VEGF receptors. Nevertheless, the histological features showed only a moderate inflammatory reaction for both conditions. Additionally, the molecular analysis showed that the introduction of fibrin sealant, ASCs and growth factors enhanced the expression of inflammatory mediators compared with scaffolds themselves. Either for short or long term subcutaneous implantations of SPCL-WS and SPCL-FB scaffolds no severe inflammatory reaction has been previously observed (chapter 6).

When the hASCs were added, the expression of VEGFR2 showed to be similar to the SCPL-based constructs with fibrin sealant. However, at the molecular level, while the VEGF expression was detected for all the conditions, the expression of VEGFR1 was only detected for the SPCL-FB+FS+hASCs construct. A possible explanation for this finding may be the differences on the SPCL-FB and SPCL-WS scaffolds, which can be additionally altered by the incorporation and interaction of the different components of the construct.

Conversely, the assembled constructs, by inducing the expression of those pro-inflammatory cytokines, showed to have an inflammatory potential. Comparing the histological images with these molecular biology results, they do not coincide. This means that, although there is molecular information to express the genes of the inflammatory cytokines, the proteins do not reach the production, justifying the inexistence of persistent acute inflammation by the histological evaluation.

VEGF and its receptors, among others VEGF-R1 are important factors in the establishment, progression and maturation of new blood vessels [53-56]. During normal wound healing [57] VEGF expression correlates temporally and spatially with the proliferation of new blood vessels [58]. Additionally to VEGF, Fibroblast Growth Factors (FGFs) are homeostatic factors with function in tissue repair and response to injury in adult organisms [59].

While the incorporation and subsequent release of both VEGF and FGF-2 from the SPCL-WS did not induce a significant effect over VEGFR2 expression, the expression of this receptor was significantly increased in the SPCL-FB+FS+hASCs+VEGF and SPCL-FB+FS+hASCs+FGF-2 implantation sites in comparison to unloaded constructs. The VEGFR2 expression was significantly higher upon exposition to VEGF or FGF-2. The observed differences may be substantiated by the strict relation of those two growth factors with inflammation [57], tissue repair and proliferation of new blood vessels [59]. Additionally, the expression of VEGFR2 translates the vascularisation status at the implantation sites [50]. Due to previous indications on the behaviour of VEGF and FGF-2 on their release [20-22] and effect on VEGFR-2 expression [46], the obtained results were expected.

7.6 Conclusions

Taken together, the presented results show that; a) the starch-based scaffolds obtained by different processing methodologies are a rather suitable support for human adipose tissue derived cells (ASCs); b) the starch-based scaffolds may be used to assemble a complex TE construct composed by a fibrin sealant, ASCs and growth factors (VEGF and FGF-2); c) after 2 weeks of implantation, the assembled TE constructs did not elicit an adverse host reaction, showing a moderate inflammatory response typically observed for implanted devices and; d) the addition of VEGF and FGF-2 to the TE construct showed to be favourable, at the molecular level, for the expression of neovascularisation specific markers.

In summary, the overall results indicate that the combination of SPCL-WS with fibrin sealant, human adipose derived stem cells and FGF-2 seems to be the TE construct with promising features for vascularisation of the newly formed tissue and thus, may be considered for further studies for bone TE applications.

References

1. Mikos, A.G., et al., *Engineering complex tissues.* Tissue Eng, 2006. **12**(12): p. 3307-3339.
2. Langer, R. and J.P. Vacanti, *Tissue engineering.* Science, 1993. **260**(5110): p. 920-6.
3. Gomes, M.E., et al., *Starch-poly(epsilon-caprolactone) and starch-poly(lactic acid) fibre-mesh scaffolds for bone tissue engineering applications: structure, mechanical properties and degradation behaviour.* J Tissue Eng Regen Med, 2008. **2**(5): p. 243-252.
4. Tuzlakoglu, K., et al., *A new route to produce starch-based fiber mesh scaffolds by wet spinning and subsequent surface modification as a way to improve cell attachment and proliferation.* J Biomed Mater Res A, 2009.
5. Huang, Y.C., et al., *Combined angiogenic and osteogenic factor delivery enhances bone marrow stromal cell-driven bone regeneration.* J Bone Miner Res, 2005. **20**(5): p. 848-857.
6. Peters, M.C., P.J. Polverini, and D.J. Mooney, *Engineering vascular networks in porous polymer matrices.* J Biomed Mater Res, 2002. **60**(4): p. 668-678.
7. Kaigler, D., et al., *Role of vascular endothelial growth factor in bone marrow stromal cell modulation of endothelial cells.* Tissue Eng, 2003. **9**(1): p. 95-103.

8. Martins, A.M., et al., *The Role of Lipase and alpha-Amylase in the Degradation of Starch/Poly(epsilon-Caprolactone) Fiber Meshes and the Osteogenic Differentiation of Cultured Marrow Stromal Cells.* Tissue Eng Part A, 2008.
9. Gerber, H.P. and N. Ferrara, *Angiogenesis and bone growth.* Trends Cardiovasc Med, 2000. **10**(5): p. 223-228.
10. Hausman, M.R., M.B. Schaffler, and R.J. Majeska, *Prevention of fracture healing in rats by an inhibitor of angiogenesis.* Bone, 2001. **29**(6): p. 560-564.
11. Fuchs, S., et al., *Contribution of outgrowth endothelial cells from human peripheral blood on in vivo vascularization of bone tissue engineered constructs based on starch polycaprolactone scaffolds.* Biomaterials, 2009. **30**(4): p. 526-534.
12. Gomes, M.E., et al., *Effect of flow perfusion on the osteogenic differentiation of bone marrow stromal cells cultured on starch-based three-dimensional scaffolds.* J Biomed Mater Res A, 2003. **67**(1): p. 87-95.
13. Jabbarzadeh, E., et al., *Induction of angiogenesis in tissue-engineered scaffolds designed for bone repair: a combined gene therapy-cell transplantation approach.* Proc Natl Acad Sci U S A, 2008. **105**(32): p. 11099-11104.
14. Santos, M.I., et al., *Crosstalk between osteoblasts and endothelial cells co-cultured on a polycaprolactone-starch scaffold and the in vitro development of vascularization.* Biomaterials, 2009.
15. Unger, R.E., et al., *Tissue-like self-assembly in cocultures of endothelial cells and osteoblasts and the formation of microcapillary-like structures on three-dimensional porous biomaterials.* Biomaterials, 2007. **28**(27): p. 3965-3976.
16. Tao, J., et al., *Induced Endothelial Cells Enhance Osteogenesis and Vascularization of Mesenchymal Stem Cells.* Cells Tissues Organs, 2009.
17. Yang, P., et al., *Prefabrication of vascularized porous three-dimensional scaffold induced from rhVEGF(165): a preliminary study in rats.* Cells Tissues Organs, 2009. **189**(5): p. 327-237.
18. Schumann, P., et al., *Consequences of seeded cell type on vascularization of tissue engineering constructs in vivo.* Microvasc Res, 2009.
19. Gerber, H.P., et al., *VEGF couples hypertrophic cartilage remodeling, ossification and angiogenesis during endochondral bone formation.* Nat Med, 1999. **5**(6): p. 623-628.
20. Elcin, Y.M., V. Dixit, and G. Gitnick, *Extensive in vivo angiogenesis following controlled release of human vascular endothelial cell growth factor: implications for tissue engineering and wound healing.* Artif Organs, 2001. **25**(7): p. 558-565.

21. Fujita, M., et al., *Vascularization in vivo caused by the controlled release of fibroblast growth factor-2 from an injectable chitosan/non-anticoagulant heparin hydrogel.* Biomaterials, 2004. **25**(4): p. 699-706.
22. Nakamura, S., et al., *Effect of controlled release of fibroblast growth factor-2 from chitosan/fucoidan micro complex-hydrogel on in vitro and in vivo vascularization.* J Biomed Mater Res A, 2008. **85**(3): p. 619-627.
23. Ishihara, M., et al., *Controlled release of fibroblast growth factors and heparin from photocrosslinked chitosan hydrogels and subsequent effect on in vivo vascularization.* J Biomed Mater Res A, 2003. **64**(3): p. 551-559.
24. Martins, A.M., et al., *The Role of Lipase and alpha-Amylase in the Degradation of Starch/Poly(varepsilon-Caprolactone) Fiber Meshes and the Osteogenic Differentiation of Cultured Marrow Stromal Cells.* Tissue Eng Part A, 2009. **15**(2): p. 295-305.
25. Tuzlakoglu, K., et al., *A new route to produce starch-based fiber mesh scaffolds by wet spinning and subsequent surface modification as a way to improve cell attachment and proliferation.* Journal of Biomedical Materials Research Part A *in press*, 2009.
26. Morton, T.J., et al., *Controlled release of substances bound to fibrin-anchors or of DNA.* Drug Deliv, 2009. **16**(2): p. 102-7.
27. Rada, T., R.L. Reis, and M.E. Gomes, *Adipose Tissue-Derived Stem Cells and Their Application in Bone and Cartilage Tissue Engineering.* Tissue Eng Part B Rev, 2009.
28. Quarto, N. and M.T. Longaker, *FGF-2 inhibits osteogenesis in mouse adipose tissue-derived stromal cells and sustains their proliferative and osteogenic potential state.* Tissue Eng, 2006. **12**(6): p. 1405-1418.
29. Ehrbar, M., et al., *The role of actively released fibrin-conjugated VEGF for VEGF receptor 2 gene activation and the enhancement of angiogenesis.* Biomaterials, 2008. **29**(11): p. 1720-1729.
30. Reis, R.L., et al., *Processing and in vitro degradation of starch/EVOH thermoplastic blends.* Polym Int, 1997. **43**: p. 347.
31. Goessl, A. and H. Redl, *Optimized thrombin dilution protocol for a slowly setting fibrin sealant in surgery.* European Surgery, 2005. **37**: p. 43-51.
32. Zhang, N., et al., *Tracking angiogenesis induced by skin wounding and contact hypersensitivity using a Vegfr2-luciferase transgenic mouse.* Blood, 2004. **103**(2): p. 617-626.
33. Kirkwood, B. and J. Sterne, *Essential Medical Statistics*. 2nd Edition ed. 2003: Wiley. 512.

34. Hofmann, A., et al., *The effect of human osteoblasts on proliferation and neo-vessel formation of human umbilical vein endothelial cells in a long-term 3D co-culture on polyurethane scaffolds.* Biomaterials, 2008. **29**(31): p. 4217-4226.
35. Egana, J.T., et al., *Use of human mesenchymal cells to improve vascularization in a mouse model for scaffold-based dermal regeneration.* Tissue Eng Part A, 2009. **15**(5): p. 1191-1200.
36. Gomes, M.E., et al., *Influence of the porosity of starch-based fiber mesh scaffolds on the proliferation and osteogenic differentiation of bone marrow stromal cells cultured in a flow perfusion bioreactor.* Tissue Eng, 2006. **12**(4): p. 801-809.
37. Santos, M.I., et al., *Response of micro- and macrovascular endothelial cells to starch-based fiber meshes for bone tissue engineering.* Biomaterials, 2007. **28**(2): p. 240-248.
38. Santos, M.I., et al., *Endothelial cell colonization and angiogenic potential of combined nano- and micro-fibrous scaffolds for bone tissue engineering.* Biomaterials, 2008. **29**(32): p. 4306-4313.
39. Byk, T., et al., *Lipofectamine and related cationic lipids strongly improve adenoviral infection efficiency of primitive human hematopoietic cells.* Hum Gene Ther, 1998. **9**(17): p. 2493-2502.
40. Wolbank, S., et al., *Labelling of human adipose-derived stem cells for non-invasive in vivo cell tracking.* Cell Tissue Bank, 2007. **8**(3): p. 163-177.
41. Marit, G., et al., *Increased liposome-mediated gene transfer into haematopoietic cells grown in adhesion to stromal or fibroblast cell line monolayers.* Eur J Haematol, 2000. **64**(1): p. 22-31.
42. Domashenko, A., S. Gupta, and G. Cotsarelis, *Efficient delivery of transgenes to human hair follicle progenitor cells using topical lipoplex.* Nat Biotechnol, 2000. **18**(4): p. 420-423.
43. Daldrup-Link, H.E., et al., *Comparison of iron oxide labeling properties of hematopoietic progenitor cells from umbilical cord blood and from peripheral blood for subsequent in vivo tracking in a xenotransplant mouse model XXX.* Acad Radiol, 2005. **12**(4): p. 502-510.
44. Millauer, B., et al., *High affinity VEGF binding and developmental expression suggest Flk-1 as a major regulator of vasculogenesis and angiogenesis.* Cell, 1993. **72**(6): p. 835-846.

45. Rissanen, T.T., et al., *Expression of vascular endothelial growth factor and vascular endothelial growth factor receptor-2 (KDR/Flk-1) in ischemic skeletal muscle and its regeneration.* Am J Pathol, 2002. **160**(4): p. 1393-1403.
46. Mittermayr, R., et al., *Sustained (rh)VEGF(165) release from a sprayed fibrin biomatrix induces angiogenesis, up-regulation of endogenous VEGF-R2, and reduces ischemic flap necrosis.* Wound Repair Regen, 2008. **16**(4): p. 542-550.
47. Martin, P., *Wound healing--aiming for perfect skin regeneration.* Science, 1997. **276**(5309): p. 75-81.
48. Dvorak, H.F., et al., *Vascular permeability factor/vascular endothelial growth factor, microvascular hyperpermeability, and angiogenesis.* Am J Pathol, 1995. **146**(5): p. 1029-1039.
49. Risau, W., *Mechanisms of angiogenesis.* Nature, 1997. **386**(6626): p. 671-674.
50. Clauss, M., et al., *The vascular endothelial growth factor receptor Flt-1 mediates biological activities. Implications for a functional role of placenta growth factor in monocyte activation and chemotaxis.* J Biol Chem, 1996. **271**(30): p. 17629-17634.
51. Barleon, B., et al., *Migration of human monocytes in response to vascular endothelial growth factor (VEGF) is mediated via the VEGF receptor flt-1.* Blood, 1996. **87**(8): p. 3336-33343.
52. Shen, H., et al., *Characterization of vascular permeability factor/vascular endothelial growth factor receptors on mononuclear phagocytes.* Blood, 1993. **81**(10): p. 2767-2773.
53. Buschmann, I., et al., *Influence of inflammatory cytokines on arteriogenesis.* Microcirculation, 2003. **10**(3-4): p. 371-379.
54. Ferrara, N., H.P. Gerber, and J. LeCouter, *The biology of VEGF and its receptors.* Nat Med, 2003. **9**(6): p. 669-676.
55. Maharaj, A.S., et al., *Vascular endothelial growth factor localization in the adult.* Am J Pathol, 2006. **168**(2): p. 639-648.
56. Folkman, J. and Y. Shing, *Angiogenesis.* J Biol Chem, 1992. **267**(16): p. 10931-10934.
57. Brown, L.F., et al., *Expression of vascular permeability factor (vascular endothelial growth factor) by epidermal keratinocytes during wound healing.* J Exp Med, 1992. **176**(5): p. 1375-1379.
58. Brown, L.F., et al., *Overexpression of vascular permeability factor (VPF/VEGF) and its endothelial cell receptors in delayed hypersensitivity skin reactions.* J Immunol, 1995. **154**(6): p. 2801-7.

59. Ornitz, D.M. and N. Itoh, *Fibroblast growth factors.* Genome Biol, 2001. **2**(3): p. 3005.1-3005.12.

Chapter VIII

Final Remarks

The rational of the work presented in this thesis was to understand the host reaction provoked by the implantation of natural-based biomaterials, aimed for skin wound healing and bone regeneration, respectively chitosan/soy-based membranes and starch-based scaffolds.

While deeper knowledge was previously gathered by other works regarding the *in vitro* performance of the starch-based scaffolds [1-3], the chitosan/soy-based membranes were rather new [4], thus demanding an *in vitro* analysis prior to the *in vivo* studies. In a first approach, the ability of chitosan/soy-based membranes to activate human inflammatory cells was assessed *in vitro*. The obtained data showed that stimulation potential of the cht/soy membranes towards PMNs was low, as indicated by the reduced lysozyme release and ROS production normally resulting from the PMNs "respiratory burst". The *in vivo* activation of PMNs by the implantation of any medical device for tissue engineering purposes is required at controlled levels, since their function in wound hound healing precedes the adaptive changes if the tissue recovers from injury and returns to normal function. Thus, the low *in vitro* stimulation of the PMNs induced by these cht/soy-based membranes seems to be a good indicator for the development of a normal wound healing process, when implanted *in vivo*, as well as the normal restoration of the tissue function. Furthermore, PMNs retained their capacity of activation, and it is important to consider that the stimulation and activation of these cells is highly influenced by the type of molecules or mediators adsorbed to the surface of materials [5, 6] once they are implanted *in vivo*. In fact, improved host response considering inflammatory cells recruitment and overall inflammatory reaction after subcutaneous implantation of chitosan, soybean and cht/soy membranes was observed when chitosan was added to soybean. Soybean powders elicited the recruitment of higher numbers of inflammatory cells compared to chitosan powders. Thus, soybean powders were considered more reactive to the host as compared to the chitosan powders, which elicited leukocyte recruitment comparable to the negative control. Additionally soybean isolate protein induced a persistent recruitment of all inflammatory cell types in comparison with the chitosan powders, since mononuclear cells (macrophages and lymphocytes), the hallmark of a chronic inflammation, were extensively present at the latter stage of reaction. Despite the absence of physiologic signs of inflammation or infection, the histological analysis of the explants revealed a severe host inflammatory reaction. Comparing the soy-based membranes and their denaturated form, it was

possible to observe that the reaction to the second was much more intense, including some necrosis of the surrounding tissue. The extension of the inflammatory infiltrate was representative of an acute persistent reaction characterised by the presence of PMNs at longer implantation periods. The higher degradation rate of the denaturated form of the soy-based membranes, in comparison to the simplest membrane and subsequent presence of smaller fragments of the membrane, might be responsible for the stronger reaction since a higher surface area is available for PMNs to respond to. The metabolites secreted by the PMNs in this situation lead to the decrease of the physiological pH and to the apoptosis and necrosis of neighbouring cells that was evident at later stages of implantation. The addition of chitosan to the soy-based membranes improved, as would be expected, the host response which showed the features of a typical inflammatory response to implanted materials. These results were to forsee, not only because the blends of chitosan and soy were not able to activate *in vitro* human PMNs, but also because of the inflammatory recruitment kinetics after intraperitoneal injection of chitosan and soybean powders. All together, these results may assert the influence of chitosan on masking specific soy reactive epitopes or even on suppressing leukocyte activation, namely PMNs. The cht/soy-based membranes showed the induction of a normal inflammatory reaction and the features characterizing this reaction are crucial for the integration of the material, as well as for the ongoing process of wound healing and tissue regeneration. This influence, and thus the suitability of these membranes for wound dressing were confirmed after application in a partial-thickness excision model. The newly developed cht/soy-based membranes produced by solvent casting methodology and that had proven to promote low *in vitro* activation of human PMNs isolated from circulating blood, decreased the healing time period of partial-thickness skin wounds in rats. The cht/soy-based membranes perform better, in comparison to the negative and positive controls, inducing re-epithelialisation.

In conclusion, chitosan/soy-based membranes showed to improve skin wound healing, enhancing the progression of the reaction from an inflammatory process to tissue healing and regeneration, in part due to their proved incapability to activate human PMNs *in vitro*. Hence, in a future approach, these cht/soy-based membranes can be considered for further studies of wound dressing, including the study of cellular and molecular mechanisms involved in skin wound healing in advanced wound healing models, such as excisional skin wounds in pigs.

Starch-based biomaterials have been extensively studied and showed promising features for bone tissue engineering (TE) applications [2, 3, 7-10]. However, not too much is known in what concerns to the host reaction after *in vivo* implantation of those natural-based biomaterials. Thus,

the main objectives of studying SPCL scaffolds in this thesis were to evaluate the host tissue reaction, tissue integration and systemic response elicited after its implantation, as well as to understand the influence of the addition of human adipose derived stem cells, fibrin sealant and angiogenic factors, on the vascularisation and host reaction after implantation.

The data showed that SPCL scaffolds produced by two different methodologies, wet spinning (SPCL-WS) and fibre-bonding (SPCL-FB) did not induce a severe soft tissue inflammatory reaction. This was observed by the low host reaction detected after subcutaneous and intramuscular implantations of both types of SPCL scaffolds in rats for 1 and 2 weeks. Additionally, the a long-term implantation in the subcutaneous tissue of rats for 8 and 12 weeks showed a good integration of the SPCL scaffolds into the host tissue and a pro-wound healing cytokine profile expression. Nevertheless, SPCL-WS seemed to be less reactive, particularly when the cytokine profile was evaluated, showing an early resolution of the inflammatory process compared with the SPCL-FB scaffolds. Additionally, it was shown that the intramuscular implantation of the same type of materials induced a slight intense inflammatory response in comparison to the SC model, which may indicate that intramuscular implantation is a more sensitive model to address the inflammation and immune host response to biomaterial's implantation.

However, the performance of a tissue engineering construct does not rely only on its scaffolding structure but also on their cellular and/or bioactive components. Thus bone TE constructs, composed by the SPCL-FB and SPCL-WS scaffolds, human adipose derived stem cells (hASCs), fibrin sealant (FS) and key angiogenic growth factors (VEGF and FGF-β) were assembled. The purpose of using those factors was to induce bone formation, enhance healing and vascularisation of the newly formed tissue, respectively. Murine models of subcutaneous implantation were used to evaluate the motility of the seeded cells after implantation and the effect of each of the constituents of the TE construct on tissue reaction and new vascularisation. The behaviour of transfected hASCs seeded onto the scaffold after transplantation in an immunocompromised mouse model was similar for the SPCL-WS and for the SPCL-FB scaffolds. As the implants were subcutaneously implanted, the transfected cells started to migrate from the scaffolds and moved to the dorsum of the animals. Despite a speculated interference of the scaffold over the luminescence signal at the implant site, an increased signal with a similar kinetics profile was observed from day 2 onward both at the implantation sites and at the dorsum of the animals indicative of cell proliferation and integration within the host tissue. When the expression of VEGFR2 was evaluated using a transgenic murine model FVB/N-Tg(VEGF-r2–luc)Xen mice (VEGFR2-LUC) in which the VEGFR2 promoter directly correlates with the

expression of the luciferase reporter it was noticed that at the SPCL-WS implantation sites VEGFR2 expression was comparable to the control without any implanted material. Conversely, VEGFR2 expression at the SPCL-FB implantation sites was higher than the controls. The addition of hASCs to the SPCL scaffolds induced a similar VEGFR2 expression at all times of implantation in comparison to SPCL-WS+FS except at day 6 in the incision site. In addition, along the time of SPCL-WS+FS+hASCs implantation, the VEGFR2 expression was similar, decreasing from pre- to post-implantation. Contrarily to what was observed for the SPCL-WS+FS, the addition of hASCs to the SPCL-FB+FS construct did not induce significant differences in the detected luminescence. However, the decrease from the pre- to the post-implantation time and the subsequent increase of the detected signal until day 3 was significant. Furthermore, the VEGFR2 expression pattern at the incision region, although at a lower level, was comparable to what was observed at the implantations sites. This was certainly due to the inflammatory process kinetic at the incision healing site. While the incorporation and subsequent release of both VEGF and FGF-β from the SPCL-WS did not induce a significant effect over VEGFR2 expression, the expression of this receptor was significantly increased in the SPCL-FB+FS+hASCs+VEGF and SPCL-FB+FS+hASCs+FGF-β implantation sites in comparison to unloaded constructs. The VEGFR2 expression was significantly higher upon exposition to VEGF or FGF-β. The observed differences may be substantiated by the strict relation of those two growth factors with inflammation [11], tissue repair and proliferation of new blood vessels [12]. Additionally, the expression of VEGFR2 translates the vascularisation status at the implantation sites [13]. The observed inflammatory reaction was considered of moderate intensity and characterized by the presence of some polymorphonuclear neutrophils (PMNs), mononuclear cells (lymphocytes and macrophages) and some foreign body giant cells. Furthermore, RT-PCR analysis complemented these observations by showing the expression of IL-4 and IFN-, two inflammatory cytokines, for all the tested conditions except when only the SPCL scaffolds were implanted. These results were in accordance with the previous indications of low inflammatory response and good tissue integration of the SPCL scaffolds after subcutaneous and intramuscular implantation in rats. In addition, TNF- expression was detected in all the test groups except the controls in which IL-4 and IFN- were also not detected. In fact in the control animals a residual inflammatory infiltrate, comprising PMNs and mononuclear cells was found as a reaction to the created pockets. Thus, these data showed that after 2 weeks of implantation, the assembled TE constructs did not elicit an adverse host reaction, showing a moderate inflammatory response typically observed for implanted devices.

As a concluding remark, one might say that starch-based scaffolds, processed either by wet spinning or fibre bonding technologies, can be integrated in the host tissue without eliciting an adverse reaction or provoking any systemic response, which is not typical for other biodegradable systems. Furthermore, as SPCL scaffolds were assembled into bone TE constructs, they supported hASCs and angiogenic mediators, were well tolerated by the host tissue and were able to induce the expression of vascularisation specific markers, without major differences between the different processing methodologies.

References

1. Marques, A.P., R.L. Reis, and J.A. Hunt, *The effect of starch-based biomaterials on leukocyte adhesion and activation in vitro.* J Mater Sci Mater Med, 2005. **16**(11): p. 1029-43.
2. Gomes, M.E., et al., *In vitro localization of bone growth factors in constructs of biodegradable scaffolds seeded with marrow stromal cells and cultured in a flow perfusion bioreactor.* Tissue Eng, 2006. **12**(1): p. 177-188.
3. Tuzlakoglu, K., et al., *A new route to produce starch-based fiber mesh scaffolds by wet spinning and subsequent surface modification as a way to improve cell attachment and proliferation.* Journal of Biomedical Materials Research Part A *in press*, 2009.
4. Silva, S.S., et al., *Physical properties and biocompatibility of chitosan/soy blended membranes.* J Mater Sci Mater Med, 2005. **16**(6): p. 575-9.
5. Jackson, J.K., et al., *Neutrophil activation by plasma opsonized polymeric microspheres: inhibitory effect of pluronic F127.* Biomaterials, 2000. **21**(14): p. 1483-91.
6. Nimeri, G., et al., *The influence of plasma proteins and platelets on oxygen radical production and F-actin distribution in neutrophils adhering to polymer surfaces.* Biomaterials, 2002. **23**(8): p. 1785-95.
7. Gomes, M.E., et al., *Starch-poly(epsilon-caprolactone) and starch-poly(lactic acid) fibre-mesh scaffolds for bone tissue engineering applications: structure, mechanical properties and degradation behaviour.* J Tissue Eng Regen Med, 2008. **2**(5): p. 243-252.
8. Santos, M.I., et al., *Response of micro- and macrovascular endothelial cells to starch-based fiber meshes for bone tissue engineering.* Biomaterials, 2007. **28**(2): p. 240-8.
9. Martins, A.M., et al., *The Role of Lipase and alpha-Amylase in the Degradation of Starch/Poly(varepsilon-Caprolactone) Fiber Meshes and the Osteogenic Differentiation of Cultured Marrow Stromal Cells.* Tissue Eng Part A, 2009. **15**(2): p. 295-305.

10. Balmayor, E.R., et al., *A novel enzymatically-mediated drug delivery carrier for bone tissue engineering applications: combining biodegradable starch-based microparticles and differentiation agents.* J Mater Sci Mater Med, 2008. **19**(4): p. 1617-1623.
11. Brown, L.F., et al., *Expression of vascular permeability factor (vascular endothelial growth factor) by epidermal keratinocytes during wound healing.* J Exp Med, 1992. **176**(5): p. 1375-9.
12. Ornitz, D.M. and N. Itoh, *Fibroblast growth factors.* Genome Biol, 2001. **2**(3): p. 3005.1-3005.12.
13. Clauss, M., et al., *The vascular endothelial growth factor receptor Flt-1 mediates biological activities. Implications for a functional role of placenta growth factor in monocyte activation and chemotaxis.* J Biol Chem, 1996. **271**(30): p. 17629-34.